CRANFIELD UNIVERSITY

DEPARTMENT of ENVIRONMENTAL and ORDNANCE SYSTEMS

FOR PRESENTATION as Ph.D. THESIS

SUBMITTED BY

JOHN ALLUM

A STUDY OF THE BEHAVIOUR OF EMULSION EXPLOSIVES

Supervisor: Dr. Michael Cartwright

March 2002

This thesis is submitted in partial fulfilment of the requirements for the Degree of Ph.D.

CRANFIELD UNIVERSITY

DEPARTMENT of ENVIRONMENTAL and ORDNANCE SYSTEMS

FOR PRESENTATION as Ph.D. THESIS

SUBMITTED BY

JOHN ALLUM

A STUDY OF THE BEHAVIOUR OF EMULSION EXPLOSIVES

Supervisor: Dr. Michael Cartwright

March 2002

This thesis is submitted in partial fulfilment of the requirements for the Degree of Ph.D.

Abstract

This study investigated the formulation and characterisation of emulsion explosives. This included the manufacture of more than 120kg of emulsion explosive of which around 105kg was used on the explosive ordnance range in over 350 individual firings. For each emulsion composition, an average of eight firings was undertaken with which to substantiate the explosive performance data. The formulation was varied to determine the effects of water content upon the physical characteristics of the emulsion. These physical effects included thermal conductivity, particle size, viscosity and the explosive performance of the emulsion. In respect of explosive performance, microballoons were added to sensitise the emulsion and the proportions of microballoons added were altered to look at their effect on velocity of detonation, sensitivity and the brisance of the emulsions.

Emulsion explosives are commonly referred, in literature, as Type II non-ideal explosives. This is due to their non-linear behaviour with respect to the variation of velocity of detonation with density. Traditionally, when an emulsion explosive was commercially manufactured, the water content has been kept at a minimum (12-17%). This was accepted as the way to achieve the best explosive performance, based upon the belief that an emulsion with the highest concentration of active ingredients, ammonium nitrate and oil, would give the best explosive performance.

This study examined a wider range of emulsion explosive water contents than has been previously studied, from 12% to 35% water. It was found, during this study, that higher water content emulsions, specifically 25% water, had a marked increase in explosive performance. The highest velocity of detonation recorded was in a 39mm diameter tube, at 25% water content with 3% microballoons, was 5558ms^{-1}. This was some 15% higher than any other VOD recorded in this study. The high velocity of detonation, at 25% water content, was one of a number of physical characteristics in which this water content varied from the other emulsion water contents.

This study endeavored to show that emulsion explosives could exhibit two differing types of explosive reaction, thermal explosion and grain burning. This was based on the velocity of detonation and plate dent data, both of which indicated that there was a change in reaction with water content. Emulsion explosives, with a high water and high microballoon content, exhibited a thermal explosion type reaction. They exhibited Type I ideal explosive behaviour, with increasing velocity of detonation with density. Lower water content emulsion explosives, displayed the more commonly expected Type II non-ideal behaviour and reacted in a grain burning type detonation.

Acknowledgments

I would like to acknowledge the help that I have received throughout my research from a great many people. Dr Michael Cartwright for his supervision, help and support throughout the period of my research and a good while beyond! Professor Alan Bailey for his pragmatic advice, which has saved me many hours of fruitless work. The personnel from the field chemistry laboratory, Arthur Burns, Jim Clements Mike Warden and Adrian Rothan for all their advice and help throughout some very foul weather!

I would also like to thank all my work colleagues for their help and advice and for many borrowed and purloined pieces of equipment, specifically Dr Anthony Bellamy, Richard Hall, Lindsay Dunn, Dr Simon Ward and Dr Michael Williams.

Contents

Figures

Glossary

λ - Thermal conductivity.

$\propto$ - Burning Rate Index- The linear burning rate is the rate at which the chemical combustion reaction is propagated by both thermal conduction and radiation.

β - Coefficient of burning rate (dependent on the material).

ρ - Density in $kgdm^{-3}$.

δ - Shape factor 0.88 for an infinite slab, 2.00 for an infinite cylinder, and 3.32 for a sphere.

λ - Thermal conductivity in J/cm/s/K.

γ - Ratio of specific heats (C_p/C_v).

ΔH – Enthalpy of reaction.

ΔH -The heat of decomposition reaction in J/mol.

AN- Ammonium Nitrate.

ANFO- Ammonium Nitrate Fuel Oil mixture. Oil is mixed with ammonium nitrate prills to give a cheap explosive, widely used in quarrying.

C - Heat capacity.

Chapman-Jouguet Point- The point at which the Hugoniot curve and Rayleigh line meet. At this point, the velocity of detonation is a minimum subject to the constraints of the theory.

Continuous phase- In a water-in-oil emulsion the phase that surrounds the water droplets.

Critical Diameter- The minimum diameter of explosive required for detonation to be sustained.

DDT- Deflagration-Detonation-Transfer. The process of going from a burning (deflagration) reaction to a detonation.

Disperse Phase- The phase surrounding droplets in solution; see also continuous phase.

DSC -Differential Scanning Calorimetry, a method of thermal analysis.

E_a -The activation energy in J/mol.

Emulsion -A colloid in which small particles of one liquid are dispersed in another liquid.

FK- Frank-Kamenetskii equation for heat transfer.

Glass Microballoons- Small glass microballoons which can vary in both size and collapse pressure. In this study 3M B15/250 Silica glass balloons with an average diameter of 15μm and a collapse pressure of 250MPa were used.

Inviscid- A hypothetical fluid without any viscosity effects.

Ionisation Probes- Polyurethane coated wires inserted into the explosive column in order to determine velocity of detonation.

Lead Azide- $Pb(N_3)_2$ a primary explosive mainly used in detonators.

P – Pressure.

PIBSA- Polyisobutylene Succinic Anhydride Ethanolamine- a dark brown viscous liquid with a density 0.91 - 0.93 kg/dm^{-3}.

Prills- Spheres of ammonium nitrate used as fertiliser.

Q - Rate of heat evolved per unit volume.

R - Universal gas constant.

r - Linear burning rate.

Solid Solution- A crystalline material that is a mixture of two or more components, with ions, atoms, or molecules of one component replacing some of the ions, atoms, or molecules of the other component in its normal crystal lattice.

Sorbitan Mono-Oleate- Viscous, amber liquid, insoluble in water. Density 1 $kgdm^{-3}$, Viscosity 100 MPa (25°C).

T - Temperature.

Tc - The critical temperature in K.

TNT Trinitrotoluene, a yellow highly explosive, crystalline solid, $CH_3C_6H_2(NO_2)_3$.

VOD- Velocity of denotation.

Z - The pre-exponential factor in s^{-1}.

Δ - Laplacian operator (x, y and z co-ordinates).

1 Introduction

1.1 Explosives background

An explosion is defined as a violent expansion of gas that usually generates heat, sound and a pressure wave. They can be conveniently separated into three distinct categories.

- Physical explosions, these are the most common in nature. They are pressure bursts that do not release heat, but release large amounts of gas. A balloon bursting would be a common example. Physical explosions can be much more violent than this, a volcano being an example of a huge pressure burst.
- Nuclear explosions can occur naturally, with the sun being the prime example of nuclear fusion. This results in the liberation of immense quantities of heat, but no gas. A nuclear explosion is by far the most energetic type of explosion.
- Chemical explosions are the result of very rapid chemical reactions that release large quantities of heat and gas. Chemical explosives are discussed in more detail below and they are the most important type to the explosive industry.

An explosive is material, with fuel and oxidiser elements, that is capable of undergoing an exceptionally fast reaction without the participation of external reactants. In general, explosives have three basic characteristics:

1) They are chemical compounds or mixtures ignited by heat, shock, impact, friction or a combination of these conditions

2) Upon ignition, they decompose very rapidly (detonation and deflagration).

3) Upon detonation, there is a rapid release of heat and gas, which expand rapidly, usually with sufficient force to overcome confining forces.

A chemical reaction involves the conversion of reactants to products. For this to occur, without a significant energy input, the reactants must have a higher internal energy than products. Energy is required to produce activated molecules and to initially break some of the bonds in the molecule, in an endothermic process. Once this has occurred products are then formed. The formation of products results in liberation of energy, which, overall, yields an exothermic reaction. After initiation, the reactions involved in the burning and detonation process are always exothermic, and therefore always liberate energy.

1.1.1 Chemical explosives

Chemical explosives contain both fuel and oxidiser components. There are, however, two major types of chemical explosives:

Composite explosives- these have two, separate fuel and oxidiser components, which react to form the products. In order for a rapid reaction to proceed, the fuel and oxidiser must be intimately mixed. The smaller the particle size, for solids, the faster the reaction can occur. An example of a composite explosive is ammonium nitrate fuel oil (ANFO). This comprises solid prills of ammonium nitrate, the oxidiser, surrounded by oil, the fuel. The smaller the ammonium nitrate prill size is the faster the reaction can occur. This is an effect, which is due to surface area, the smaller the particle size the larger the surface area. Composite explosives are commonly used in the commercial blasting industry, with only limited use in military blasting charges, usually amatol/TNT fillings. Cost and availability are the main reasons for their widespread use in commercial blasting, with poor performance the reason for their limited military use. Safety is an important parameter with any explosive and composite explosives can often be stored as separate non-explosive ingredients.

Single molecule explosives- the oxidiser and fuel elements are contained within the same molecule. This can be considered an intimate mix on the atomic scale with a separation of nanometres between the fuel and oxidiser. A single molecule explosive commonly reacts much faster than two-phase explosives, leading to a

higher velocity of detonation. Single molecule explosives are commonly used in military ordnance due to their superior performance characteristics.

Single molecule explosives can be further subdivided into three distinct categories based on the ease of ignition for each type:

Primary explosives are the most sensitive and are therefore easily initiated. Examples of primary explosives are substances such as lead azide, silver azide, and mercury fulminate. Primary explosives have a limited use due to their high sensitivity and poor performance. The most common use for primary explosives is as an initiator in detonators. Some primary explosives are able to transit from surface burning to detonation within a very small distance. A 0.2mm thick grain of lead azide when ignited will transit from burning to deflagration to detonation (DDT) within the grain thickness. The lead azide molecule decomposes in a two-step reaction producing high molecular weight reaction products. The reaction products are generated at the surface faster than they can expand away, which results in build up of pressure at the burning surface leading to detonation [1].

Secondary explosives, substances such as trinitrotoluene (TNT) and cyclotrimethylenetrinitramine (RDX) can also burn to detonation. However, a larger quantity of explosive and some form of confinement is often required. With small quantities, they will often burn with an example of this being a stick of TNT, which, if lit, will burn slowly without undergoing DDT. This is because there is little pressure build up from the reaction products, so the reaction does not speed up and transfer to detonation does not often occur. When the quantity is increased or the explosive is confined a pressure build usually occurs and transfer to detonation often results.

Tertiary explosives, which include ammonium nitrate, are extremely difficult to initiate and usually require a sensitising agent. Notwithstanding this, they are, under certain conditions, capable of undergoing a burning to detonation transition. Some of the largest accidental explosions have involved ammonium nitrate, without any obvious sensitising agent.

Most secondary explosive compounds contain nitrogen and oxygen. When oxygen combines with nitrogen, little energy is released. However, when oxygen combines with carbon or hydrogen a relatively large amount of energy is released. As the explosive detonates, the nitrogen-oxygen bond is broken and the oxygen combines with carbon or hydrogen to form bonds. This results in the formation of compounds such as carbon monoxide, carbon dioxide, water vapour and free nitrogen. This is formed in varying proportions, which depend on the relative proportions of fuel and oxidiser. These reactions liberate considerable quantities of heat and gas, with the amount of energy actually released dependent upon the explosive compound involved. An example reaction of a common secondary explosive, RDX, is shown below.

Equation 1 Decomposition of RDX

$$C_3H_6N_6O_6 \rightarrow 3N_2 + 3H_2O + 3CO$$

This is the initial decomposition sequence of RDX but some of the products remain reactive after the initial reaction is complete. These products expand and undergo further reactions. As the products expand, they may mix with oxygen in the air, thereby oxidising the carbon monoxide and producing a secondary fireball. This occurs as the enthalpy of formation for carbon dioxide is such that 283 kJ/mol of energy is released by this reaction ($\Delta H^{\cdot}_f$ kJ/mol CO_2 –393.5, $\Delta H^{\cdot}_f$ kJ/mol CO –110.5).

In this reaction, RDX decomposes to give three main product gases. The fact that explosives are mostly self sufficient in oxygen gives rise to a distinction between explosives and other flammable substances. Whilst the combustion of explosives can take place equally well in the presence or absence of air, the combustion of a flammable substance requires oxygen. As explosives supply their own source of oxygen, less energy is available compared to a flammable substance such as petrol. Burning an explosive in air will generate about eight times more heat than detonation does. The reason explosives are so destructive, in comparison to flammable substances, is the speed at which an explosive releases its energy.

An explosion can be differentiated from combustion by the speed and type of reaction. The speed of the reaction allows an explosive to do useful work and, on an energy basis, explosives do not have a high internal energy in comparison to fuels such as petrol. As petrol contains no oxidiser, it burns with oxygen from air, which is a rate-determining step in its combustion. As an explosive has its own oxidiser and fuel, it is not therefore limited by this step. A good solid explosive, such as RDX, converts energy, at the detonation front, at a rate of approximately 10^{10} Wcm^{-2}. As a comparison, the total solar energy intercepted by earth is about $4 \times 10^{16}W$. Therefore, a 20m square detonation wave gives the same power output as that the earth receives from the sun[2].

An explosive is a material capable of a violent exothermic chemical reaction[3], but the normal resting state is at a metastable chemical equilibrium. An explosive is stable under 'normal' conditions because the reaction rate is so slow. A local stimulus can initiate a reaction wave, which spreads through the material. This reaction wave can be one of two types: a deflagration or a detonation wave. Deflagration is a surface-burning phenomenon and a detonation is characterised by the presence of a shock wave. These are described in the following section.

1.2 Deflagration

A deflagration (flame) is a slow (subsonic) wave where transport processes such as viscosity, heat conduction and matter diffusion are dominant. Changes in momentum and kinetic energy are small and the pressure change through the wave, to an approximation, can be neglected.

Burning reactions are surface phenomena and as such, the flame will spread over the surface of the material quicker than through the main body. In 1893, Paul Vieille determined a mathematical relationship between burning speed and pressure. He showed that linear burning rate, the speed of burning, r, is determined by the pressure P according to the equation below, Vieille's law[4].

Equation 2 Vieille's burning rate law

$$r = \beta P^{\propto}$$

r = Linear burning rate

β = Coefficient of burning rate (dependent on the material)

P = Pressure

$\propto$ = Burning rate index (dependent on the material)

The rate of burning index, $\propto$, can vary from 0.3 to greater than 1.0. With values of less than one, a flame front is generated and the reaction proceeds rapidly, but only as a surface burning phenomena. An example of this is black powder, which when unconfined will burn at a rapid rate (~0.1kms^{-1}), which is below that of detonation. If the explosive has a burning rate index of greater than 1.0, then pulses are generated. These pulses can accelerate the linear burning rate to sonic velocity, thereby leading to detonation. When an explosive is ignited, they often burn with no oxygen being required for this process to occur. If the explosive was confined, such that the reaction product gases cannot escape, then the

pressure, at the reaction zone, builds up. Burning reactions are functions of pressure and temperature; therefore, the reaction rate increases as the pressure increases. The high pressure forces the hot gases into the surrounding material thereby accelerating the process. Pressure waves are generated in the deflagrating region, these compact and compress the explosive material, causing greater confinement and hence even greater pressure build up. The compressional waves cause shock pile up, which, given sufficient time and distance, form the conditions necessary for detonation to occur. A shock wave is then formed, and the transition to detonation occurs. This process is commonly referred to as deflagration-to-detonation transition, DDT. DDT transition is an important mechanism for the initiation of explosives and Mallard[5], in 1881, was the first person to show that this could occur.

There have been many examples of DDT occurring accidentally, such as the Texas container ship explosions[6]. A container ship carrying ammonium nitrate had a minor fire in the main hold, which was not considered a risk. After burning for many hours, the ammonium nitrate eventually exploded. The ammonium nitrate underwent DDT due to the large mass of explosive present (~3000 tons), which then destroyed everything within a 2-mile vicinity.

1.3 Detonation

A detonation runs at supersonic speeds, 2000 to 8000 ms^{-1} in solids and liquids, with the velocity limited to the local speed of sound in the explosive. The transport properties, which were important for combustion, become relatively unimportant in a detonation. Changes in momentum and kinetic energy are dominant, with compressibility and inertia being important properties. The leading element of a detonation wave is a shock front, and the high temperature and pressure produced by this shock front is maintained by inertial confinement. That is the outer layers of the material are not appreciably displaced before the reaction in the centre is over.

The process of an explosive going from an undisturbed state to an explosion is described as the detonation process. The detonation process can be explained by

Detonation theory, which is based on the study of shock propagation through inert materials. Both Berthelot[7] and Vieille[8] determined the existence of detonation waves in 1881. Using a Le Boulenge chronograph, they measured the propagation velocity of detonation waves in approximately 50 different mixtures of fuels and oxidisers. Their conclusions were that the propagation velocity of an explosive is a constant, which depends upon the mixture and not on external conditions, such as tube diameter or tube material. This discovery, within twenty-five years, allowed the growth of detonation theory, in thermodynamic and hydrodynamic terms, to be developed.

This development began, in the 19th century, with theoretical studies of the detonation process. Much of the understanding of detonation phenomena was based on research into gas explosions. This began with the early work of Berthelot[9] (1882) and Dixon[10] (1893), who attributed the high detonation velocities to the properties of explosion product molecules. Schuster (1893) was the first to point out similarities between detonations and unreactive shock waves. He suggested, the now accepted view, that detonation is a shock wave supported by chemical reaction.

A shock wave[11,12,13,14,15] is a region of very high pressure that passes through a material at the local speed of sound for that material. An important feature is that the local speed of sound is the speed of sound at the shock front, where the material is under high pressure. A representation of a shock wave in an explosive material is shown in Figure 1. This shows the shock impinging on the material and immediately exerting a maximum pressure, referred to as the Von Neumann spike. After the shock front has passed, the pressure reduces in an exponential manner.

In an explosion, the shock wave and reaction zone are called the detonation front. The shock wave compresses the explosive, which breaks apart the chemical bonds, causing a chemical reaction. This chemical reaction continuously adds energy to the shock front, which as well as driving the shock front forwards, is also lost laterally. This is because the detonation wave expands sideways as well as forwards through the column. If more energy is added to the shock front, by the chemical reaction, than is lost laterally, then the velocity at the front increases.

This process of acceleration continues until the energy added, to the detonation front, equals the lateral losses due to expansion and heat flow. Once this has occurred, and the losses from the system equal the energy being added to it, then a steady state velocity of detonation is achieved.

Figure 1 Structure of a shock wave

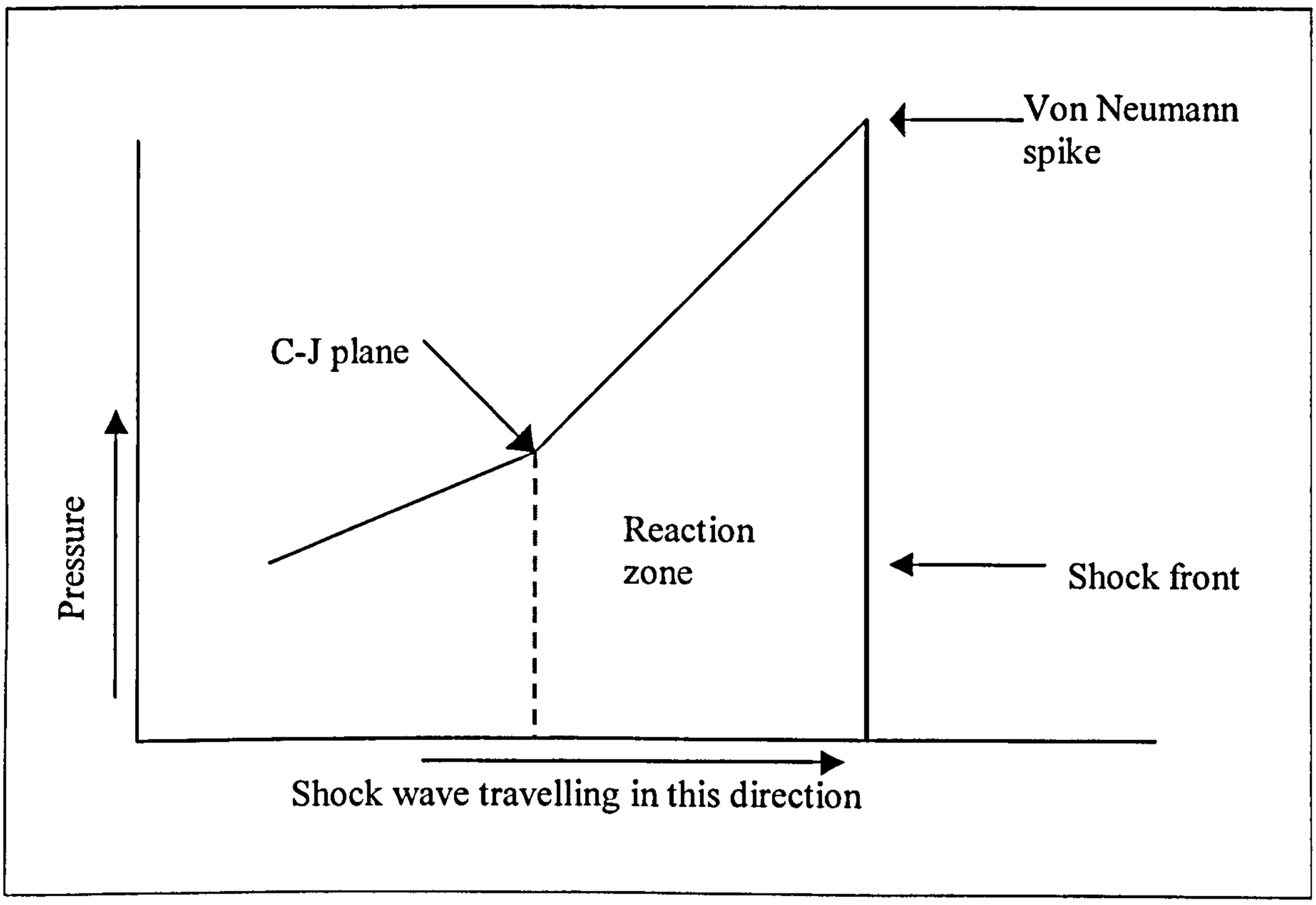

1.3.1 Simple detonation theory

The first attempts at a thermodynamic[16] analysis of a detonation were independently reported by Chapman[17] (1899), Jouguet[18] (1903), and Michelson[19] (1891). This is commonly referred to as the Chapman-Jouget theory. In Chapman-Jouguet (CJ) theory, the detonation process is treated as a one-dimensional wave of infinitesimal thickness, without mass, momentum or energy

loss, in an inviscid (no viscosity) fluid; this is done for mathematical simplicity. The detonation process is shown schematically in Figure 2[20].

Figure 2 Schematic of the detonation process in a condensed explosive.

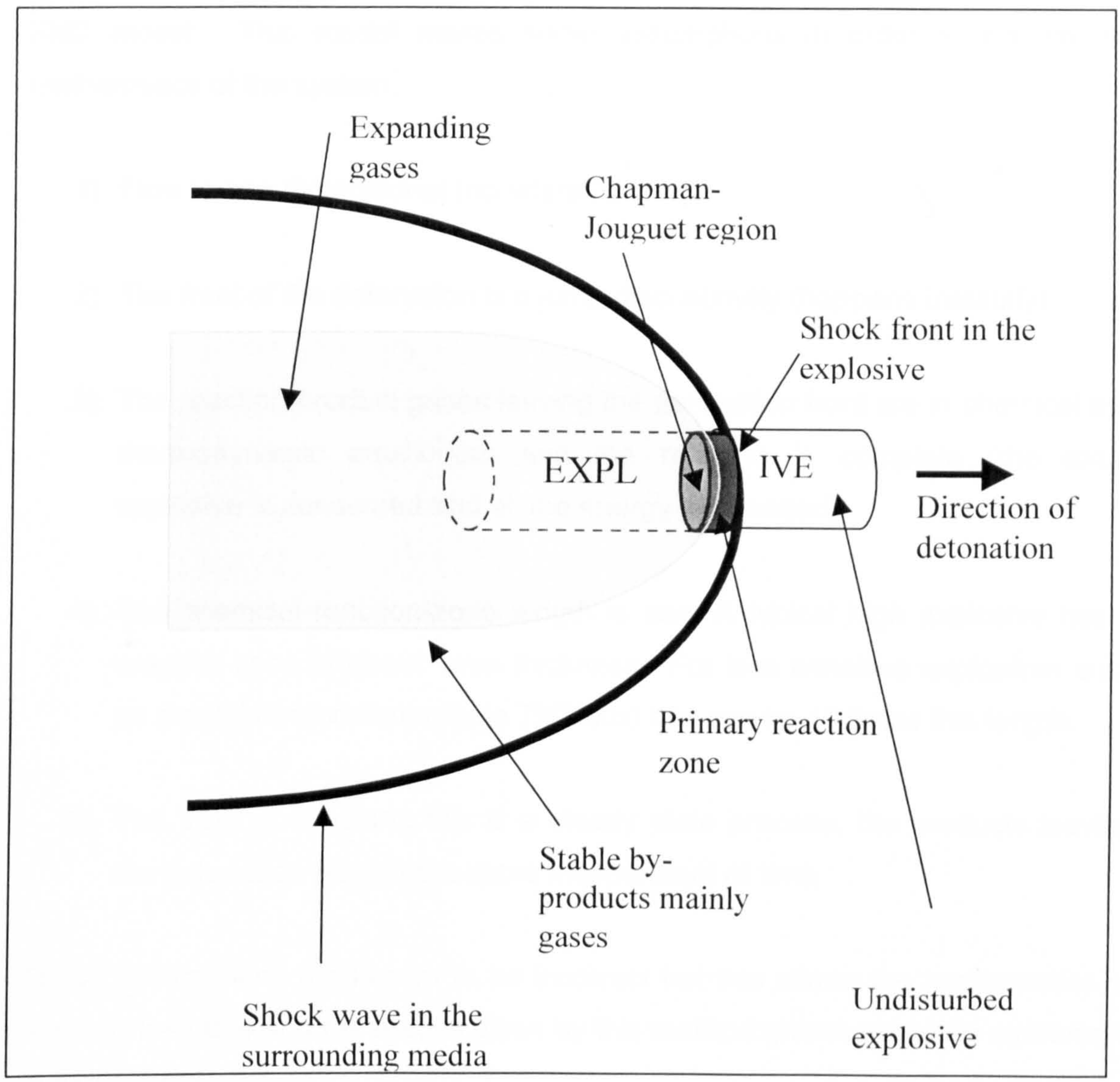

It can be seen, from Figure 2, that the CJ region, described by the equations of conservation, is at the end plane of the reaction zone. This is a point after the shock wave has passed through the material and the initial reactions are complete, although the gases produced have not expanded and reactions with oxygen in the air have yet to take place.

Detonation theory has significantly advanced since the 1900's, but the Chapman-Jouguet theory is still used as the basis for modern interpretation. In the 1940s Zeldovich[21], Von Neumann[22] and Doering[23] independently developed a model to describe the detonation process. This is referred to as the simple theory or the ZND model. This model makes some assumptions in order to simplify the mathematics of the system.

1) Flow is one-dimensional (no lateral losses).

2) The front of the detonation is a jump discontinuity (happens instantly).

3) The reaction-product gases leaving the detonation front are in chemical and thermodynamic equilibrium and the reaction is complete (the entire explosive is consumed and all the energy is released).

4) The chemical reaction-zone length is zero A typical high explosive has a reaction zone of about 1mm thickness. For less sensitive explosives such as amatol (ammonium nitrate TNT mix) this can be 10 times this length.

5) The VOD is constant; this is a steady state process; the products leaving the detonation remain the same independent of time

These assumptions are known to be incorrect but this allows the mathematics to become tractable and the results given by this method give reasonable agreement to experiment.

The basic theory allows profiles for temperature, pressure and density to be determined through the reaction zone and Figure 3 shows this variation across the reaction zone.

Figure 3 Variation of pressure, density and temperature across a detonation wave.

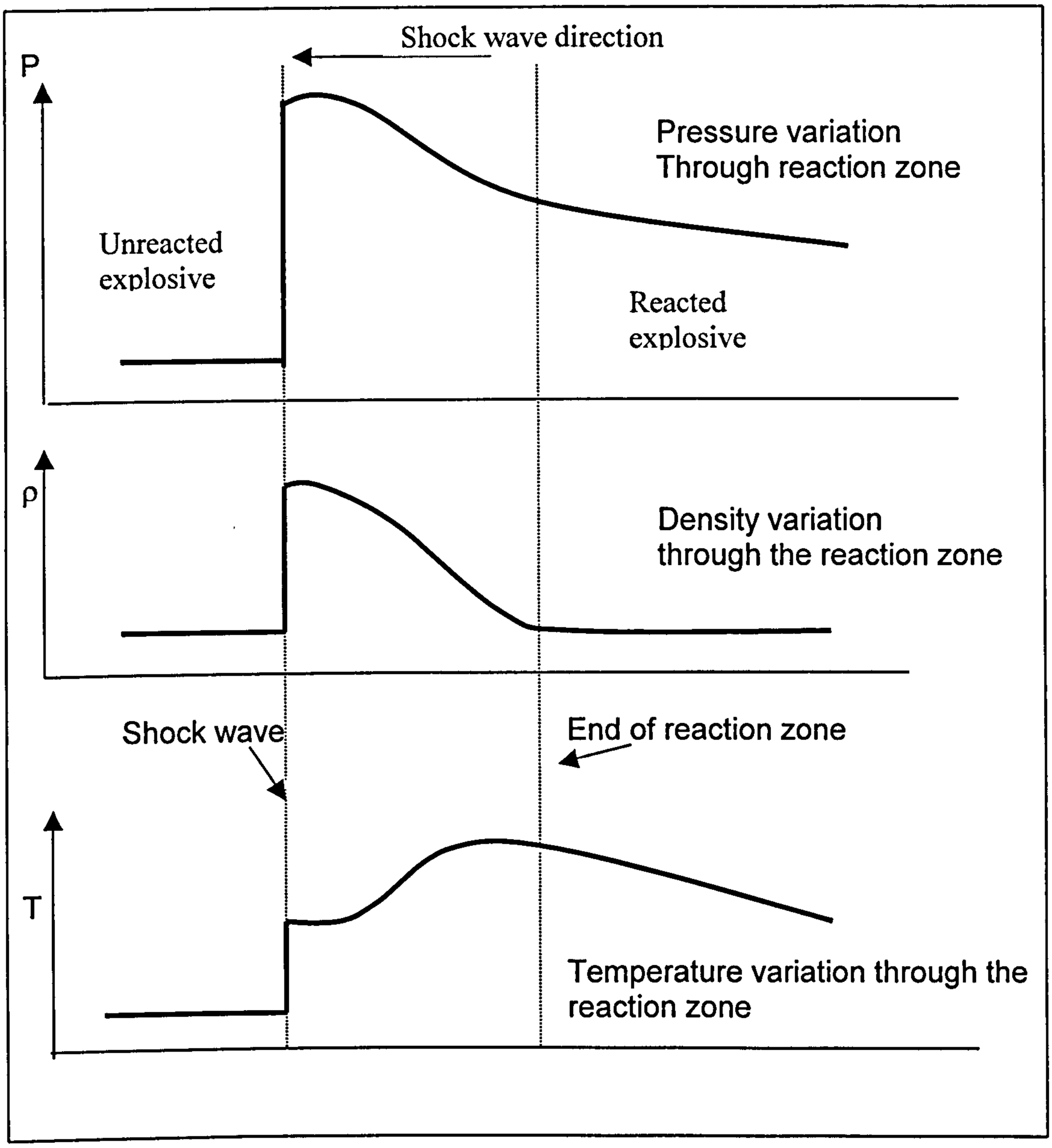

This shows that the pressure and density reach an instant maximum at the shock front, which then drops off through the reaction zone. Whereas the temperature continues to rise throughout the reaction zone, as secondary reactions occur.

1.4 Initiation Theory

An explosive can be initiated[24] by various different forms of energy delivery. These stimuli could be friction, shock, electrical or thermal. Using the Frank-Kamenetskii equation (see later), with Arrhenius kinetics, bulk heating and thermal initiation can treated. Bowden and Yoffe[25] came up with a treatise in 1952 on the mechanism of initiation in explosives.

Whatever form of energy is supplied to an explosive to cause initiation, once the activation energy for that mechanism is exceeded, the detonation process will begin. An explosive can be initiated by applying a shock of greater energy than its critical activation energy. Below this critical energy, the reaction will not generate enough energy to support itself. This does not mean that reaction does not occur, but that the reaction 'fades'. If the explosive contains sensitising agents, such as grit or bubbles then the minimum shock pressure required for initiation is decreased by approximately one order of magnitude [25]. Voids in the explosive cause irregularities in the mass flow when shocked and the explosive is initiated by local hot spots formed at these irregularities. The hot spot mechanism is important in the propagation and failure of the detonation wave.

1.4.1 Hot Spots

Hot spots have been well characterised[26,27,28,29,30,31,32,33,34,35,36,37,38,39,40] and are small areas where heat is generated when an explosive is subjected a variety of stimuli. Although they are large, compared to molecular dimensions they are small, within the range of ~10^{-5} to 10^{-3} cm^3, in comparison to the physical dimensions of the charge. Stimuli, which can produce hotspots in explosives, are described below.

- Adiabatic compression of small entrapped bubbles of gas
- Frictional hot spots
  1) Inter-crystalline friction
  2) Grit particles
  3) On confining surfaces
- Viscous heating of rapidly flowing explosive
- Shear of crystals

For emulsion explosives, the main area of interest is the adiabatic compression of gas bubbles. When an adiabatic reaction occurs there is no transfer of heat in or out of the system, all the work supplied being converted to heat at the hot spot site. An emulsion explosive usually has micro-balloons or gas bubbles added to the emulsion to provide a source of hotspots. Micro-balloons (3M B15/250) are glass balloons with an average diameter of 60μm; they are filled to 0.2 bar with sulphur dioxide and molecular oxygen.

The initiation of an explosion, when small gas bubbles are trapped in liquid, is due to the adiabatic compression of the bubble. For an ideal gas the temperature reached inside the bubble (T_2 degrees absolute) depends on the compression ratio given by;

Equation 3 Compression ratio for hot spot temperature determination.

$$T_2 = T_1 \left(\frac{P_2}{P_1} \right)^{\frac{(\gamma-1)}{\gamma}}$$

P_1 = Initial pressure in gas bubble.

P_2 = Final Pressure in gas bubble.

γ = Ratio of specific heats (C_p/C_v) (γ has an accepted value of 1.4 for air and 1.29 for sulphur dioxide[41]).

T_1 = Initial temperature. T_2 = Final temperature.

The initial pressure would usually be atmospheric pressure but micro-balloons are filled at a reduced pressure of 0.2 bar. The higher the initial pressure of the bubble the lower the temperature obtained by the hot spot. By having, the micro-balloons filled to only 0.2 bar pressure the pressure differential is greater and hence temperature obtained will be higher. This gives a means of determining the hotspot temperature obtained from an applied pressure.

There are other processes, beyond adiabatic compression, which occur when a bubble is subject to a shock wave. These include jetting, where the top surface of the bubble forms a jet, which impinges on the bottom surface generating a high-pressure, high temperature zone, and vaporisation where a small amount of the explosive is vaporised in the cavity as it collapses causing it to violently react. Although both these processes are important, they are not the dominant process in hotspot initiation.

1.4.1.1 Frank-Kamenetskii Equation

Frank-Kamenetskii[42] proposed the classical three-dimensional heat transfer equation, which relates the rate of heat production to the rate of temperature rise in a reacting material. The equation shows that if heat is evolved by a reaction faster than it can be transferred away, then the temperature of the reacting material must increase. Increasing the temperature increases reaction rate, as shown by the Equation 4.

Equation 4 Rate of heat evolved to reaction temperature.

$$Q = \rho \Delta H Z e^{-E_a / RT}$$

Q - Rate of heat evolved per unit volume.

ρ - Density.

ΔH – Enthalpy of reaction.

Ea - Reaction activation energy.

R - Universal gas constant.

T - Temperature.

Z - Pre-exponential factor

The heat produced by a reaction is transferred to the surrounding material; this can be shown using the Frank-Kamenetskii equation. This equation gives the heat transfer rate, a figure that is dependent upon temperature, as well as thermal conductivity, heat capacity and density.

Equation 5 Frank-Kamenetskii (FK) equation for heat transfer.

Where;

$$-\lambda \nabla^2 T + \rho C\left(\frac{dT}{dt}\right) = \rho \Delta H Z e^{-E_a/RT}$$

λ - Thermal conductivity

C - Heat capacity

∇- Laplacian operator (x, y and z co-ordinates)

The FK equation predicts that for each explosive a critical temperature can be obtained, which, if exceeded, will result in explosion. This critical temperature is the point at which heat loss exactly equals heat gain, any increase in heat gain results in a runaway reaction and thereby an explosion. The heat transfer rate given by the equation depends upon sample size and geometry. With the same geometry, the larger the mass of the explosive, the slower the rate of internal heat conduction. This leads to the conclusion that the critical temperature is dependent on the size and geometry of the explosive, as well as its composition. When the FK equation is solved, to obtain the critical temperature, the following expression is obtained[43].

Equation 6 Frank-Kamenetskii equation for critical temperature.

$$\frac{E_a}{Tc} = R \ln\left(\frac{r^2 \rho \Delta H Z E_a}{T_C^2 \lambda \delta R}\right)$$

Where;

r	The radius of a sphere, cylinder, or half slab thickness in cm
ρ	Density in kg/dm^{-3}
ΔH	The heat of decomposition reaction in J/mol
Z	The pre-exponential factor in s^{-1}
E_a	The activation energy in J/mol
Tc	The critical temperature in K
R	The universal gas constant
λ	Thermal conductivity in J/cm/s/K
δ	Shape factor 0.88 for an infinite slab 2.00 for an infinite cylinder and 3.32 for a sphere

The shape factors are used to correct for sample geometry, as different shapes will have a different surface areas and therefore lose heat at different rates. The equation represents a condition where the rate of heat generation exactly matches that of heat lost.

1.4.2 Priming

Priming is the energy required by the explosive to successfully propagate to allow detonation to occur. In order that adequate priming is achieved, the minimum detonation pressure of a primer must be at least equal to that of the explosive, preferably it should be higher. If the detonation pressure applied to the explosive is higher than required, then the explosive will be overdriven. This means that the explosive will initially detonate faster than its theoretical maximum velocity of detonation. This is an effect, often used in the commercial quarrying industry, where a more powerful explosion is often required at the toe of a quarry face. This

is only a short-lived effect, which rapidly dies away with distance. The distance the over-driven state exists for is dependent on the diameter of the explosive and the source of initiation. With a primer of equal diameter to that of the explosive charge, the overdriven state can exist for up to three charge diameters.

This is an important effect and must be accounted for when measuring the VOD of an explosive initiated with a primer. Conversely, if the pressure of detonation and VOD applied by the primer is lower than the explosive's own VOD then the explosive will be under-driven, reacting at a rate lower than its theoretical VOD, until the detonation wave either fades or picks up. This is often referred to as the run up distance, and if the explosion is to propagate, the VOD will pick up within three charge diameters. Figure 4 illustrates the effect of under-driving and over-driving the explosive.

Figure 4 Effect of priming.

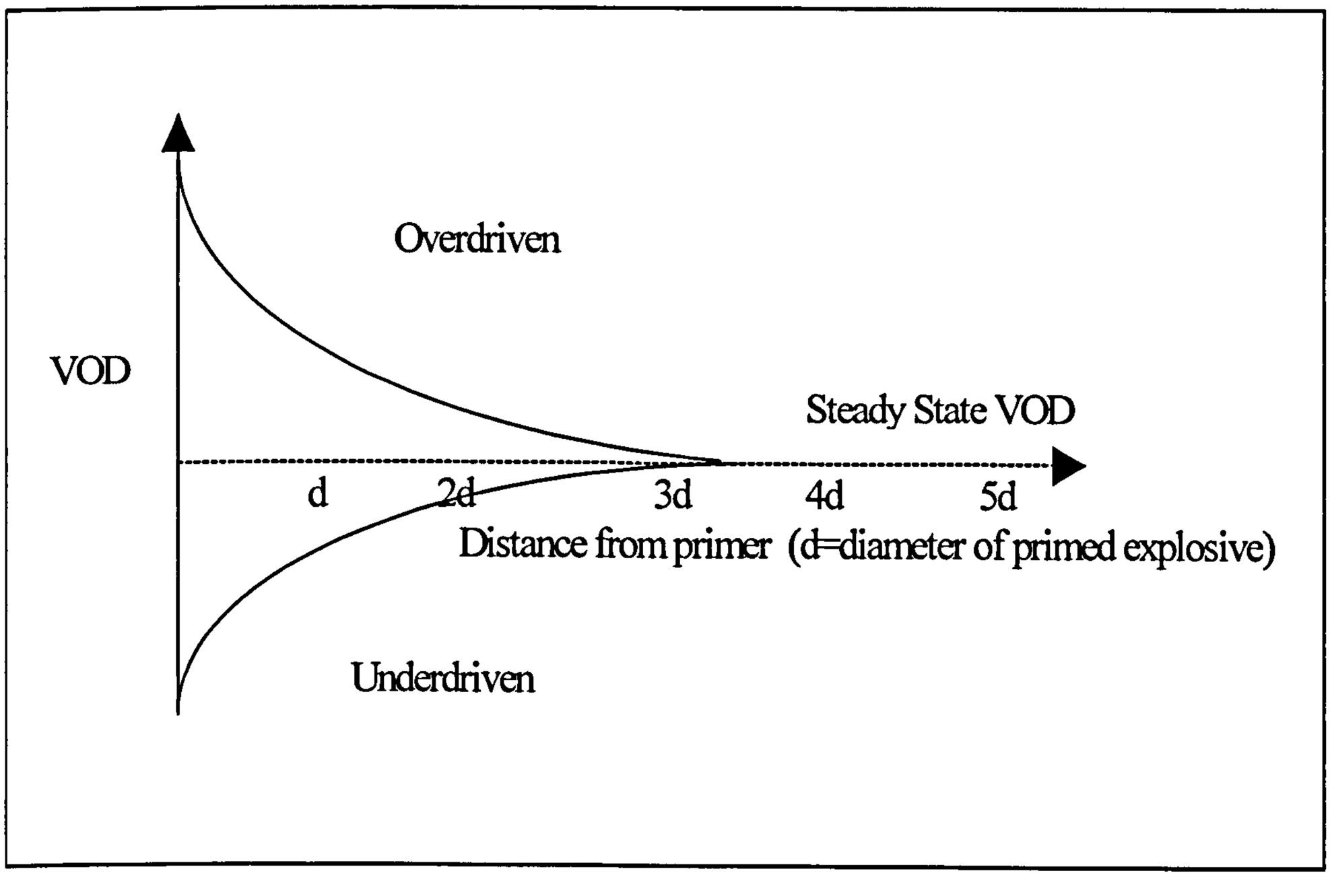

3.1.1 Calculation of detonation pressure

Cook[44] developed an empirical method for determining the detonation pressure, if the density and the velocity of detonation are known. It can be shown that the Chapman-Jouguet pressure can be determined by:

Equation 7

$$Pcj = \frac{\rho D^2}{\gamma + 1}$$

Where Pcj is the CJ or detonation pressure in gigapascals (GPa)

ρ is density in kg/dm^{-3}

γ is the ratio of specifics heats of the detonation product gases

D is the velocity of detonation in km/s

This allows the detonation pressure to be predicted to within an error of less than 5%. An alternative method, which allows the calculation of detonation pressure to a similar degree of accuracy, without requiring the ratio of specific heats for the detonation gases, the following equation can be applied.

Equation 8

$$Dp = 2.325 * 10^{-7} * VOD^2 * \rho$$

As Equation 8 shows, a high density and a high VOD lead to high detonation pressures. An emulsion explosive has both a low VOD and a low density; it therefore follows that the detonation pressure will be low. This signifies that to successfully initiate an emulsion explosive, a primer with a high detonation pressure of detonation is not necessarily required.

1.5 Explosive behaviour classification

Chemical explosives, as described by Price[45], can be classified as one of two distinct categories. The first, and most common category, is type I ideal explosives and the second, less common, is type II non-ideal explosives. This classification is based upon the variation in velocity of detonation as a function of density.

1.5.1 Type 1 Ideal explosives

Type 1 explosives are the standard military high explosives such as, RDX, HMX and TNT. The density of an explosive affects its performance in terms of the velocity of detonation, heat and pressure. The term of most interest is velocity of detonation (VOD) and for a Type 1 explosive, increasing density leads to higher velocity and pressure of detonation. For type I explosives, the relationship between VOD and the density of the unreacted explosive is close to linear. This leads to the relationship shown in Equation 9, which is shown graphically as Figure 5.

Equation 9 Relationship between VOD and density.

$$D = a + b\rho$$

D - Velocity of detonation.

a, b - Empirical constants specific for each particular explosive and identified from experimental studies.

ρ- Density.

The density of an explosive is an important factor in determining the properties of an explosive although direct comparison of performance cannot be made from the density alone. Comparing lead azide with RDX shows this, lead azide is four times more dense than RDX, but its velocity of detonation is half that of RDX. For the same type 1 explosive the higher the density of the explosive the higher the

higher the VOD will be. As a result of this, type I ideal explosives, are often packed at maximum loading density to give maximum performance. [46]

Figure 5 Variation of VOD with density for a type I explosives VOD (ms^{-1})

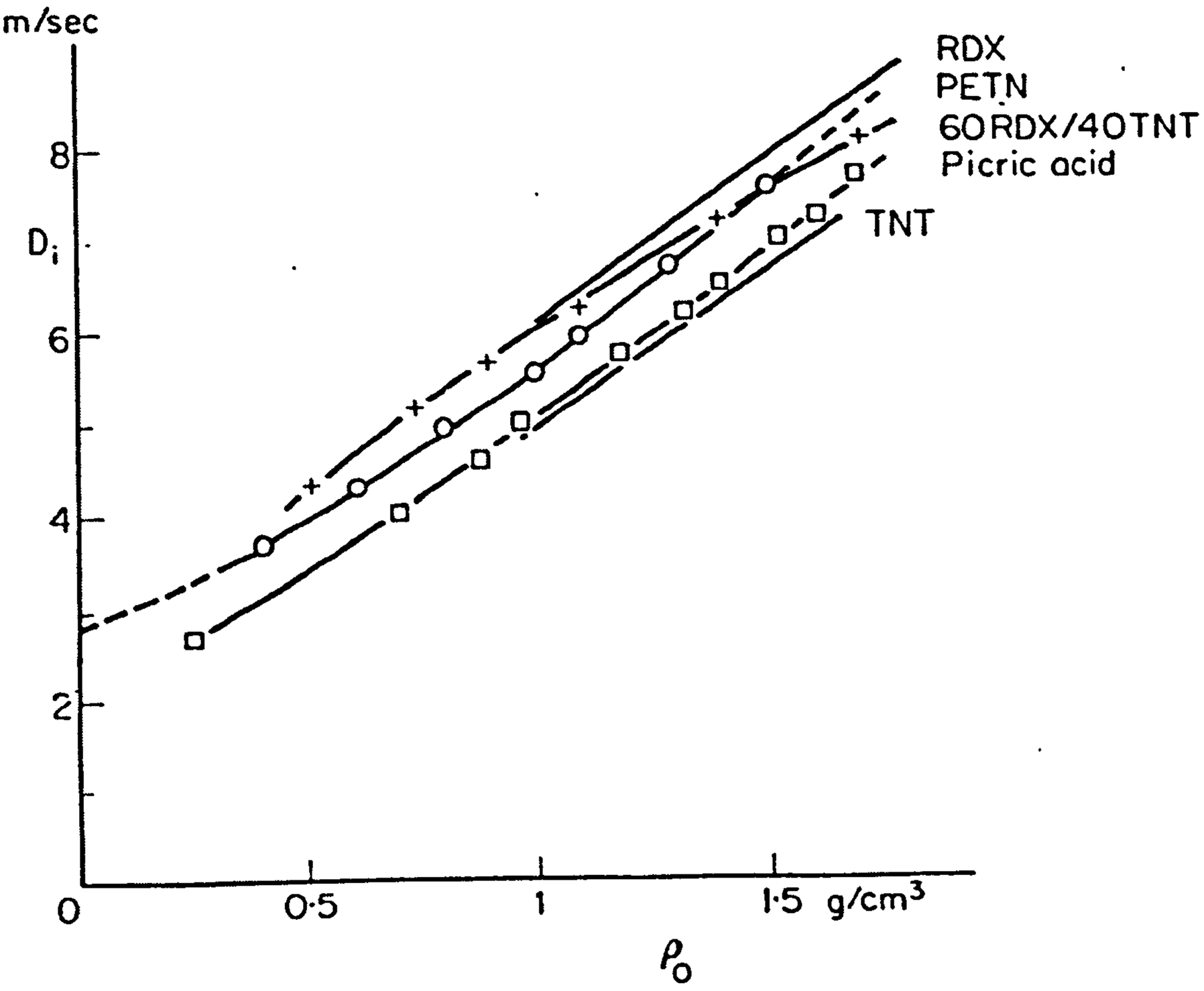

1.5.2 Type II non-ideal explosives

The behaviour of type II explosives is more complex, although density is still a parameter of interest. Examples of type II explosives are ANFO, emulsions and slurries. These are not single molecule explosives and increasing the density often causes differing reaction mechanisms to be observed. At low densities, the velocity of detonation increases as a linear function of density, but as the density is increased, the velocity of detonation drops off rapidly until failure occurs. A graph of this behaviour, as first reported by Price, is shown in Figure 6.

Figure 6 Type II non-ideal explosive. Decrease in detonation velocity with increasing density of ammonium perchlorate. (According to Price,1967.)[45]

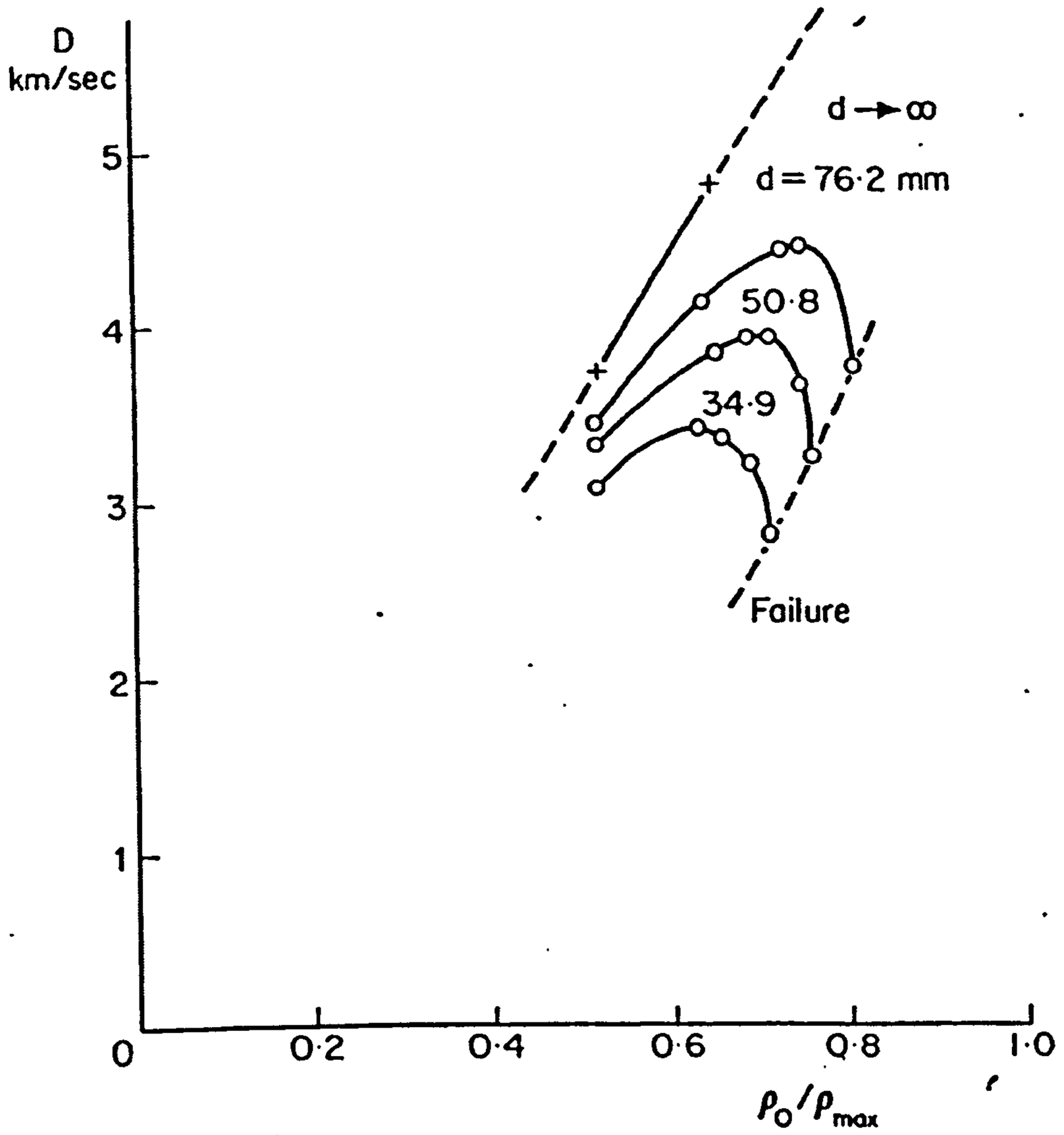

There are many explanations for this process, with reaction zone length being of prime importance, but at present, the process has not been fully elucidated. Emulsion explosives, as used in this study, have been categorized as type II non-ideal explosives, although there has been little published data on the characterisation of them.

1.5.3 Methods for VOD determination

VOD can be measured by a variety of different methods, varying from point methods such as ionisation probes and fibre optic lines to continuous systems such as resistance wire and streak camera's.

One of the original methods, and a method that is still sometimes utilised, was the Dautriche method for measuring velocity of detonation. It was developed (1906) as a method of measuring the velocity of detonation in short columns of explosive. The practice before this had been developed was to use columns of explosive tens of meters long.

Figure 7 Dautriche method of VOD measurement.

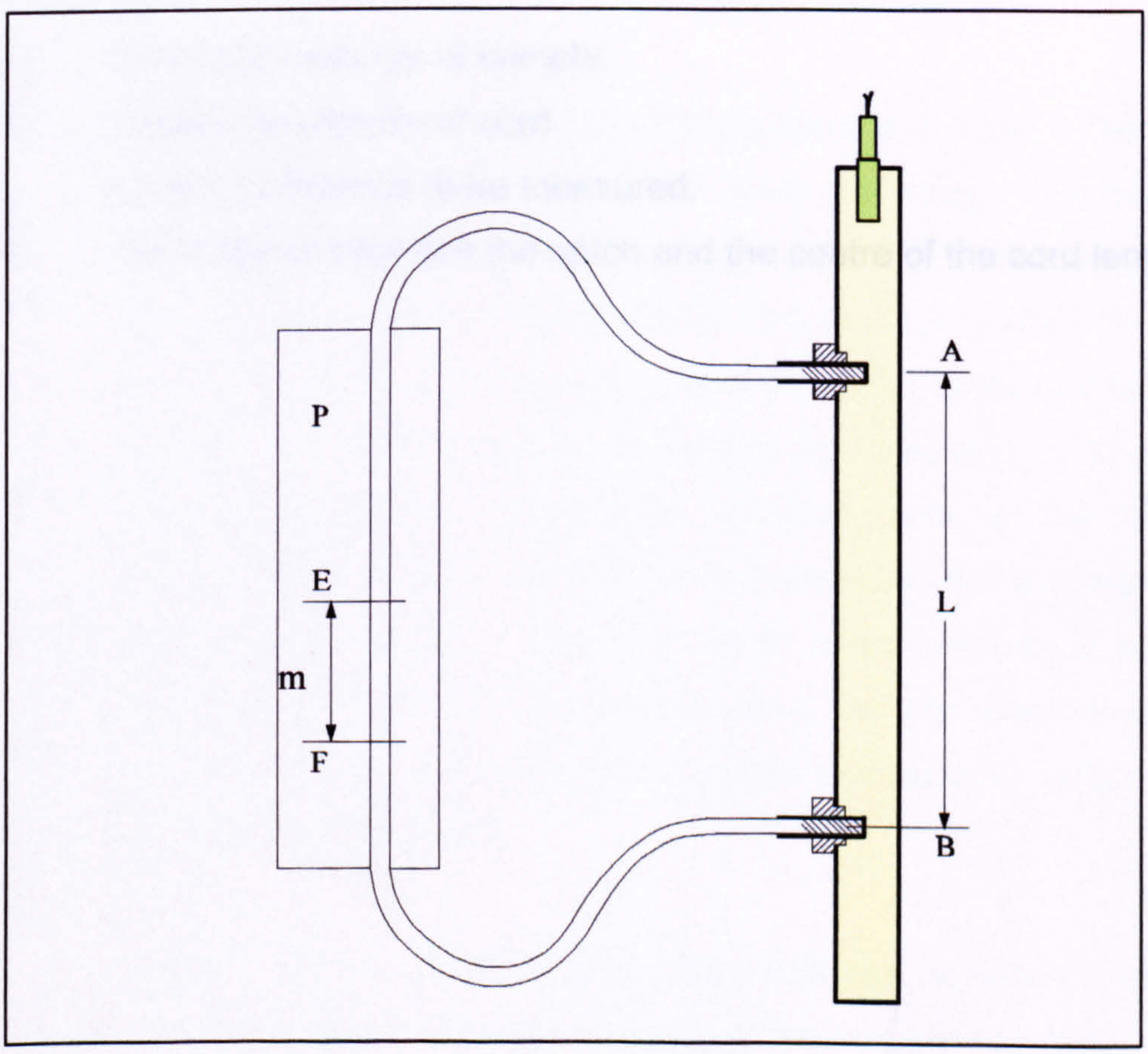

The[47] test sample is inserted into a cylindrical column and blasting caps are inserted into the sample at a set distance apart (L) (see Figure 7). A loop of detonating cord, of known VOD, is connected to the blasting caps and placed on a lead sheet (P). On the lead sheet, the centre of the cord is marked out (E). The explosive column is then initiated at one end. The cord is ignited as the detonation wave passes over the blasting caps and sets them off. The meeting point of the two detonation waves in the cord makes a notch in the lead witness plate (F). The distance between the meeting point and the centre of the cord (m) is a measure of the reciprocal detonation rate to be determined as shown by Equation 10.

Equation 10 Determination of VOD using the Dautriche method.

$$D_x = \frac{D \times L}{2m}$$

D_x- Detonation velocity of sample.

D- Detonation velocity of cord.

L- Length of distance to be measured.

M- The distance between the notch and the centre of the cord length.

1.6 Emulsions

1.6.1 Introduction

An emulsion comes under the broad heading of a colloid, which Thomas Graham originally defined, in 1861, as substances, such as starch or gelatine, which will not diffuse through a membrane. He distinguished colloids from crystalloids (i.e. inorganic salts), which would pass through membranes. Later it was recognized that colloids could be distinguished from true solutions by the presence of particles that were too small to be observed with a normal microscope, yet were much larger than normal molecules. Colloids are now regarded, as systems in which there are two or more phases with one, the dispersed phase, distributed in the other, the continuous phase. Moreover, at least one of the phases has small dimensions (in the range 10^{-9}–10^{-6} m). Colloids can be classified by various subdivisions.

- Sols are dispersions of small solid particles in a liquid. The particles may be macromolecules or clusters of small molecules. Lyophobic sols are those in which there is no affinity between the dispersed phase and the liquid. An example is silver chloride dispersed in water. In such colloids, the solid particles have a surface charge, which tends to stop them coming together. Lyophobic sols are inherently unstable and, in time, the particles aggregate and form a precipitate. Lyophilic sols, on the other hand, are more like true solutions in which the solute molecules are large and have an affinity for the solvent. Starch in water is an example of such a system. Association colloids are systems in which the dispersed phase consists of clusters of molecules that have lyophobic and lyophilic parts. Soap in water is an association colloid.

- Gels are colloids in which both dispersed and continuous phases have a three-dimensional network throughout the material, so that it forms a jelly-like mass. Gelatine is a common example. One component may sometimes be removed (e.g. by heating) to leave a rigid gel (e.g. silica gel).

- Other types of colloid include aerosols (dispersions of liquid or solid particles in a gas, as in a mist or smoke) and foams (dispersions of gases in liquids or solids).

- Emulsions are colloidal systems in which the dispersed and continuous phases are both liquids, e.g. oil-in-water or water-in-oil. Such systems require an emulsifying agent to stabilize the dispersed particles.

Emulsions, formed by the process of emulsification[48,49,50,51,52,53] are heterogeneous systems consisting of at least one immiscible liquid intimately dispersed in another in the form of droplets. The preparation of an emulsion requires the formation of a large interfacial area between two immiscible liquids. They are described as thermodynamically unstable mixtures that are stabilised by the presence of a third phase, an emulsifying agent. The diameter of the dispersed phase droplets is generally in the range of about 0.1 to 10μm, though droplets as small as 0.01μm and as large as 100μm are often observed. Simple geometric calculations indicate that if a sample of 10ml of oil is emulsified in water to give an average droplet diameter of 0.2μm, the resulting interfacial area will have been increased by a factor of approximately 10^6.

Milk is the most common food emulsion with cow's milk comprising about 87% water, 3.6% lipids 3.3% protein, 4.7% lactose, and, in much smaller amounts, vitamins and minerals. The stability of raw milk[54] is accomplished by a complex interfacial lipid-protein membrane, formed during the secretion of milk. To avoid separation of the fat phase during storage, milk is homogenised. This process reduces the fat globule size to below 1 micron in diameter, and thus keeps the fat in suspension by Brownian motion. During the homogenisation process, the surface area of the fat phase is greatly increased due to the formation of many new fat particles. These new fat particles are covered with absorbed milk proteins, stabilising them against coalescence. If the particle size of the fat droplets is lowered too much (below 0.5μm), the surface load of absorbed proteins may cause the oil droplets to precipitate due to the increased density.

Some common food emulsions are shown in Table 1, they are distinguished by which is liquid is the disperse phase.

Table 1 Emulsion types

Oil-in-water	Particle size	**Water-in-oil**	Particle size
Milk	>1μm	Margarine	5-20μm
Mayonnaise	1-5μm	Butter	1μm

There is a large variation in droplet size between differing foods and this has significant effects on their properties and behaviour. Other common emulsions include oil products such as bitumen and a whole range of medical and cosmetic products. Figure 8 shows two electron micrographs of butter and a low fat spread, these show the variation in droplet size between them. [55]

Figure 8 Electron micrographs of butter and a low fat spread. (Both at the same magnification).

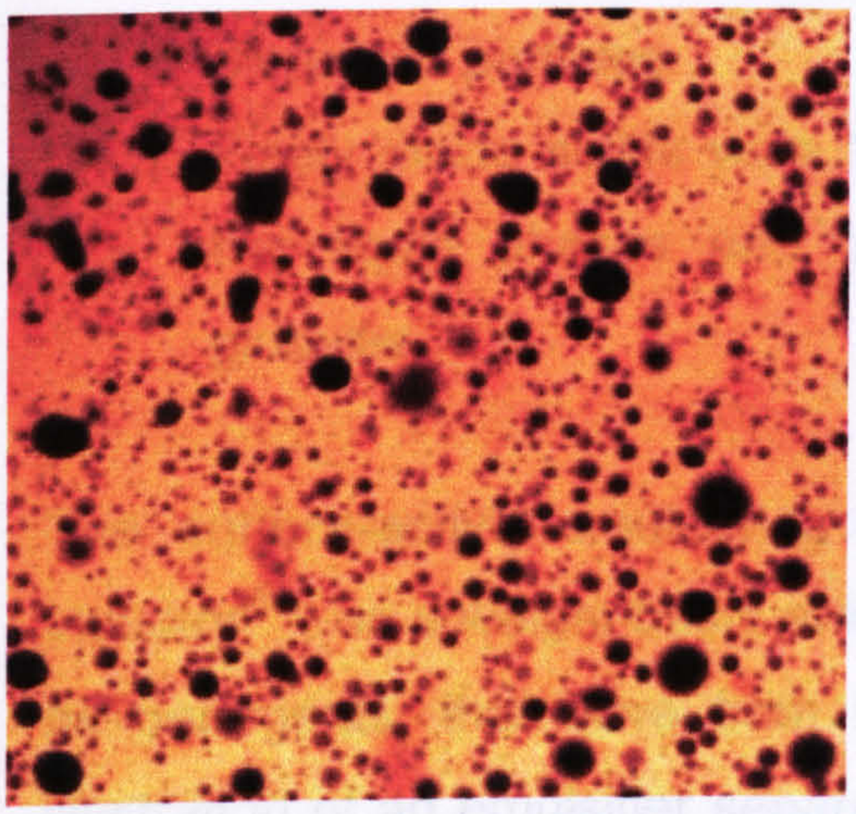

Butter
Confocal laser scanning microscopy image of butter. Dark water droplets in the continuous fat phase. A water in oil emulsion. Image by Grethe Hyldig

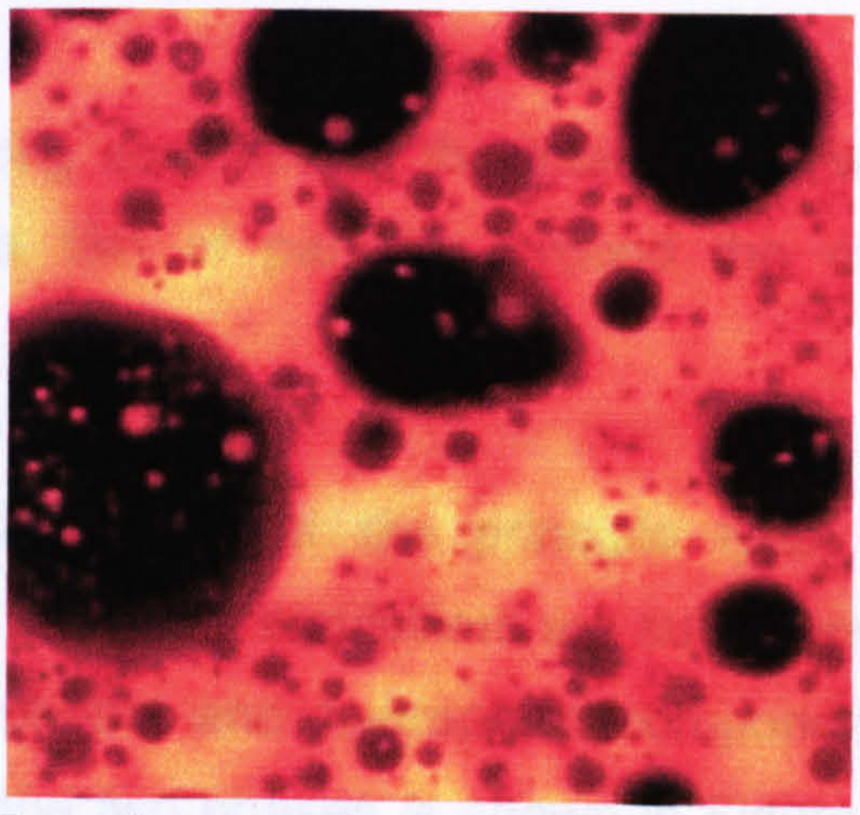

Low fat spread
Confocal laser scanning microscopy image of a low fat spread. Dark water droplets in the continuous fat phase, inside the globular water droplets. An oil in water in oil emulsion
Image by Grethe Hyldig.

1.6.2 Emulsifiers

In order for an emulsion to successfully disperse droplets in a continuous phase, it is often necessary to use an emulsifier. The addition of an emulsifier allows a thermodynamically unstable system to achieve a degree of stability, by separating the two phases. The emulsifying agent minimises the tendency of the globules to coalesce, or join to form larger globules, which would eventually lead to the separation of the two liquids. The stability of an emulsion is dependent upon the properties of the emulsifier and the film it forms at the interface between the two phases. The film at the interface must be tough and elastic and should be rapidly formed during the preparation.

Emulsifying agents can be divided into three categories:

1. Surface-active agents work by congregating at the oil-water interface reducing the interfacial tension.
2. Hydrophilic colloids work by forming multi-molecular films about the dispersed particles.
3. Finely divide solids work by being absorbed at the interface between the two liquid phases and form a film of particles around the dispersed globules.

The surface-active emulsifying agents represent the principle type used in industry[56], on a weight basis at least. Common emulsifiers are substances, such as detergents, that have both hydrophobic and hydrophilic components. An illustration of an emulsifier separating the two phases is shown in Figure 9. The emulsifier that surrounds the droplet will often be more than one molecule thick, frequently several layers separates the two systems.

Figure 9 Action of emulsifying agents in a water-in-oil emulsion.

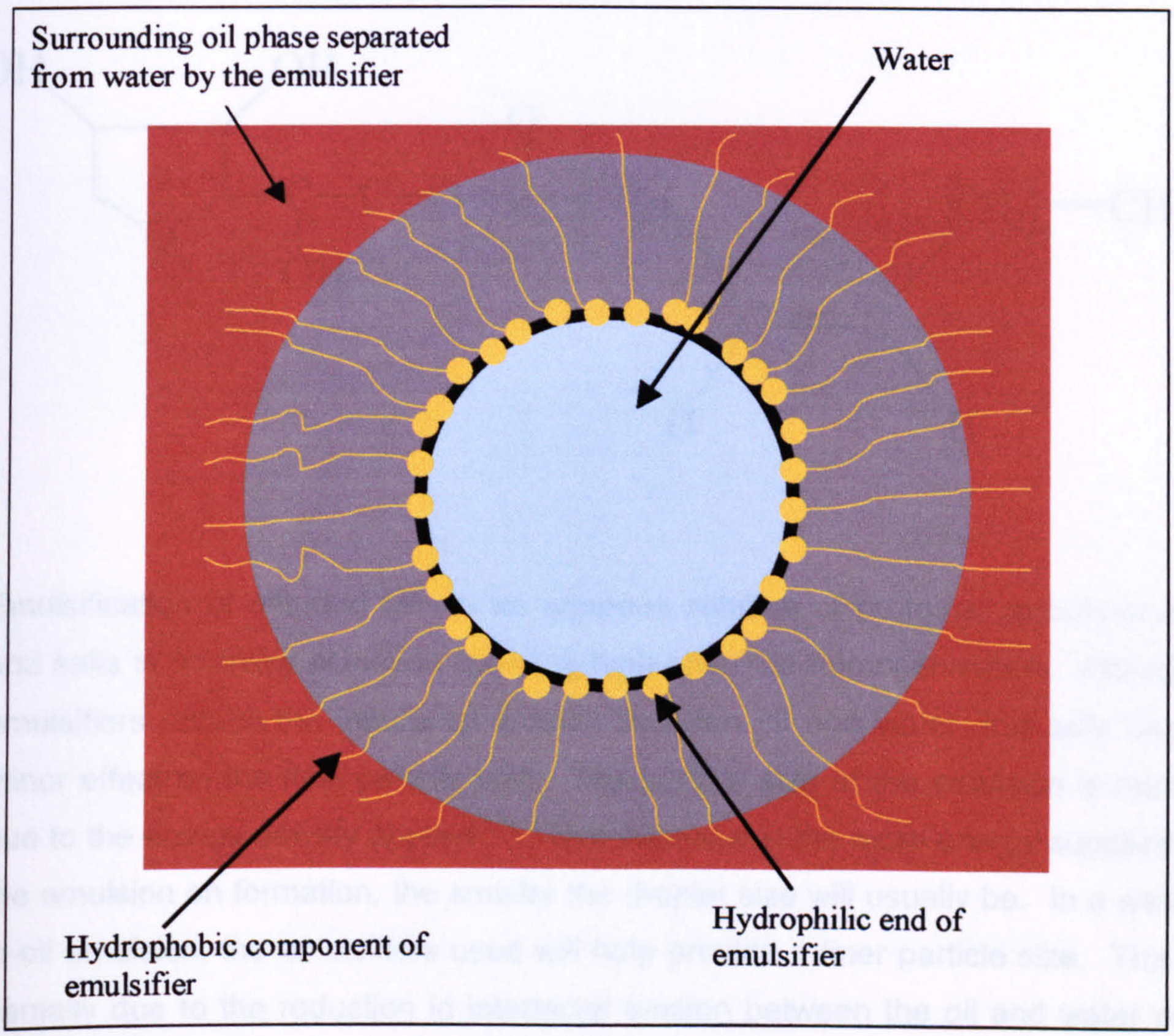

The choice of emulsifier depends on the type of emulsion required, oil-in-water or water-in oil, and on the solubility of the emulsifier in each phase. As a rough rule, the phase in which the surfactant is more soluble forms the continuous phase. The exact mechanism of emulsion formulation and emulsifier choice is as much an art as science, with trial and error along with previous experience often deciding the choice of emulsifier.

The most common emulsifier for emulsion explosives, and one of the emulsifiers used in this study, is sorbitan monooleate. Sorbitan monooleate has low water solubility and acts as a good solubiliser of water-in-oils. The structure of this is shown in Figure 10

Figure 10 Sorbitan monooleate molecule.

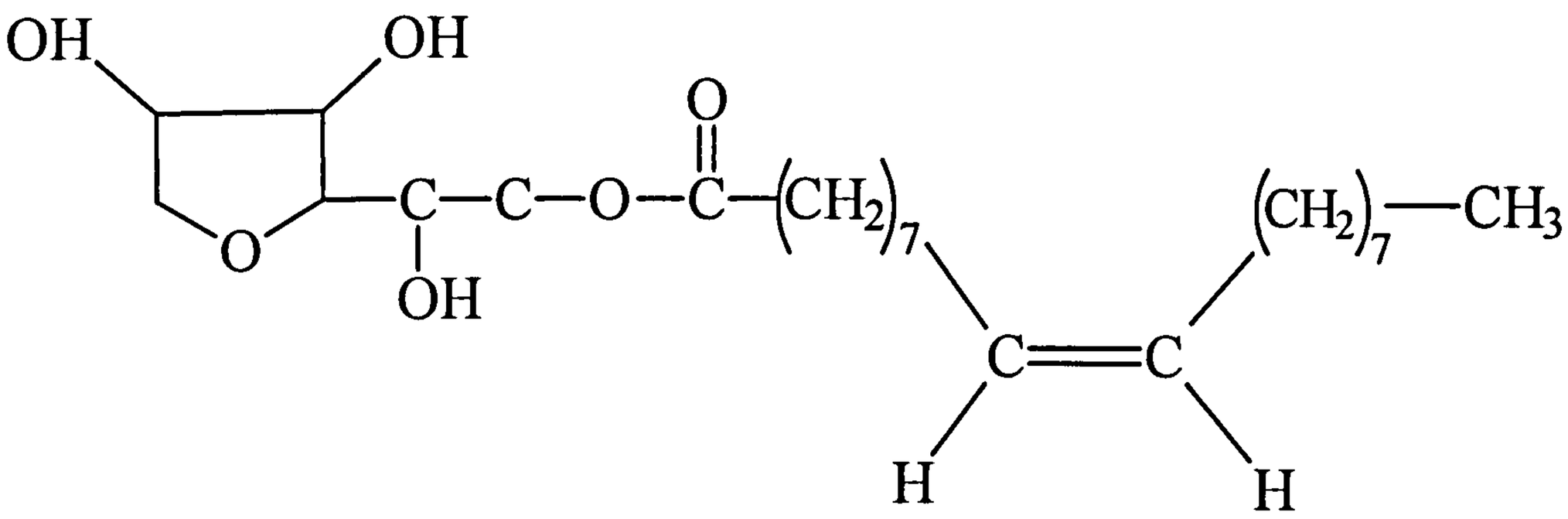

Emulsification of oils and fats in an aqueous solution of proteins, carbohydrates and salts is normally achieved by using high-pressure homogenisation. Although emulsifiers reduce the interfacial tension between oil and water, this only has a minor effect on the final particle size. The particle size of the emulsion is mainly due to the energy density applied[57]. This means that the more energy supplied to the emulsion on formation, the smaller the droplet size will usually be. In a water-in-oil emulsion, the emulsifiers used will help provide a finer particle size. This is partially due to the reduction in interfacial tension between the oil and water and due to a reduction in the rate of re-coalescence of water droplets before the fat phase crystallises.

1.6.3 Break down of emulsions

Emulsions are thermodynamically unstable, and their relative stability is affected by factors such as flocculation and aggregation. Lowering the interfacial tension, with emulsifiers, allows the emulsion to form, if the interfacial tension then increases, the emulsion will begin to breakdown. An emulsion can breakdown in one of four different modes of failure, as shown in Figure 11.

Figure 11 Processes of emulsion breakdown.

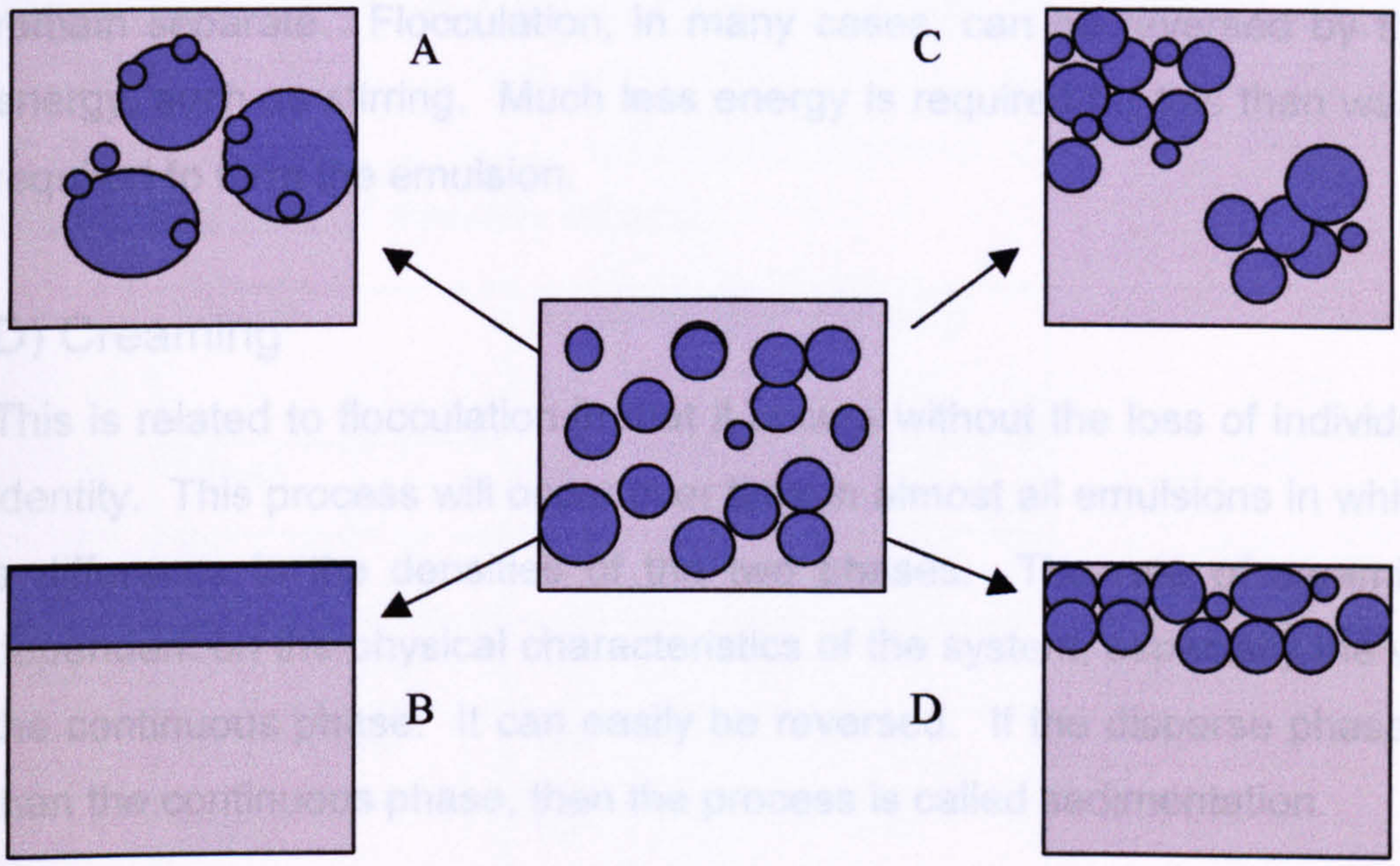

A) Coalescence B) Breaking C) Flocculation D) Creaming

A) Coalescence

This is the joining of two (or more) drops to form a single drop of greater volume, but smaller interfacial area. Such a process is energetically favourable in all cases in which there exists a positive (even if small) interfacial tension. Although coalescence results in significant microscopic changes in the condition of the dispersed phase (size and distribution) it may not immediately result in macroscopic change.

B) Breaking

This refers to the process of gross separation of the two phases. The process is the macroscopically apparent consequence of the microscopic process of coalescence.

C) Flocculation

This is the process where individual droplets in the emulsion congregate to form flocs or loose assemblies of particles in which the identity of each droplet is maintained. This condition is clearly different from coalescence, as the droplets remain separate. Flocculation, in many cases, can be reversed by the input of energy, such as stirring. Much less energy is required for this than was originally required to form the emulsion.

D) Creaming

This is related to flocculation in that it occurs without the loss of individual droplet identity. This process will occur over time in almost all emulsions in which there is a difference in the densities of the two phases. The rate of creaming will be dependent on the physical characteristics of the system, especially the viscosity of the continuous phase. It can easily be reversed. If the disperse phase is denser than the continuous phase, then the process is called sedimentation.

1.7 Emulsion Rheology

1.7.1 Viscosity

Viscosity is a measurement of the flow properties of a product. It is the ratio of shear force applied and the amount of resulting deformation. The deformation of the fluid is expressed as the rate of shear. Therefore, viscosity is the relationship between shearing stress and the rate of shear. The concept of viscosity came about with Newton's postulate (1690's) that; Shear stress σ is related to the velocity gradient or shear rate $\dot{y}$ through the equation;

Equation 11 Shear stress.

$$\sigma = \eta \dot{y}$$

Where η is the shear viscosity.

In the simplest cases, like water or aqueous solutions, the shearing stress is directly proportional to the rate of shear. The proportionality constant is called the viscosity coefficient. Fluids where the proportion is direct are called Newtonian fluids. For Newtonian fluids η is independent of $\dot{\gamma}$ and therefore does not change with respect to $\dot{\gamma}$. For Newtonian fluids η is usually called the viscosity.

Table 2 Example of viscosity values.

Liquid	Approximate Viscosity (P)
Glass	10^{40}
Bitumen	10^{8}
Liquid Honey	10^{1}
Bicycle Oil	10^{-2}
Water	10^{-3}
Air	10^{-5}

There are many types of non-Newtonian fluids, each having distinct properties. Measurement of these viscosities is more involved, requiring the additional function of time. The viscosity behaviour, when the stress is applied over time, determines the type of a non-Newtonian fluid. With emulsions it is usual for the apparent viscosity to lower with increasing shear.

1.7.2 Particle size analysis

An important parameter for emulsions is the droplet size, with this possibly having the greatest effect on the rheological and physical properties of the emulsion. There are a number of ways to determine particle size, although particle sizing of emulsions is not an exact science, errors compound every process but these can often be minimised by careful selection of methods and the use of good practice to minimise error.

The most common method, of particle size analysis involves the use of microscopy. Samples of emulsion are placed on a microscope slide and a digital picture taken. This is converted by computer manipulation to a black and white image, which allows the size of each droplet to be interpolated. A histogram report of droplet size and number of drops is then obtained from this. The larger the sample group size, the greater the accuracy of this method.

An alternative technique for particle size characterisation is hydrodynamic chromatography. Hydrodynamic chromatography has emerged, in the last 20 years, as a method of choice for particle size analysis. Samples are isolated in a solvent and by passing them through a column packed with tiny, porous beads separation occurs. The carrier liquid used is inert to the particles and the beads are packed in long columns, usually with no immobilised coating. Separation depends on the hydrodynamic flow of the fluid flowing in the Poiseuille regime. This means that large particles move quickly with the inert flow and smaller particles move at a slower speed. The turbulence generated around the beads causes the smaller particles to take a longer path and therefore pass more slowly through the column. Mixed particle sizes introduced at the head of the column are separated according to size. The large particles emerge first, followed in order by smaller and smaller particles.

1.8 Background to Emulsions Explosives

Emulsion explosives consist of three basic ingredients, an aqueous phase, an oil phase and a surfactant. The aqueous phase, which makes up 85% or more of the formulation, usually, consists of a supersaturated aqueous solution of ammonium nitrate (AN). Other oxidisers such as sodium and calcium nitrate are sometimes added as an alternative to AN. The salts are dissolved in hot water (~90°C), as the solubility of these salts greatly increases with temperature. These solutions often have a crystallisation point around 70°C and have to be mixed above this temperature. This solution is added to a heated oil phase and mixed. Once properly formulated, the emulsion can be stable down to temperatures as low as minus 20°C, although at low temperatures crystallisation is encouraged, so prolonged storage at low temperature leads to emulsion failure.

The oil phase plays a critical role in the stability of the emulsion system, as well as providing the fuel for the ammonium nitrate oxidiser. Oils such as refined paraffin or microcrystalline waxes are often used. A variety of chemicals has been investigated, but paraffin is by far the most commonly used oil.

Surfactants help to form and stabilise, the high internal phase water-in-oil emulsion, at processing temperatures. Once the emulsion has formed, it is allowed to cool to ambient temperature. This means that the water solution becomes supersaturated, so the emulsifier has to be capable of limiting nucleation of the nitrate salts. The surfactants surround each of the water droplets with the hydrophilic layer limiting the nucleation of the nitrate salt. A basic emulsion explosive composition, as used in commercial applications, is shown in Table 3. This contains about 13 times as much ammonium nitrate by mass, or about 10 times as much AN solution by volume, as oil.

Table 3 Emulsion formulation.

Component	% by weight
Water	15
Oil	6
Nitrate salts	78
Surfactant	1

The reaction between ammonium nitrate and fuel oil is relatively simple, with water, carbon dioxide and nitrogen gas formed as reaction products.

Equation 12 Stoichiometry of the reaction between AN and oil.

$$3NH_4NO_3 + \frac{1}{n}C_nH_{2n} \Rightarrow CO_2 + 7H_2O + 3N_2$$

The reaction is an idealized one involving ammonium nitrate and oil, which assumes the complete reaction of the ammonium nitrate with the hydrocarbon.

1.8.1 Development and use of Emulsion explosives

Emulsions explosives were first formulated in the early sixties. Egly disclosed, in a US patent in 1964[58], a water-in-oil emulsion that was explosive. This was based on a concentrated solution of a metal nitrate in paraffin oil. Atlas powder applied for a whole series of patents covering the use of nitric acid in an oil phase[59]. Their emulsion was based upon a solution of 30 to 80% aqueous nitric acid mixed with ammonium nitrate and a carbonaceous fuel, such as diesel oil. This formed a dispersion that was stable for at least eight months. These early emulsions gave VOD figures, using the Dautriche method, of 1700ms^{-1} to 4500ms^{-1}. The patent stated that these figures were obtained from firings with a 3" (76mm) diameter and 10" (254mm) long cylinder. The emulsion was primed with ¾lb (340g) of composition B. Using the Dautriche[60] method of VOD determination, with the

size of priming used, there is some ambiguity over the velocity of detonation data obtained.

In the results reported by Egly, the first blasting cap (for the Dautriche VOD measurement) was well within three charge diameters of the initiation point. The detonation wave from the composition B primer would not have had time to fade, thereby producing erroneously high VOD values. This could be a reason for the lack of further work on nitric acid emulsions, notwithstanding the extremely corrosive nature of the emulsion, which made storage and use of the explosive difficult. There was also the toxicity and safety aspect of using bulk quantities of an explosive containing up to 80% nitric acid.

Bluhm's patent[61] led to the development of the first commercially viable emulsion explosive. This was based upon a water-in-oil emulsion, made with a mixture of hot nitrate solution and hot oil. Micro-balloons (gas bubbles) were used to sensitise the emulsion and to lower the density. Other studies have since produced refinements to this initial system. The problem with the initial formulation was that it was not detonator sensitive and required extensive priming.

The next major advance was in 1977 when Wade[62] of Atlas powder patented an emulsion explosive system using a closed void material as a sensitising material. The preferred material was glass micro-balloons, which gave the emulsion greater sensitivity to initiation. Using the glass micro-balloons, the emulsion could be initiated with a standard detonator. The closed void material sensitises the emulsion by providing a source of hot spots. When the emulsion is shocked, the glass micro-balloons collapse and heat the immediate area around them via adiabatic compression.

Emulsion explosives are water-in-oil emulsions with the water forming the disperse phase. Emulsions offered an intrinsic advantage over more basic ammonium nitrate fuel oil (ANFO) explosives in that they are water resistant. The emulsion does not break down in water because of the impervious oil layer surrounding the disperse phase. ANFO is composed of ammonium nitrate prills and fuel oil and is extremely sensitive to water. A thin oil layer surrounds the prills but does not

completely cover them. This layer is easily washed away by water allowing the ammonium nitrate to be dissolved. This desensitises the explosive leading to detonation failure or possibly, more significantly, partial detonation. Emulsions with water resistance do not suffer from this problem. This is probably the single most important fact that has lead to the success of emulsion explosives[63].

Emulsions are widely used in tunnelling where a most important feature is the explosive's fume characteristics. In addition to the production of gases such as CO_2 and H_2O, some explosives produce nitrogen oxides and carbon monoxide. These gases are poisonous with low exposure limits and compositions that produce high concentrations of them are inappropriate for tunnelling. A high oxygen balance leads to the production of nitric oxide and nitrogen dioxide in the explosion fumes, which are highly toxic. When the explosive is not oxygen balanced, it develops a lower heat of explosion. This is due to an incomplete reaction occurring and products being formed that result in a lower energy release, such as CO rather than CO_2.

Equation 13 Energy of CO and CO_2 formation.

$$C + O_2 \rightarrow CO_2 \qquad \text{Energy of Formation } -393.5 \text{ kJ/mol}$$

$$C + \tfrac{1}{2}O_2 \rightarrow CO \qquad \text{Energy of Formation } -110.5 \text{ kJ/mol}$$

For composite explosives, the intimacy of mixing of the ingredients influences the overall fume characteristic of the explosive. Oxygen balanced explosives with coarse ingredients produce higher quantities of noxious gases than products that are more intimately mixed. This is due to kinetics and homogeneity of the explosive. As the reacting material rapidly expands not all the reactions go to completion and explosives that are not resistant to water will, often, form large quantities of noxious gases when fired wet. Re-entry times to the tunnel face are critical to the overall rate of advance of a tunnel and emulsion products have shown up to a tenfold reduction in the quantity of nitrogen dioxide and a two fold reduction in the quantity of carbon monoxide produced when they have replaced nitroglycerine based explosives[64].

1.9 Ammonium Nitrate (AN)

In 1659 Glauber first synthesised AN by reacting nitric acid with ammonium carbonate. In the eighteenth century, it was considered to have medicinal value and by 1867, a patent was issued in Sweden to cover its use as an explosive additive. Following World War 1, when large stocks of AN were abundant, AN was first used as a fertiliser[65]. The main difference between fertiliser and explosive grade AN is that explosive grade AN has smaller sized prills and have larger pore spacing. This is because the major use of explosive grade AN is for ANFO explosives and the smaller prill gives a larger surface area, whilst the larger pore spacing allows more oil to enter the prill. The increased porosity of explosive grade AN is obtained by adding extra water to the AN liquor before the prilling process. The prill is dried out and as the water escapes away, void spaces are created. For this study, fertiliser grade prills were used, but since it was dissolved in water, there is no discernible difference between the two grades.

AN is used in massive quantities, with world usage of AN in 1985 being about 44 million metric tons[66]. About 75% of this is used for fertiliser production, with the majority of the remainder being used for explosives.

AN[67] is stable in different allotropic forms below its melting point of 442K. These phases are shown in Table 4, as reported by Ahtee[68] and Fedoroff[69]. The data shown is that obtained from moist AN, with a residual amount of water present in the AN before analysis.

Table 4 Ammonium nitrate phases.

Phase	Symmetry	Density (kg/dm^{-3})	Temperature Range (°C)
V	Tetragonal	1.710 at -25°C	-170.0 to –16.0
IV	Orthorhombic	1.725 at 25°C	-16.0 to 32.1
III	Orthorhombic	1.661 at 40°C	32.1 to 84.2
II	Tetragonal	1.666 at 93°C	84.2 to 125.2
I	Cubic	1.594 at 130°C	125.2 to 169.6
Melt			169.6

Dry AN has a different thermal profile to that of moist AN and this is shown in the Table 5, which gives the temperatures at which each phase change occurs[70].

Table 5 Phase change temperatures for dry AN compared to moist AN.

Phase	Moist transition temperature	Dry transition temperature
V-IV	-18	-18
IV-III	32	-
III-II	84	-
IV-II	-	50
II-I	125	124

The important phase changes, in the commercial use of AN, is the phase IV to III transition. This occurs at approximately 32°C in moist AN, whilst in dry AN the 32°C phase change does not occur. Instead there is a transition straight to phase II, which occurs at about 50°C, with the exact temperature dependent upon the water content. The phase change at 32°C is important, as this increases the volume of the AN by about 3.6%[71], which can have major implications in the use of AN.

1.10 Objective of the research project

The objectives of this research project were to characterise the behaviour and physical characteristics of emulsion explosives. Emulsion explosives, as a system, are used by the quarrying and mining industry, but as such, little core research, beyond that required for commercial use, has been carried out into their characteristics. This project set out to determine how the behaviour of the explosive varies with formulation. The parameters for this were closely controlled, with the water content and microballoon content of the emulsion being changed, whilst keeping a constant ratio between the oil and AN. This ratio was kept constant throughout all of the experimentation undertaken in this project. Other studies[84,85] have looked at varying the ratio between the oil phase and the AN, usually replacing a proportion of AN with sodium nitrate or aluminium.

The overall objective was to determine if increased explosive performance could be achieved by varying the water and microballoon content. If this varied the performance, then how this affected the physical properties of the emulsion, such as the thermal and viscosity properties, was to be investigated. If a positive link could be established between the physical properties and the explosive properties of the emulsion, then the mechanism for the explosive reaction could be further understood. The objective was, the development of emulsion explosives on a scientific basis, rather than on an empirical basis, as much of the data is at present.

2 Experimental

2.1 Material Sources

Ammonium nitrate was manufactured by ICI and was fertiliser grade 'Nitram', which had a 34.5% Nitrogen content and was supplied in 50kg bags. This was prilled AN, which had 0.1% of an anticaking agent, which limited water absorption.

Sorbitan mono-oleate was supplied by Sigma Aldrich (catalogue number 38,891-2) and came in 1L glass bottles.

Glass micro-balloons were supplied by 3M (B15/250) and came in a 25kg sealed box.

Oils as used to manufacture the emulsion, polyisobutylene succinic anhydride ethanolamine adduct in xylene and mineral oil, Eldex 13, were supplied by ICI Nobel Explosives.

All other materials, such as plastic tubing, wires and metal plates were locally sourced.

2.2 Emulsion Preparation

Aspects of emulsion explosives have been characterised[72,73,74,75,76,] with limited features having been investigated. However, only limited research has been undertaken on the effect that varying the water content has on explosive performance. Research has been undertaken to investigate the effect of adding different microballoon types and ratios to the emulsion[77], but only at a single fixed water content. By altering the water content the sensitivity, and the performance, of the emulsion explosive can be modified. The aim of this work was to characterise emulsion explosives systems and these were prepared in an adapted commercial food mixer, as shown in Figure 12.

The study initially investigated a single type of emulsion explosive. The microballoon and water content were varied, whilst keeping a constant fuel to oxidiser ratio. The water and microballoon content were altered, as these were considered the two most pertinent factors affecting performance. The fuel/oxidiser ratio was not altered, as this ratio (an approximate fuel/oxidiser ratio of 6.7/100) gives an oxygen-balanced explosive.

Figure 12 Mixing apparatus.

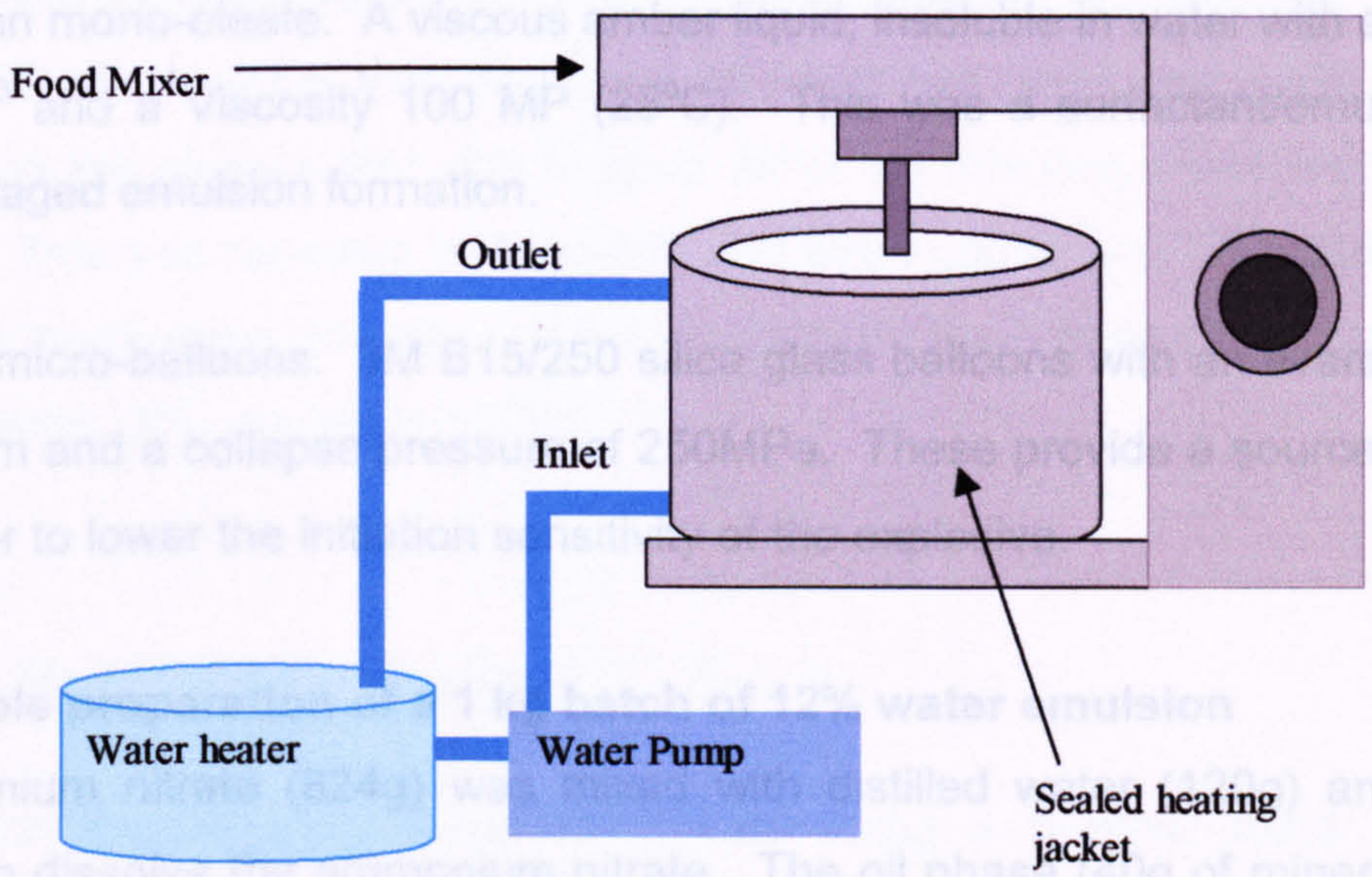

The compositions of the emulsions, as used in this study, are shown in Table 6.

Table 6 Composition of emulsion matrix.

Water	12% H_2O	15% H_2O	20% H_2O	25% H_2O	30% H_2O	35% H_2O
Ammonium nitrate	82.4%	79.6%	74.9%	70.3%	65.6%	60.9%
Oil	4.0%	3.8%	3.6%	3.4%	3.2%	2.9%
Polyisobutylene succinic anhydride ethanolamine (PIBSA)	1.3%	1.2%	1.1%	1.1%	1.0%	0.9%
Sorbitan mono-oleate	0.30%	0.30%	0.29%	0.27%	0.25%	0.23%

PolyIsoButylene Succinic Anhydride ethanolamine adduct in xylene (PIBSA). A mainly amide derivative of succinic anhydride, which is a dark brown viscous liquid with a density of 0.91-0.93 kg/dm^{-3}. PIBSA is a surfactant/emulsifier and was used to stabilise the emulsion system. This was a proprietary mixture supplied by ICI Explosives.

Mineral oil. Eldex 13, a light paraffin oil, which was the foundation fuel for the explosive.

Sorbitan mono-oleate. A viscous amber liquid, insoluble in water with a density of 1 kg/dm^{-3} and a Viscosity 100 MP (25°C). This was a surfactant/emulsifier, which encouraged emulsion formation.

Glass micro-balloons. 3M B15/250 silica glass balloons with an average diameter of 15μm and a collapse pressure of 250MPa. These provide a source of hot spots in order to lower the initiation sensitivity of the explosive.

Example preparation of a 1 kg batch of 12% water emulsion

Ammonium nitrate (824g) was mixed with distilled water (120g) and heated to 90°C to dissolve the ammonium nitrate. The oil phase (40g of mineral oil, 13g of PIBSA and 3g of sorbitan mono-oleate) was placed in an adapted Kenwood Chef Major food mixer, which was heated by water jacket to 90°C. The aqueous ammonium nitrate solution was slowly added to the hot oil phase, with slow stirring, until an emulsion just started to form. Once the emulsion had formed, the remaining aqueous ámmonium nitrate was then quickly added and the speed of the mixer increased to maximum. This was maintained for five minutes to ensure a homogeneous mixture. The hot emulsion was then transferred to a plastic bag (high temperature cooking bag), allowed to cool naturally to ambient and stored until required.

Micro-balloons (3M B15/250) were added to the emulsion at room temperature within 24h of using the explosive. They were combined with the emulsion by slowly adding the required weight fraction and mixing at a programmed mixing

speed for five minutes. The emulsion was then split into five 200g portions, with one portion being retained for later analysis.

2.3 Physical Characterisation

2.3.1 Emulsion densities

The densities of the emulsions were determined by weight measurements. Initially small containers were filled with water and weighed to determine their volume. Emulsions samples were then placed in the container and weighed to determine their densities. This was repeated, at least ten times, for each emulsion to eliminate the chance that any trapped air or an inhomogeneity would affect the result. This was repeated in three different sized containers. The containers used were a small glass container ~75µl, a standard aluminium DSC container ~50µl and a large DSC container ~100µl

2.3.2 Particle size analysis

Emulsion droplet sizes were determined using a Kontron IBAS 2000 image analyser, a dedicated particle size analyser. The emulsion sample was placed on a microscope slide covered and placed under a light microscope. The microscope was then manually focused and the resulting image was converted into a digital image. A computer then measured the number and size of each of the droplets. The instrument was capable of measuring droplet sizes from 1µm to 40µm and a printout was produced from this giving a histogram analysis of the sample, which showed droplet size as a percentage of the total number of droplets.

2.4 Thermal Analysis

Thermal analysis includes a group of techniques in which the specific physical properties of a material are measured as a function of temperature. In differential thermal analysis, DTA, a sample is heated, usually in an inert atmosphere, and a plot of temperature of sample versus reference material is made. In differential scanning calorimetry, DSC, heat is electrically added to or removed from a sample as the temperature is increased. This allows enthalpy changes, due to phase changes and thermal decomposition, to be studied. The thermal properties of a substance are important in determining its behavioural characteristics. DSC was used in order to determine the level of crystallinity in emulsion samples. The re-dissolution of ammonium nitrate crystals into the emulsion matrix should produce an endotherm. Thermal conductivity has been determined as an important parameter[78] for explosive materials as evidenced by the Frank-Kamenetskii equation, where the rate of heat loss is dependent on thermal conductivity. Thermal conductivity is not easily measured using DSC or DTA, so a method for examining relative thermal conductivities was developed.

2.4.1 Differential scanning calorimetry (DSC)

DSC and DTA measure the rate and degree of heat change as a function of time and temperature[79]. In addition to direct energy measurements, the precise temperature of the sample material, at any point during the experiment, is also monitored. As DSC can measure both the temperature and heat of transition or reaction, it has replaced DTA as the main thermal analysis technique, except in certain high-temperature applications.

The DSC instrument, a Mettler TA4000 control unit fitted to a Mettler DSC 30 head with a CDL50 liquid nitrogen attachment, was capable of cooling samples to –170°C and heating to 600°C. Sample size was usually 5 to 10mg but the head could also accommodate larger containers, which can take up to 100mg of

sample. Samples were contained in sealed aluminium cups. After the cups have been sealed, they are gas tight. Initially the containers were pierced in order to stop a build up of gas pressure. However, since this could cause an event that would damage the sensor, it eventually became apparent that a sealed system could be used. The advantage of using a sealed system is that any gas created by the heating of the sample could be later analysed. The essential components of this are shown in Figure 13. Heat is supplied to the sample and the reference, allowing the enthalpy changes due to phase changes to be studied.

Figure 13 DSC Schematic.

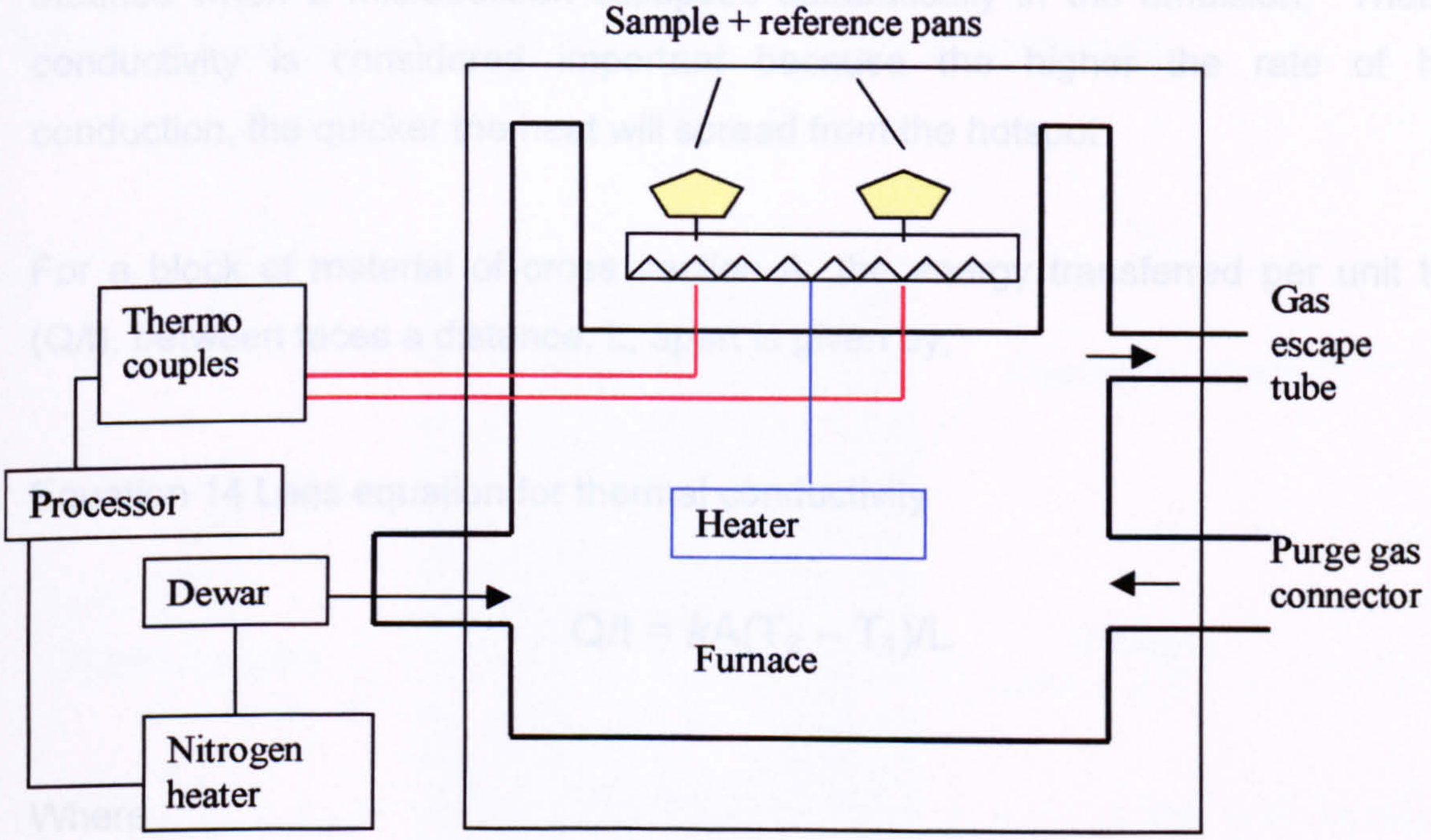

A DSC trace highlights phase changes, which take place within a sample, these increase or decrease the temperature of the sample in comparison to a reference and this difference is measured. It is a quantitative technique with the area enclosed by the curve of signal against time being directly proportional to the energy change.

In power compensated DSC[80], the sample and a reference material are maintained at the same temperature ($T_\delta = T_s - T_r = 0$) throughout the controlled temperature program. Any energy differences, in the independent energy supplies to the sample and reference, are then recorded against the program temperatures

2.4.2 Thermal Conductivity

Thermal conductivity is a measure of the ability of a substance to conduct heat. This was measured to determine the rate of heat transfer through the emulsion with respect to time. This allows a determination of the maximum temperature attained when a microballoon collapses adiabatically in the emulsion. Thermal conductivity is considered important because the higher the rate of heat conduction, the quicker the heat will spread from the hotspot

For a block of material of cross section A, the energy transferred per unit time (Q/t), between faces a distance, L, apart is given by;

Equation 14 Lees equation for thermal conductivity

$$Q/t = kA(T_2 - T_1)/L$$

Where

k is the conductivity,

T_2, and T_1 are the temperatures of the faces.

This equation assumes that the opposite faces are parallel and that there is no heat loss through the sides of the block. The SI unit for thermal conductivity is $Wm^{-1}K^{-1}$.

Thermal conductivity was measured using a self-designed Lees apparatus[81]. The sample was sandwiched between two aluminium blocks as shown Figure 14. This widely used apparatus was designed by Lees for measuring the thermal

conductivity of bad conductors that can be made in the form of a slab. To make the heat flow measurable, the area A is made large and the temperature gradient is made high.

The aluminium block was heated from above by a metal beaker of boiling water. This provided a constant heat conduction source that limited the affect of convection and radiation, allowing them to be neglected. Samples were placed in the centre of the blocks with an insulator surrounding it; this was used to stop the emulsion escaping. The temperature at the top and bottom of the two aluminium tubes, along with room temperature, was continuously recorded until a steady state was achieved.

Figure 14 Lee's apparatus for thermal conductivity measurement.

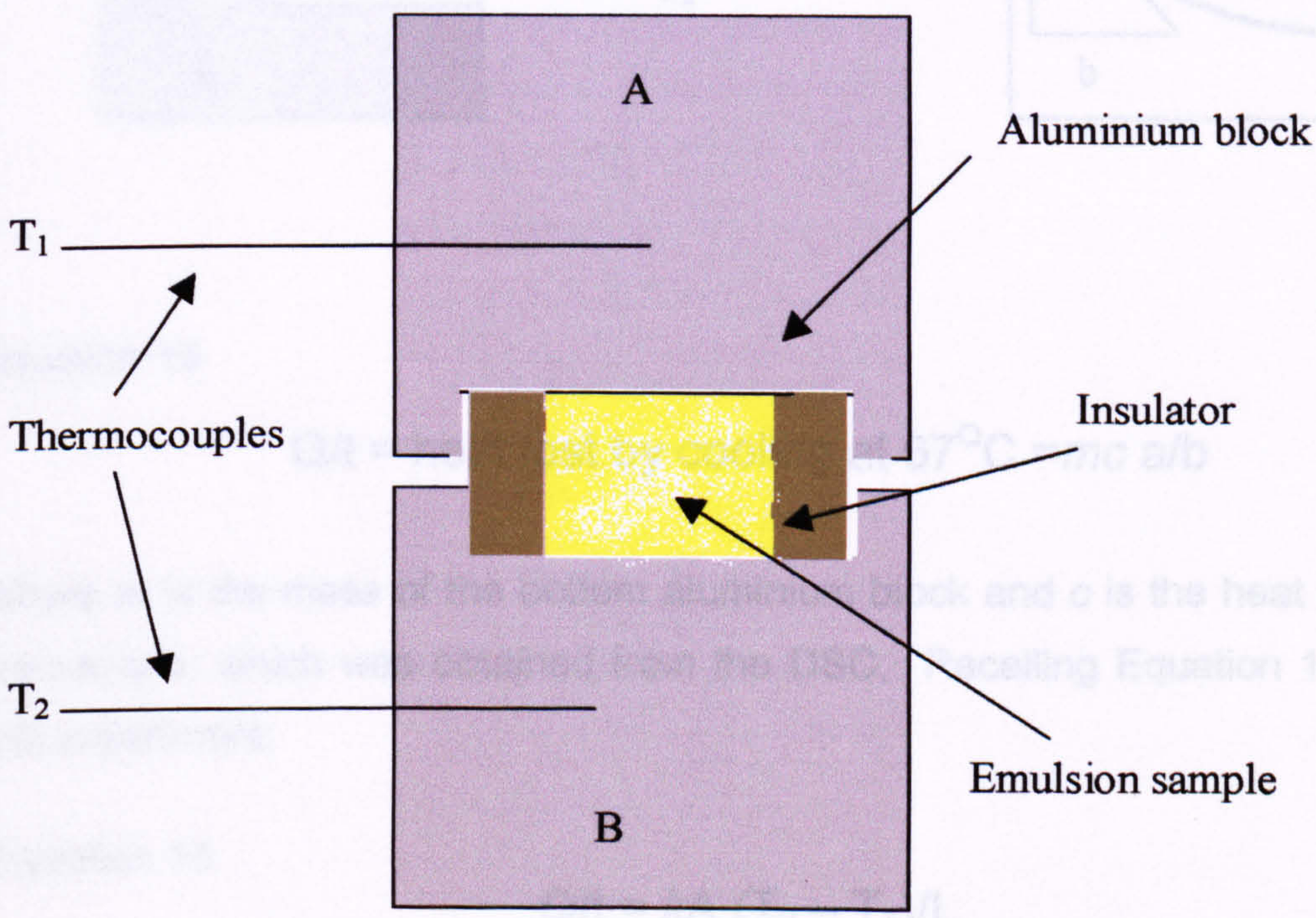

If, for example, T_2= 67°C the heat per second (Q/t) flowing through the sample in the steady state is equal to the heat per second lost by B due to radiation and convection at 67°C.

A second experiment was necessary to find the rate of loss of heat by B, see Figure 15. The top block and heater were removed and with the sample still in place, B was heated to a few degrees above its steady state temperature. The heating was removed and the sample allowed to cool, and readings of its temperature fall with respect to time were taken. From the temperature time graph, the tangent at its steady temperature was taken to give the slope of the line. This allowed the thermal conductivity of the sample to be determined using Equation 15.

Figure 15 Cooling Experiment

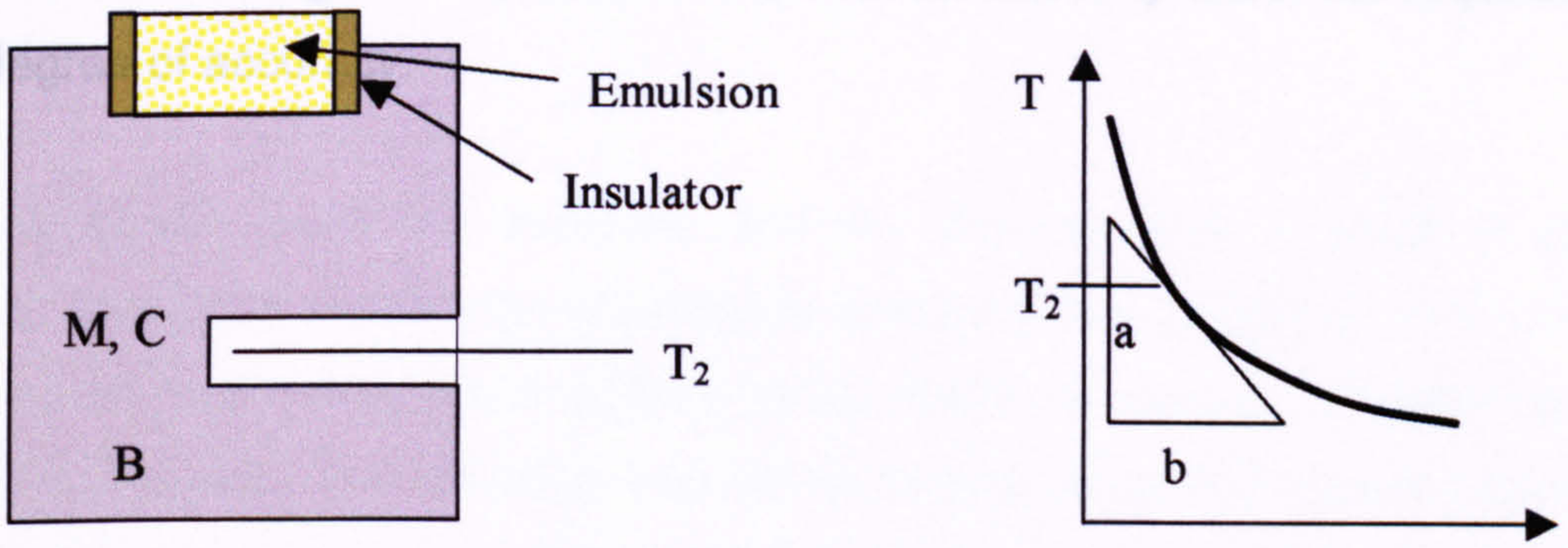

Equation 15

$$Q/t = \text{heat lost by cooling at } 67^{\circ}C = mc\ a/b$$

Where *m* is the mass of the bottom aluminium block and *c* is the heat capacity of the sample, which was obtained from the DSC. Recalling Equation 14 from the first experiment:

Equation 14

$$Q/t = kA\ (T_2 - T_1)/L$$

Where *A* is the area and *L* is the thickness of the sample. This allows *k*, the thermal conductivity to be calculated.

This method gave the thermal conductivity values for emulsions on a comparative basis. The method was validated using a thermal paste of known conductivity. The value obtained from this paste was used as a reference value. It is known that the method is not rigorous, but it did give comparative thermal conductivity data for the emulsions. This allowed the different emulsions to be ranked according to their relative thermal conductivity.

There are several methods, which could be used to obtain more rigorous thermal conductivity values but these all require high value instrumentation. The reasons for not applying them in the present study were both fiscal and time limitations. It was also felt that rigorous results for thermal conductivity were not required to a high degree of accuracy.

2.4.3 Viscosity

Viscosity is an important physical parameter for characterising emulsion behaviour. It was measured using a Viscometers UK Ltd Viscolog MRV-8 instrument. The Viscolog operates on the principle of a rotating cylinder or disc immersed in the material being tested, and measures the torque necessary to overcome the viscous resistance to rotation. The rotating disc (spindle) is coupled via a spring to a drive shaft, which is turned at a known speed. The angle through which the spindle is deflected is measured electronically, giving a measurement of torque. Calculations performed within the Viscolog from the torque measurement, the spindle speed and the spindle characteristics give a direct readout of apparent viscosity.

Various spindle sizes are available and the Viscolog has a range of spindle speeds, giving it a wide range of viscosity measurement capability. For a fluid of given viscosity, the drag will be greater as the rotational speed of the spindle, or its size, is increased. The Viscolog was set up to take account of speed setting and spindle size to give readings in P. Measurements can be made using the same spindle at different speeds, to determine the rheological properties of a material at different shear rates. Figure 16 Schematic of Viscolog MRV-8 shows the Viscolog. Samples, for analysis, were placed in 500ml plastic, wide-mouth bottles with a minimum of 300g of emulsion placed in each bottle. The spindle was inserted up to the immersion point, and the speed varied from 0.5 to 100rpm.

Table 7 shows the full-scale readings for the spindle, an R7, used. The maximum sensitivity of the instrument is 0.1% of full-scale deflection, which means that at 1 rpm the maximum sensitivity was 4P.

Table 7 Spindle speed to maximum viscosity reading for an R7 spindle

Spindle speed/rpm	100	50	20	10	5	2.5	1.0	0.5
Viscosity/P	40	80	200	400	800	1,600	4,000	8,000

Figure 16 Schematic of Viscolog MRV-8.

1 INPUT/OUTPUT SOCKETS
2 IMMERSION POINT
3 SPINDLE
4 SPINDLE NUT
5 SHAFT
6 SPEED CONTROL
7 MEASURING HEAD
8 BUBBLE LEVEL
9 SUPPORT
10 HEAD CLAMP
11 POWER SWITCH
12 FUNCTION SWITCH
13 SPINDLE SWITCH
14 SG CONTROL
15 LIQUID CRYSTAL DISPLAY
16 LEVELLING FEET

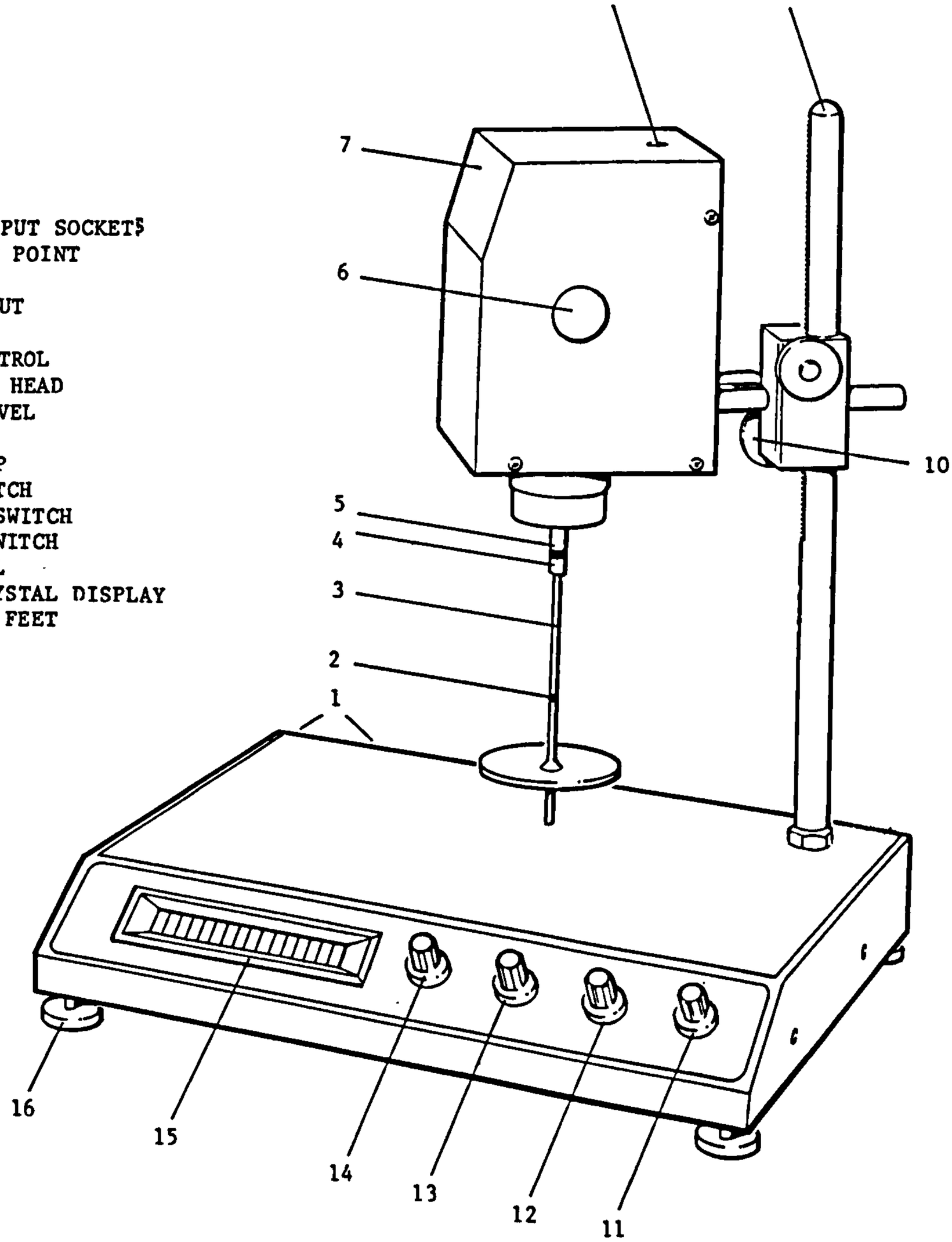

Figure 16 Schematic of Viscolog MRV-8.

1 INPUT/OUTPUT SOCKETS
2 IMMERSION POINT
3 SPINDLE
4 SPINDLE NUT
5 SHAFT
6 SPEED CONTROL
7 MEASURING HEAD
8 BUBBLE LEVEL
9 SUPPORT
10 HEAD CLAMP
11 POWER SWITCH
12 FUNCTION SWITCH
13 SPINDLE SWITCH
14 SG CONTROL
15 LIQUID CRYSTAL DISPLAY
16 LEVELLING FEET

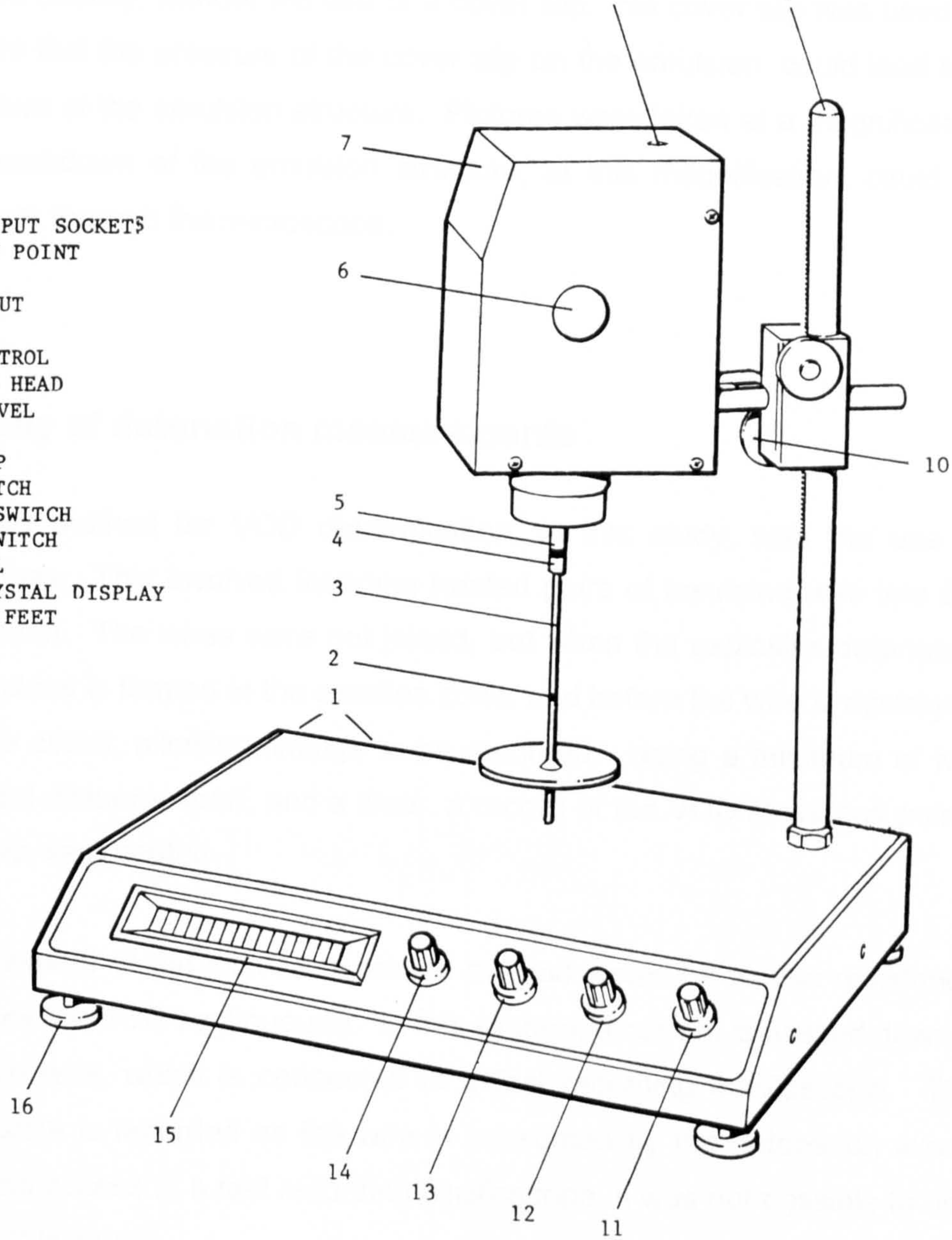

2.4.4 Emulsion breakdown

Emulsion breakdown was determined by examining the emulsion with a light microscope. A standard microscope with a camera attachment was used for this purpose. This was connected to a Polaroid printer, which produced photographic images from the eyepiece perspective. Emulsions were placed on a glass slide and examined directly, without the use of a cover slip. No cover slip was used as it was thought that the pressure of the cover slip on the emulsion, could lead to a distorted picture of the emulsion structure. Pictures were taken at a magnification of 1550. Breakdown of the emulsion structure, at this magnification, could be observed easily through the microscope.

2.4.5 Velocity of detonation measurements

The only used method for VOD determination, in this study, was the use of ionisation probes. This involved inserting twisted pairs of insulated wire into the explosive column. The wires were not joined, but when the explosive detonates, an ionisation cloud is formed in the reaction zone, and before the wire is destroyed this shorts the circuit, allowing timings to be recorded. Using a minimum of two probes, at a set distance apart, and a timer, a record of the VOD at various points in the explosive was created.

A further refinement of the ionisation probes method would be to use resistance wire to measure the VOD continuously. In this system, a current is passed down a high resistance wire, which is connected to a fast recording oscilloscope. The drop in resistance is recorded as the wire is consumed by the detonation wave. As there was no access to a fast recording oscilloscope, it was not possible to use this method in this study

Firings were carried out on the Explosive Ordnance Range. Cylindrical polypropylene pipes (39mm diameter) were cut to the required length and small holes, for the ionisation probes, were cut into the pipe exactly 100mm apart. Each

cylinder was sealed, with bathroom sealant, onto to steel witness plate and filled with 200g of emulsion. The density of the emulsion varied from 0.8 to 1.2 kg/dm^{-3}. Due to the variations in density, the length of the pipe varied from 180 to 280mm. The explosive was initiated by detonator, usually an 8*, and if priming was required Demex 200 sheet explosive was used. On one set of firings number 8 detonators were used due to a misunderstanding (8 contains 0.69g of PETN base charge whilst 8* contains 0.85g of PETN). Ionisation probes (polyurethane coated wires) were inserted through the pre-cut holes in the wall of the cylinder to determine the velocity of detonation of the emulsion (Figure 17).

Figure 17 Measurement of VOD with ionisation probes.

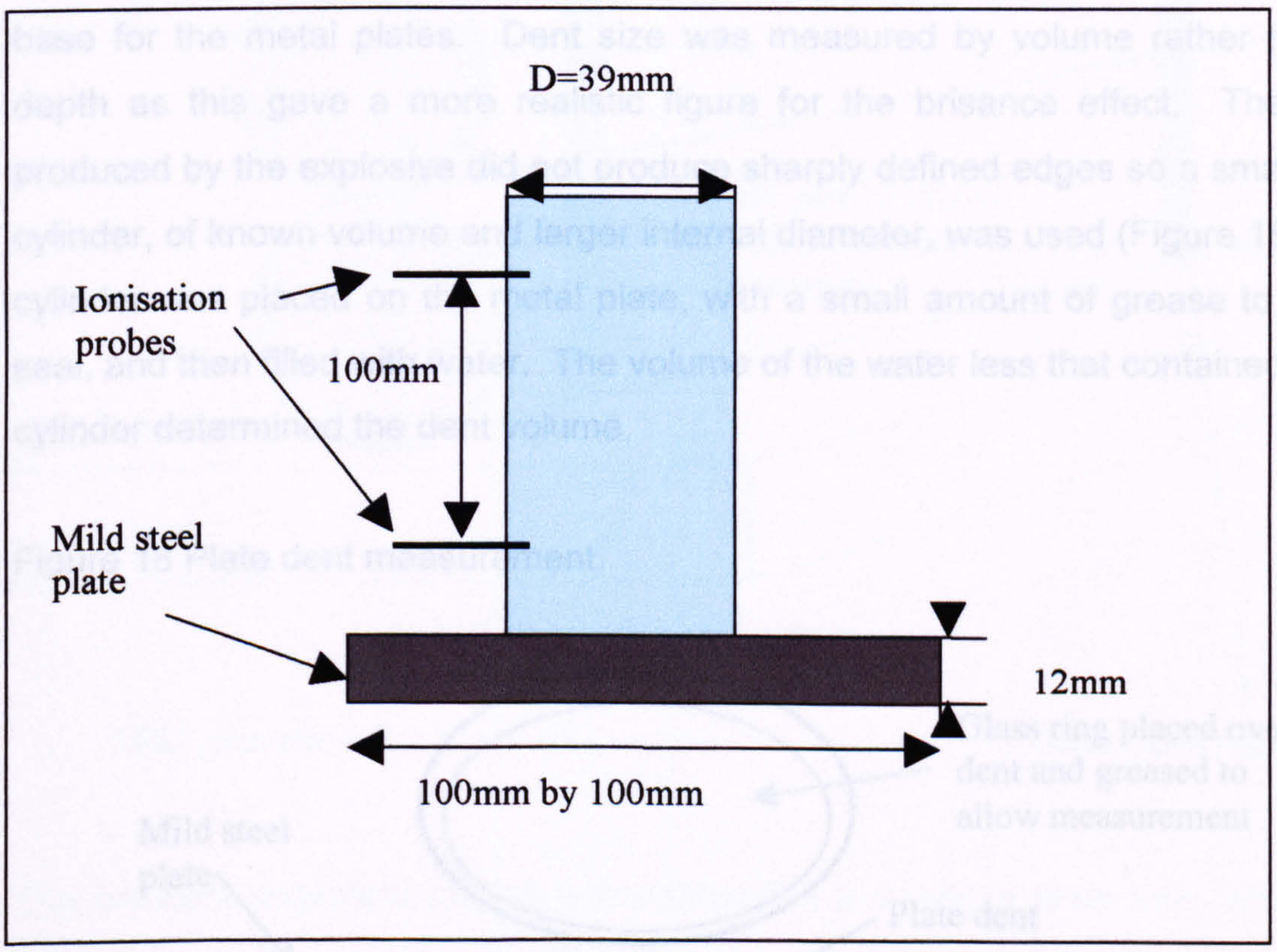

Ionisation probes were connected by wire to an electronic interface unit, which operated an electronic timer (Gould Advance Timer Counter TC314). The shock wave on reaching the wires causes a current to pass starting the timer. When the shock wave reaches the second probe the timer stops. The velocity of detonation is determined by the time taken for the shock front to travel between the probes. Velocity of detonation data was recorded for each emulsion type. Each emulsion

type was tested at least 4 times, with many undergoing 8 firings, to allow for statistical variation and eliminate anomalous results. Results of particular interest, such as 25% water content emulsion at 3% microballoon content, had up to 32 individual firings.

2.4.6 Plate dent measurement

The plate dent test was used as a technique to determine the brisance of the explosive[82]. The charge was placed on a mild steel plate (100mm x 100mm x 12mm) and the dent size, after the event, was measured. The charge and plate were placed on a steel anvil, ~150mm by 150mm by 500mm, to provide an infinite slab below the plate. Although the slab is in no way infinite, it did give a consistent base for the metal plates. Dent size was measured by volume rather than by depth as this gave a more realistic figure for the brisance effect. The dents produced by the explosive did not produce sharply defined edges so a small glass cylinder, of known volume and larger internal diameter, was used (Figure 18). The cylinder was placed on the metal plate, with a small amount of grease to form a seal, and then filled with water. The volume of the water less that contained by the cylinder determined the dent volume.

Figure 18 Plate dent measurement.

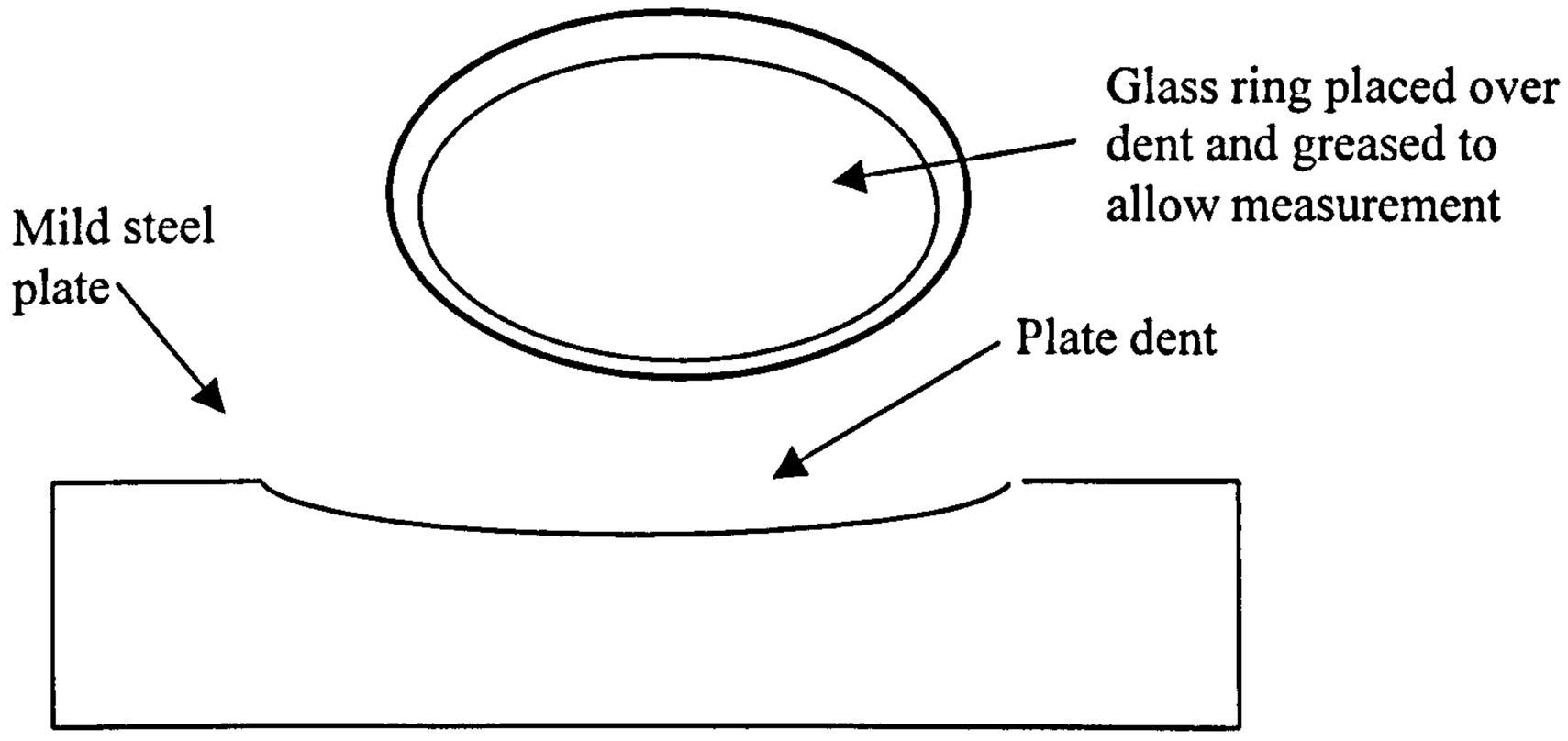

2.4.7 Double Pipe Test

The double pipe test was used as a method to determine the brisance of the explosive and the degree of reaction, as the detonation proceeds through the explosive column[83] as shown in Figure 19.

Figure 19 Double Pipe Test.

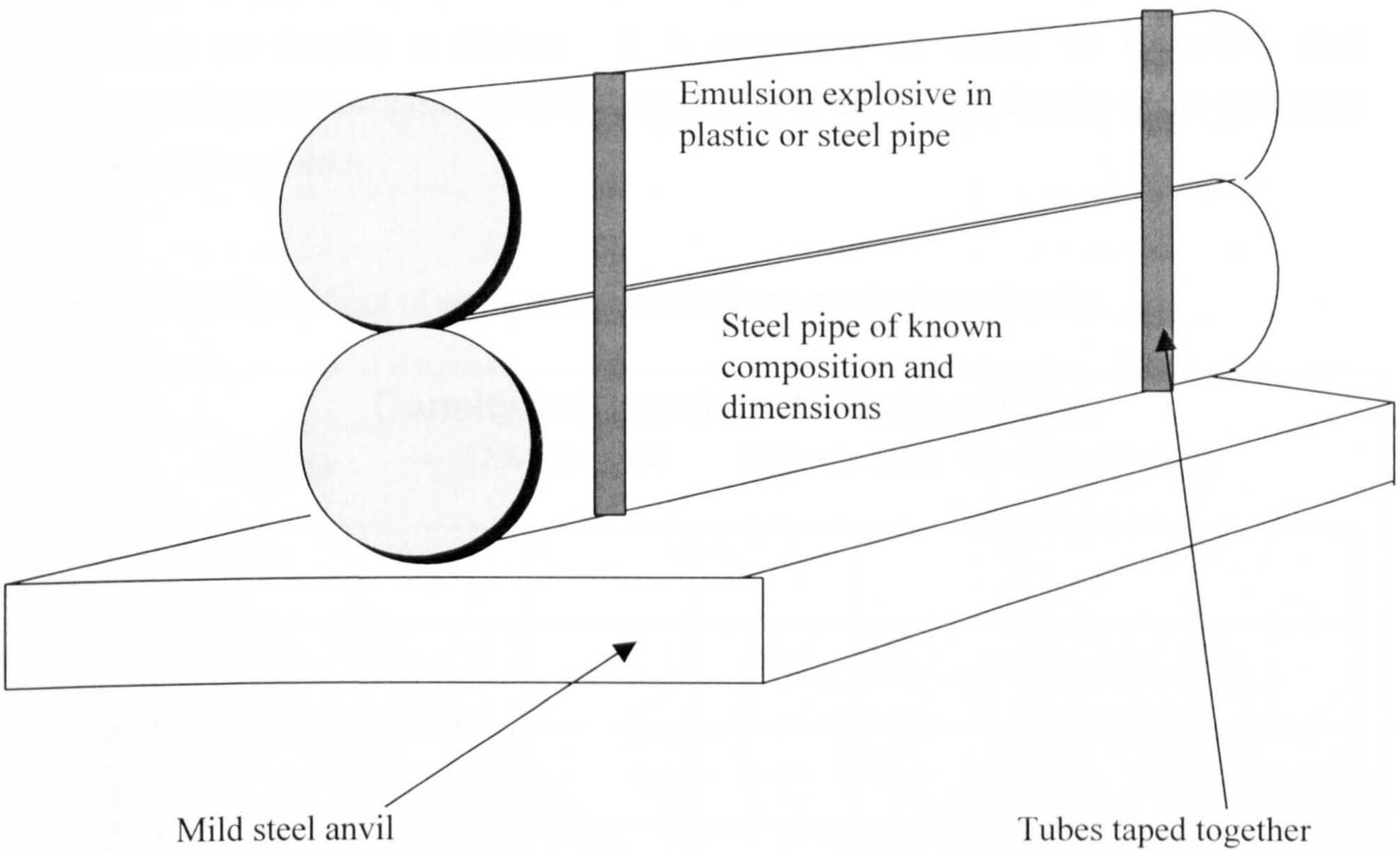

The emulsion explosive charge was confined in a plastic or steel tube, which was taped to a hollow mild steel pipe of known dimensions and composition. The assembly was then placed on a steel anvil and the charge detonated. The test can be used to determine the sensitivity, the output and a figure for the brisance of the explosive. Pivotal to the procedure is that it places an emphasis on monitoring the performance of the emulsion explosive under conditions which match, as closely as possible, those under which the explosive is used for rock blasting. The tests allow parameters to be altered, such as pipe size and wall thickness, to simulate differing conditions in boreholes.

3 Results and Discussion

3.1 Emulsion densities

The effect of water and microballoon content on the density and the explosive properties, of the emulsion, was examined. The error in the density measurement was minimised by repeating the experiment, until at least eight consistent results were obtained. The density of the emulsion matrix is controlled, in part, by the water and microballoon content. Changing either of these variables affects the density of the emulsion. In Figure 20, the effect of water and microballoon content on density is shown. It is apparent, as would be expected, that microballoon content had a more pronounced effect on the density of the emulsion than water content.

Figure 20 The effect of water and microballoon content on density.

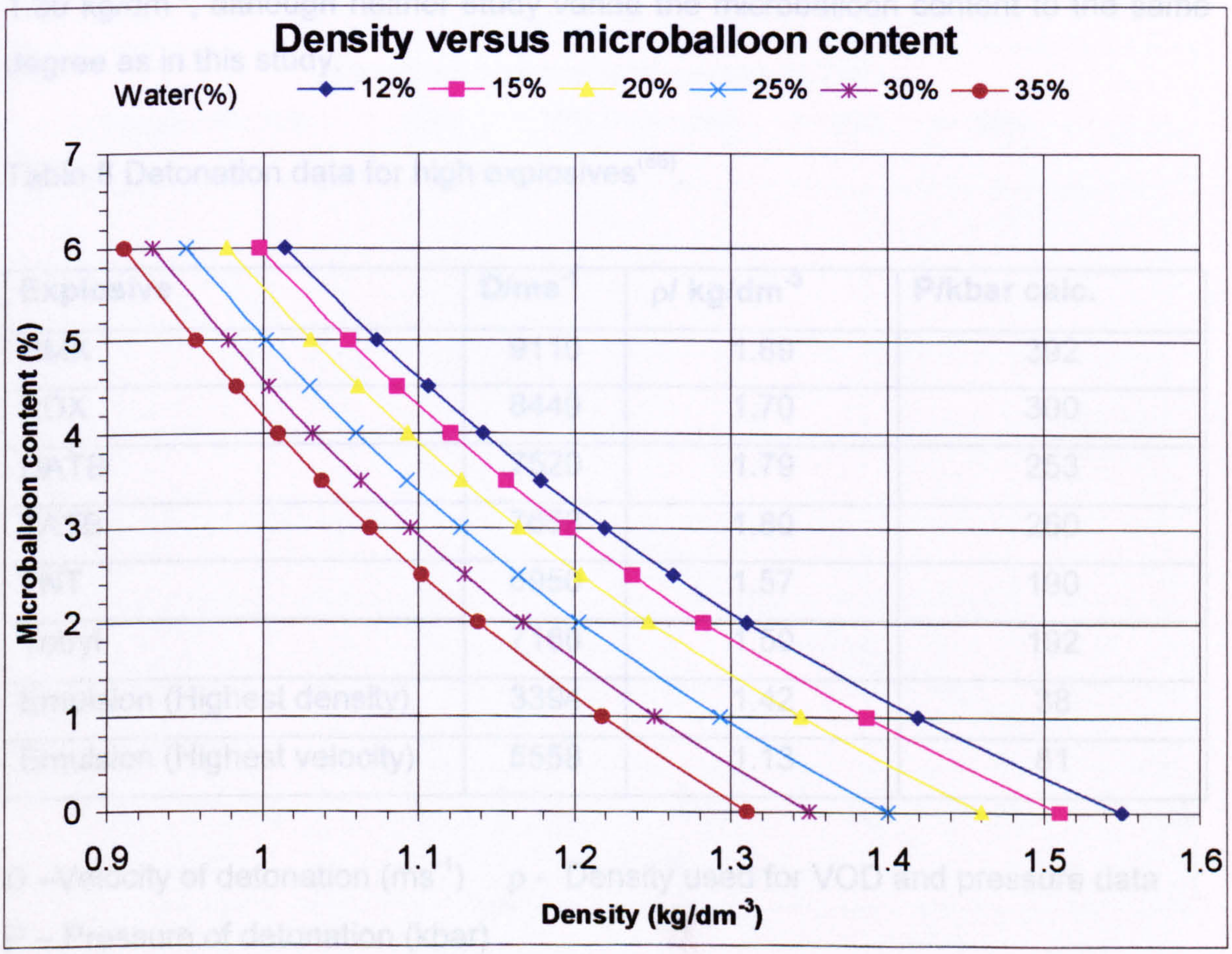

The average density of the microballoons used in this study was 0.15 kg/dm^{-3} and, therefore, even a small percentage increase in microballoon content significantly alters the density of the emulsion. Water, having a much higher density (~1 kg/dm^{-3}), has a less pronounced effect on density. Variation of the microballoon content allows the direct comparison of density for differing water contents. The microballoons are made of silica glass, with a sulphur dioxide and molecular oxygen filling (0.2 bar). Microballoons provide hotspots in the emulsion, when subjected to shock, but they provide no energy contribution to the explosive. Therefore, as the microballoon content is increased, the total explosive energy of the emulsion decreases.

Figure 20 shows that emulsion explosives have a narrow density range (0.92-1.55 kg/dm^{-3}). The observed densities compare well with those of similar studies by Lee and Hattori. Lee[84] et al, prepared similar emulsions and reported a density range of 0.80-1.31 kg/dm^{-3}. Hattori[85] et al noted a variation in density of 1.00-1.30 kg/dm^{-3}, although neither study varied the microballoon content to the same degree as in this study.

Table 8 Detonation data for high explosives[86].

Explosive	D/ms^{-1}	ρ/ kg/dm^{-3}	P/kbar calc.
HMX	9110	1.89	392
RDX	8440	1.70	300
DATB	7520	1.79	253
TATB	7658	1.80	260
TNT	6950	1.57	190
Tetryl	7160	1.50	192
Emulsion (Highest density)	3394	1.42	38
Emulsion (Highest velocity)	5558	1.13	81

D –Velocity of detonation (ms^{-1}) ρ - Density used for VOD and pressure data

P – Pressure of detonation (kbar)

In comparison to standard high explosives, emulsions have a low density. Table 8 compares the data for highest density emulsion to successfully initiate and the highest VOD emulsion in this study, to that of standard military explosives. The density, VOD and detonation pressure of the military explosives are all appreciably higher than the emulsion.

A more useful measurement, for explosives, than density is the percentage of theoretical maximum density (TMD). Percentage TMD is used in place of density in analysis of explosive performance as this allows direct comparisons of different explosives to be undertaken. TMD is taken, for solid explosives, as the actual density divided by the maximum theoretically calculated density, and is quoted as a percentage. Emulsions as used in this study are thick liquids and as such are at their maximum density before the microballoons are added. Figure 21 shows a graph of microballoon content versus %TMD.

Figure 21 % TMD versus % microballoon content

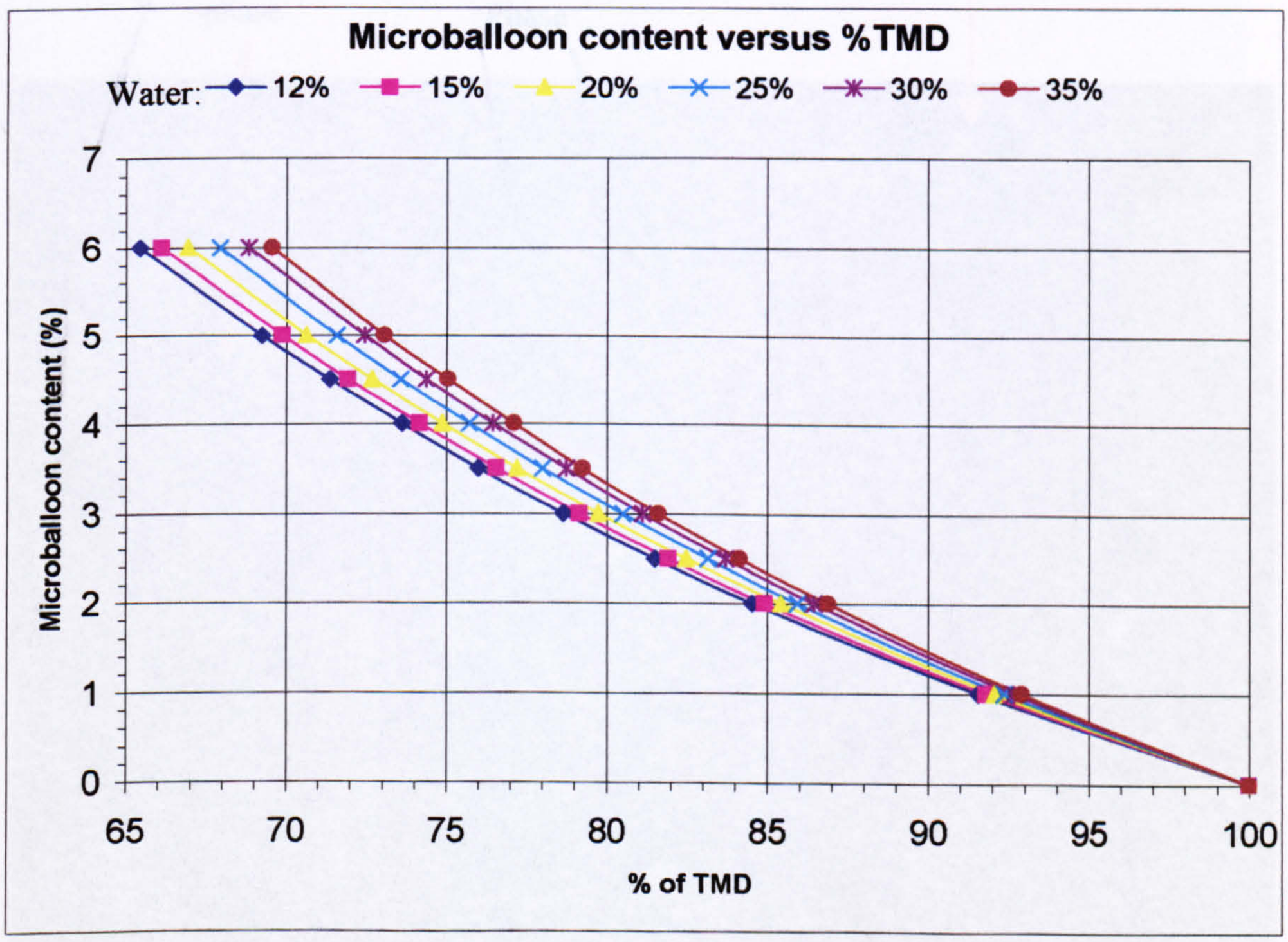

3.2 Emulsion breakdown

Emulsions degrade slowly over time and one of the most effective ways to monitor this is using microscopy. Emulsions were examined under a light microscope for early signs of failure, which eventually, would lead to more severe macroscopic failure. Pictures of the emulsion samples were taken over time, and comparisons taken between new and aged samples.

Figure 22 shows a recently manufactured emulsion, less than a week old, with a typical particle size and distribution. The two phases can be seen with the disperse phase (water droplets), containing dissolved ammonium nitrate, surrounded by the continuous oil phase.

Figure 22 Picture of an emulsion from an optical microscope x1550 (expanded for report).

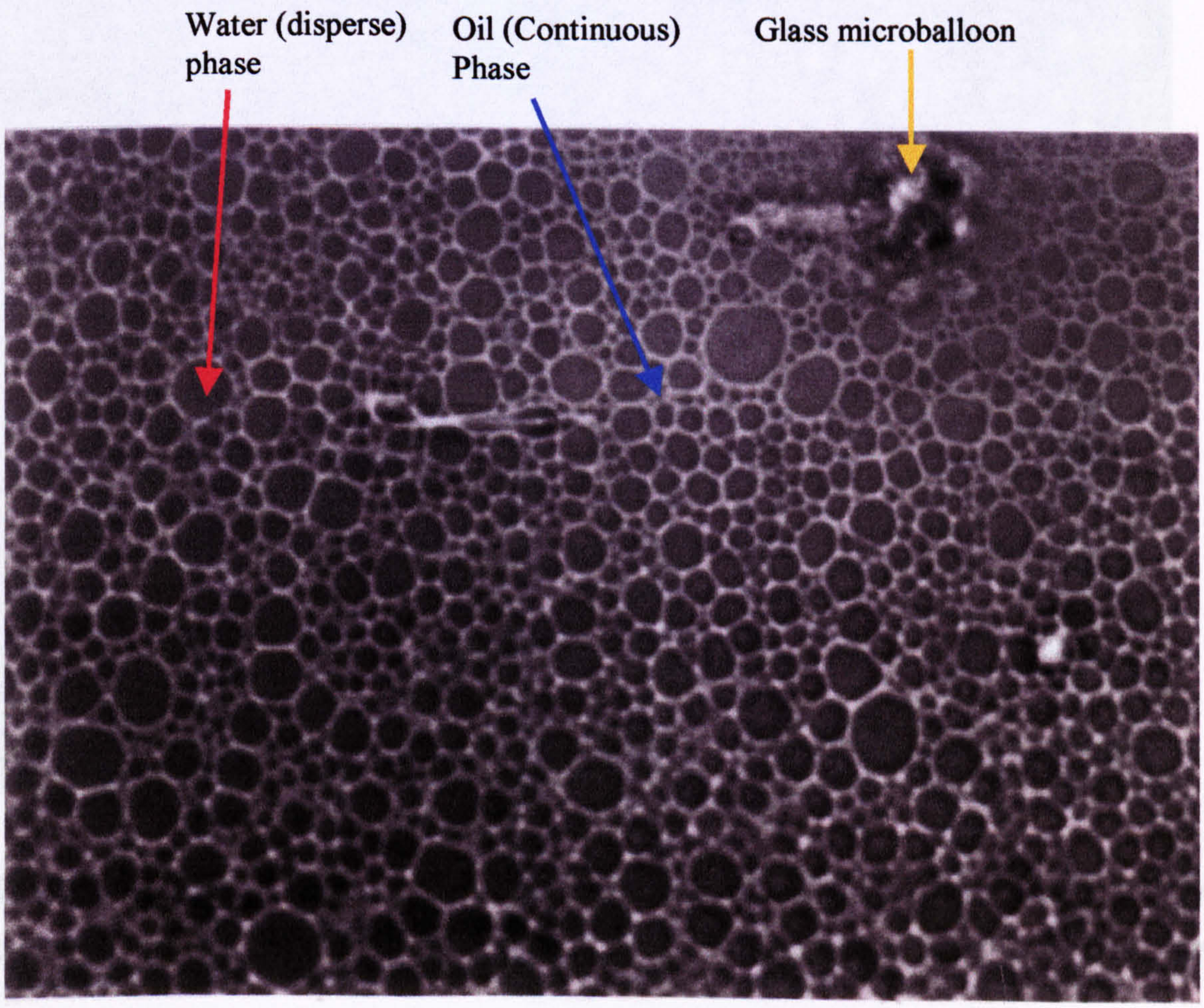

It can be seen from Figure 22 that there was a significant, and large, variation in droplet size, but the emulsion was stable and most of the droplets were spherical. This, Figure 22, was a typical emulsion explosive, which has been well mixed and is stable. The droplets correspond to a closely packed sphere model, with little wasted space between the droplets.

After time the emulsion begins to break down and the two phases separate by either coalescence or flocculation. Figure 23 shows an emulsion sample at the onset of coalescence. This was a two-year-old emulsion explosive sample with a 25% water and 1% microballoon content. The overall droplet size has started to increase with more medium to large droplets being observed.

Figure 23 Shows the onset of coalescence occurring in an aged sample (x1550) (expanded for report).

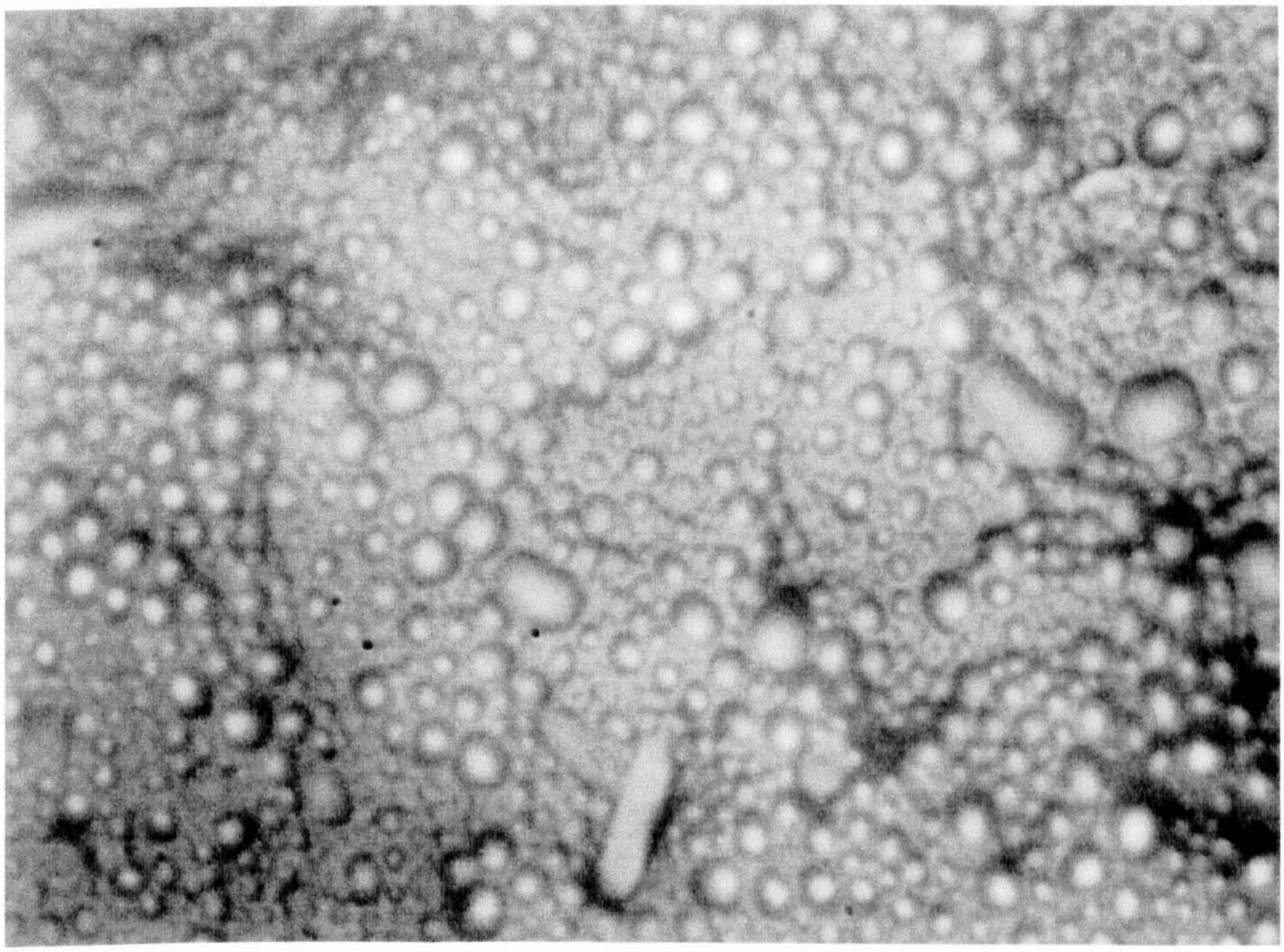

The gap between droplets has also increased and the disperse phase can be clearly seen. At this early stage, almost no difference in the sample can be seen

on the macroscopic scale. The sample can become slightly more opaque and less free flowing, but this change was minimal.

Figure 24 shows an aged sample in a more advanced stage of coalescence. It can be seen that the droplets were far less numerous and were no longer spherical. There were still a number of small droplets, but droplets can be seen amalgamating with others, their shape matching that of the joined droplets. At this stage, macroscopic changes were observed in samples. At the edge of large samples, there was a small amount of crystallised ammonium nitrate. Samples, at this stage, were very opaque and noticeably less free flowing, although the sample could still be easily converted back to a stable emulsion. The action of stirring caused the droplets to reform as a stable emulsion. This occurs when little or no crystallisation in the bulk of the sample has occurred. Even if the coalescence was slightly more advanced, the emulsion could still be recovered by the combined action of heat and stirring. The colour and flow properties of the emulsion were both affected at this stage, but macroscopically it still behaved as an emulsion.

Figure 24 Coalescence now more advanced in sample (x1550) (expanded for report).

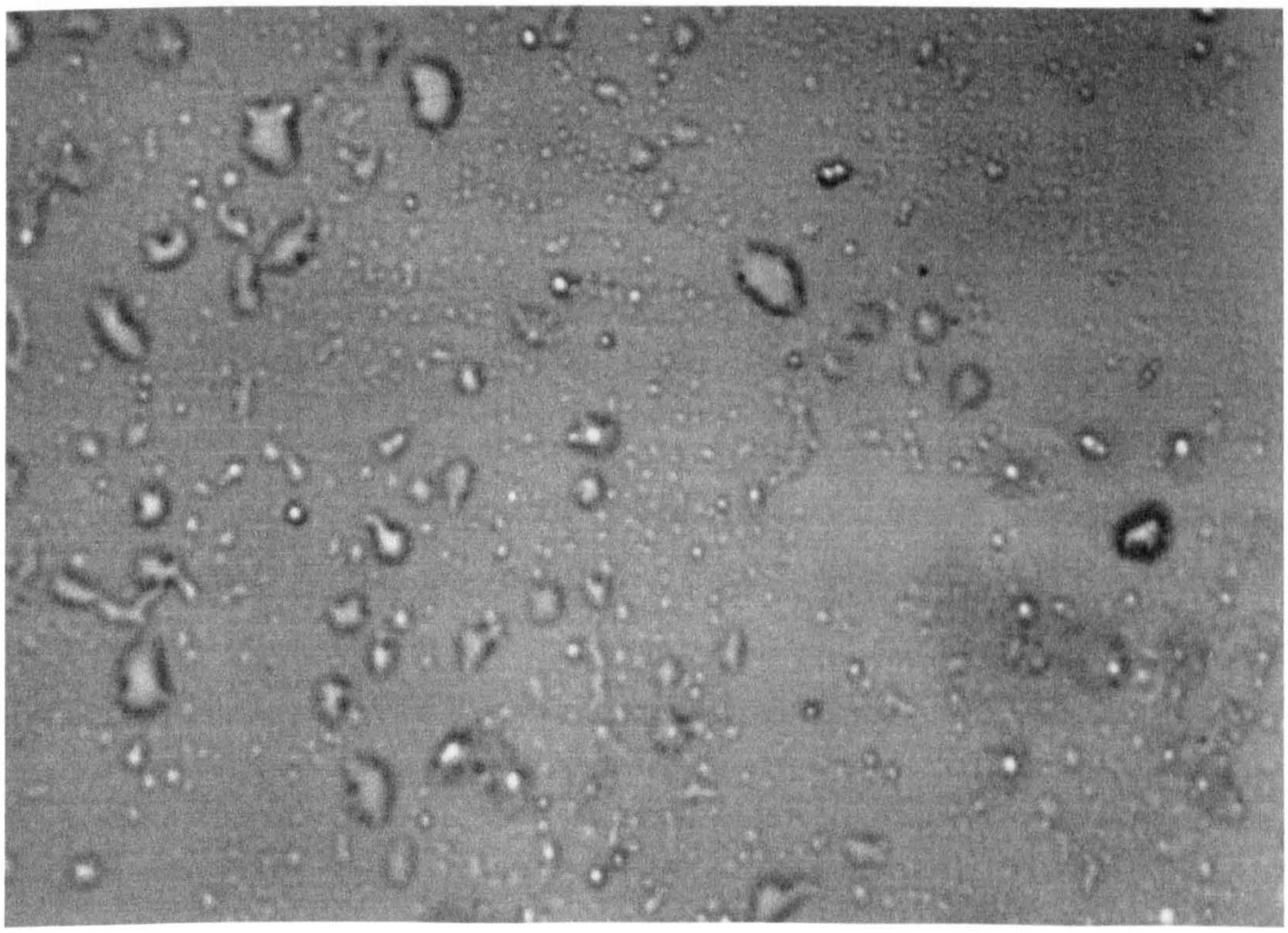

Figure 25 show the most advanced stage of coalescence with the effects very apparent on the macroscopic scale. The sample was completely opaque, extremely viscous and did not flow, but behaved more like a solid. At this stage, the effects of coalescence were irreversible and the droplets were very large, with virtually no small droplets. The shape of the droplets was haphazard, with no real structure to them. This sample was a 12% water emulsion with 5% microballoons, aged for 2½ years.

Figure 25 Coalescence, now catastrophic and seen on a macroscopic scale (x1550) (expanded for report).

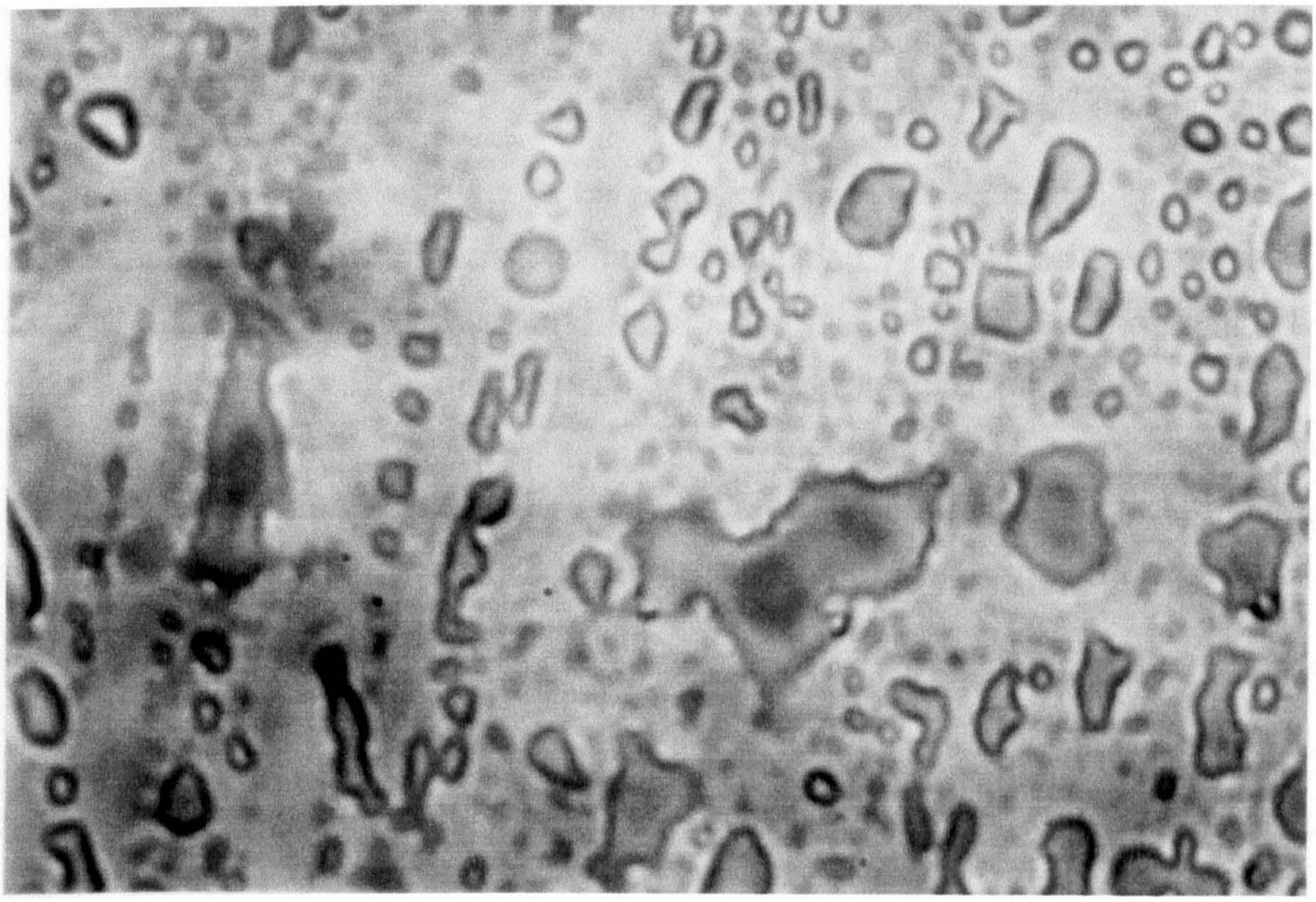

Crystallisation of samples sometimes occurred, but usually only on a minor scale. This was noted from the texture of the emulsion, which felt 'gritty' to touch. This, and the opaque colour, showed that a degree of crystallisation had occurred in the emulsion. Crystallisation was easily reversed, by heating the emulsion above 60°C and mixing, forcing the AN back into solution.

Initially 10% water content emulsions were manufactured, but these continually suffered catastrophic failures, due to crystallisation. This occurred spontaneously, either on cooling of the emulsion, or on the addition of microballoons. A 10% water emulsion was never manufactured in a stable enough state for explosive testing.

The lower water content emulsions, 12, 15 and 20%, showed a much greater propensity to spontaneously crystallise. On three separate occasions, 12% water emulsions began to crystallise on addition of microballoons. This was corrected by heating and stirring, which restored the emulsion matrix. Above 20% water content, crystallisation was rarely seen and this never occurred spontaneously on addition of microballoons.

An alternative breakdown process for emulsions is that of flocculation. Figure 26 shows a 20% water emulsion with no microballoons. This had been kept in a sealed container for 6 months and before analysis. Figure 26 shows that the droplets, although having grouped together, have still kept their individual identity. The size of this large 'droplet' is substantial in comparison to the normal droplet size for the emulsion. Emulsion explosives are not generally thought to undergo flocculation[87] and this was only noted in a few samples. This process was easily reversed with a minimum of stirring of the sample.

Coalescence and crystallisation were the more common processes of emulsion failure, and subsequent breakdown. By adding microballoons to the emulsion within 24h of explosive testing, this alleviated the problem of failure of the emulsion, by mixing the emulsion and thereby reforming a stable system before explosive testing.

Figure 26 Example of flocculation in emulsion sample (x1550) (expanded for report).

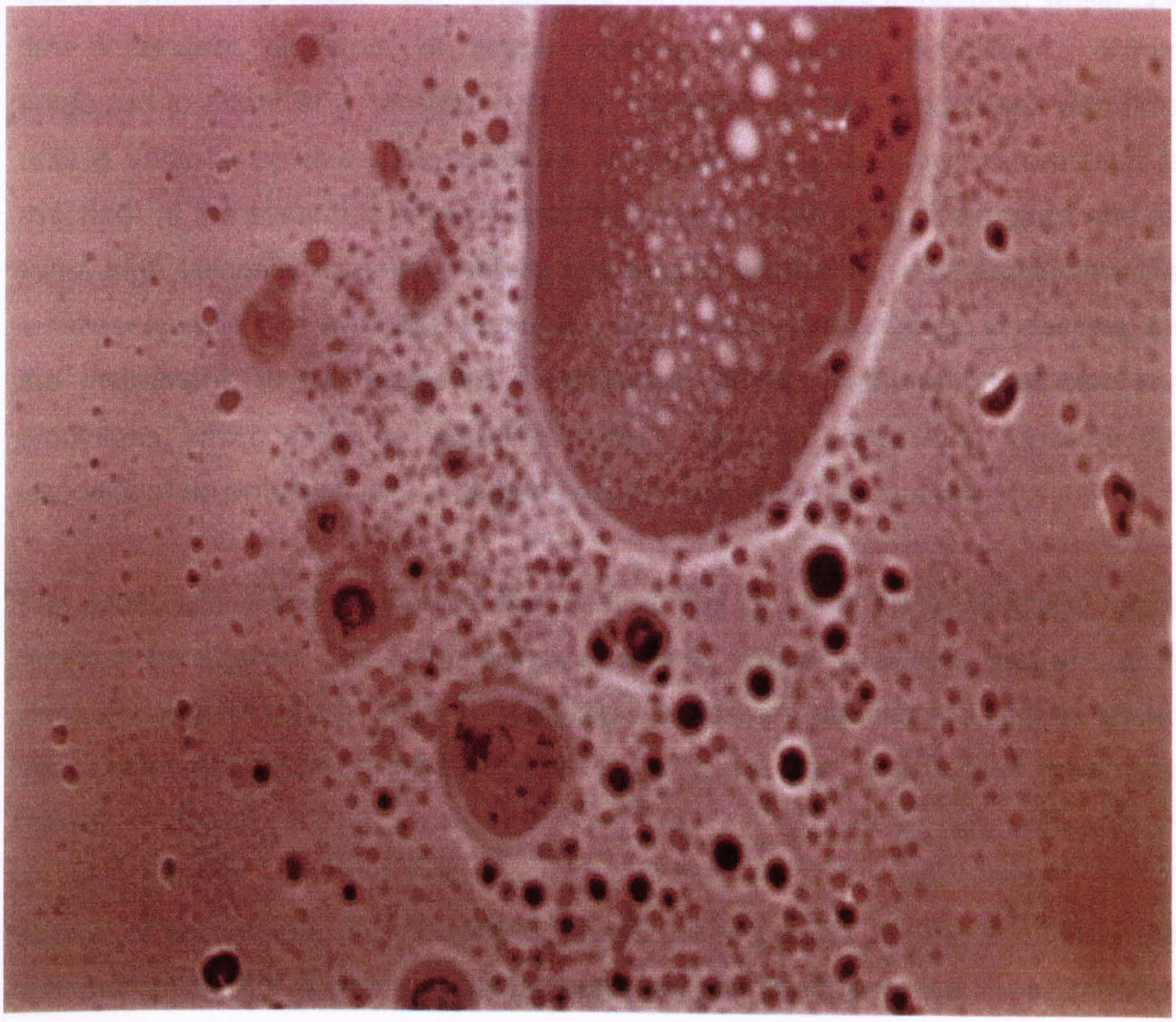

3.3 Rheology

Rheological measurements were made on the emulsions, specifically viscosity, using a Brookfield viscometer. Emulsions exhibit thixotropic behaviour, which is a time-dependant analogue of shear thinning and plastic behaviour. When subjected to shear at a constant rate, the apparent viscosity decreases with time until a balance between the structural breakdown and structure re-formation is reached. If the system is allowed to stand, it regains its original structure and an initial high viscosity is noted, before this again decreases. For emulsions, the smallest spindle size available was used, which allowed the highest viscosities, for the instrument, to be measured. Limitations of the instrument restricted the emulsions, which could be examined, and it was not possible to measure the viscosity of an emulsion with a higher than 1% microballoon content.

The speed of the spindle through the medium has an effect on the viscosity range that can be studied. By using a slower spindle speed, mediums that are more viscous can be studied. With the emulsion explosives, varying the spindle speed has a dramatic effect on the apparent viscosity; this was due to their thixotropic nature.

Figure 27 shows the effect of spindle speed on viscosity. As the spindle speed was increased, the apparent viscosity dropped; this effect is called shear thinning. This is a well-known property of emulsions, which has been utilised by paint manufacturers, for emulsion paints. The solution viscosity decreases with applied force, being initially thick and viscous at low force and becoming free flowing as the force is increased. The drop in apparent viscosity can be seen as the spindle speed increases. When the apparent viscosity becomes stable, the emulsion matrix turns with the spindle, at low speed. However, as the spindle speed increases the apparent viscosity dramatically drops. This was shown for every emulsion composition, with the apparent viscosity dependent upon the water content.

Figure 27 Variation of viscosity with spindle speed (viscosity/log plot).

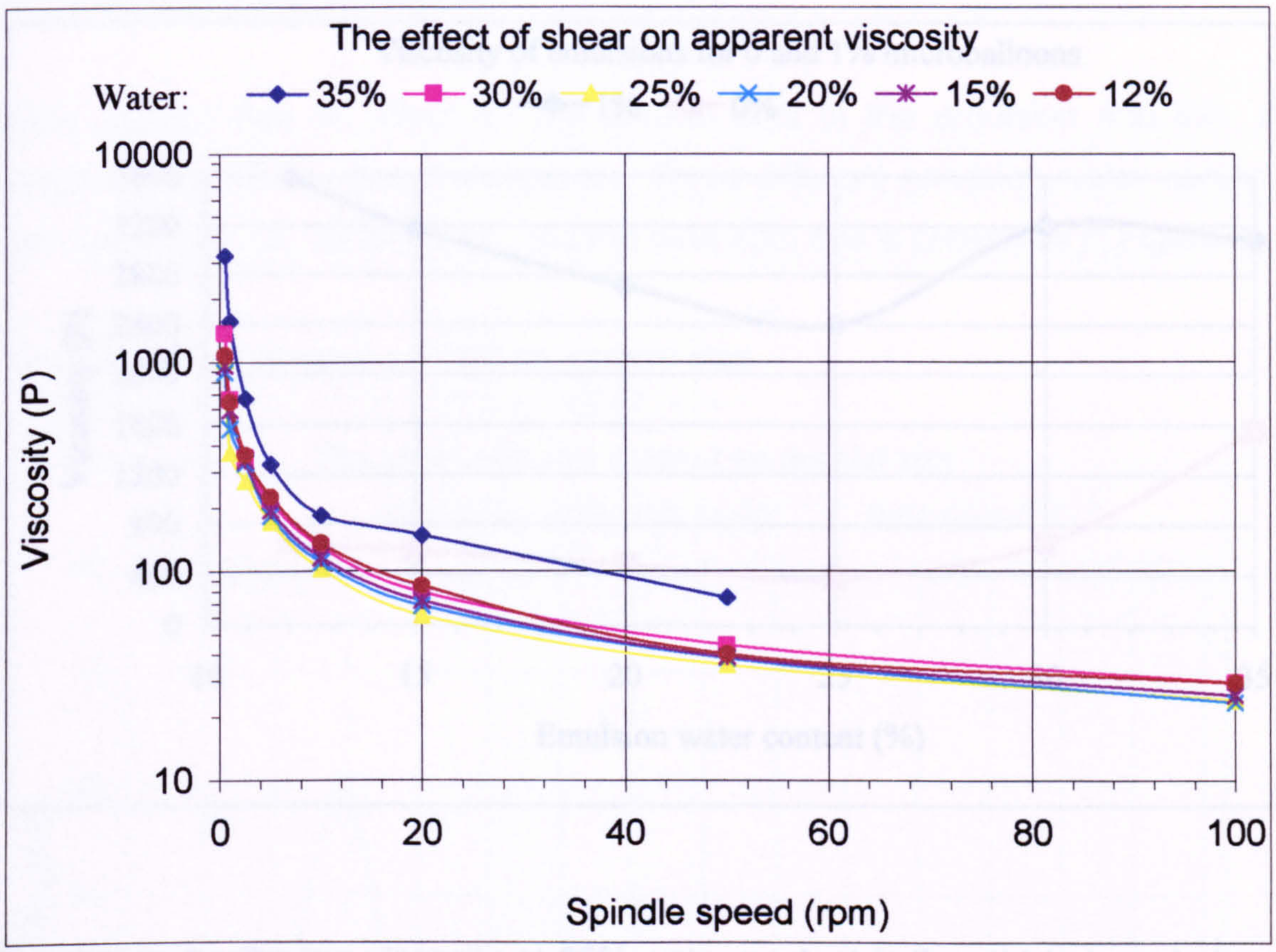

Figure 28 shows the data obtained at 1rpm. At this speed the most stable viscometer readings were obtained. With no microballoons in the emulsion matrix, it can be seen that as the water content dropped from 35%, the viscosity began to drop. At lower than 25% water content, where the lowest viscosity was recorded, the viscosity increased with decreasing water content. With the addition of microballoons, the overall viscosity of the emulsion increased for all water contents and again, at 25% water content, the lowest viscosity is recorded.

Figure 28 Viscosity's for emulsions.

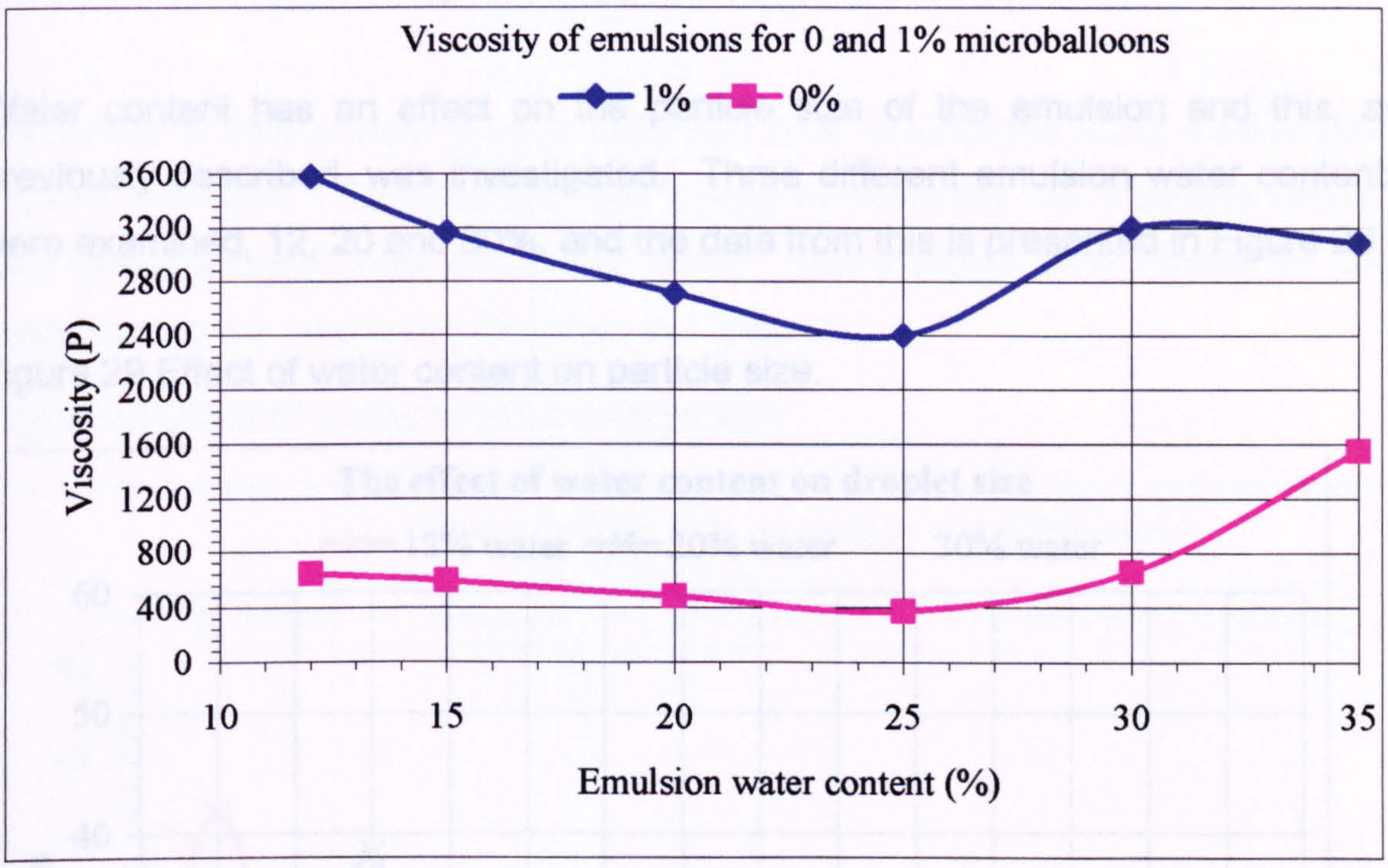

The reason for the low viscosity at 25% water content is thought to be a balance between the water, ammonium nitrate and the disperse phase droplet size. Increasing the percentage of water, in comparison to ammonium nitrate content, initially has the effect of lowering the viscosity. This is believed to occur because the density of the ammonium nitrate solution, the disperse phase, decreases. With further increase in water content, the continuous phase becomes, in comparison, sparser, leading to a greater number of disperse phase droplets. It is thought that this has the effect of increasing the viscosity, as noted when the water content increases from 25% to 35%. At 25% water, these two interactions, the droplet size and droplet density, are thought to be at a mutual low point. This would account for the lowest viscosity readings being recorded at 25% water content.

3.4 Particle size analysis

Water content has an effect on the particle size of the emulsion and this, as previously described, was investigated. Three different emulsion water contents were examined, 12, 20 and 30%, and the data from this is presented in Figure 29.

Figure 29 Effect of water content on particle size.

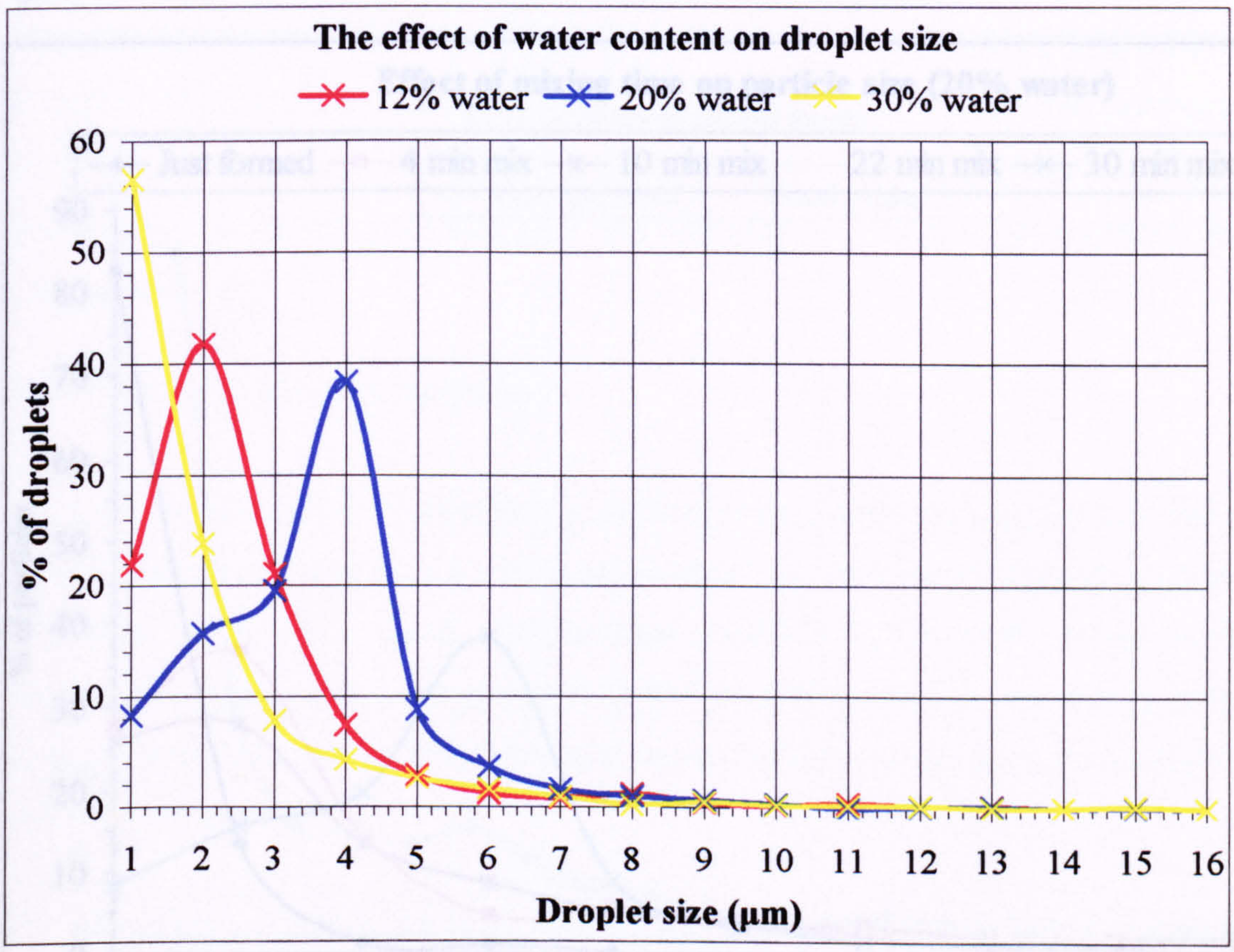

The chart shows droplet size as a percentage of the total, however, due to limitations of the instrument the maximum droplet size that could be recorded was 50µm. From Figure 29 it can be seen that 30% water emulsion had the lowest average droplet size. This was notwithstanding the fact there could have been a greater proportion of large, but not recorded, droplets in the emulsion. At 20% water content, the highest average particle size, 4µm, was recorded, although there was only a limited difference in droplet size between the various emulsions. The difference in droplet size could be linked to the viscosity of the emulsions, but

no clear trend was observed in the data. Overall, there was only a limited difference in the particle sizes between the differing water contents.

The effect of time of mixing on particle size was investigated using a 20% water content emulsion. The emulsion was prepared, following the standard method, and samples taken from this at set times. The samples were stored for later analysis with the results of this shown in Figure 30.

Figure 30 Effect of mixing time on particle size.

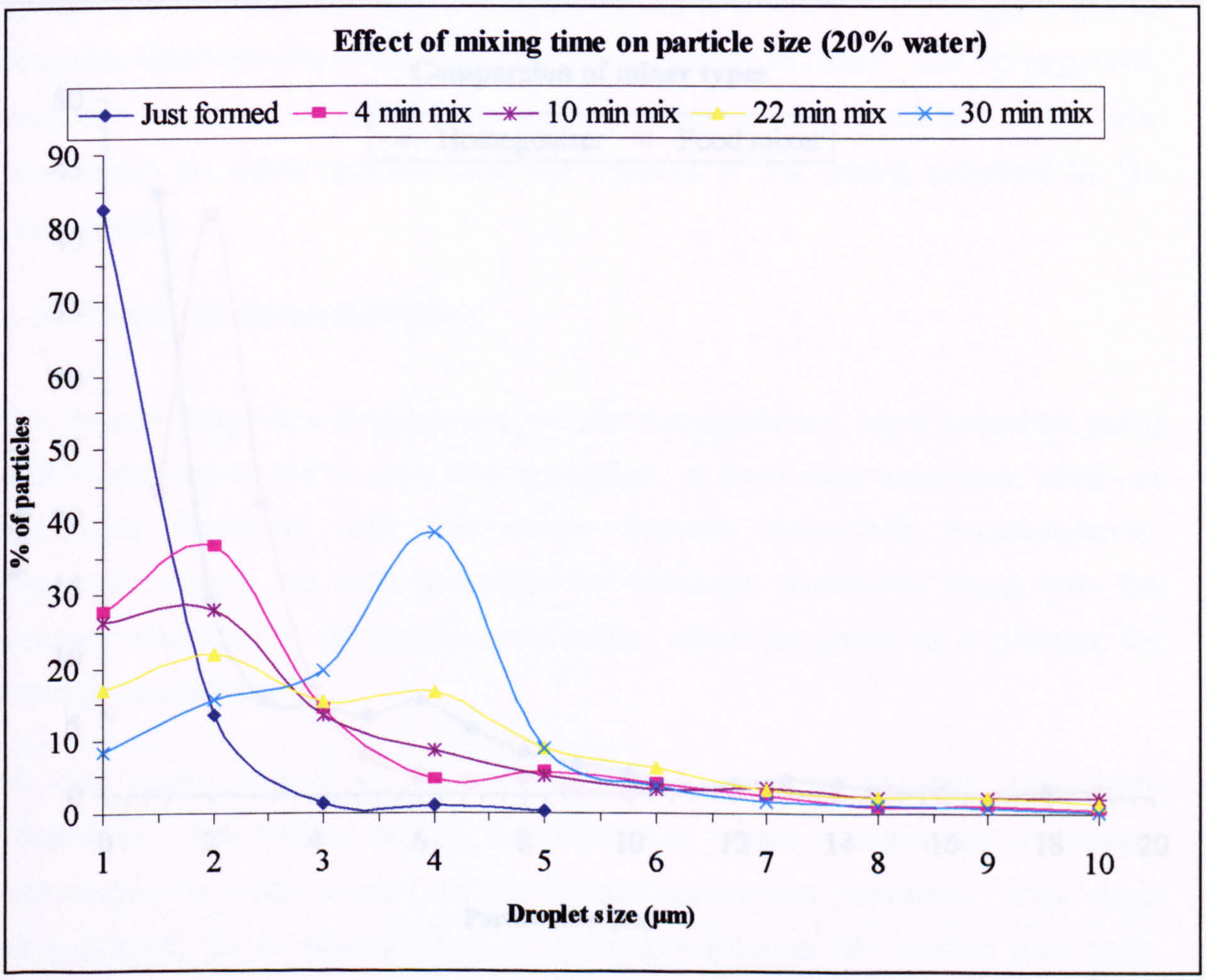

The lowest average droplet size was recorded in a newly formed emulsion and in this sample over 80% of comprised 1µm droplets. Notwithstanding this, it should be stressed that as the instrument could only record a maximum droplet size of 50µm, the true state of the sample cannot be ascertained. By increasing mixing time the average droplet size of the emulsion increased.

Further mixing of the emulsion after formation can cause catastrophic failure of the emulsion. After the emulsion is formed, and is then subjected to further vigorous mixing, flocculation and coagulation can occur as failure of the emulsion matrix begins. A degree of mixing after the initial emulsion formation is necessary but this was limited to stop these effects. On this basis, emulsions were mixed for two minutes after formation, before being used in explosive testing.

Figure 31 Effect of mixer type on particle size.

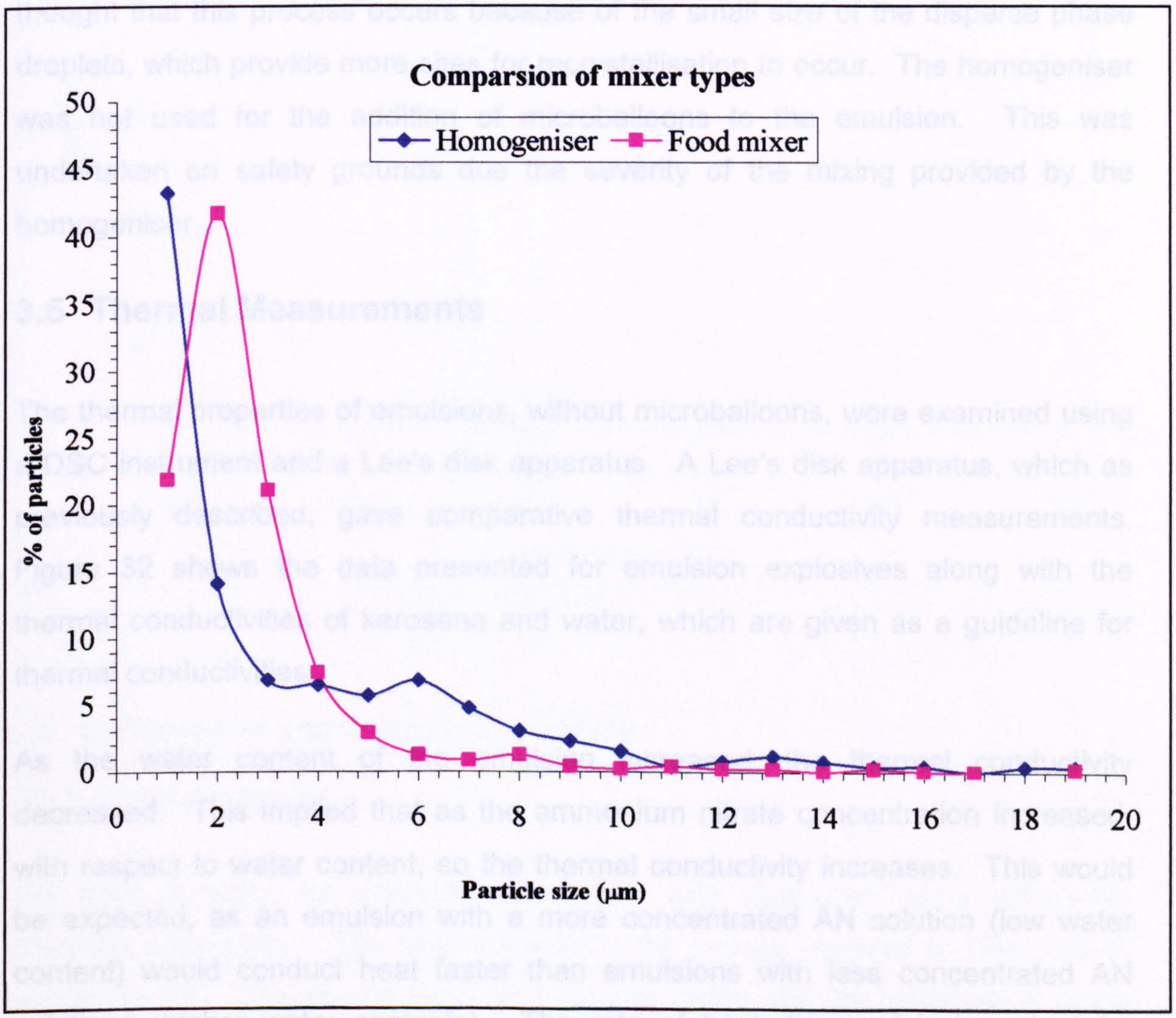

As an alternative to the standard mixing apparatus, a homogeniser was tested in an attempt to lower the droplet size, to gain an increase in explosive performance. To this end, a 25% water content emulsion was mixed with the standard mixer and then compared to a 25% water content emulsion mixed with a homogeniser. The results of this are shown in Figure 31.

The homogeniser produced a refined emulsion much more quickly than the standard mixer. The average droplet size of the emulsion produced by the homogeniser was lower, the majority of the droplets being at or below 1μm. However, when the homogeniser was used to mix the emulsion, water was prone to separate out from the emulsion matrix. The mixing head provided a much more severe environment than a standard food style mixer, which led to phase separation. Emulsions formed with the homogeniser were prone to catastrophic failure, the ammonium nitrate crystallising out of solution in the emulsion. It is thought that this process occurs because of the small size of the disperse phase droplets, which provide more sites for recrystallisation to occur. The homogeniser was not used for the addition of microballoons to the emulsion. This was undertaken on safety grounds due the severity of the mixing provided by the homogeniser.

3.5 Thermal Measurements

The thermal properties of emulsions, without microballoons, were examined using a DSC instrument and a Lee's disk apparatus. A Lee's disk apparatus, which as previously described, gave comparative thermal conductivity measurements. Figure 32 shows the data presented for emulsion explosives along with the thermal conductivities of kerosene and water, which are given as a guideline for thermal conductivities.

As the water content of the emulsion increased, the thermal conductivity decreased. This implied that as the ammonium nitrate concentration increased, with respect to water content, so the thermal conductivity increases. This would be expected, as an emulsion with a more concentrated AN solution (low water content) would conduct heat faster than emulsions with less concentrated AN solutions (higher water contents). The rate of heat dispersal is important for explosives in the context of initiation, with shock and heat being two of the major mechanisms for this. This is discussed later, in more detail, in the context of explosive performance.

Figure 32 Thermal conductivity of emulsion explosives.

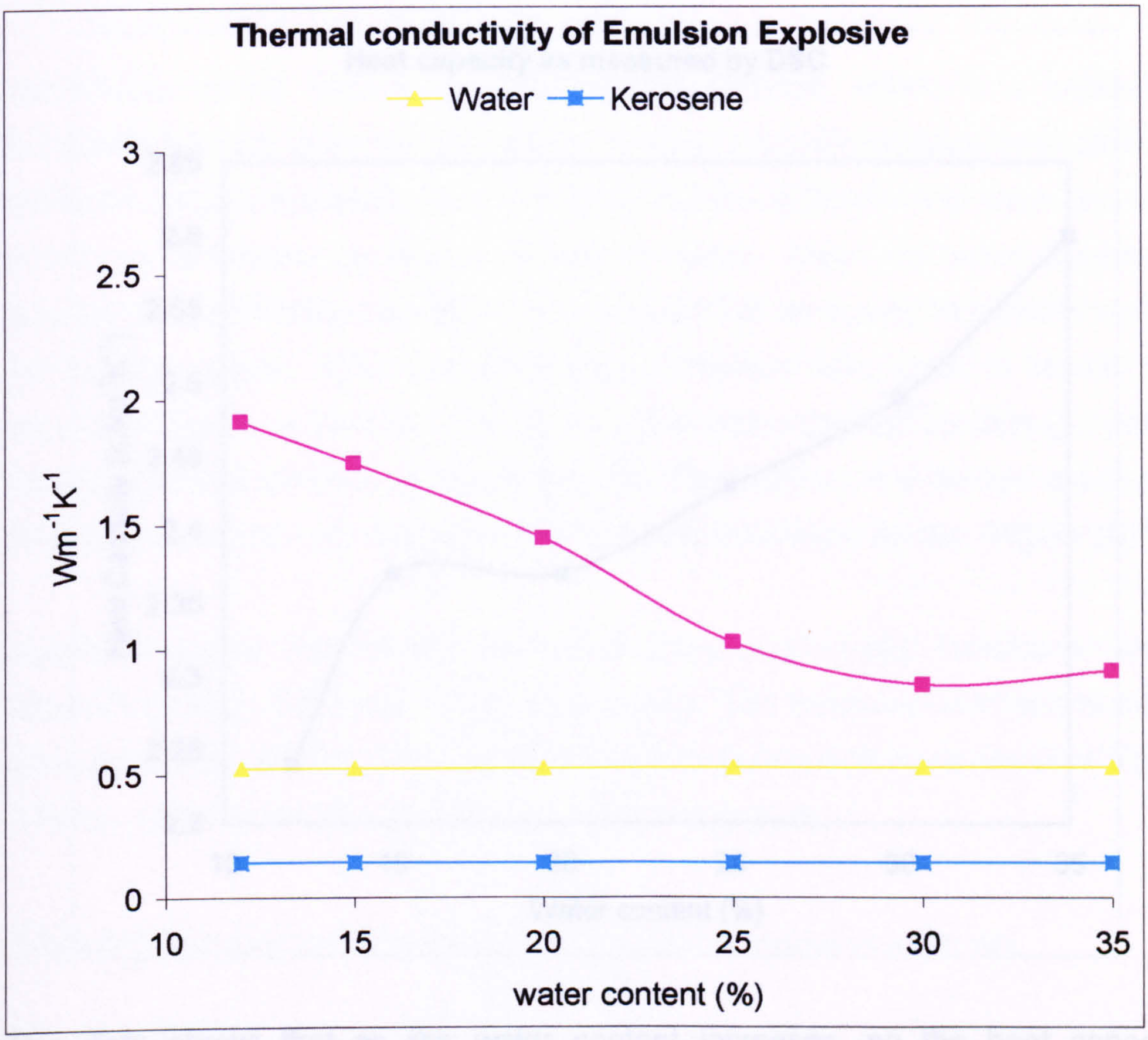

3.6 Differential scanning calorimetry

3.6.1 Heat capacity

The heat capacity, for emulsion explosives, was measured using differential scanning calorimetry. The heat capacity is the energy required to heat 1kg of sample by 1°C. The energy required to do this varies with the temperature of the sample, with heat being conducted at different rates depending on the temperature. The data presented in Figure 33 was measured for the emulsions at 40°C. This temperature was used since temperatures higher than this are unlikely to be encountered in the normal operational use of emulsion explosives and below this temperature it could be affected by phase changes.

Figure 33 Heat capacity as measured by DSC.

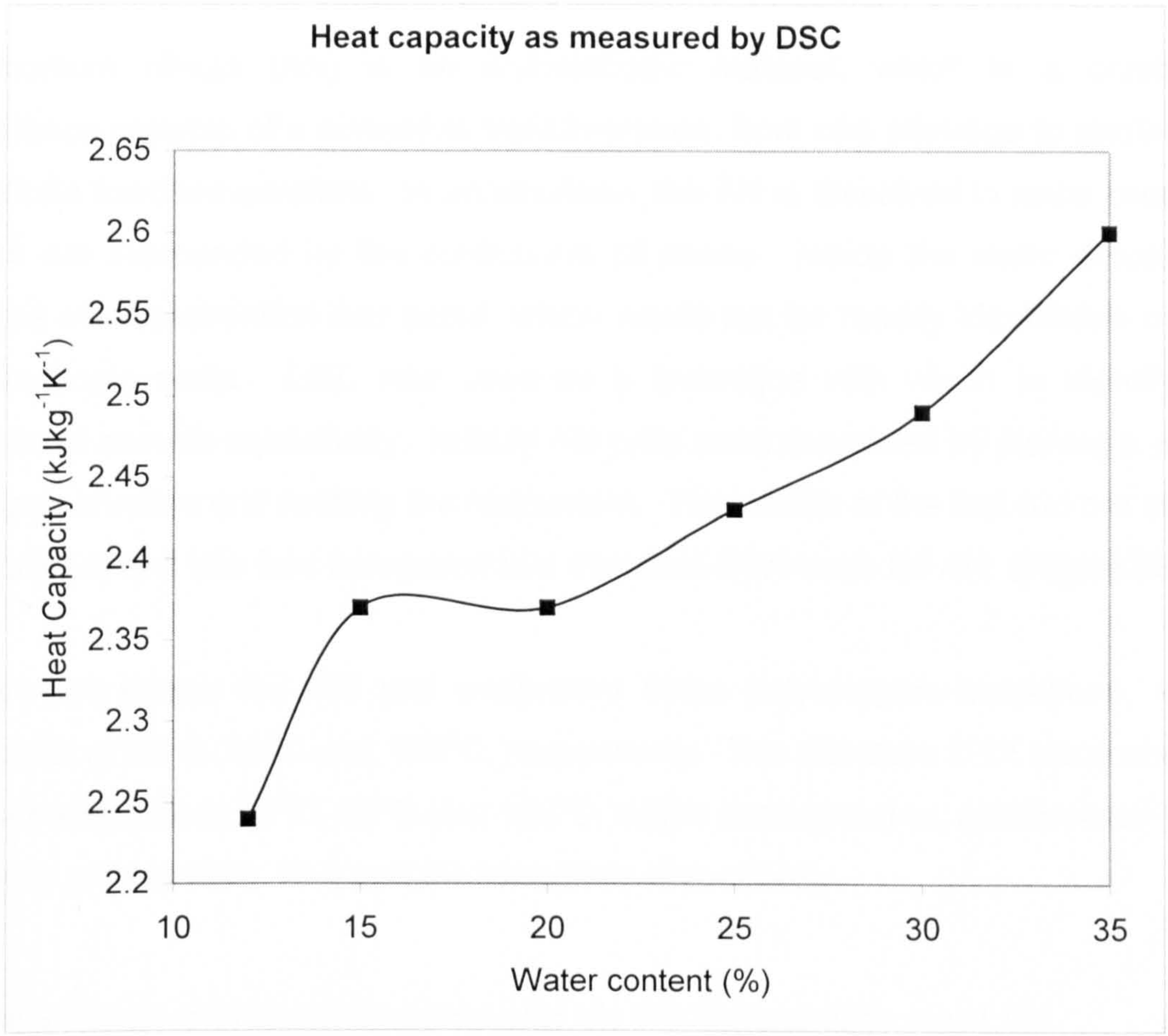

This data shows that as the water content increases, so the heat capacity increases. The data observed at 15% water content seems to be higher than would be expected. This analysis was repeated four times for each sample, although this used the same bulk sample, with respect to water content, for each emulsion. The high result recorded at 15% water content could be due to a degree of crystallinity in the sample. Energy would then be utilised redissolving some of the AN, before an increase in temperature was recorded. Overall, as water has a higher heat capacity, in comparison to oil, these results show an expected trend of increasing heat capacity with increasing water content.

3.6.2 Thermal analysis data

Ammonium nitrate (AN) is an enantiotropic material, which is a crystalline substance capable of a reversible transformation, from one allotrope to another, at a definite fixed temperature. In an emulsion, the AN is dissolved in water droplets, which are surrounded by the continuous oil phase. Inside the water droplets, a degree of crystallisation can occur, which would not be readily identifiable on the macroscopic scale. DSC was used as a technique with which to identify the degree of sample crystallinity. Initially AN prills were examined by placing a prill in an open crucible and running the instrument. The results of the first run are shown (Figure 34) and this was compared to a standard DTA trace for AN (Figure 35)[88].

Figure 34 shows the AN prill underwent three polymorphic transitions, which occurred at 52°C, 92°C and 134°C, respectively. The literature DTA trace showed three transitions at 32°C, 84°C and 125°C, which correspond to, as shown in Table 5 below, phase IV-III, III-II and II-I transitions respectively.

Table 9 Phase change temperatures for dry AN compared to moist AN.

Phase	Moist transition temperature	Dry transition temperature
V-IV	-18	-18
IV-III	32	-
III-II	84	-
IV-II	-	50
II-I	125	124

The phase transitions, in the AN prill, occurred at higher temperatures than the reported literature values for powdered AN. The initial phase change, at 52°C in the AN prill, could be the IV-II phase transition or a late IV-III transition. Whilst it would be expected that the centre of the AN prill would be free from moisture, allowing the core of the prill to undergo a direct IV-II phase transition, this would not account for the fact that the moisture rich exterior of the prill did not undergo

the IV-III phase transition at 32°C. However, as the exterior of the prills were sprayed, at manufacture, with 0.5% of an anti-caking agent and this could lower the IV-III phase transition temperature, at the moisture rich exterior of the prill. The implication of this being that the IV-III phase transition would have already occurred, at room temperature, before the DSC thermal trace began.

It could also be possible that because of the surface coating, moisture was not in direct contact with the AN, and therefore the IV-III transition did not occur as there was no moist AN. If this were the case, then there would be difficulty explaining the phase transition at 92°C, which is likely to be a late III-II phase transition, as seen in moist AN. In my opinion, it is most likely that the surface coating of anti-caking agent does in fact lower the initial IV-III transition temperature and this is the reason why it is not seen on the thermogram. There was no direct evidence to prove that this occurred, nevertheless, some of the AN in the prill must have been in the phase III, orthorhombic state, as evidenced by the III-II phase transition at 92°C.

Figure 34 DSC trace of AN prill.

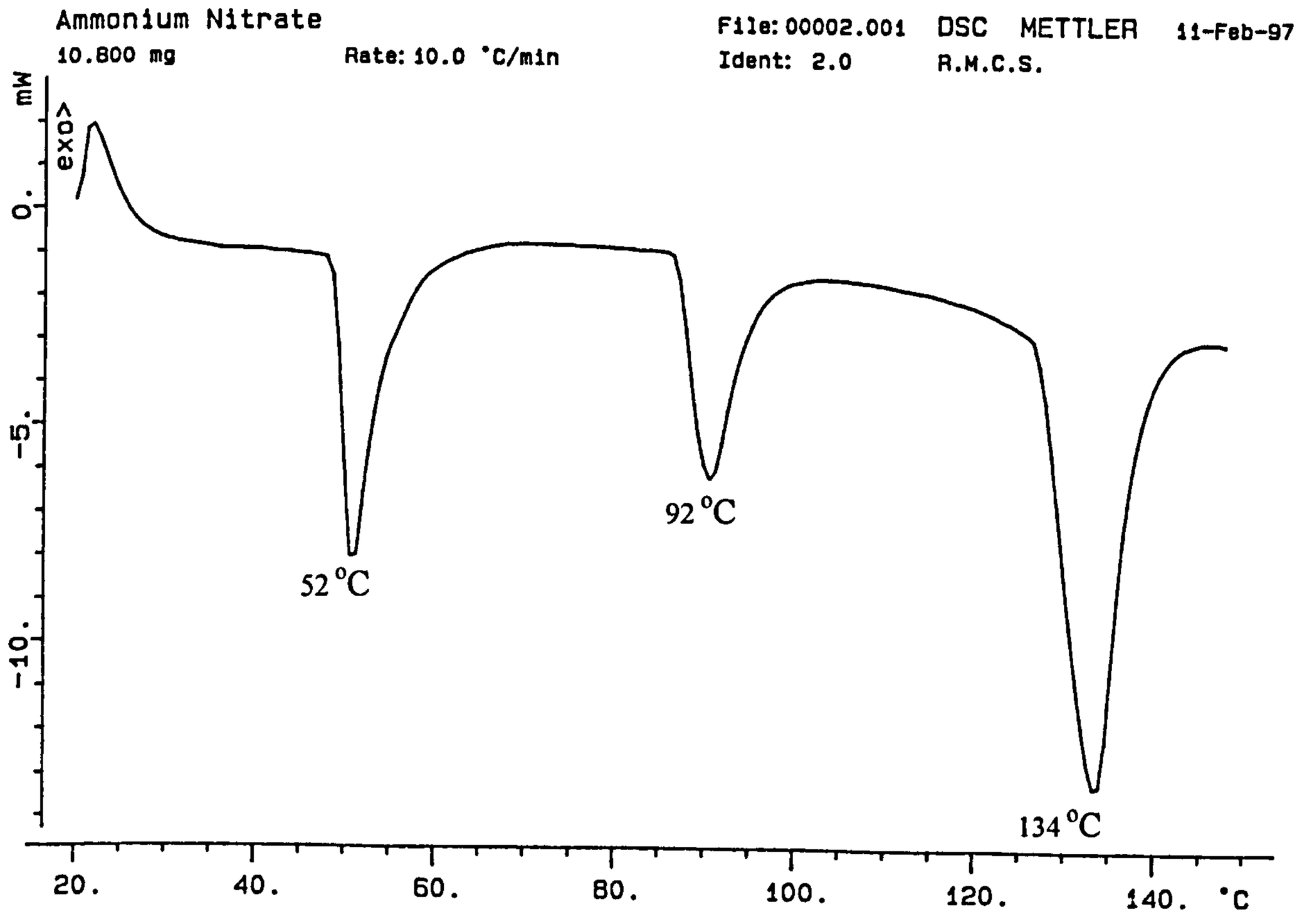

Figure 35 DTA (ΔT) and heating (T) curves for ammonium nitrate, showing three polymorphic transitions (at 32°C, 84°C and 125°C).

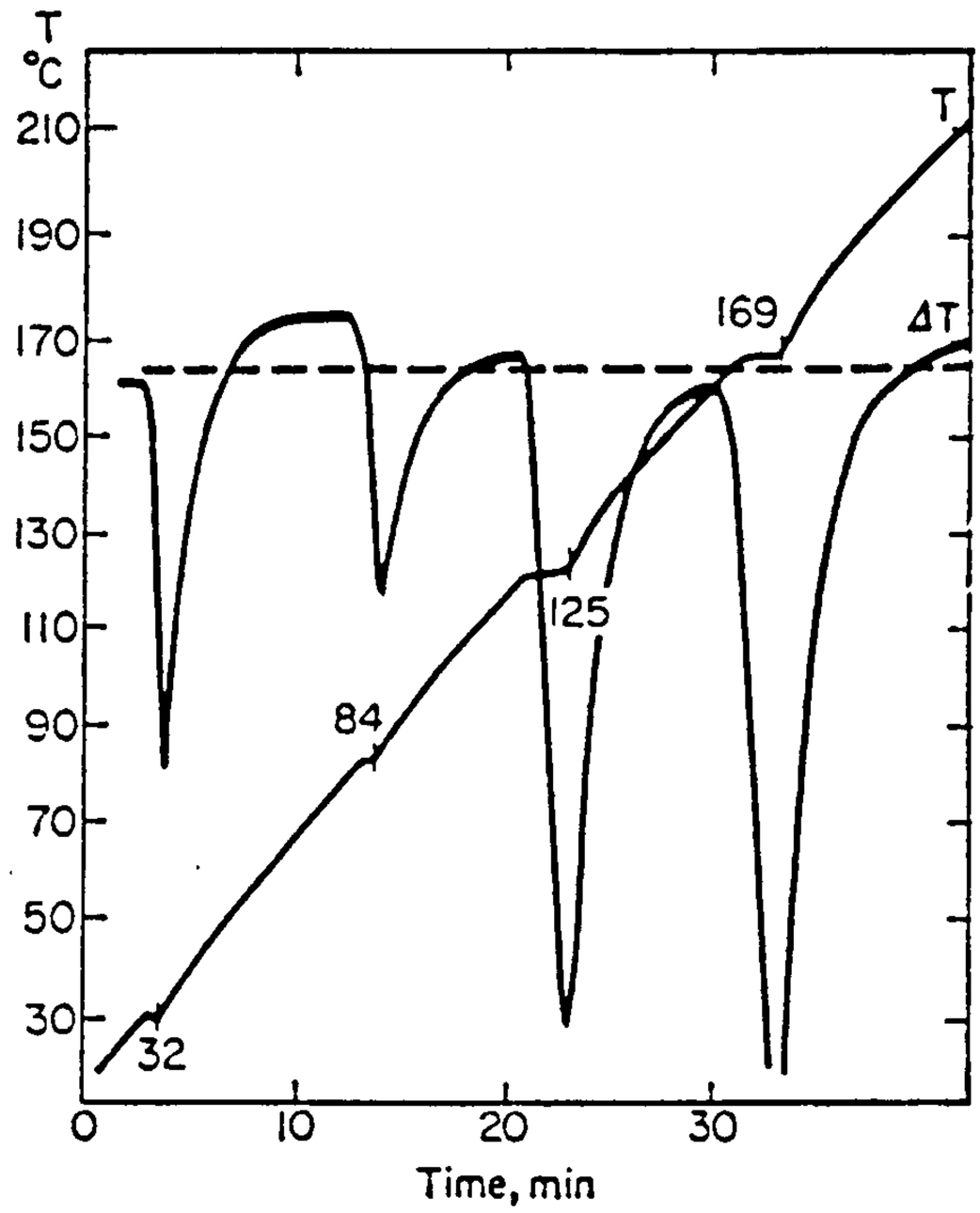

Figure 36 Ammonium nitrate phase changes from DSC.

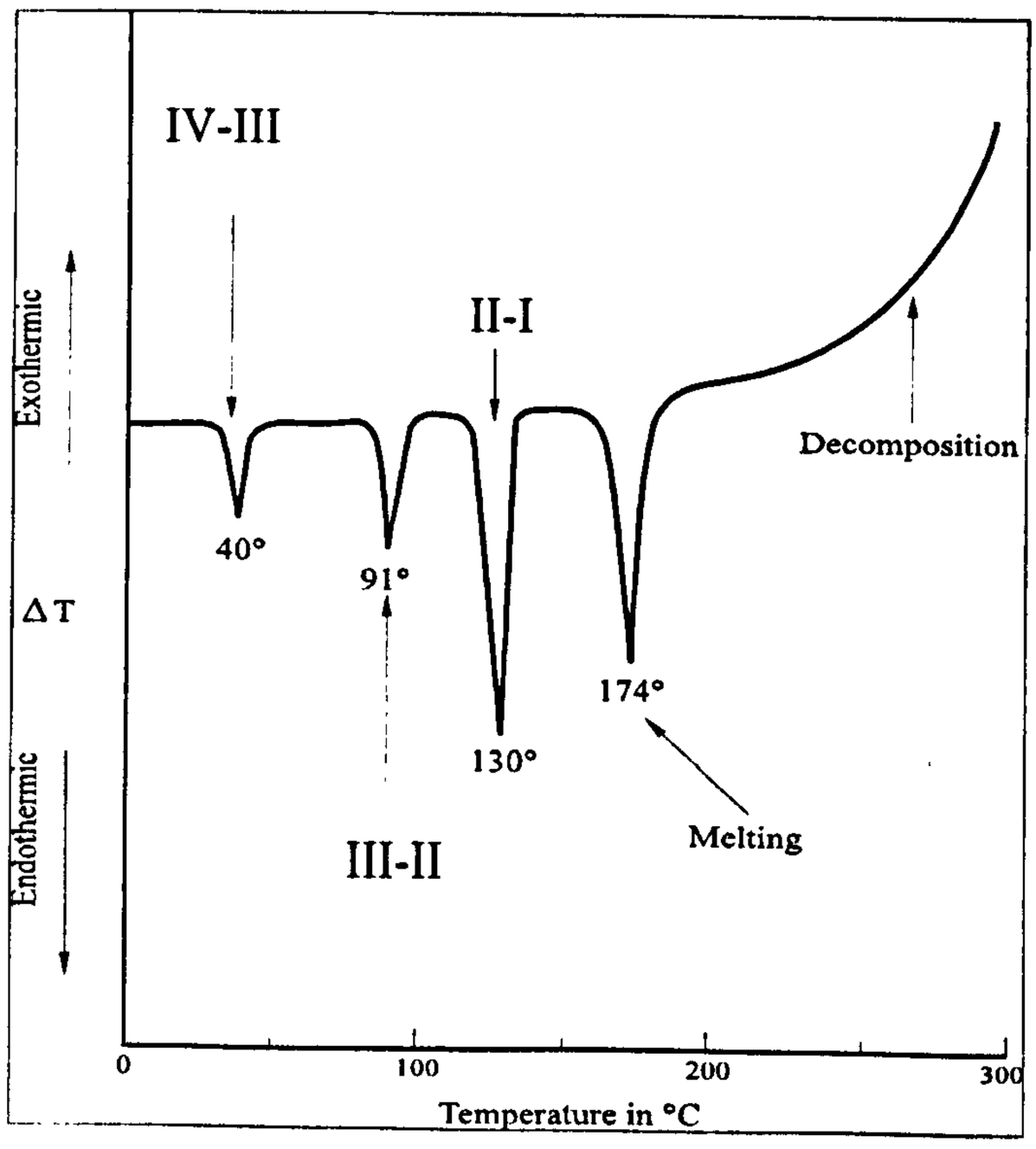

In the literature there is some ambiguity over the exact temperatures at which the phase changes occur in moist AN. Figure 36[89], a DSC trace, shows the phase transition temperatures in moist AN. The temperature that the phase changes occurred in Figure 36, in comparison to the present study and the data from Figure 35, is shown below in Table 10.

Table 10 Comparison of AN phase transition temperatures.

Phase Transition	Figure 35 DTA Trace	Figure 36 DSC Trace	Present Study DSC Trace
IV-III	32°C	40 °C	-
IV-II	-	-	52 °C
III-II	84 °C	91 °C	92 °C
II-I	125 °C	130 °C	134 °C

The phase transitions temperatures in the present study were higher than those recorded in the literature. One plausible explanation is that because the AN was in a prill form, there could be instrumental temperature lag due to uneven heating. This would be expected as the prill is spherical and has, in comparison with powdered samples, a low contact area with the surface of the DSC pan.

Figure 37 to 40 show DSC traces for emulsions with water percentages 35, 30 25, 20, 15 and 12% respectively. The traces for the higher water contents (35, 30 and 25%, Figure 37) show a smooth trace with, any phase transitions masked by the broad water evaporation band. The water evaporation band occurred because the sample containers were pierced. There is evidence of an endotherm on the 25% emulsion, but this was hidden in the water evaporation band and therefore difficult to determine quantitatively.

Figure 37 DSC trace of 35,30 and 25% water emulsions.

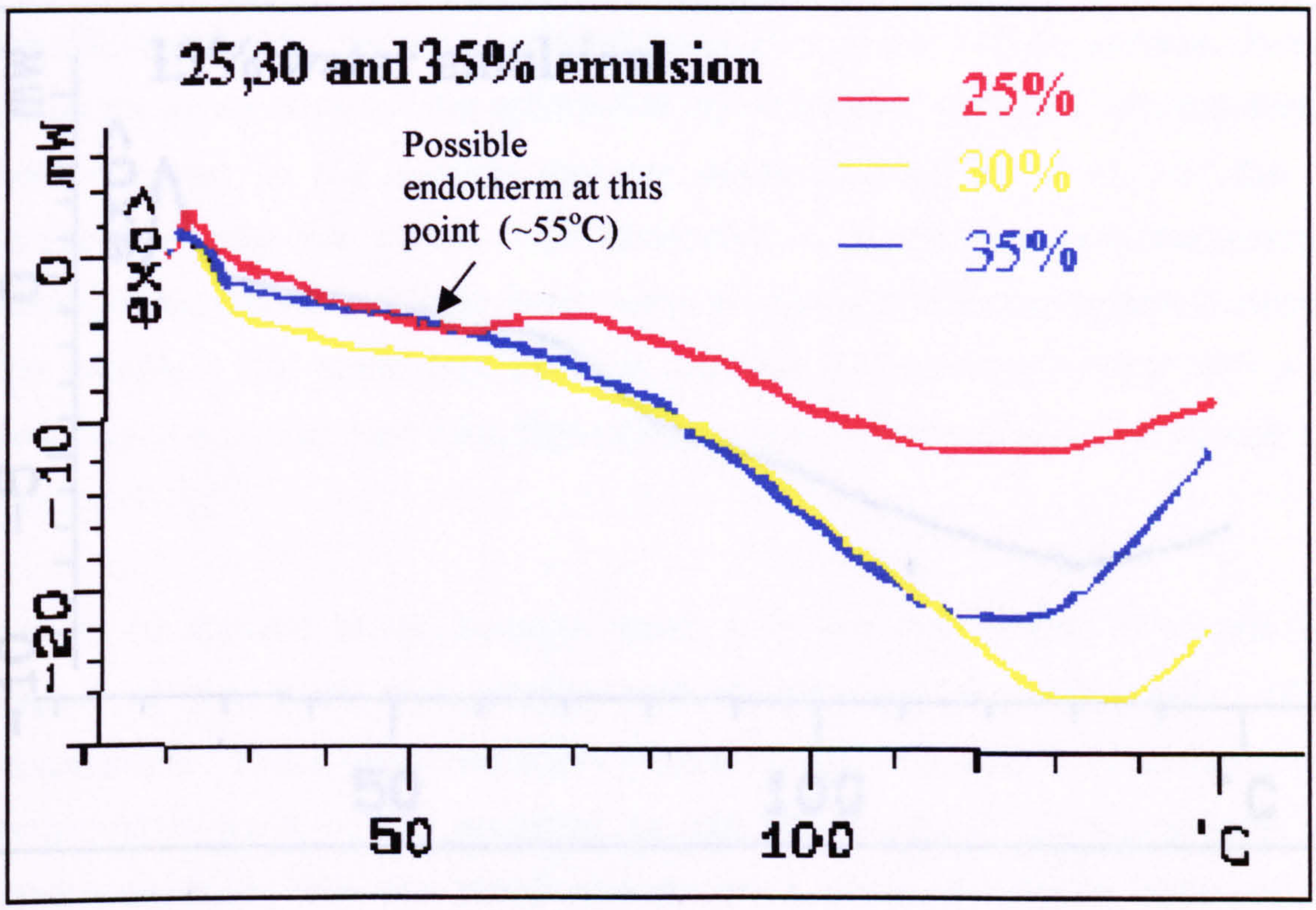

Figure 38 20% water emulsion.

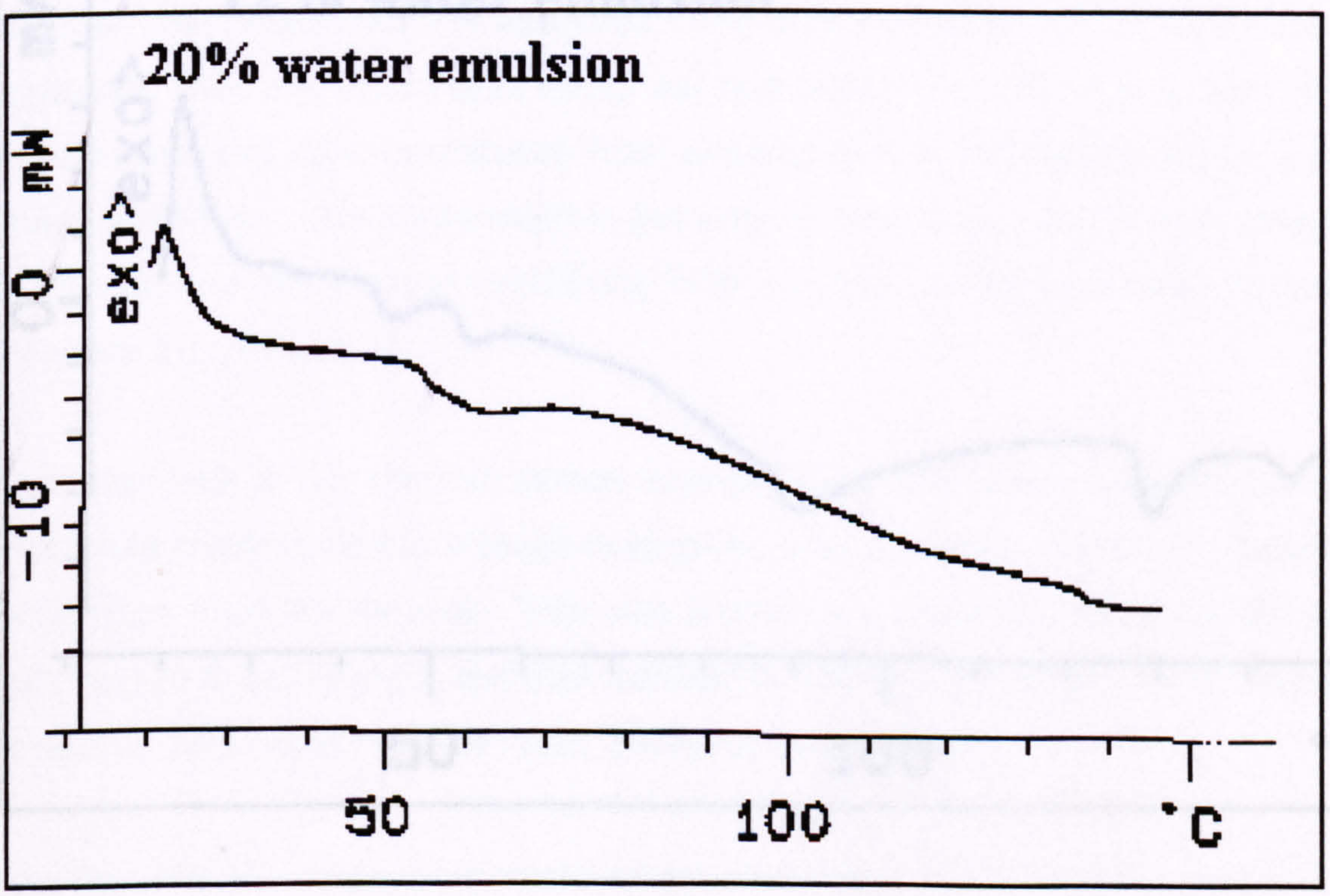

Figure 39 15% water emulsion.

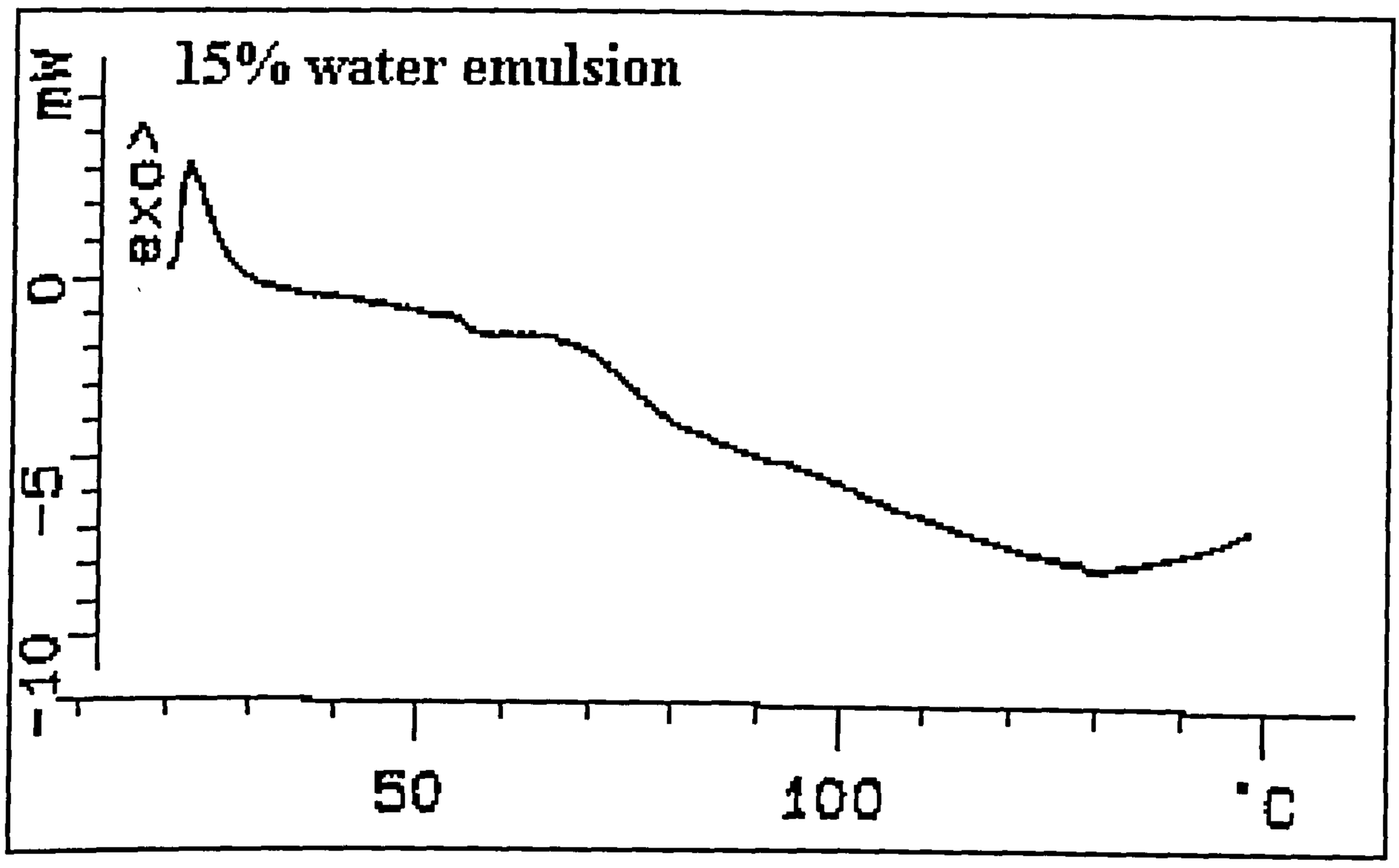

Figure 40 12% water emulsion.

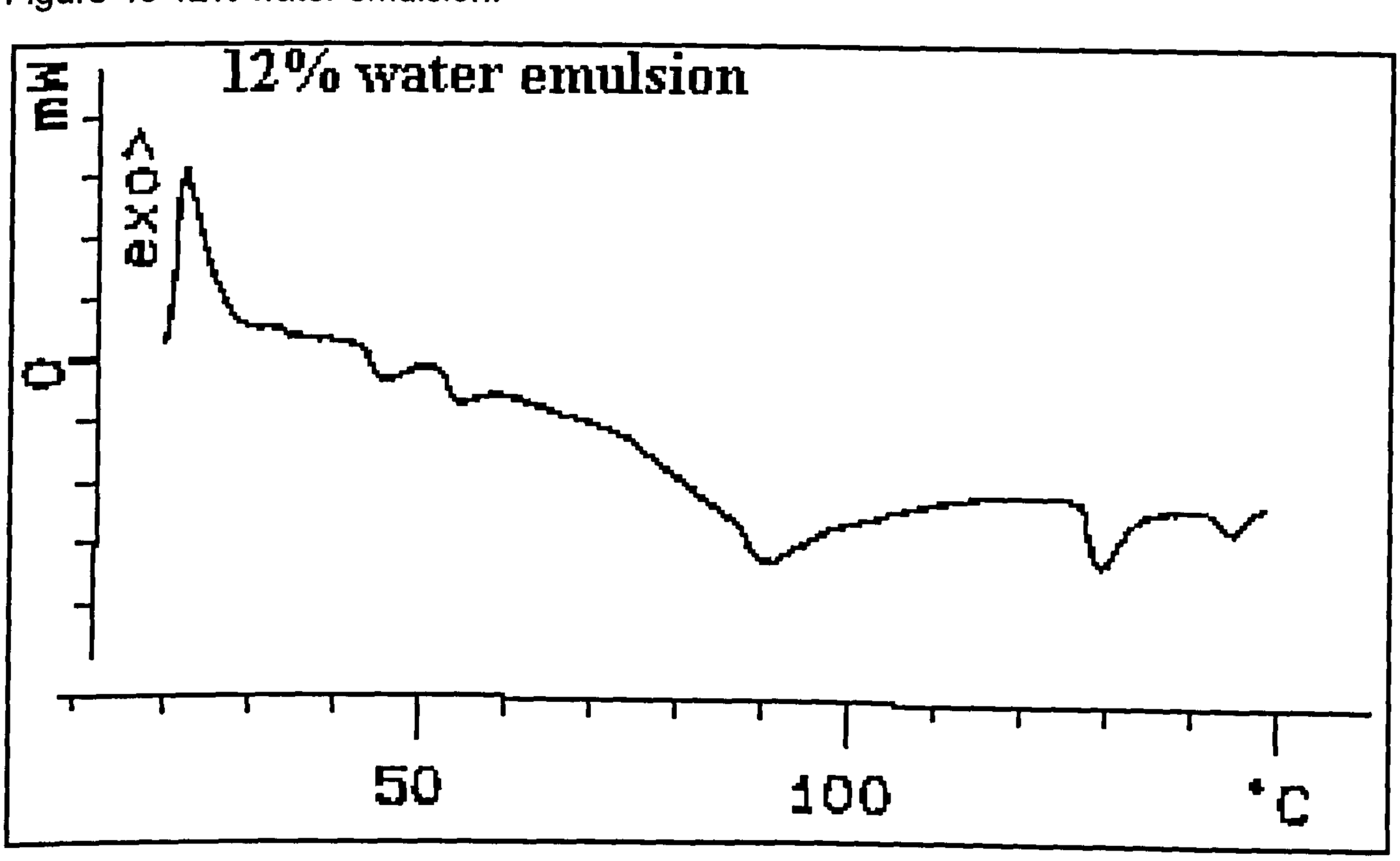

As the water content decreased from 25% to 20%, Figure 38, an endotherm can be seen at approximately 55°C. This is could be to be due to a IV-II phase transition, although this would only be expected to occur in a dry sample. A more plausible explanation for the endotherm would be that a degree of crystallisation had occurred in the sample and no phase change occurred, but the AN redissolved into the water. AN dissolving in water is a well-characterised endothermic process and this would seem an entirely plausible process to occur in the sample. The same endotherm is apparent but reduced for the 15% water emulsion, Figure 39, signifying that perhaps less crystallisation of this sample had occurred.

Figure 40 showed an unexpected result, with two endotherms in the 40-60°C region of the trace and another two endotherms at ~90°C and ~150°C respectively. These extra endotherms could be accounted for if crystallisation had occurred in parts of the emulsion to differing degrees. If the mixture was inhomogeneous, then the phase change could occur at different temperatures, due to differing conditions. An alternative explanation is that some of the AN had entirely crystallised, and come out of solution, and as heating of the sample occurred, the crystallised AN dissolved. The endotherms at ~50°C could then be separated with one endotherm being the redissolution of AN in one part of the sample, and the other endotherm from another part of the sample being a IV-II phase transition. This explanation is not entirely satisfactory and a more detailed examination of this process combining TGA and DSC could be utilised to further elucidate the process.

To further look at the effect of sample crystallinity, a 12% water emulsion sample, which had crystallised into a single solid piece, was analysed. Figure 41 shows an initial trace from this sample. This was placed in a sealed crucible, heated from 20°C to 170°C at 10K/min, and then allowed to cool to room temperature. Without removing the sample from the DSC, the cycle was repeated.

The first run shows an endotherm at approximately ~60°C, which could be the redissolution of part of the sample. There was a second endotherm at

approximately ~130°C, which, given the temperature this occurred at, is likely to be a II-I phase transition. The second run shows an initial endotherm at ~45°C rather than 60°C. This is likely to be a phase change, rather than the AN redissolving, although it was not possible to determine if this was a IV-II transition or a IV-III transition. There was another endotherm at ~90°C, which was not seen in the initial trace. This endotherm was seen in the dry AN prills and was determined to be the III-II phase transition. The process occurring in the sample, which causes the phase transitions to become apparent after initial heating was not apparent. Notwithstanding this, it is possible that the endotherms, at 60°C in the first trace, were the combination of the redissolution of AN and the III-II phase transition, which combined to form a single endotherm. Again, this is not an entirely credible explanation and more samples were run in an attempt to determine a pattern.

Figure 41 Crystallised emulsion sample (12% water) heated and allowed to cool then reheated.

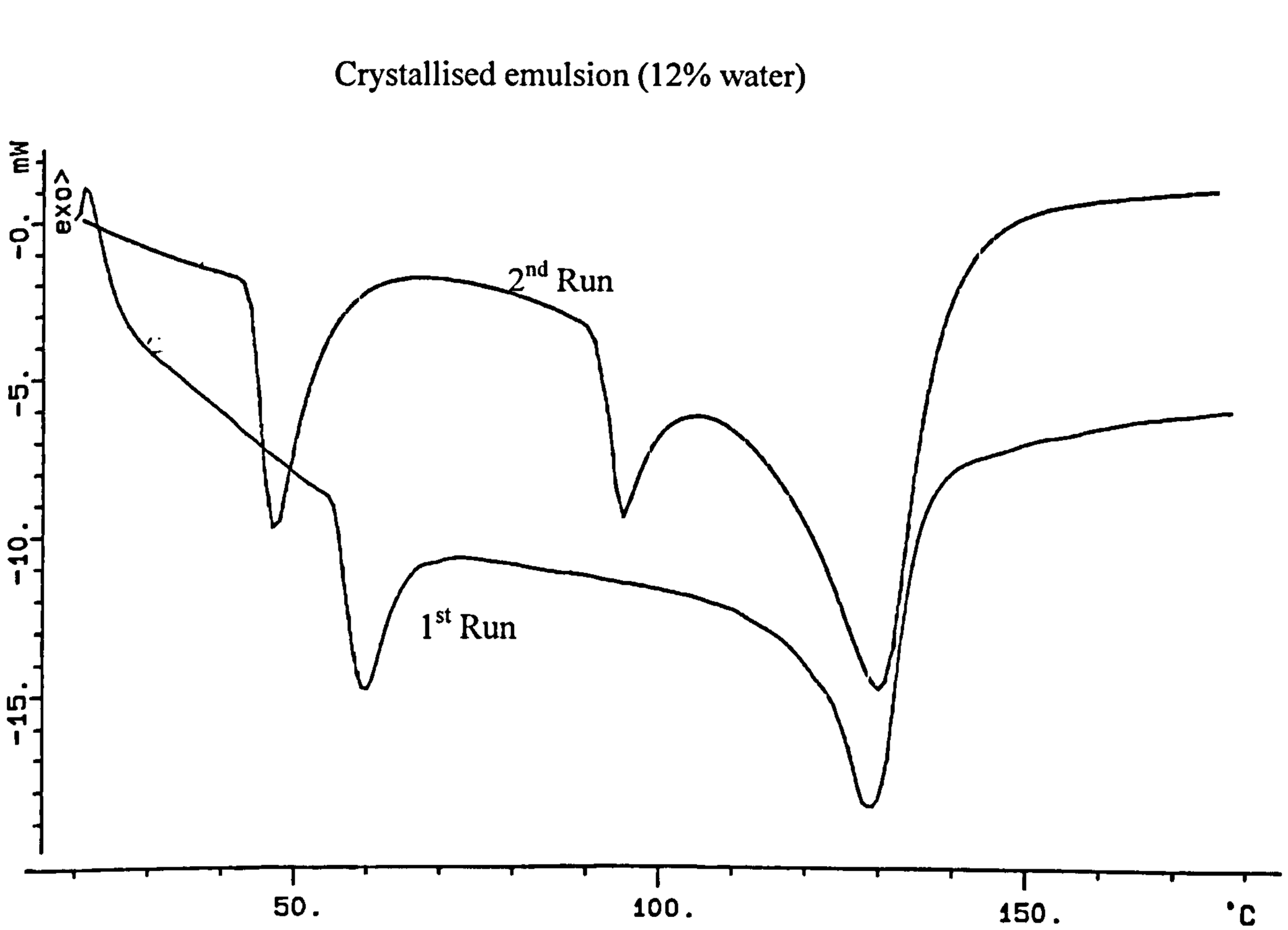

This was undertaken using the pieces of the same crystallised sample whilst keeping the conditions constant. The sample was cycled from 20°C to 180°C three times and this is shown in Figure 42.

Figure 42 Crystallised sample, (12% water) heat cycled 3 times.

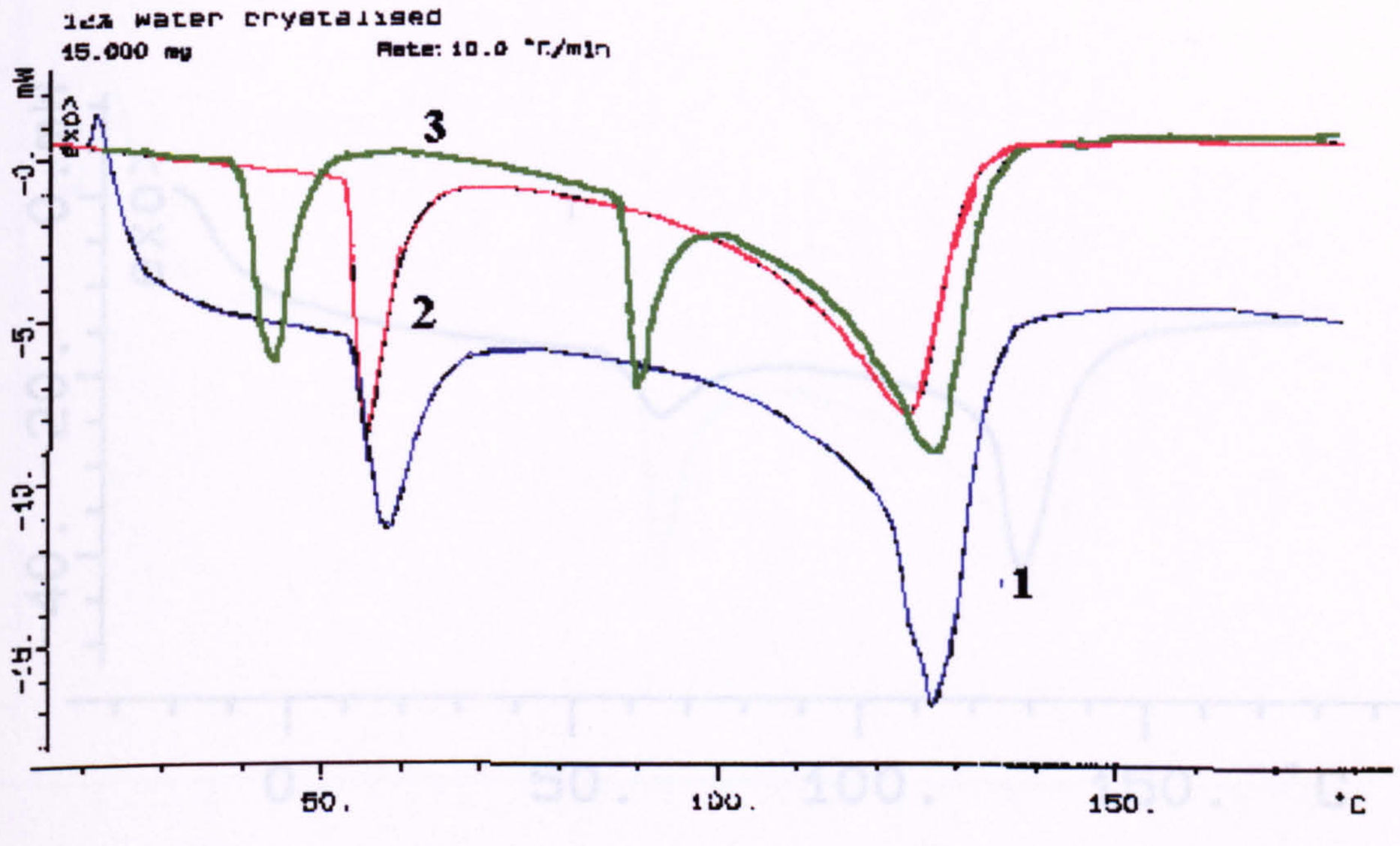

A similar pattern to Figure 42 was seen, with only two endotherms in the first run, although, in this trace, only two endotherms were seen on the second run. It was not until the third run that all three endotherms were seen. The polymorphic transitions that occur on heating of ammonium nitrate are changes in the crystal structure and as such should only occur at definite temperatures. The formation of solid solutions can cause the effects, due to polymorphic transitions to be displaced, or even disappear, owing to the retarding effect of isomorphous substitution on the process of phase transition. A solid solution being a crystalline material, which is a mixture of two or more components, with ions, atoms, or molecules of one component replacing some of the ions, atoms, or molecules of the other component in its normal crystal lattice. Compounds can form solid solutions if they are isomorphous. However, the crystallised emulsion was not a solid solution, so this would not seem to be a conceivable explanation of the process involved.

To prove that the previous results were not spurious they were repeated and some the results of this are shown on the following pages.

Figure 43 DSC trace crystallised sample (15.3mg) –20°C-180 °C.

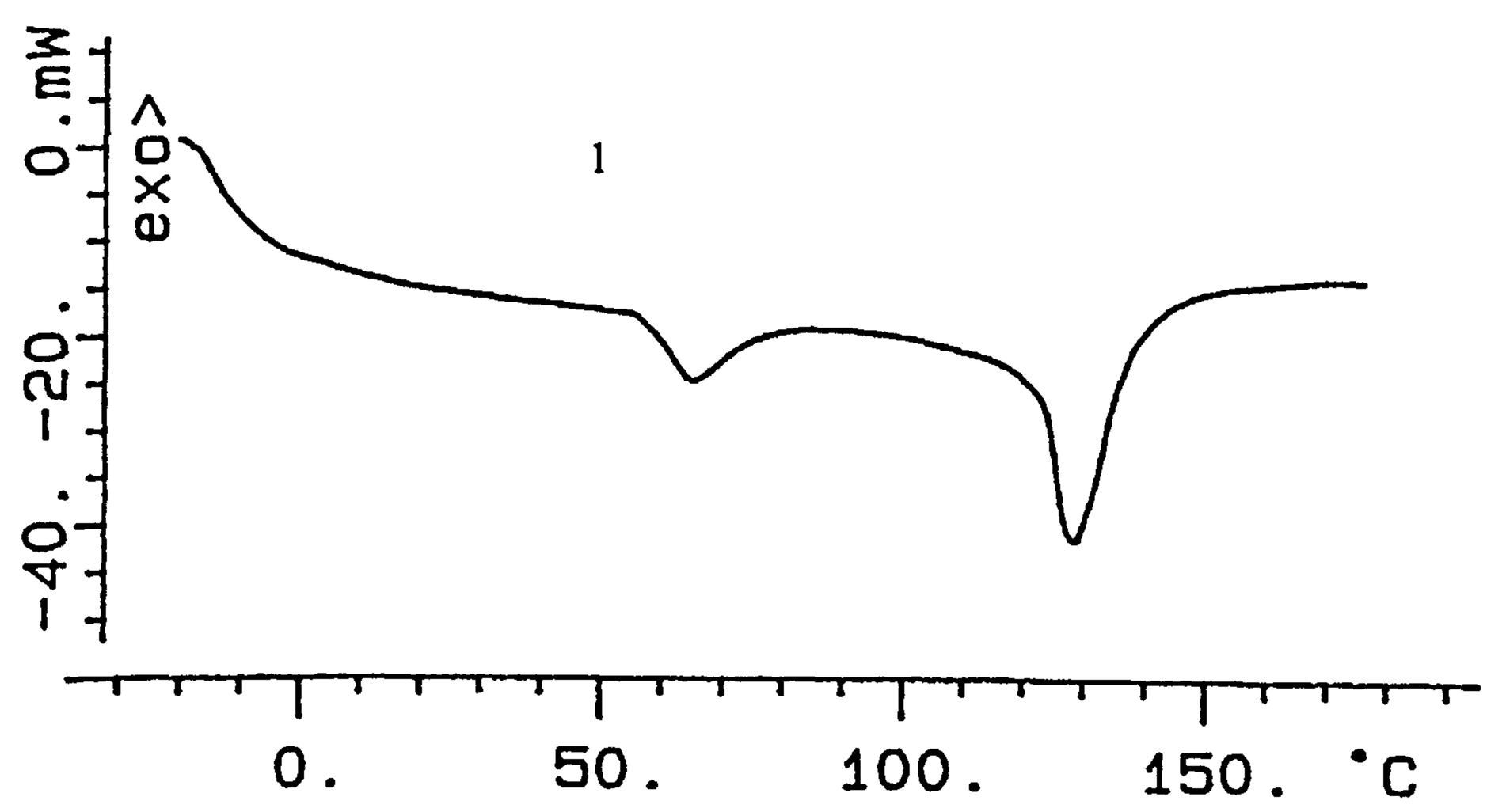

Figure 44 Second run, after Figure 43.

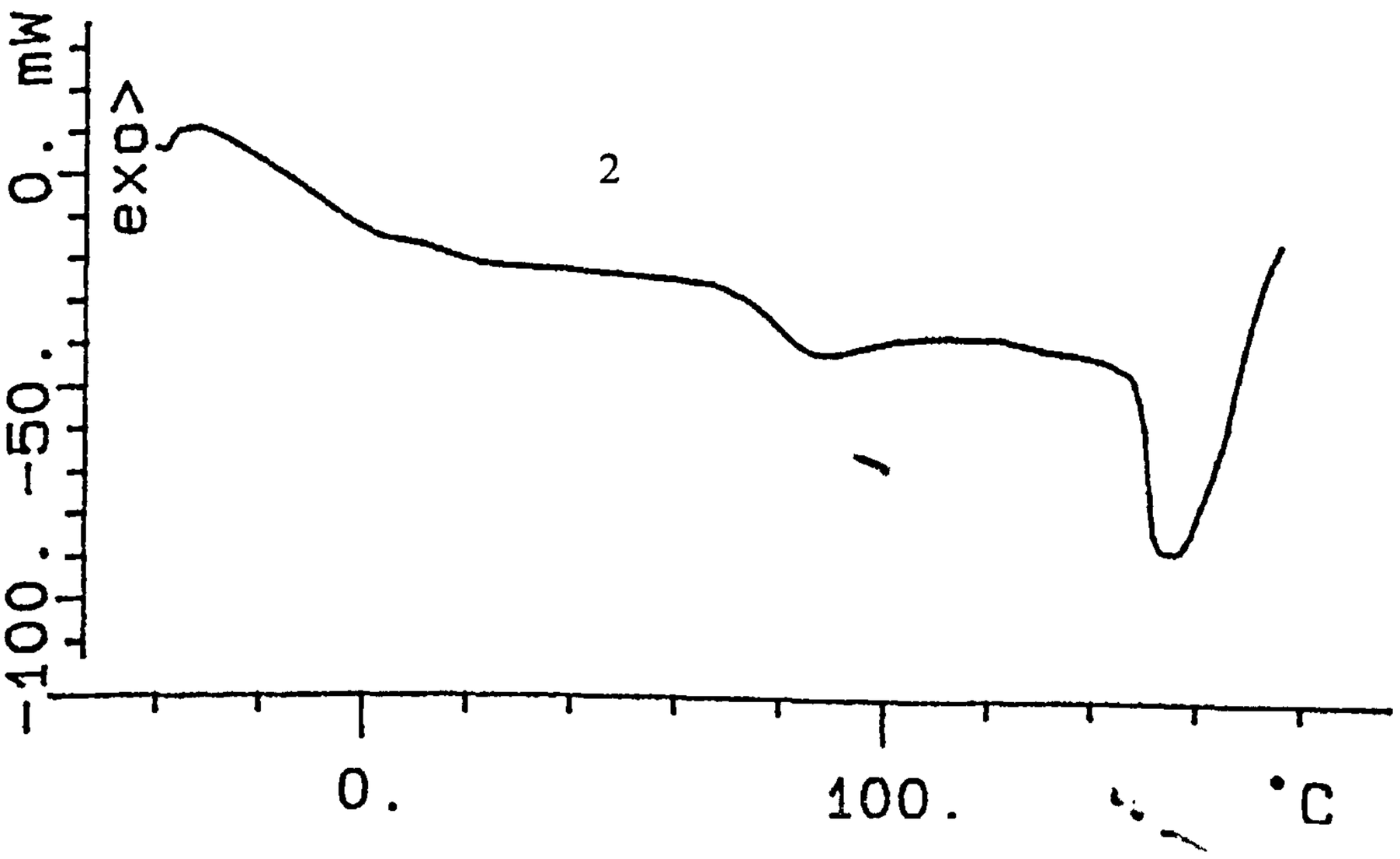

Figure 45 Final run, after Figure 44.

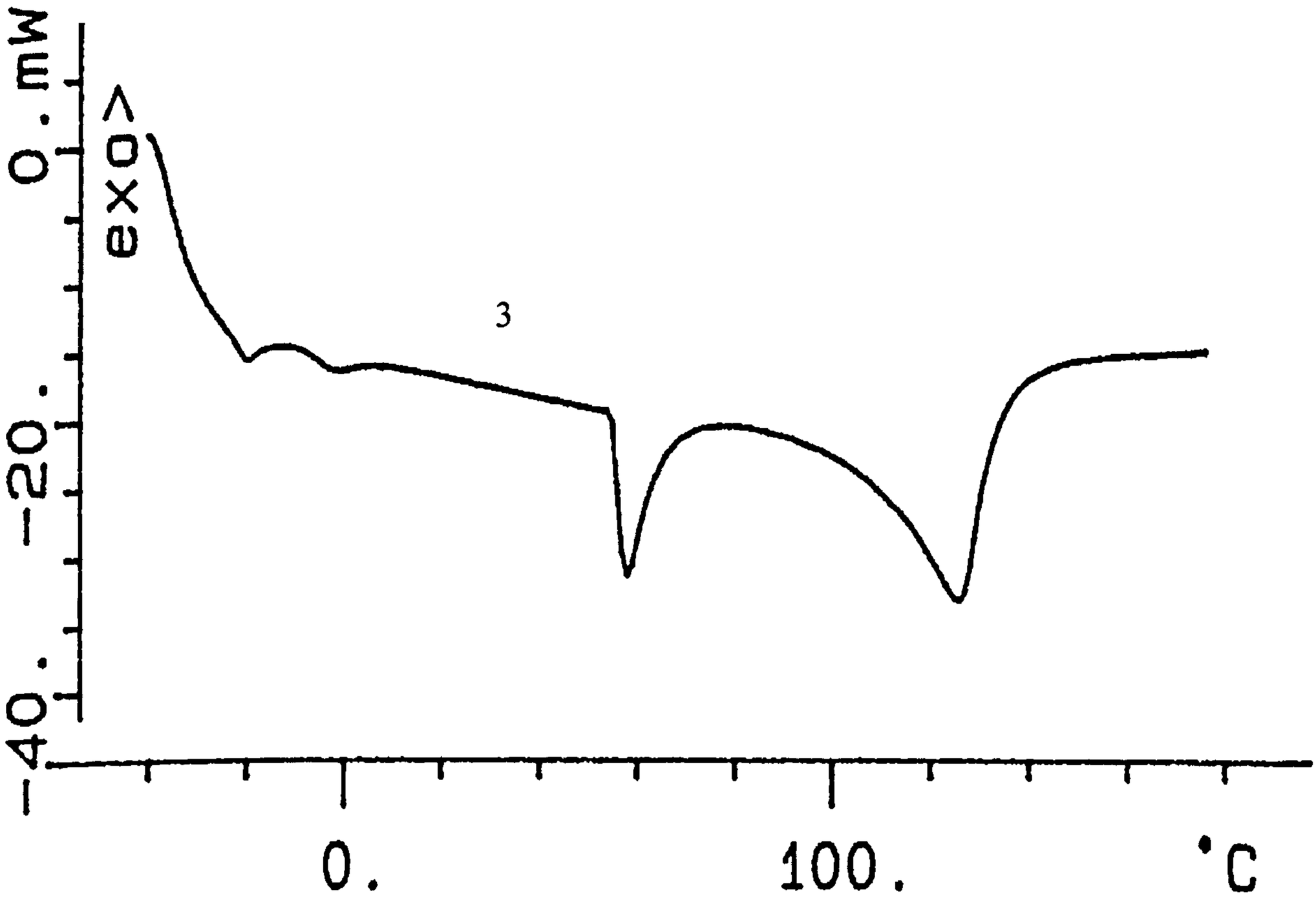

Figure 46 Large sample size, 100.8mg.

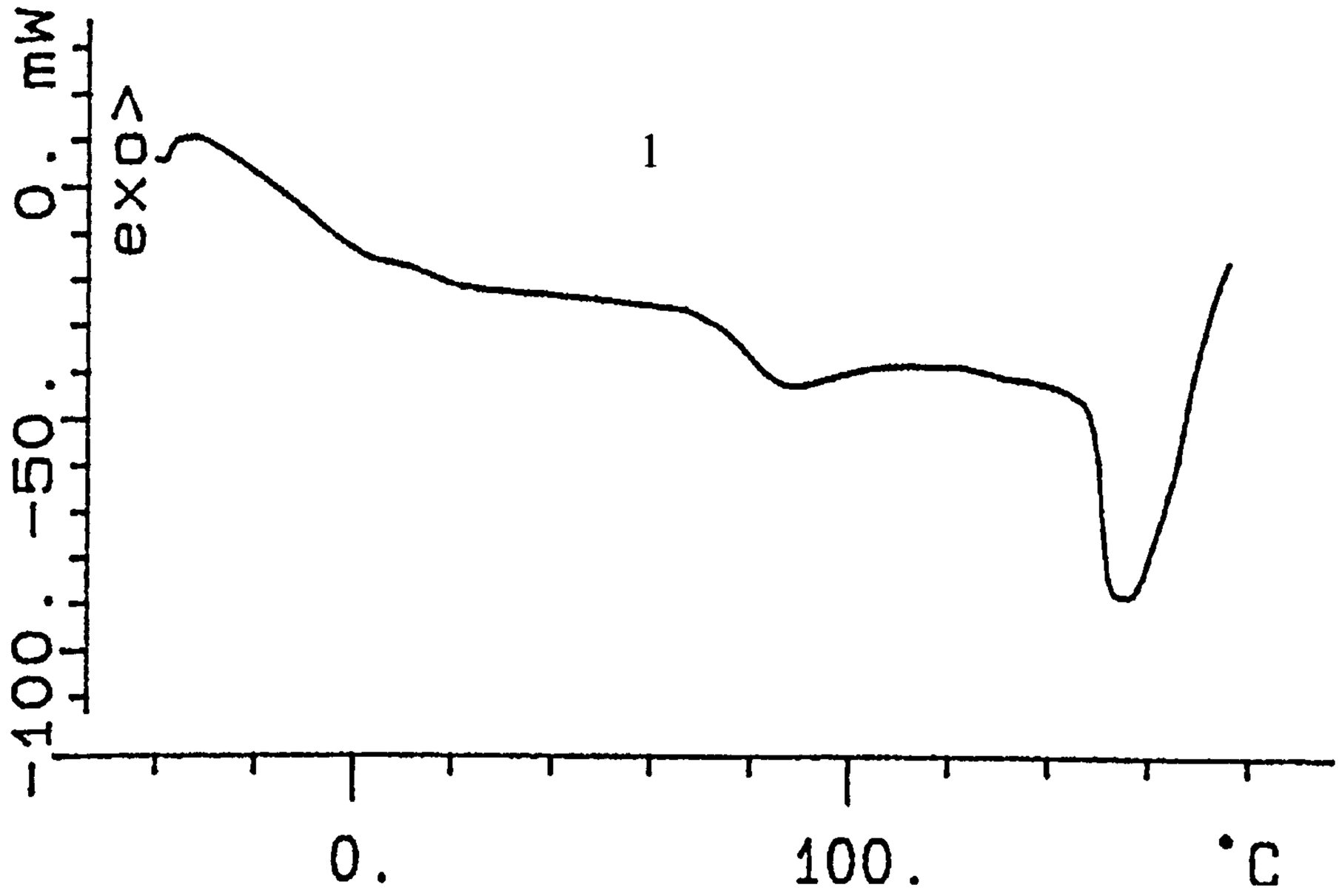

Figure 47 Second run, after Figure 46.

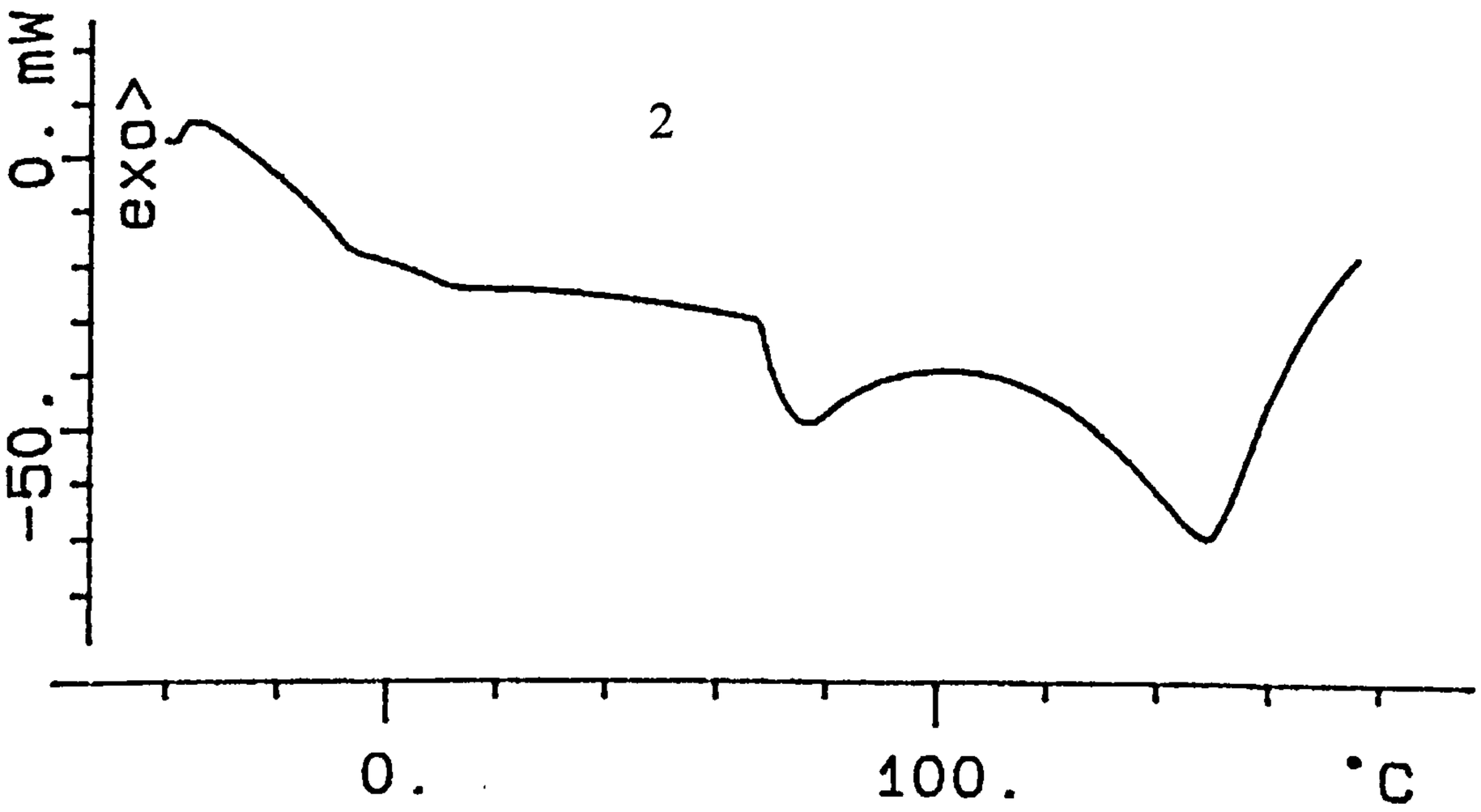

Figure 48 Third run, after Figure 47.

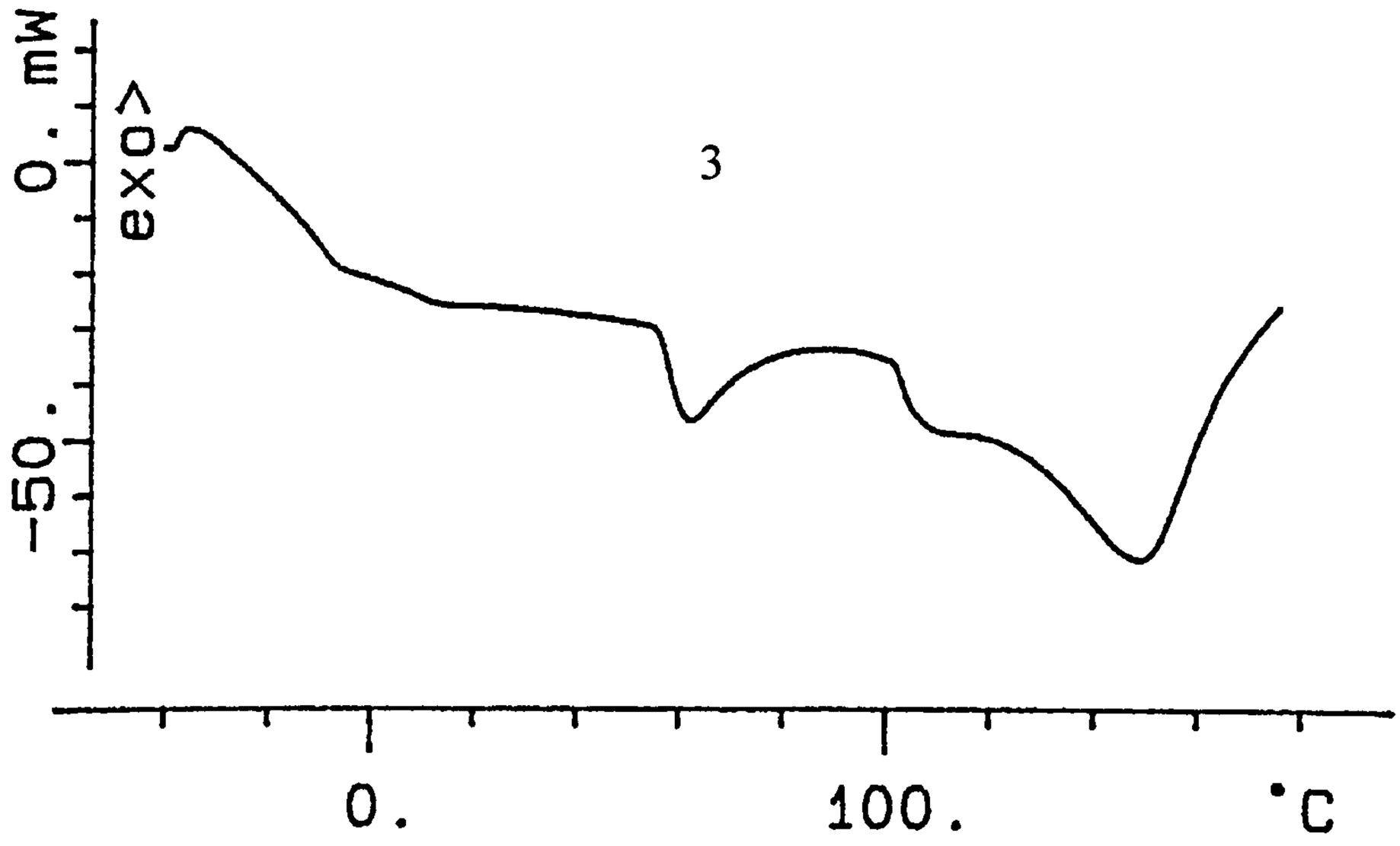

Figure 49 Final run, after Figure 48.

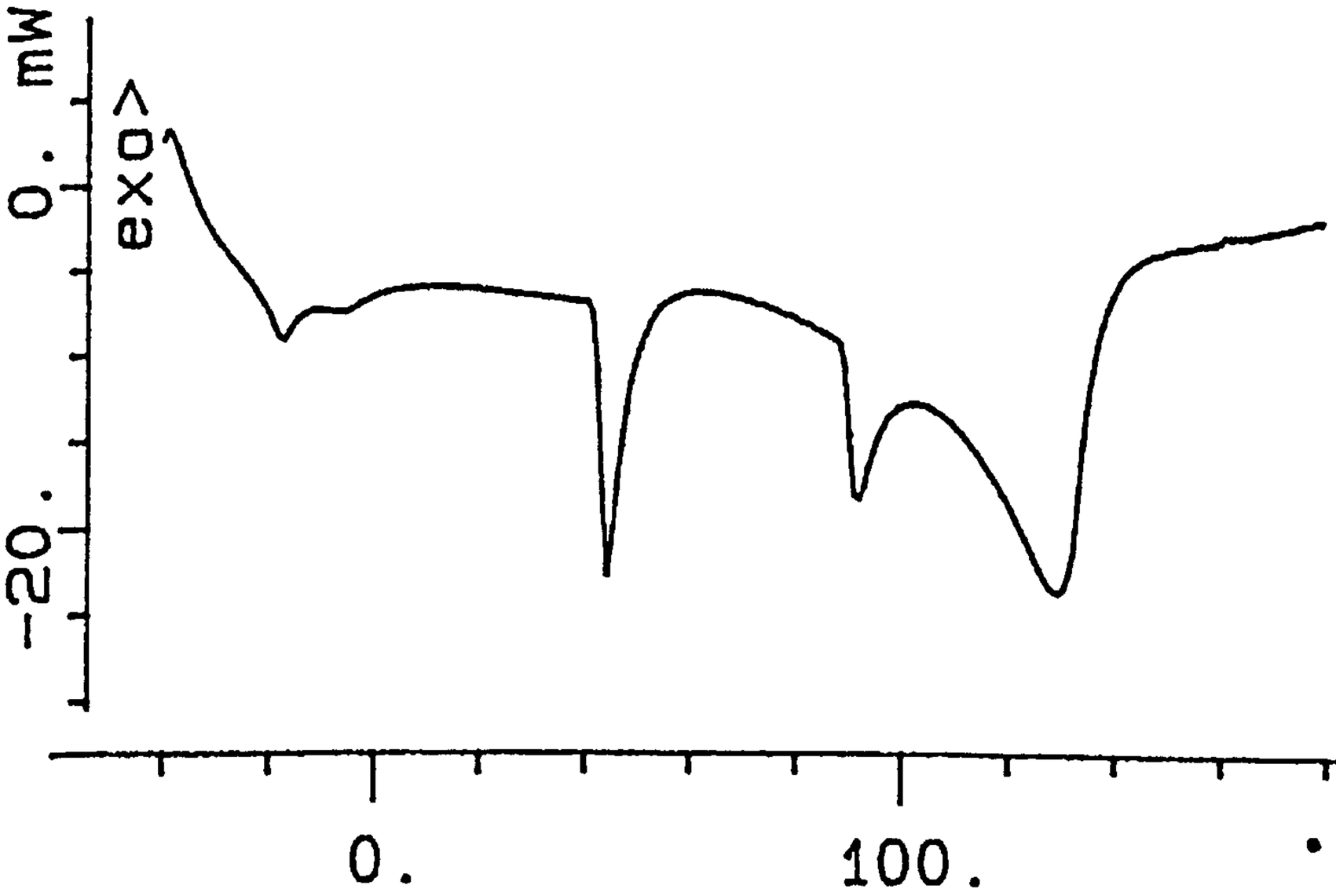

Figure 43 to Figure 49, along with numerous repeated experiments, show that the results were not abnormalities. In a crystallised emulsion sample repeated heating cycles were required before the endotherms become apparent. Although repeating the experiments confirmed that this was an actual process, it did not help to clarify the mechanism by which it occurred.

To help elucidate the reaction process occurring in the crystallised emulsion sample, analysis of the gaseous reaction products was undertaken. Large (100mg) samples, of crystallised 12% water emulsion were sealed in gas tight aluminium crucibles. The crucibles were then heated, in the DSC, in a repeated heating cycle, in the same manner as the previous samples. After the heating cycle, the crucibles were placed in a glass sample vial Figure 50, which was sealed with a self-sealing rubber septum. The crucibles were then pierced and the gaseous products were analysed by headspace GC-MS.

Figure 50 Method used for gas analysis of crucibles.

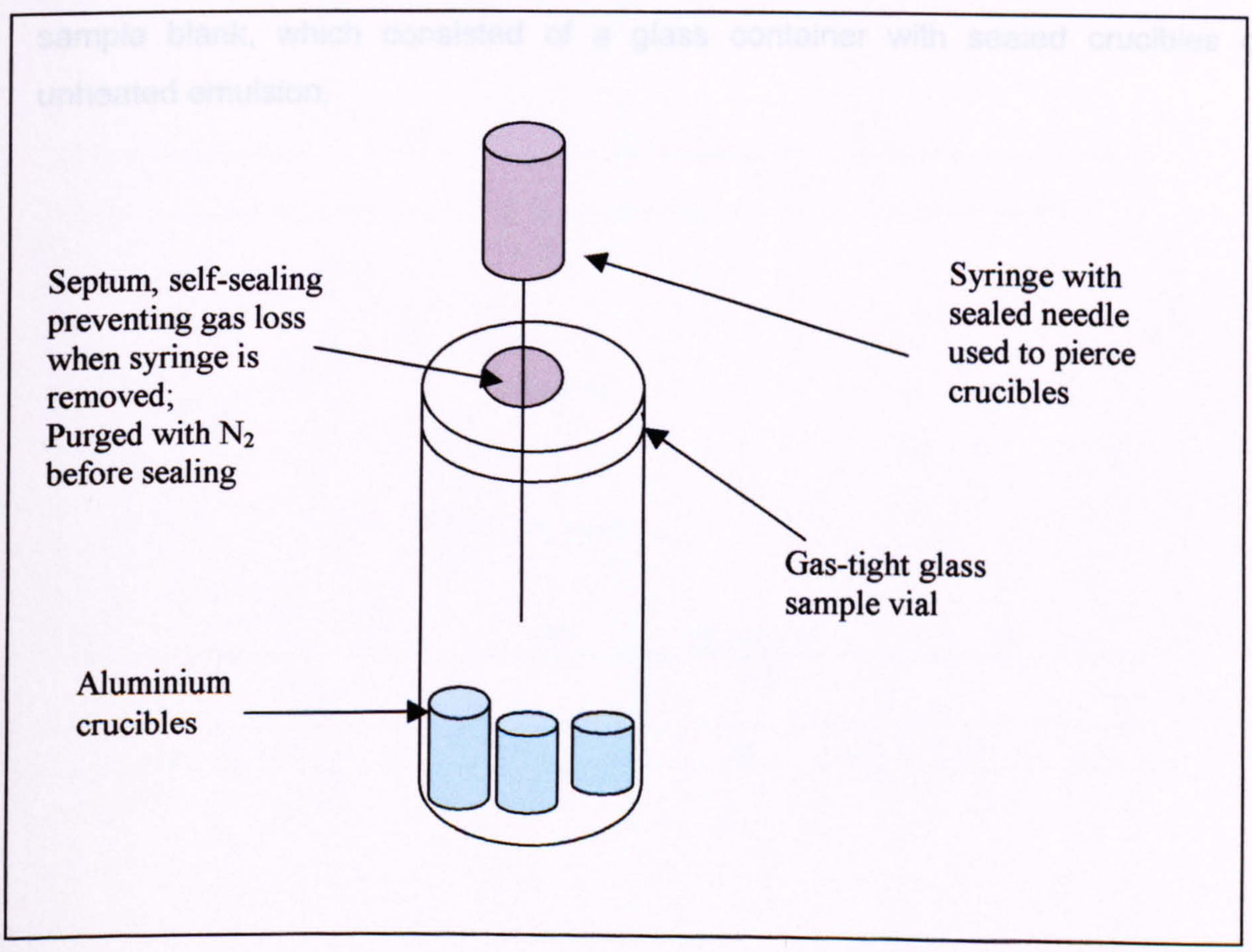

It would be expected that ammonium nitrate would begin to decompose at the upper temperature limit of the experiment (170°C). If this happened then N_2O would be formed, along with water, as shown in the reaction below.

Equation 16 Decomposition of AN.

$$NH_4NO_3 \longrightarrow N_2O + 2H_2O$$

Analysing the gas from the crucibles, for the presence of N_2O, would show whether decomposition had occurred. N_2O is a neutral oxide and does not form hyponitrous acid ($H_2N_2O_2$) with water or hyponitrites with alkali. Therefore, water should remain unreacted (if formed) in the container. If decomposition were occurring, then water could be the catalyst for the polymorphic phase changes in the ammonium nitrate.

The samples were analysed and compared to two blanks. One blank consisted of an empty sample container purged with N_2 before analysis. The other was a sample blank, which consisted of a glass container with sealed crucibles of unheated emulsion.

Figure 51 GC-MS traces m/z 44.

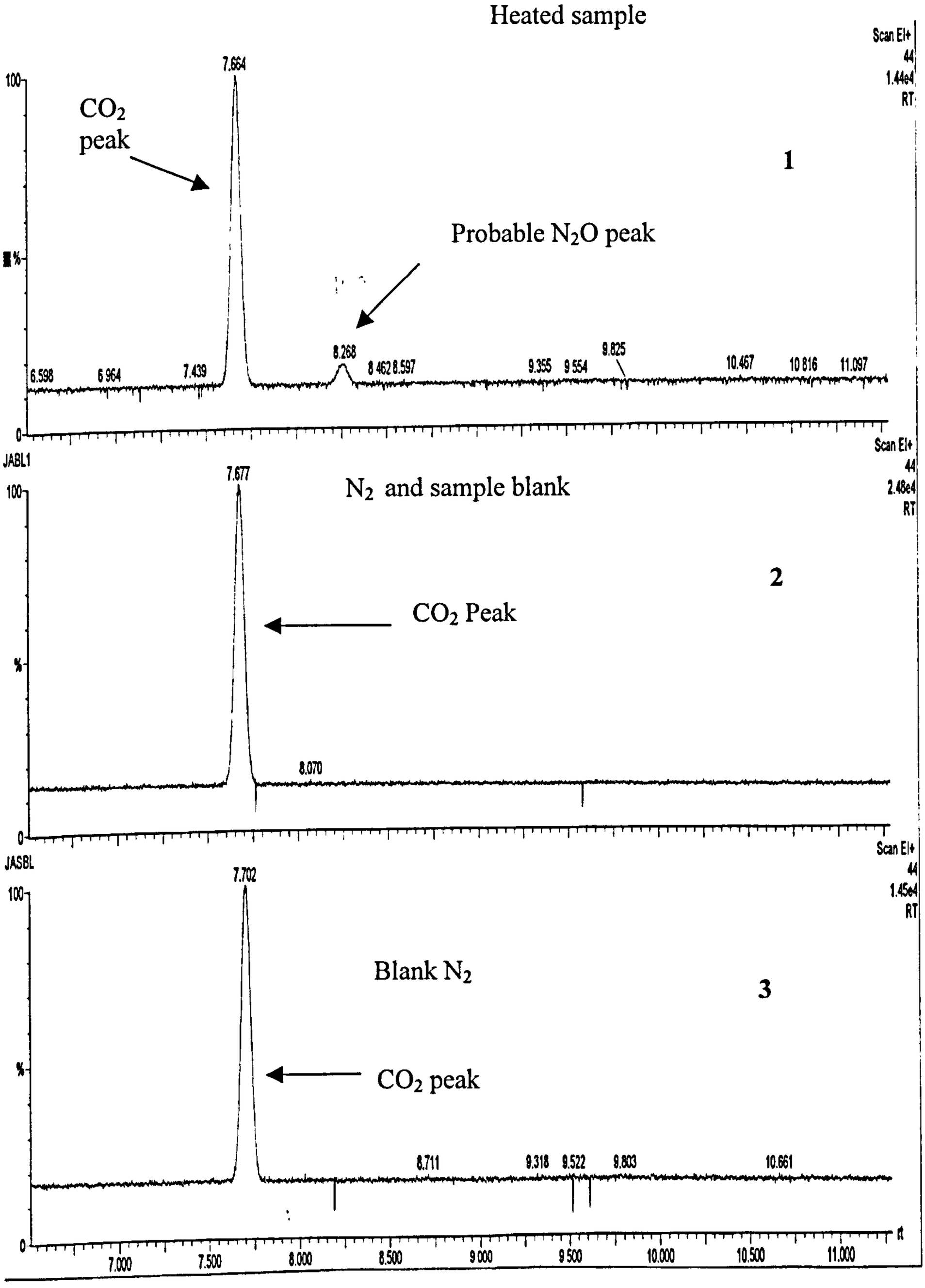

The retention time for CO_2 and N_2O was 7.6min and 8.2min respectively. It can be seen that there is a small peak at 8.2min in the sample trace, which is absent in the blank traces. The two peaks, from the sample trace, were analysed by mass spectrometry to determine their fragmentation pattern and identities. These show the expected fragmentation for N_2O and CO_2 respectively.

Figure 52 Mass analysis of peak at RT 8.2min.

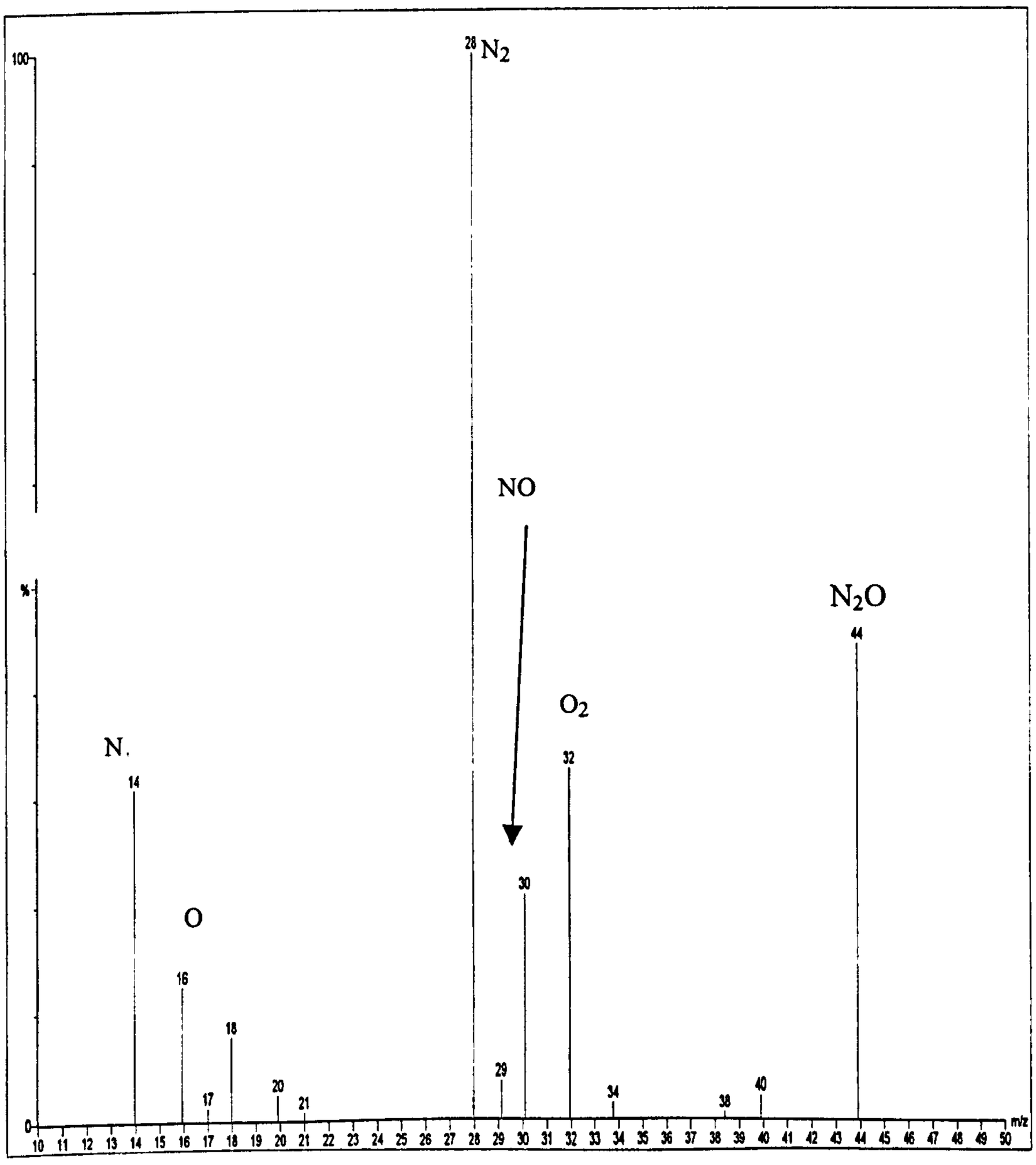

Analysis of the atomic masses, in Figure 52 shows that the peak at RT 8.2min is almost certainly N_2O. There was no peak at m/z 12 whilst there are peaks at mass weight 14, 30 and 32, which were not present in the CO_2 spectrum (Figure 53).

Figure 53 Mass analysis of CO_2 peak, RT 7.6min.

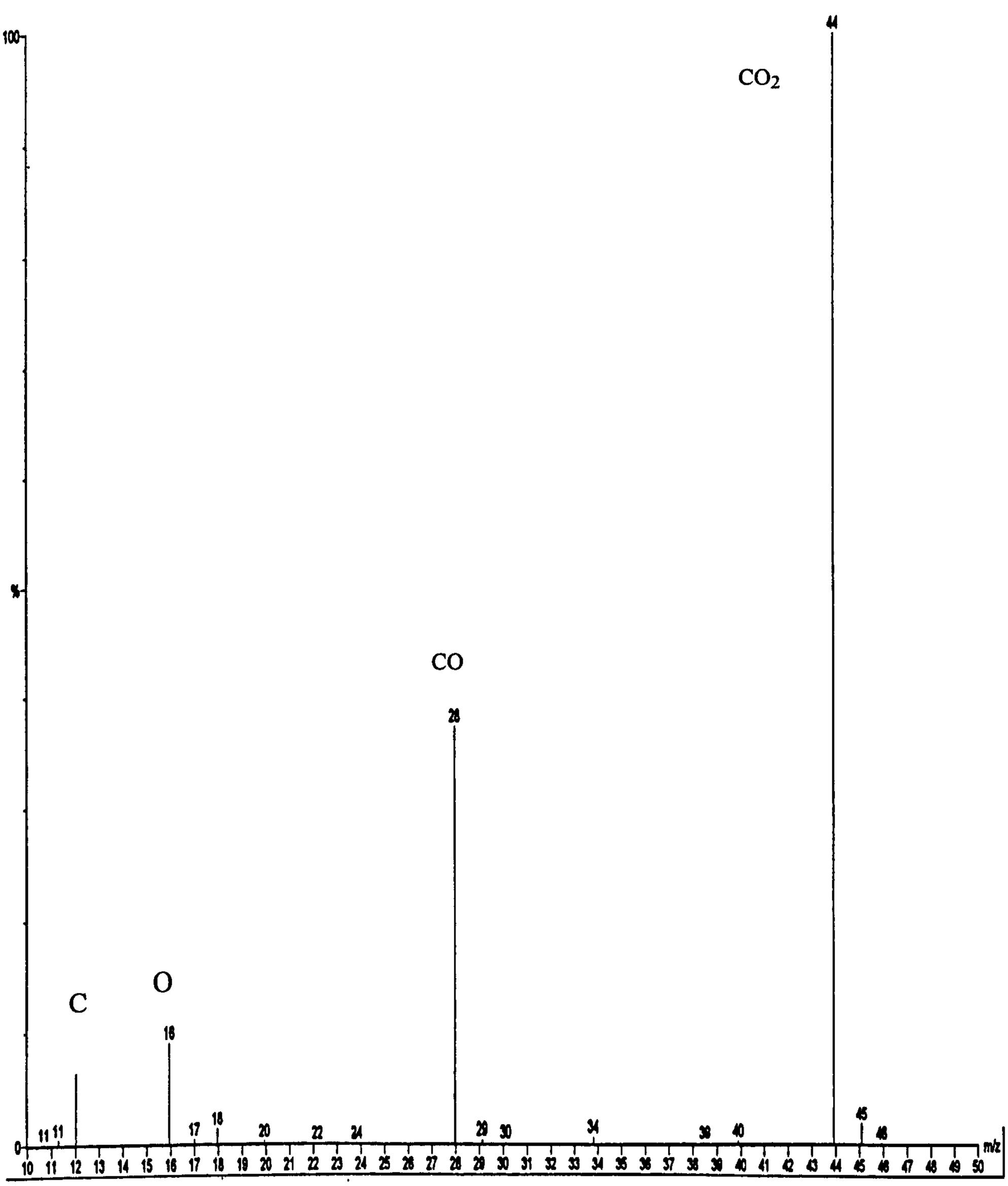

If N_2O is formed in the heating of the sample, then water will be produced as well.

$$NH_4NO_3 \longrightarrow N_2O + 2H_2O$$

Water, specifically H_3O^+, is suggested to be the catalyst for the phase transitions[90] in AN. As water is being generated through, the decomposition AN, this could be providing a source of H_3O^+ and thereby catalysing the reaction. Notwithstanding this, the crystallised emulsion sample should have water present and thereby the H_3O^+ ion should be present.

A reason for the water in the emulsion not catalysing the reaction could be that oil and emulsifiers are present in the sample. If, when the sample completely comes out of solution and crystallises, the water is expelled from around the crystal structure and oil then surrounds this, it could be argued that there is no water available to catalyse the reaction. This argument is purely based on supposition, with, as yet, no evidence and much further research beyond the scope of the present study required, but in my opinion this is plausible

3.7 Explosive performance results

3.7.1 Introduction

The explosive ordnance range (ERDA) is a purpose built facility where explosive firings can take place. Up to 400g of explosive material may be fired outside and up to 1kg inside a purpose built containment building. All firings below 400g, for this study, were conducted outside so that they could be observed. Figure 54 shows a prepared charge as seen from the firing point.

Figure 54 Explosive ordnance research range, with a charge prepared for firing.

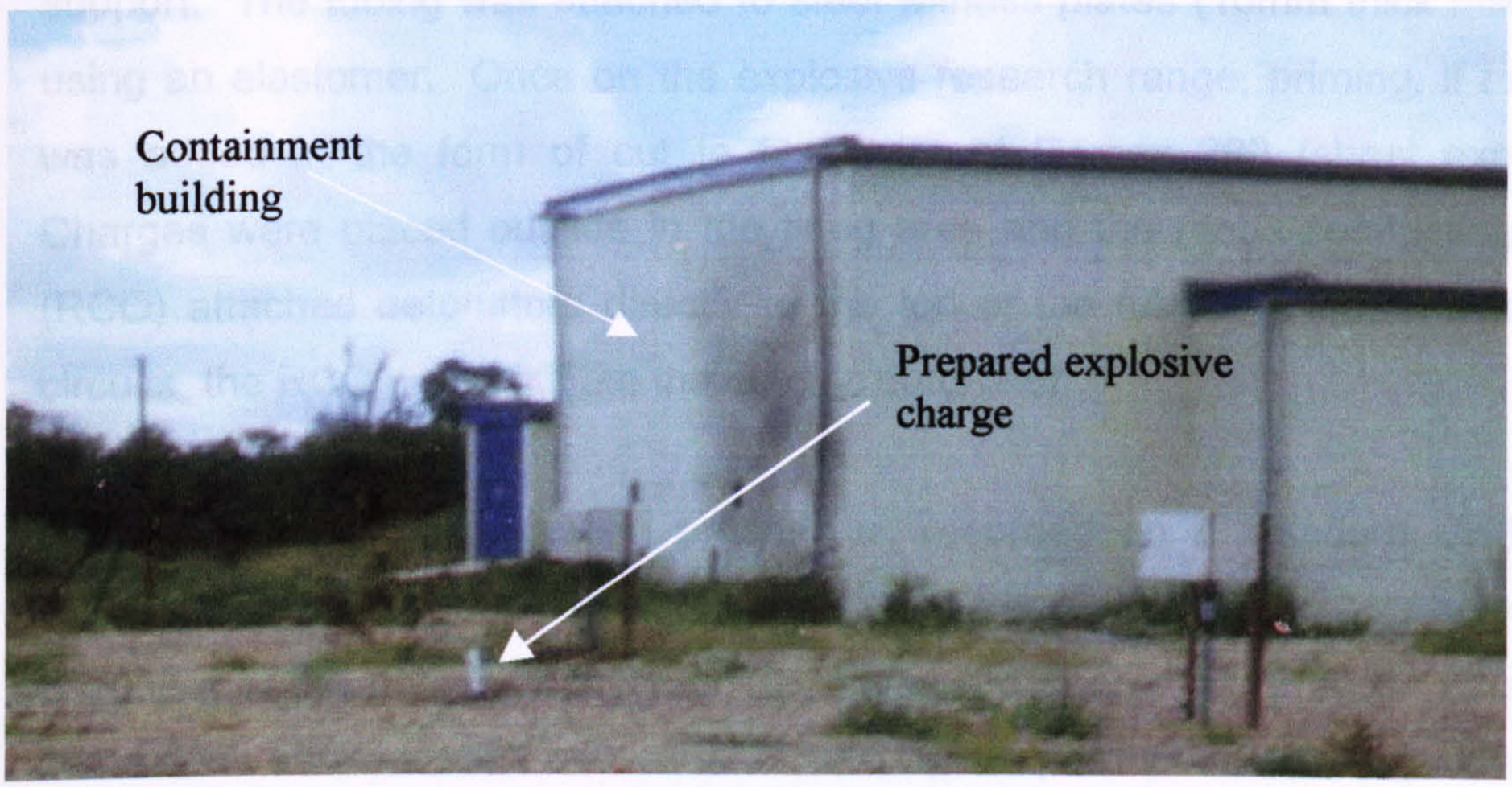

Figure 55 Detonation of charge- note the white cloud.

Figure 55 shows a charge initiating; it was noted that there was a bright yellow flash upon detonation and a large plume of white smoke. All firings that propagated showed this, with the intensity of the flash and amount of smoke produced being variable.

Charges were prepared, mixed and initiated within 24h on the ERDA range. This was done to minimise any effects of ageing on the emulsion matrix. Prepared emulsions were placed into plastic tubing (39mm polypropylene) as these provided a minimum degree of confinement whilst still providing the necessary degree of support. The tubing was attached to steel witness plates (10mm thick mild steel) using an elastomer. Once on the explosive research range, priming, if required, was added in the form of cut to fit sheets of Demex 200 (sheet explosive). Charges were placed outside in the firing area and the range-conducting officer (RCO) attached detonators directly to the top of the tubing. After checking the circuits, the RCO would initiate the electric detonator.

Figure 56 shows the initiation process as recorded on a standard VHS video camera. Standard video can only record at 15 frames per second, so only a brief snapshot of the process can be seen. Figure 56 shows this process as a bright flame flash as detonation occurred followed by the production of a large amount of gas. The smoke cloud did not disperse rapidly, but slowly dissipated into the surrounding area in a process that took minutes rather than seconds. In Figure 56 frame 2, the charge can be seen at the beginning of the initiation process. The detonator, and primer have initiated and the emulsion is just starting to propagate. The escape of the hot gases and flame can be clearly seen to be coming predominately upwards, from the top of the charge.

Figure 56 Emulsion initiating.

3.7.2 Hot spot temperatures in the emulsion

By calculating the detonation pressure applied by the priming explosive, used in the trials, Demex 200 sheet explosive, it was possible to determine the hot spot temperature of the microballoons. The detonation pressure for Demex 200 was first calculated:

Equation 17 Calculation of detonation pressure for Demex 200

$$Dp = 2.5 * 10^{-6} * VOD^{2} * \rho$$

$$VOD = 7{,}200\ ms^{-1}$$

$$\rho = 1.63$$

$$\therefore$$

$$Dp = 2.5 * 10^{-6} * 7{,}200^{2} * 1.63$$

$$= 211\ kbar$$

Using the calculated detonation pressure and knowing the initial pressure of the microballoons (0.2bar), the hot spot temperature can be determined using Bowden and Yoffe's equation.

Equation 18

$$T_2 = T_1\left(\frac{p_2}{p_1}\right)\frac{(\gamma-1)}{\gamma}$$

$$\gamma = 1.29,\ p_1 = 0.2\text{bar}$$

$$p_2 = 207.5\text{kbar}$$

$$T_1 \approx 293\text{K}$$

$$\therefore$$

$$T_2 = 293\left(\frac{207500}{0.2}\right)^{\left(\frac{1.29-1}{1.29}\right)}$$

$$T_2 \cong 6596\text{K}$$

The average hot spot temperature would be in the region of 6000°C. Eyring[91] in his treatise stated that the calculated critical hot spot temperature for initiation is dependent on the radius of the hotspot. The larger the radius the lower the critical temperature required before initiation occurs.

Table 11 Critical hot-spot temperatures for hot-spot radii as calculated by Eyring.

Explosive	$r = 10^{-3}$m	10^{-4}m	10^{-5}m	10^{-6}m
PETN	310°C	385 °C	495 °C	640 °C
RDX	380 °C	485 °C	615 °C	815 °C
HMX	410 °C	510 °C	645 °C	825 °C
Tetryl	425 °C	570 °C	815 °C	1250 °C
Ammonium nitrate	590 °C	825 °C	1230 °C	2180 °C

The average radius for the microballoons, before being crushed by the shock wave, is in the region of 3 $x10^{-5}$ m. The hot-spot temperatures achieved are therefore higher than that required to initiate ammonium nitrate, without the presence of oil. The critical temperature for emulsions is not known but, given the high temperature achieved, microballoons would be expected to provide an adequate initiation source for the shocked explosive.

3.7.3 Velocity of detonation data

Emulsions were formulated, as described in the experimental section, and velocity of detonation measurements taken. For each variant of the emulsion, change in water and microballoon content, at least four explosive firings (and an average of eight) were undertaken, to acquire representative data. The data from this was then tabulated, and is shown in Figure 57, as a plot of percentage theoretical maximum density (TMD) versus VOD. (Percentage theoretical maximum density is taken as a percentage of the density compared to the base emulsion with no added microballoons). The error bars on Figure 57, show the standard deviation calculated for each emulsion based on the variation in measured VOD. As plotted in this form the data is hard to interpret, although it is possible to see a slight parabola. This data is also presented, in a different form, in Figure 58.

From Figure 58 it is possible to see that the data shows a hill type profile. At low water contents, there is a high ridge between 2.5 and 3.5% microballoon content. As the water increases to 25%, a peak is seen where the highest VOD is observed. Beyond 25% water content, there is a rapid drop as the observed VOD falls. Figure 57 also shows that at low water contents the VOD is more stable across the microballoon range.

Figure 57 Velocity of detonation versus %TMD.

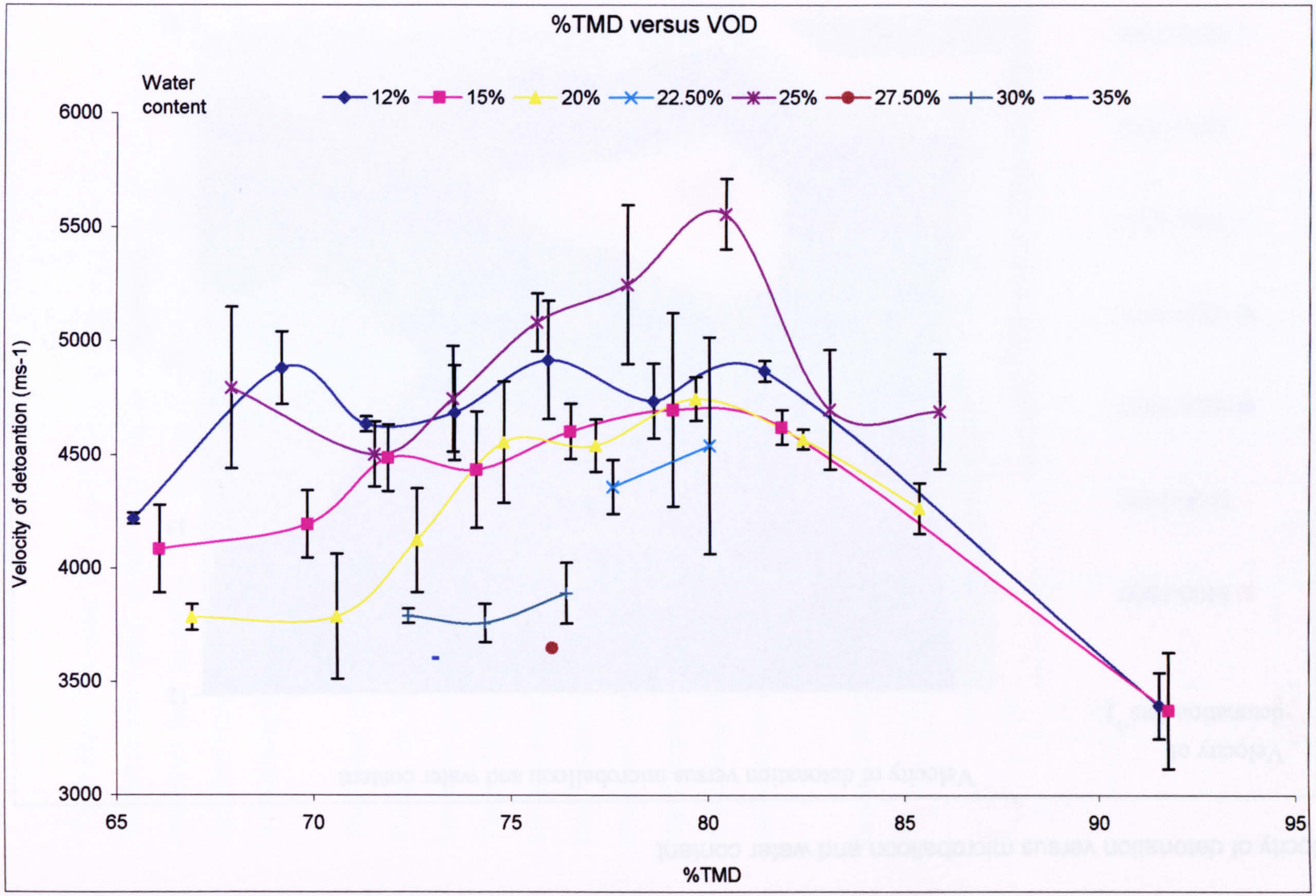

Figure 58 Velocity of detonation versus microballoon and water content

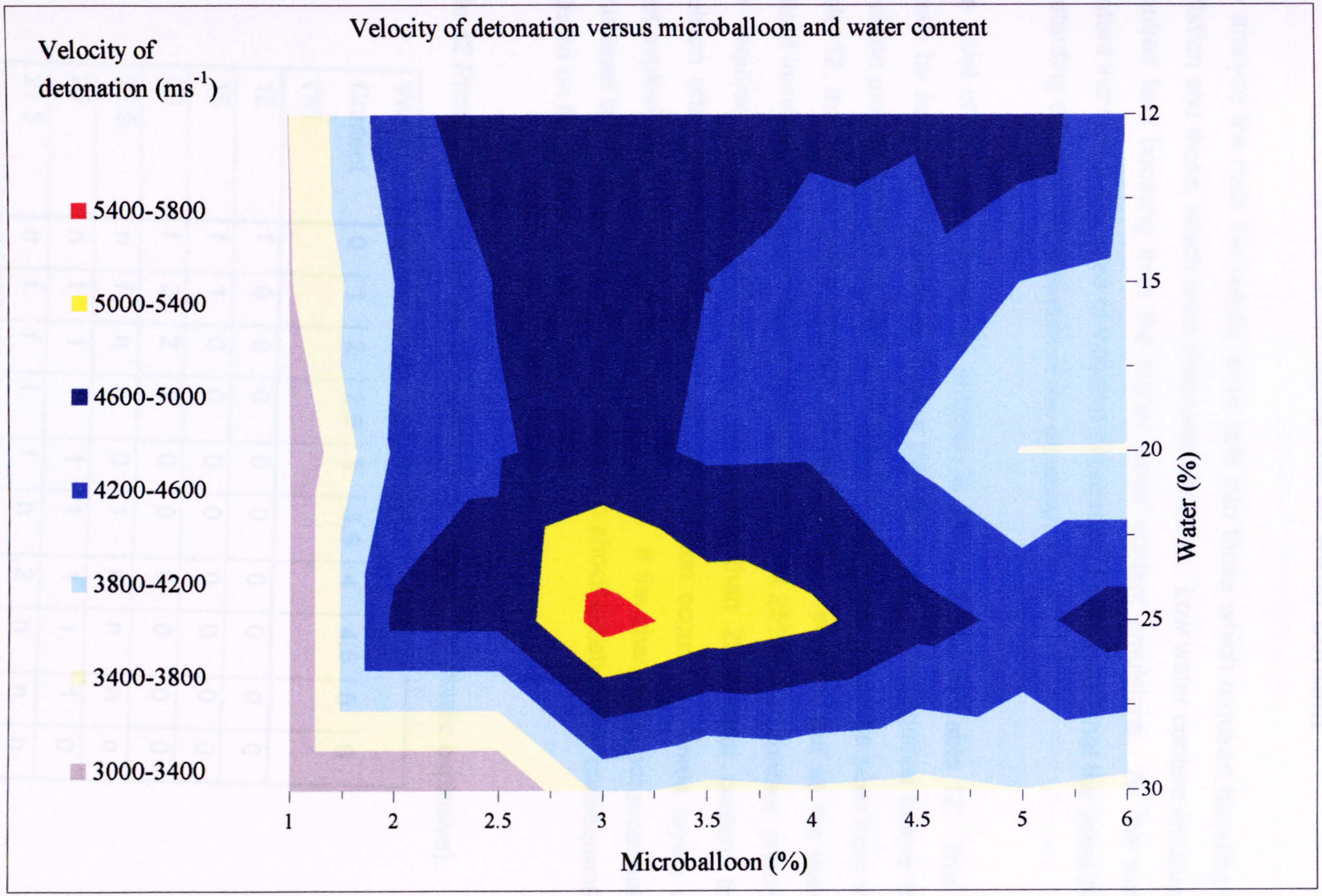

3.7.4 VOD data plotted as functions of water content

To analyse the data the results were split into those which required boosting for initiation and those, which were detonator sensitive. Low water content emulsions required less boosting than the higher water content emulsions. As the water content increased, the ease of initiation decreased; this showed that the water had a retarding effect on the initiation of the emulsion.

The level of priming required for initiation is shown below in Table 12. This is shown by how many sheets of Demex 200 explosive were required before the emulsion propagated and an explosive reaction occurred. It can be seen from the Table 12, that at low water content, no priming was required, but as the water content increased priming became a requirement. At 25% water content, priming was required for every formulation. At higher than 25% water content the emulsion often failed to propagate and no reaction occurred. Three layers of sheet explosive was the maximum priming used. If the charge did not propagate at this level then it was considered insensitive to shock initiation and consequently not listed on the table.

Table 12 Priming required for initiation (sheets of Demex 200 plastic explosive).

Water Content (%)	Microballoon content (%)									
	0	1	2	2.5	3	3.5	4	4.5	5	6
12	f	0	0	0	0	0	0	0	0	0
15	f	1	0	0	0	0	0	0	0	0
20	f	3	2	2	0	0	0	0	0	0
22.5	n	f	n	n	0	1	n	n	n	n
25	n	f	1	1	1	1	1	1	1	0
27.5	n	f	f	f	f	n	2	n	n	n
30	n	f	f	f	2	n	1	n	1	n
35	n	f	f	f	f	f	f	f	1	n

f- failed to propagate n- not tested

Table 12 shows that 12% water content emulsion required no priming, but with a microballoon content of less than 1%, it failed to propagate, even with four sheets of Demex 200. When the water content was increased to 20%, at low microballoon content, priming was required for initiation. More priming was required at 20% water content than for 25% water content for equivalent low microballoon contents. For this to have occurred there must be a change in the initiation mechanism, which increased the sensitivity of the 25% water emulsion.

To analyse the VOD data for the emulsions it was determined that splitting the data into separate water contents, and plotting these against percentage TMD, would aide interpretation of the data. The error bars, as shown in Figure 59, are the standard deviation as calculated from the data. The fitting parabolas shown are that of a line of best fit for a second order polynomial, as plotted by the spreadsheet software.

Figure 59 12% water content emulsion explosive.

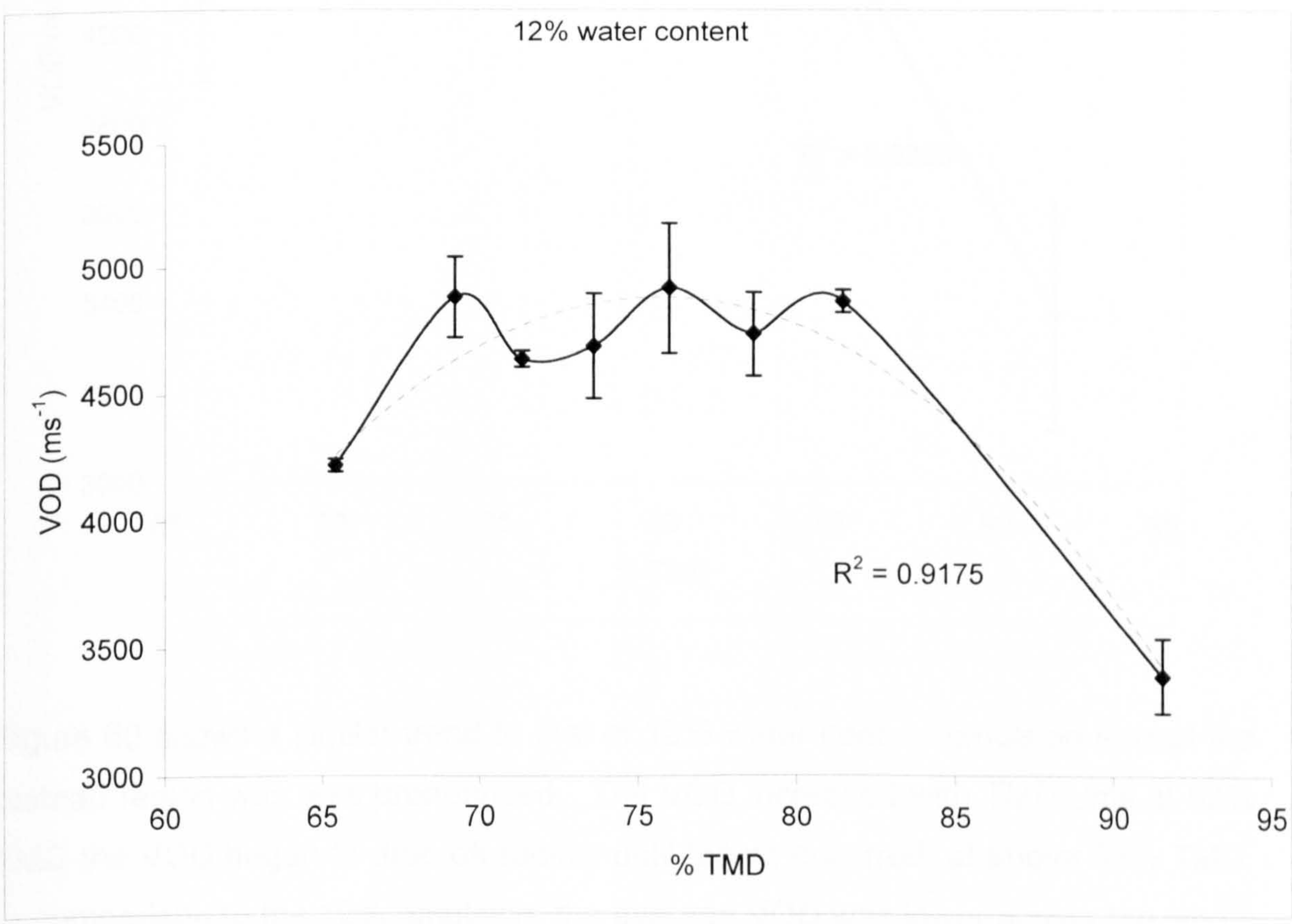

In Figure 59, the VOD showed an initial increase with increasing TMD followed by a plateau region (70-83% TMD) where the VOD remained reasonably constant at around 4750ms^{-1}. As the TMD increased beyond 83%, there was a rapid drop in VOD down to 3400ms^{-1}, followed by failure to initiate. This was a classical Type II non-ideal explosive behaviour, which mirrors the type of results recorded by Price.

Figure 60 15% water content emulsion explosive.

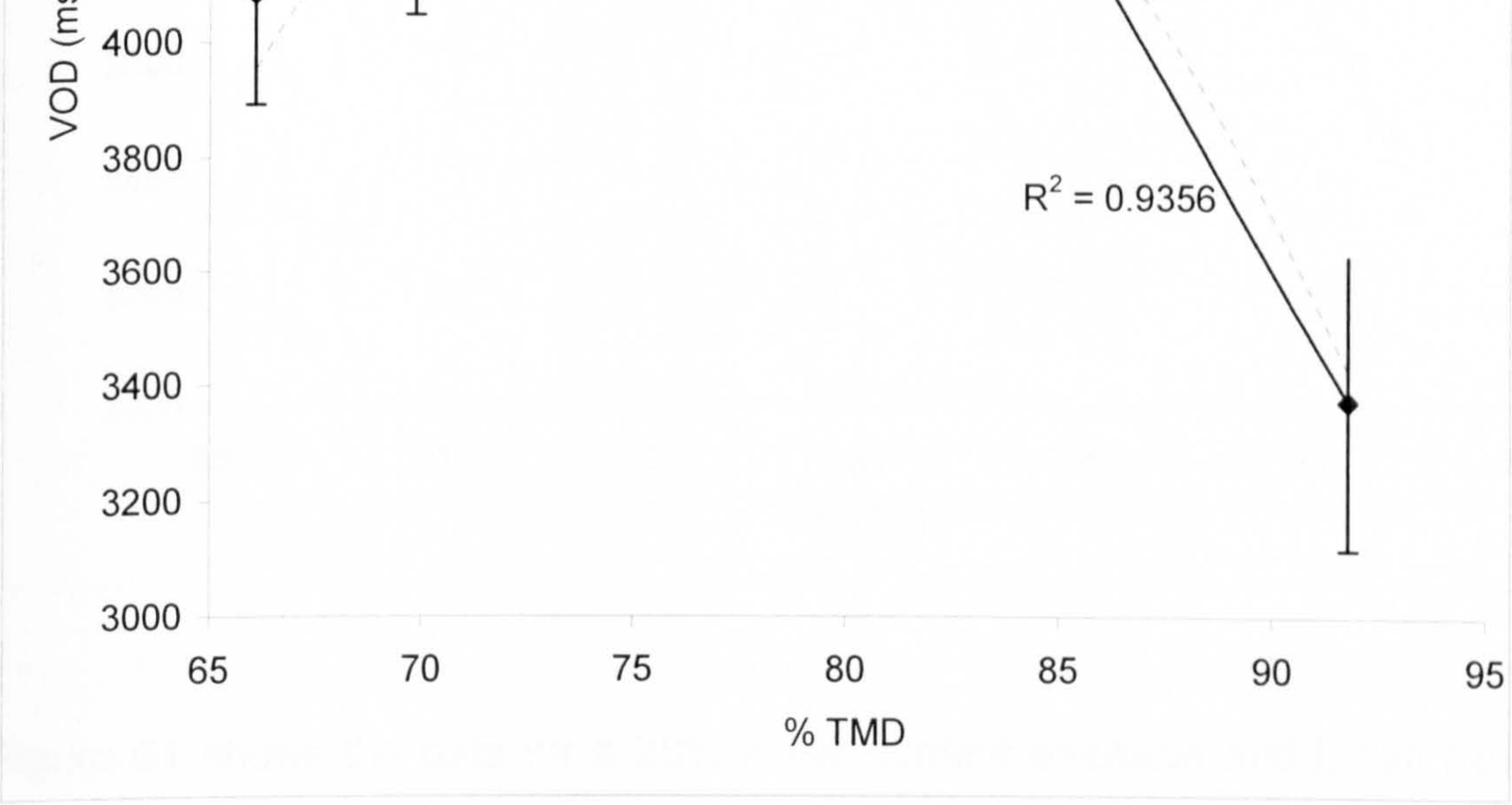

Figure 60 shows a similar trend to that of 12% water content emulsion except the plateau region was less pronounced. The VOD increased with TMD until at 82% TMD the VOD began to drop off rapidly until failure occurred, at above 93% TMD. In comparison to the 12% emulsion, the average VOD was lower across the whole

TMD range but this was not a significant drop in performance. Again, this showed a classical type II non-ideal explosive behaviour.

Figure 61 20% water content emulsion explosive.

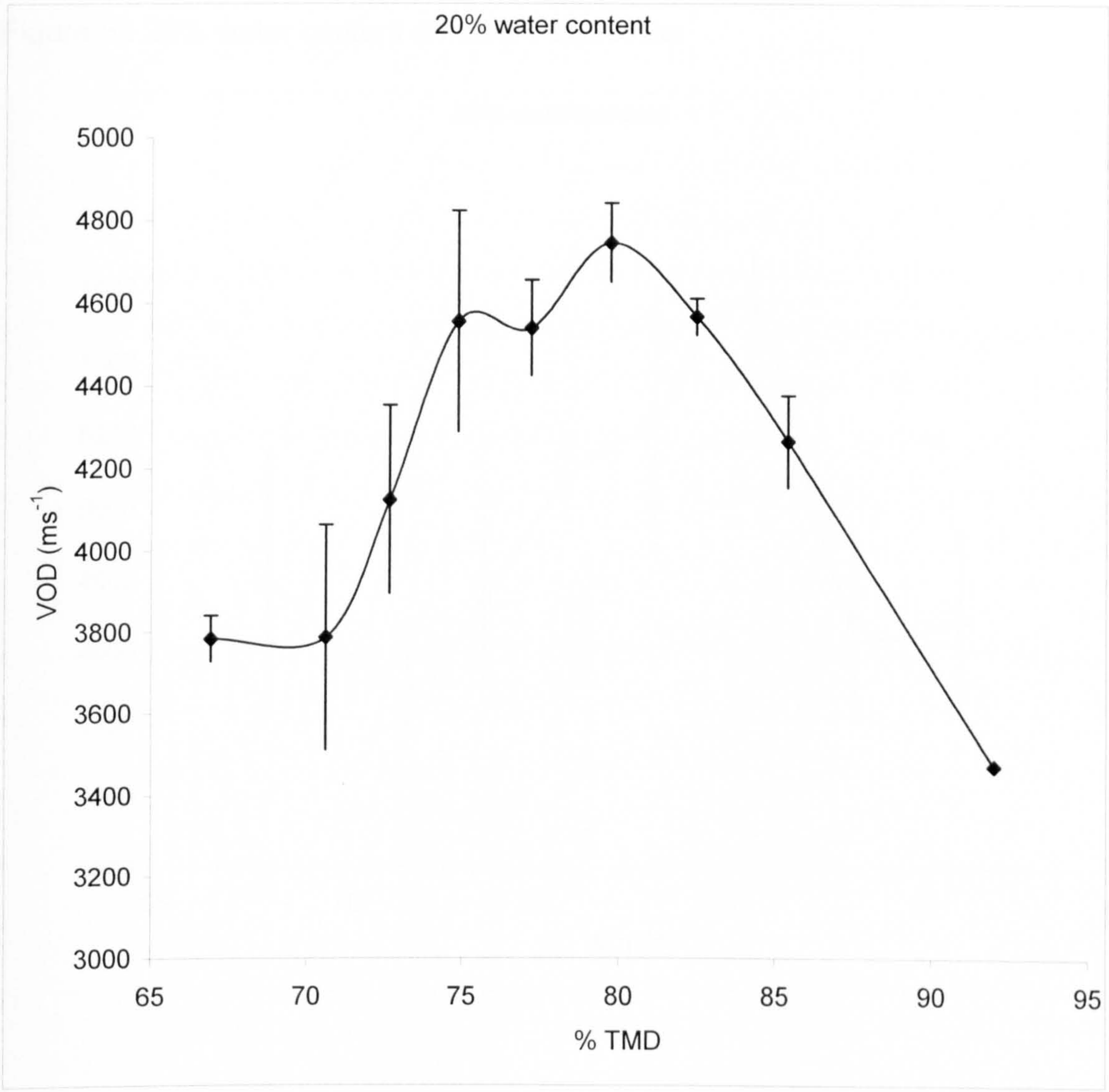

Figure 61 shows the data for a 20% water content emulsion and it can be seen that there was approximately 30% difference in VOD between the highest, 4918ms^{-1}, and lowest, 3472ms^{-1}, VOD. This was not considered excessive and would be considered typical for VOD versus TMD relationships. The data shows that the 20% water emulsion underwent a rapid rise in VOD with TMD before peaking at around 80% TMD. At higher than 80% TMD there was a slow drop off in VOD, although not as rapid a drop as observed with the lower water content

emulsions. This slow drop off could be accounted for as at high TMD the 20% water emulsion required priming for initiation, and once the reaction started it was sustained.

Figure 62 25% water content emulsion explosive.

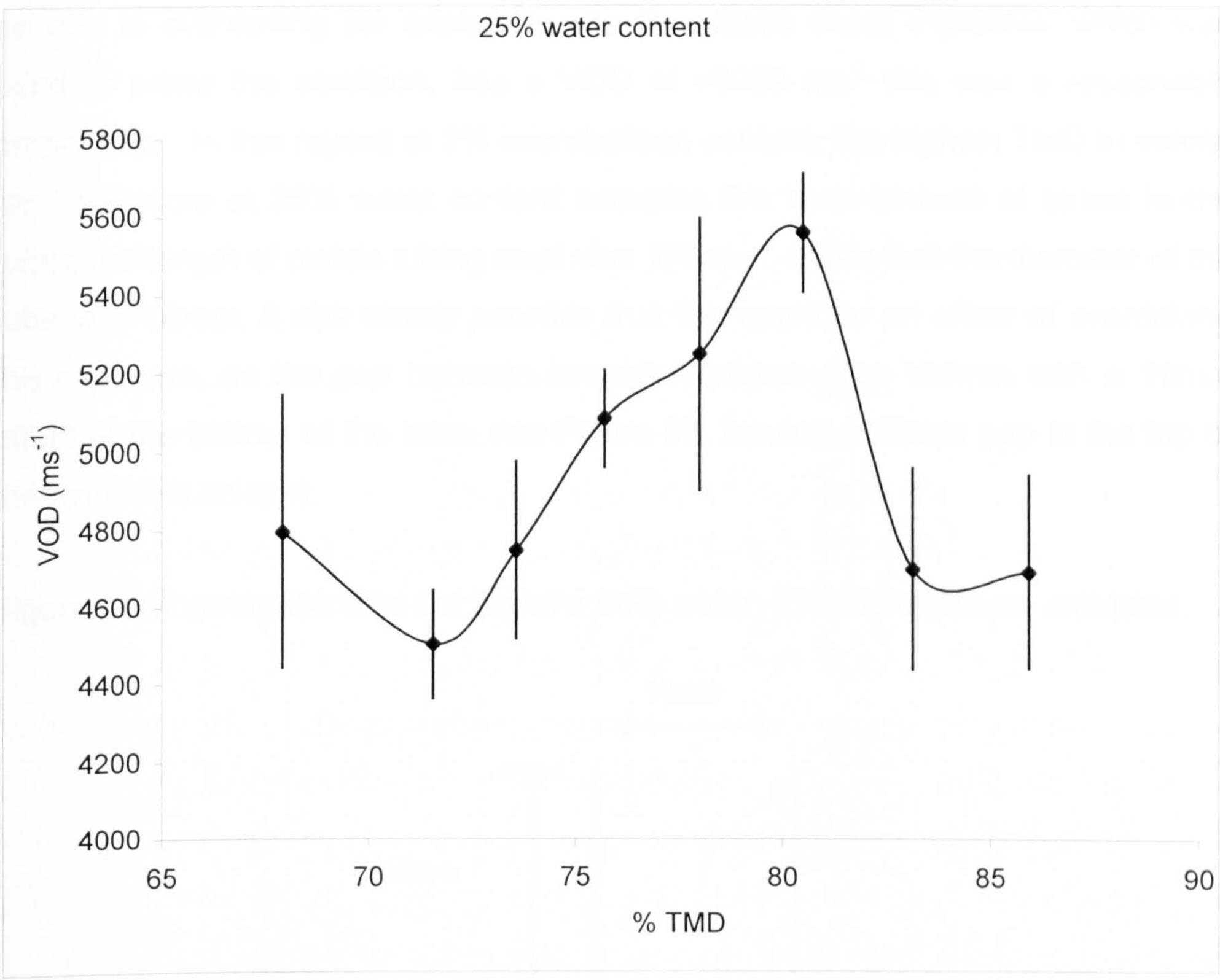

Figure 62 showed a similar pattern to the lower water content emulsions, except for the initial drop in VOD at 67 to 70% TMD, there was an upward trend in VOD followed by a rapid drop. However, this occurred at a much higher VOD than exhibited by the lower water content emulsions. The highest VOD recorded, for a 25% water emulsion with 3% microballoons, was 5558ms^{-1}. This VOD was observed at approximately 80% TMD, which was a similar TMD at which the maximum VOD for the lower water content emulsions was observed.

At 25% water, content priming was required for the entire density range except the lowest TMD. Although this showed that, the 25% water emulsion was less sensitive to shock initiation than the lower water content emulsions, once the explosive initiated the reaction occurred at a much faster rate. As the trend was similar to that of the lower water content, emulsions it must be considered plausible that the high detonation velocities recorded at 25% water content could be due to overdriving the explosive. As the plastic sheet explosive, which was used to prime the emulsion, has a VOD of ~8000 ms^{-1} this was a reasonable proposition. In this regard at 2% microballoon content, the highest TMD to initiate (and therefore at 25% water content occupies the least amount of space in the tube), the length of plastic tubing used was 170mm. Given that the diameter of the tube was 39mm, it was clearly possible that this could be an effect of overdriving the explosive, as the gap between ionisation probes was 100mm with a 10mm offset at the bottom of the tube, see Figure 63, leaving a 60mm gap to the top of the explosive column.

Figure 63 Showing the tube set up for a 25% water, 2% microballoon, emulsion.

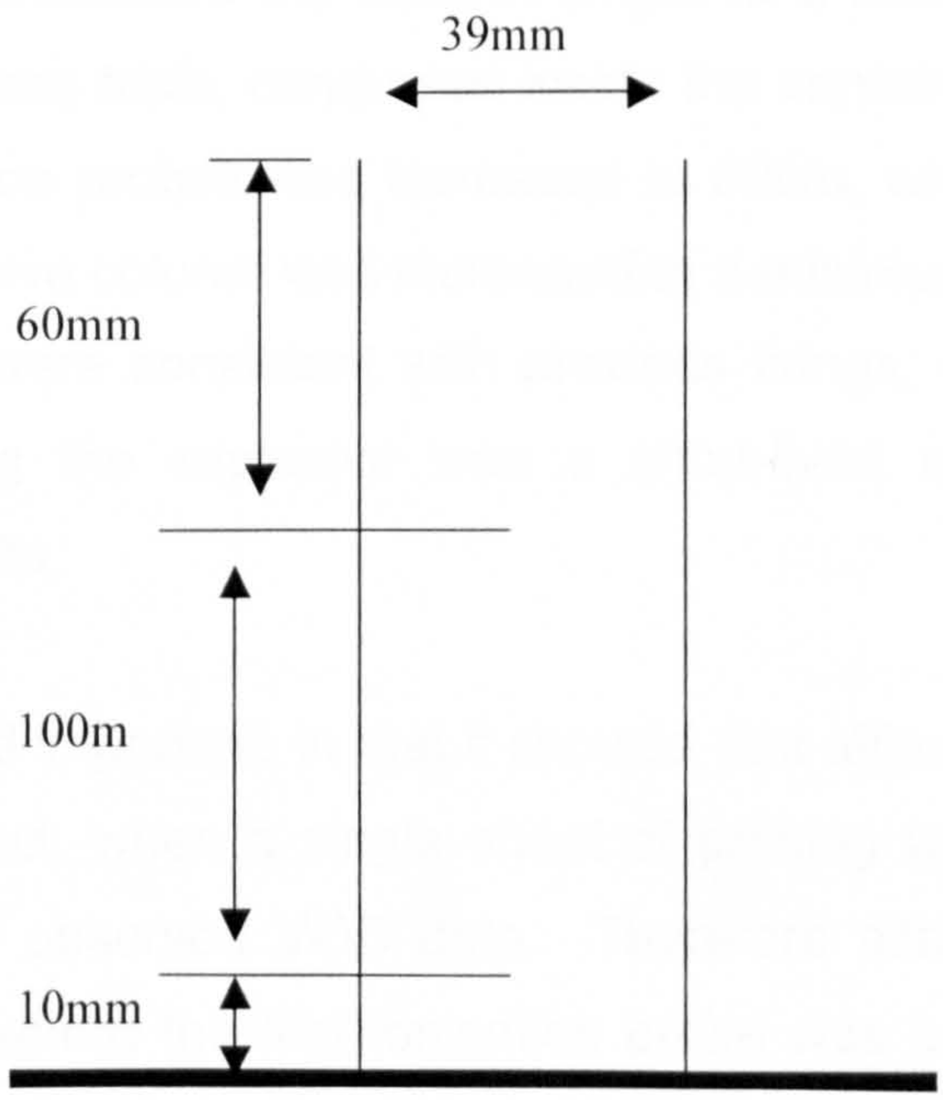

Figure 63 shows that, in this case, the separation of the first ionisation probe from the top of the explosive column was less than three times the diameter of the column. As was discussed previously (see Figure 4), this would have the effect of

At 25% water, content priming was required for the entire density range except the lowest TMD. Although this showed that, the 25% water emulsion was less sensitive to shock initiation than the lower water content emulsions, once the explosive initiated the reaction occurred at a much faster rate. As the trend was similar to that of the lower water content, emulsions it must be considered plausible that the high detonation velocities recorded at 25% water content could be due to overdriving the explosive. As the plastic sheet explosive, which was used to prime the emulsion, has a VOD of ~8000 ms^{-1} this was a reasonable proposition. In this regard at 2% microballoon content, the highest TMD to initiate (and therefore at 25% water content occupies the least amount of space in the tube), the length of plastic tubing used was 170mm. Given that the diameter of the tube was 39mm, it was clearly possible that this could be an effect of overdriving the explosive, as the gap between ionisation probes was 100mm with a 10mm offset at the bottom of the tube, see Figure 63, leaving a 60mm gap to the top of the explosive column.

Figure 63 Showing the tube set up for a 25% water, 2% microballoon, emulsion.

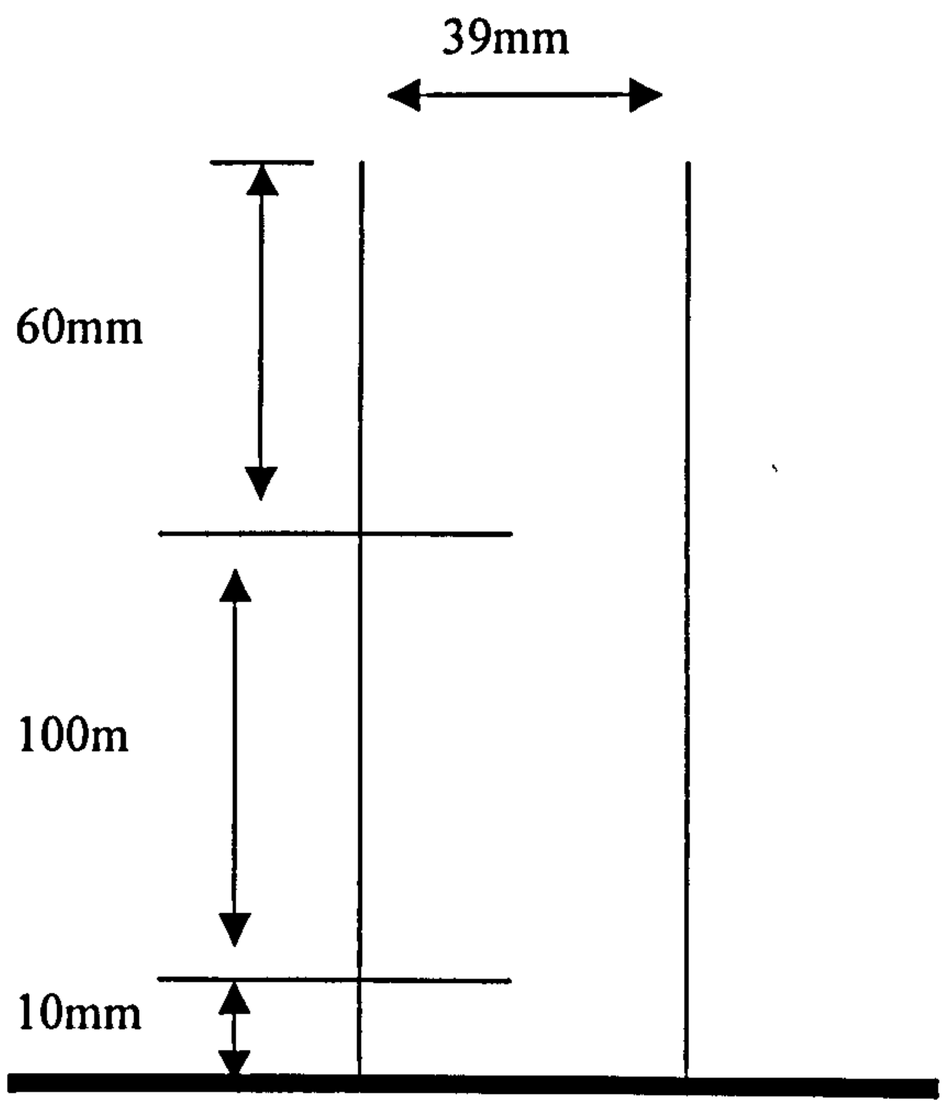

Figure 63 shows that, in this case, the separation of the first ionisation probe from the top of the explosive column was less than three times the diameter of the column. As was discussed previously (see Figure 4), this would have the effect of

overdriving the explosive causing an artificially high VOD, over the measured section, to be observed. In this regard it should be noted that the increase in VOD due to the explosive being overdriven drops off exponentially with distance and in this case the distance, was just over 1.5 times the tube diameter. The explosive could still be overdriven at the point of the first ionisation probe but not excessively so.

Two differing approaches were adopted to show that the observed VOD results were not anomalous results due to overdriving of the explosive. The first approach was to increase separation between the first probe and the top of the explosive. This was undertaken by decreasing the separation between the ionisation probes to 5cm, which gave a distance of 11cm from the top of the explosive column. This distance was still inside three times the diameter of the column, which was 11.7cm. The results from this were entirely consistent with the data already obtained from the previous firings and showed no decrease in VOD, just the normal statistical spread of results. A second approach was taken, to remove any uncertainty with the validity of the data. The amount of emulsion in a tube was increased to 1kg, which increased the column length to a minimum of 77cm, for the highest TMD. For these trials, conducted inside the containment building, the gap between the ionisation probes was increased to 50cm, whilst the separation from the top of the explosive column was increased to a minimum of 25cm. Again, data from these results were consistent with previous firings, indicating that any effect due to overdriving the explosive was a short-lived effect and did not noticeably affect the results.

This work was considered important, in that it showed that although overdriving an explosive is a noted effect, when a single sheet of priming was used it had no perceptible effect on the observed VOD data. Therefore although many of the firings were undertaken where the first ionisation probe was just within 3 charge diameters of the top of the explosive column, when a single sheet of priming was used these are considered valid results.

Figure 64 27.5, 30 and 35% water content emulsion explosives.

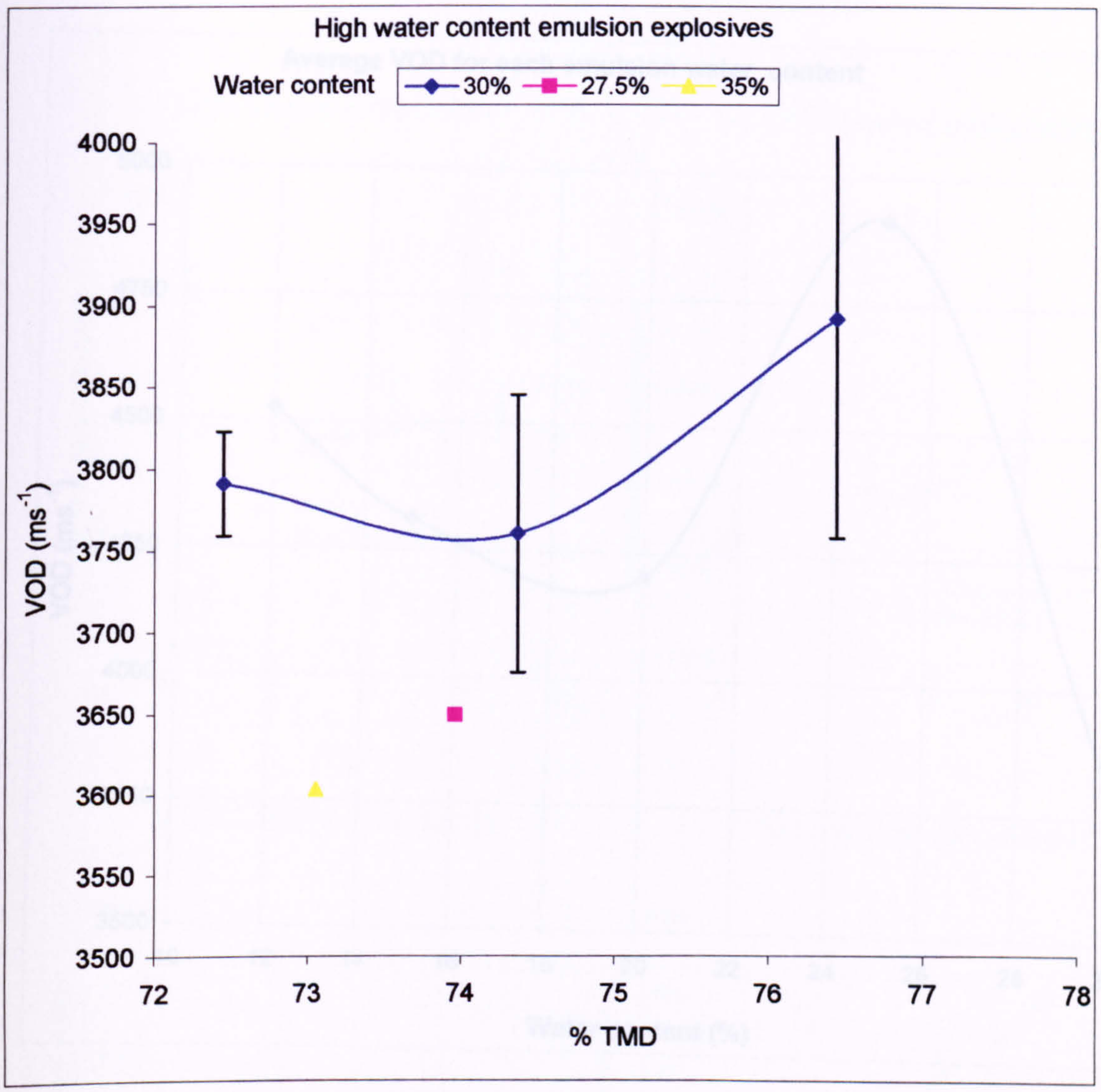

At higher than 25% water content, the emulsions became extremely insensitive to initiation. The %TMD range across which initiation could occur was narrow with the explosive often failing to successfully propagate to detonation, even inside these narrow %TMD limits. This failure would sometimes occur after the explosive had begun to initiate, which had the effect of throwing the unreacted emulsion across the firing area.

The VOD results for these high water content emulsions were consistently below that of the lower water content emulsions. It was difficult to fully characterise the high water content emulsions, as failure to detonate occurred on such a regular basis, that firing became a problem, due to the clean up operations required.

Figure 65 Average VOD for emulsion water contents

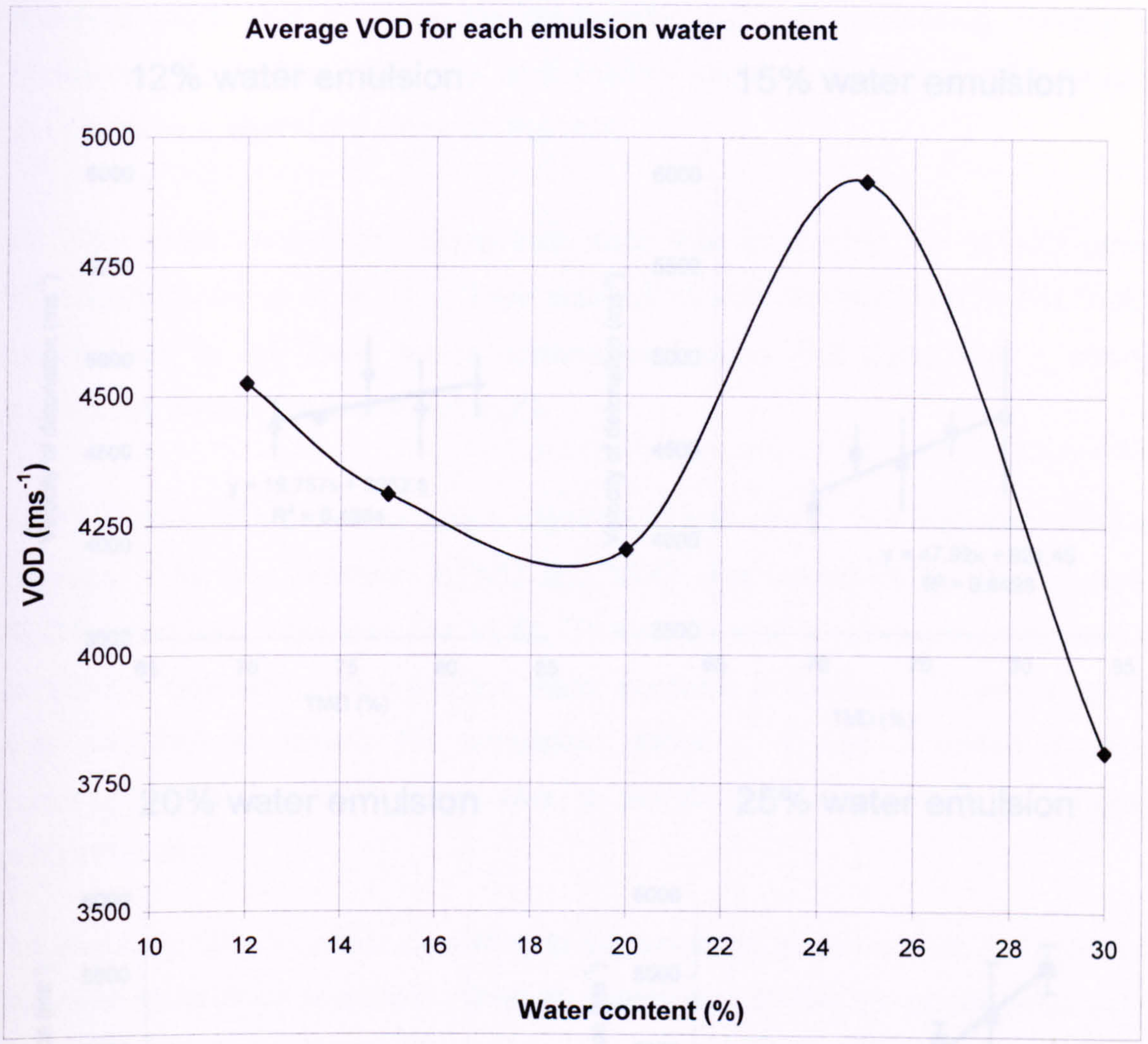

Figure 65 shows the average VOD for each emulsion water content, as calculated from every result for each emulsion, giving the average VOD for the emulsion across the entire %TMD range. This shows an expected result of decreasing VOD with increasing water content until, at 25% water content, this trend stops, and a huge rise in VOD occurs. This cannot be considered anomalous as the average was based on over sixty individual firings for the 25% water emulsion, with a similar number for the other, low water content, emulsions.

The low water content emulsions showed an initial rise in VOD with %TMD and if this initial behaviour is examined more closely, a trend can be seen in the data as Figure 66 shows.

Figure 66 The linear section of density versus VOD.

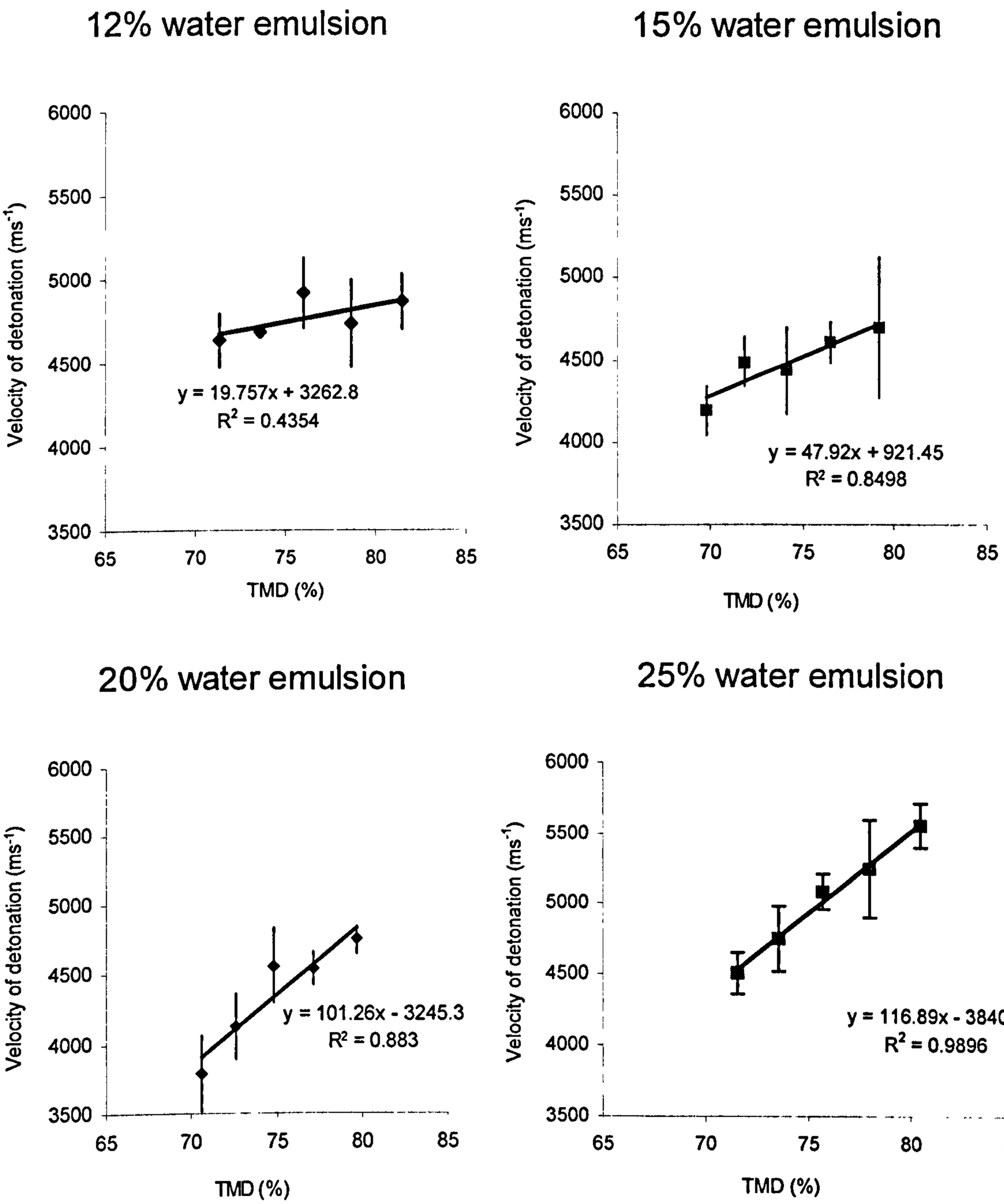

Figure 66 shows that as the water content increases, so the rate of increase in VOD with respect to %TMD increases. At 12% water content, the VOD across the entire density range is almost invariant. No priming was required and the emulsion showed a comparable VOD across the %TMD range.

Figure 66 The linear section of density versus VOD.

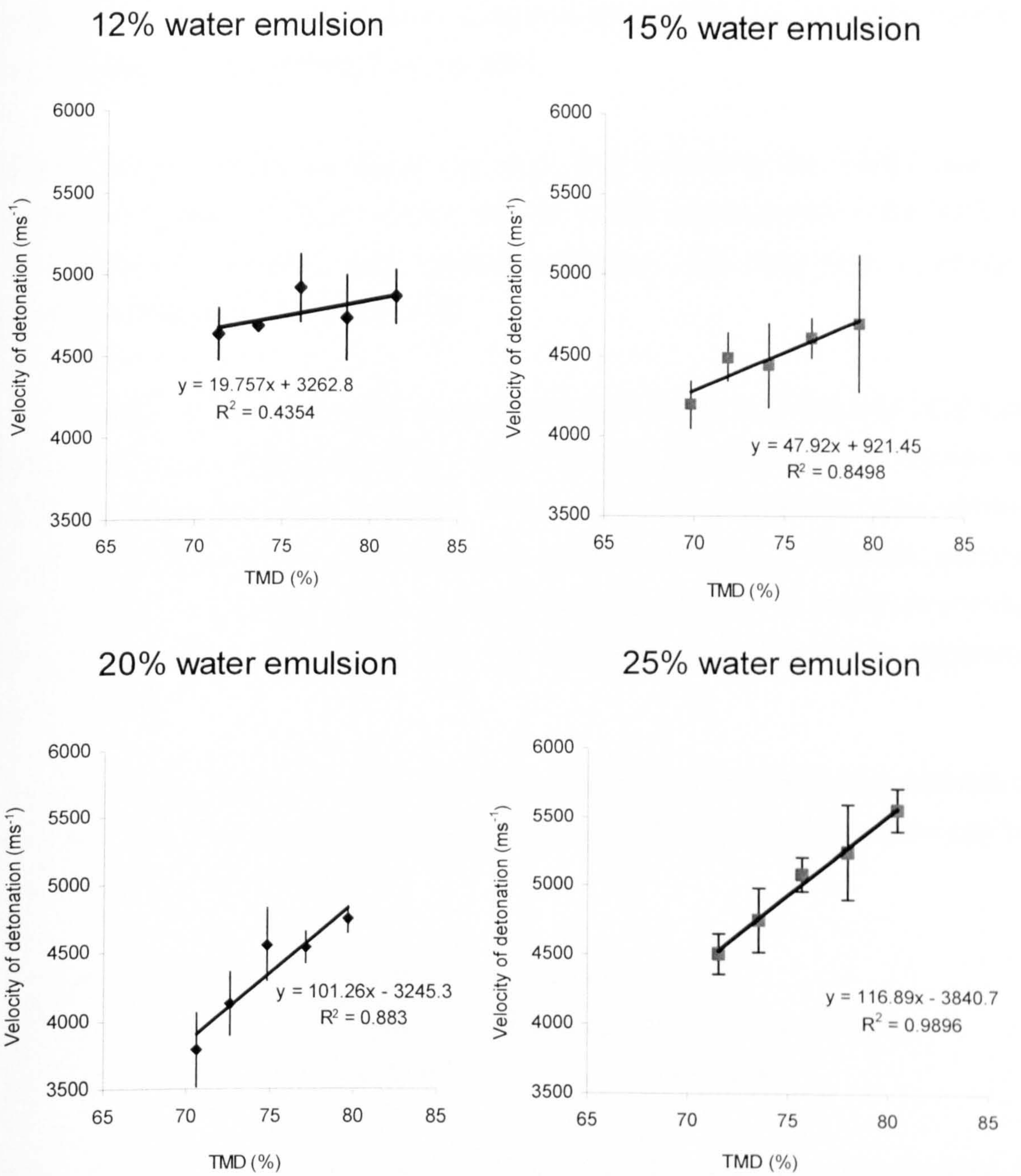

Figure 66 shows that as the water content increases, so the rate of increase in VOD with respect to %TMD increases. At 12% water content, the VOD across the entire density range is almost invariant. No priming was required and the emulsion showed a comparable VOD across the %TMD range.

As the water content was increased to 15%, still, no priming was required, however there was a noticeable relationship between increasing density and increasing VOD. The slope was at a shallow angle, and varying the formulation did not have a significant effect on the VOD.

At 20% water content the slope was such that increasing the %TMD gave a significant increase in VOD. There was no overall improvement in the VOD in comparison to the lower water content explosives, but there was a stronger correlation between density and VOD.

At 25% water content there was a significant, and strong, link between VOD and density. The link between %TMD and VOD was important as an increase in %TMD markedly increased the VOD. There was also a noteworthy improvement in VOD in comparison to lower the water contents emulsions. However, priming was required to initiate the emulsion, although it was a minimum-priming requirement and overall there was a significant improvement in explosive performance.

To elucidate the processes occurring in the emulsion at detonation, the process of initiation must be understood. When an explosive initiates, the phenomena can be separated into three stages[93];

1. The trigger mechanism or primary activation process.
2. The spreading or fading out of deflagration from the primary action.
3. The transition from deflagrating explosion into detonation.

When the initiating hot spots are small, as with microballoons, it is possible to separate the three processes, which in such a case succeed one another at some interval in both space and time.

When the area of initiation is large, the build up to detonation can occur much more rapidly, without the clearly defined stages of build up of detonation from hotspots.

As the 25% water emulsion required priming, it could be argued that, the increased VOD was an effect of a large initiation area, which caused the explosive to initiate without undergoing three separate stages for hot spot initiation.

To prove that this was not the case in this study, selected, although limited, firings at 12, 15 and 20% were initiated using single sheets Demex 200. The data from these firings were similar and within the expected range for emulsions initiated using only detonators.

Whilst this goes some way to showing that, the size of the initiator was not the cause of the high VOD's recorded at 25% water content, it has been subsequently noted that for clarity all the firings should have been conducted using the same level of priming.

3.7.5 Plate dent data

Plate dent measurements were taken, as previously described, and plotted against %TMD for each emulsion and a graph of this is shown in Figure 67.

Figure 67 Plate dent volume versus TMD.

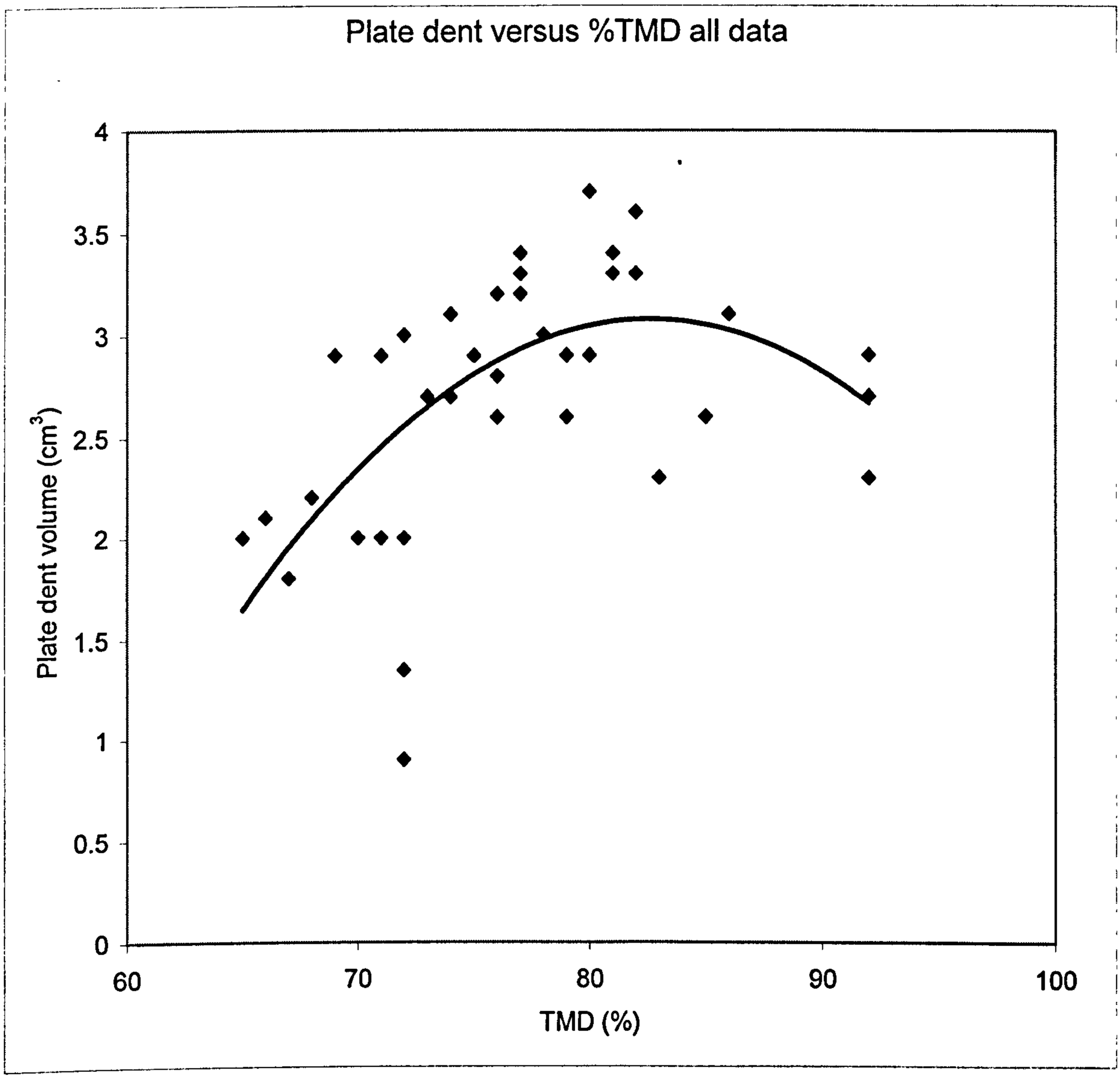

Figure 67 shows a similar spread of data to Figure 57 with no pattern easily discernable, except possibly a trend of decreasing dent volume at higher TMD, although this is not in any way clear. Again, by splitting the data up into individual water contents, the data can be more easily interpreted.

3.7.5 Plate dent data

Plate dent measurements were taken, as previously described, and plotted against %TMD for each emulsion and a graph of this is shown in Figure 67.

Figure 67 Plate dent volume versus TMD.

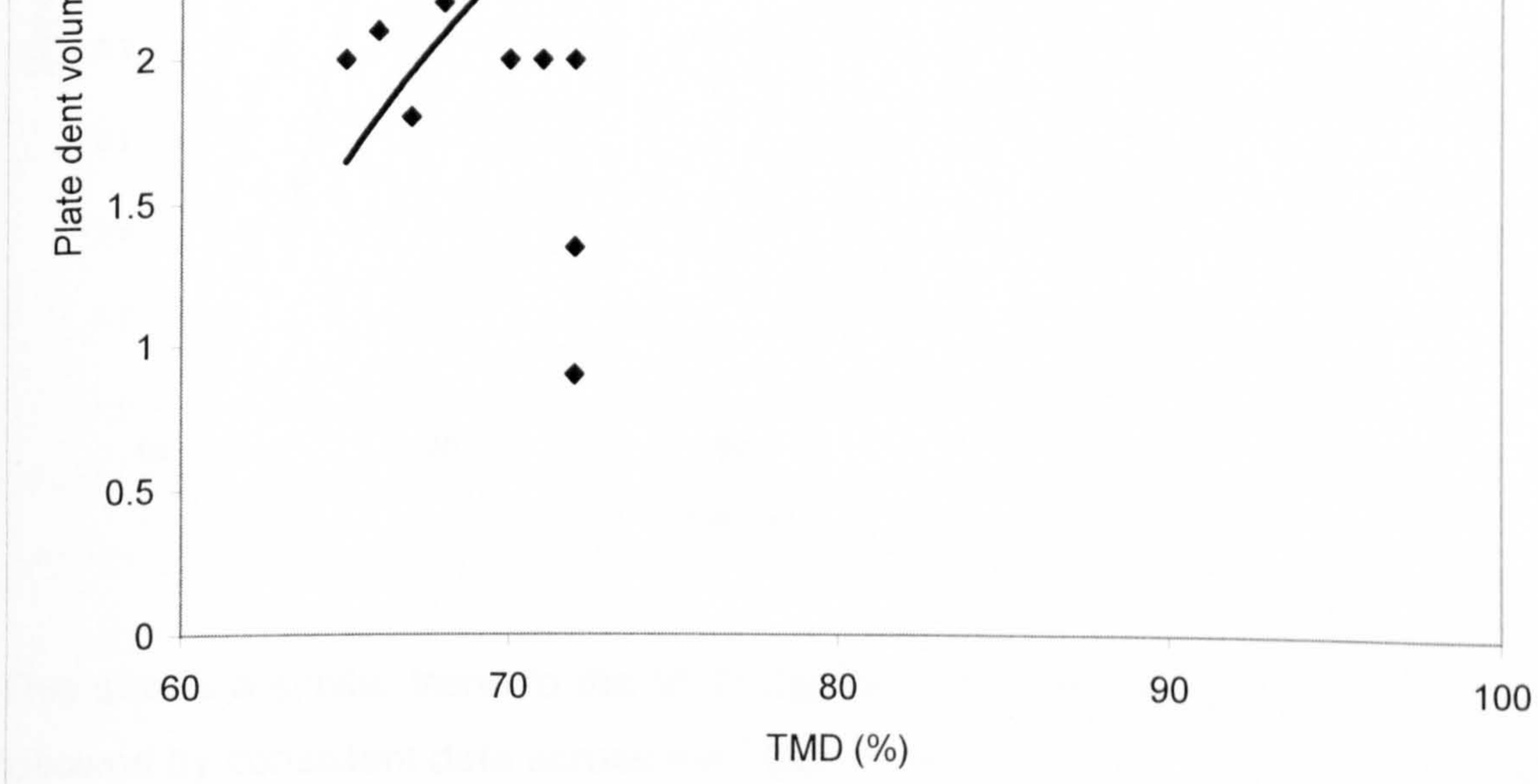

Figure 67 shows a similar spread of data to Figure 57 with no pattern easily discernable, except possibly a trend of decreasing dent volume at higher TMD, although this is not in any way clear. Again, by splitting the data up into individual water contents, the data can be more easily interpreted.

The data for 12% water content emulsion can be seen below in Figure 68, which shows, that apart from a low dent volume at ~65%TMD, the dent volume is reasonably consistent. The average volume, barring the low result, is 2.9cm^3 with little variation away from this.

Figure 68 Plate dent versus TMD for 12% water content.

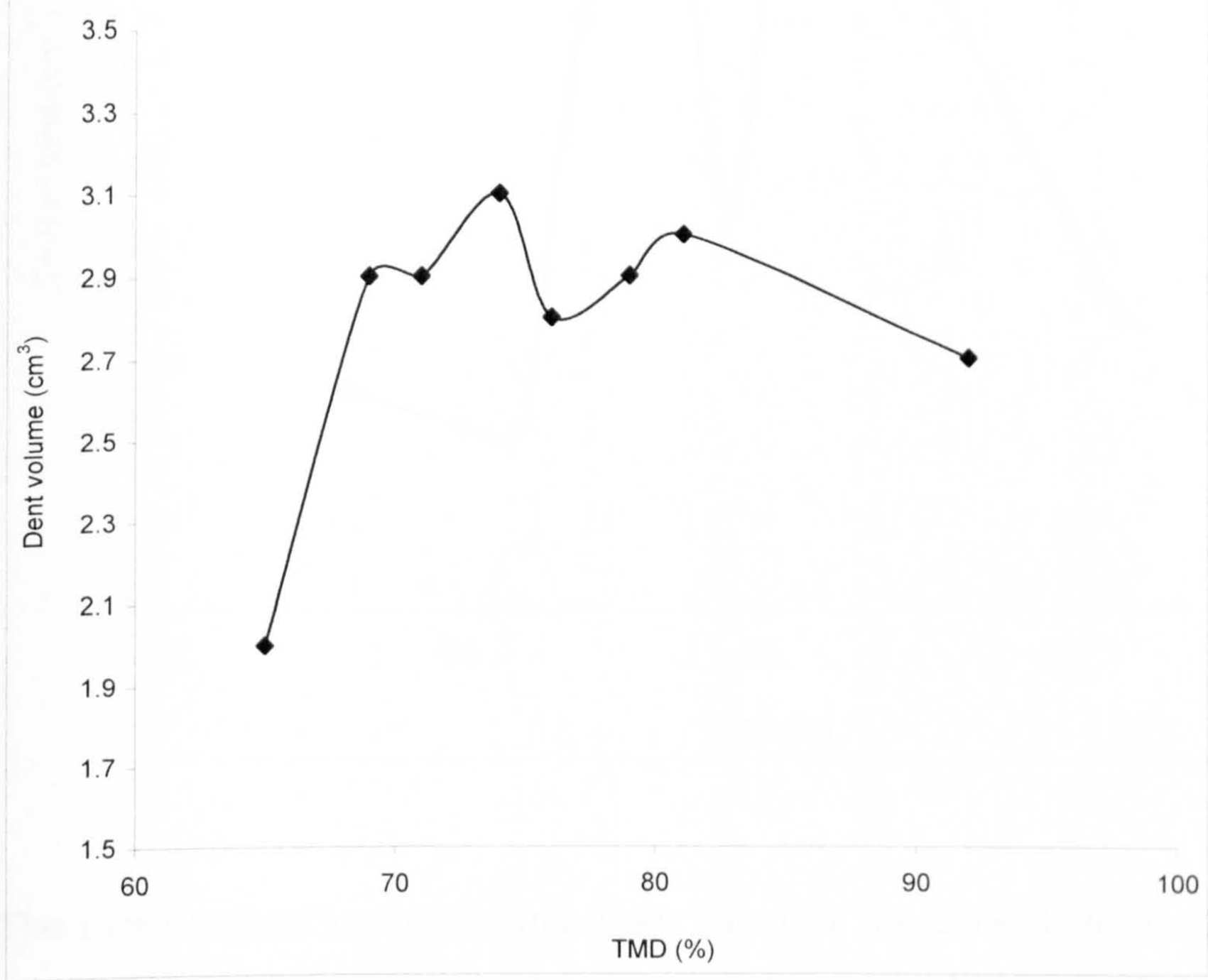

This shows a similar trend to the VOD data where there was an initial low result, followed by consistent data across the TMD range.

Figure 69, shows initially the plate dent volume is stable until around ~72%TMD when there is a large increase in dent volume. The dent volume then drops at ~79%TMD the dent volume drops before again increasing this time to a maximum at ~82%TMD.

Figure 69 Plate dent versus %TMD for 15% water content

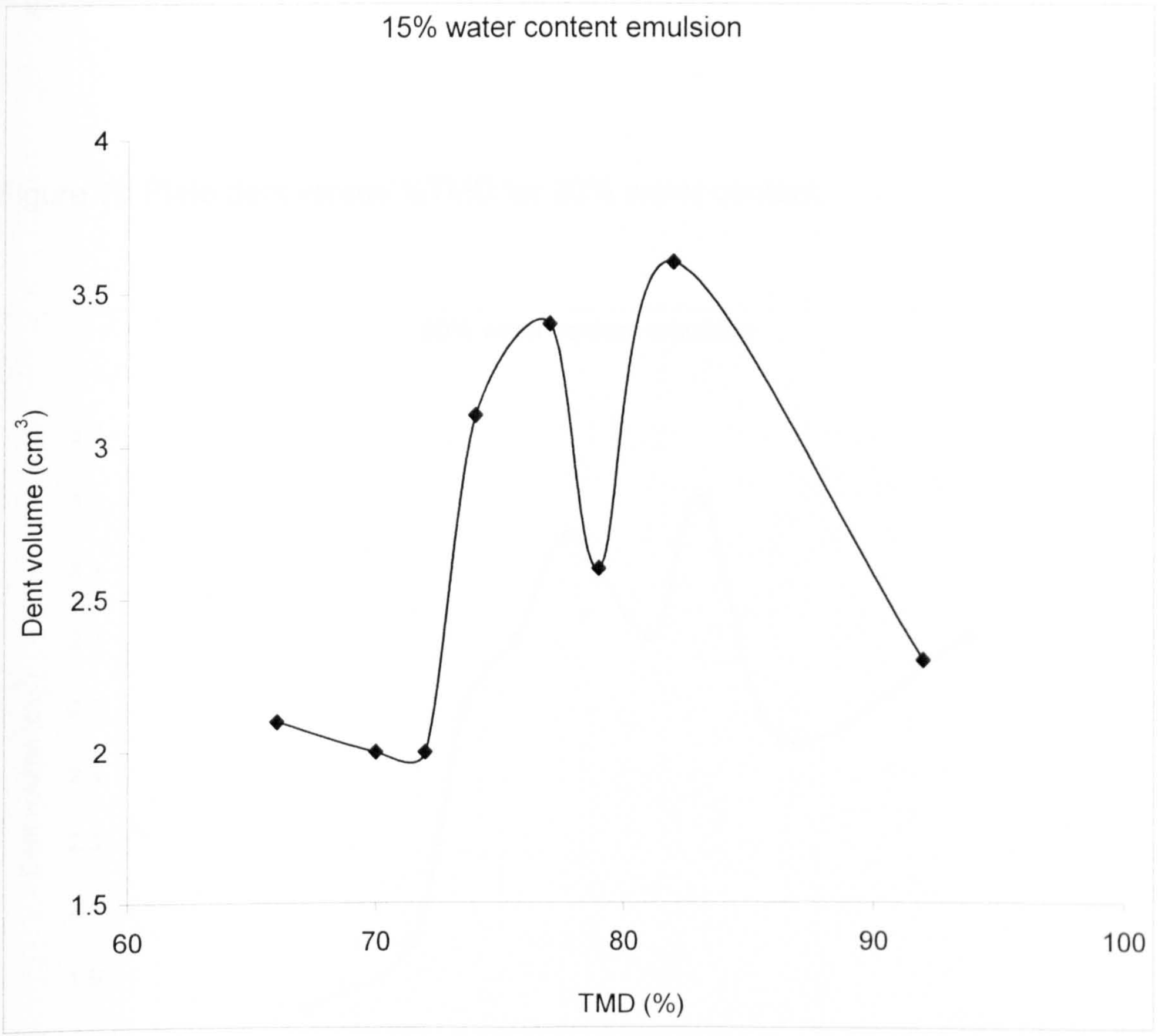

The exact reason for the up and down nature of the plate dent results cannot be adequately explained, except to comment that whilst the plate dent test gives a permanent record it is subject to a certain degree of error. These errors can permeate themselves before the explosive is initiated, one such error being that if there was an air gap at the bottom of the cylinder. If this occurs then the plate dent achieved is not an accurate refection of the brisance of the explosive. Whilst it was not certain that this occurred, measures were taken to overcome this effect. These included drilling small holes at the base of the cylinder and then pushing the emulsion down the tube with a purpose made plunger until emulsion came out of the holes. Plate dent measurements were also subject to variations due to the quality of the witness plate, and the state of the backing plate below.

Notwithstanding this, they did provide a guide that ties in with the VOD data to give a general trend.

Figure 70 Plate dent versus %TMD for 20% water content.

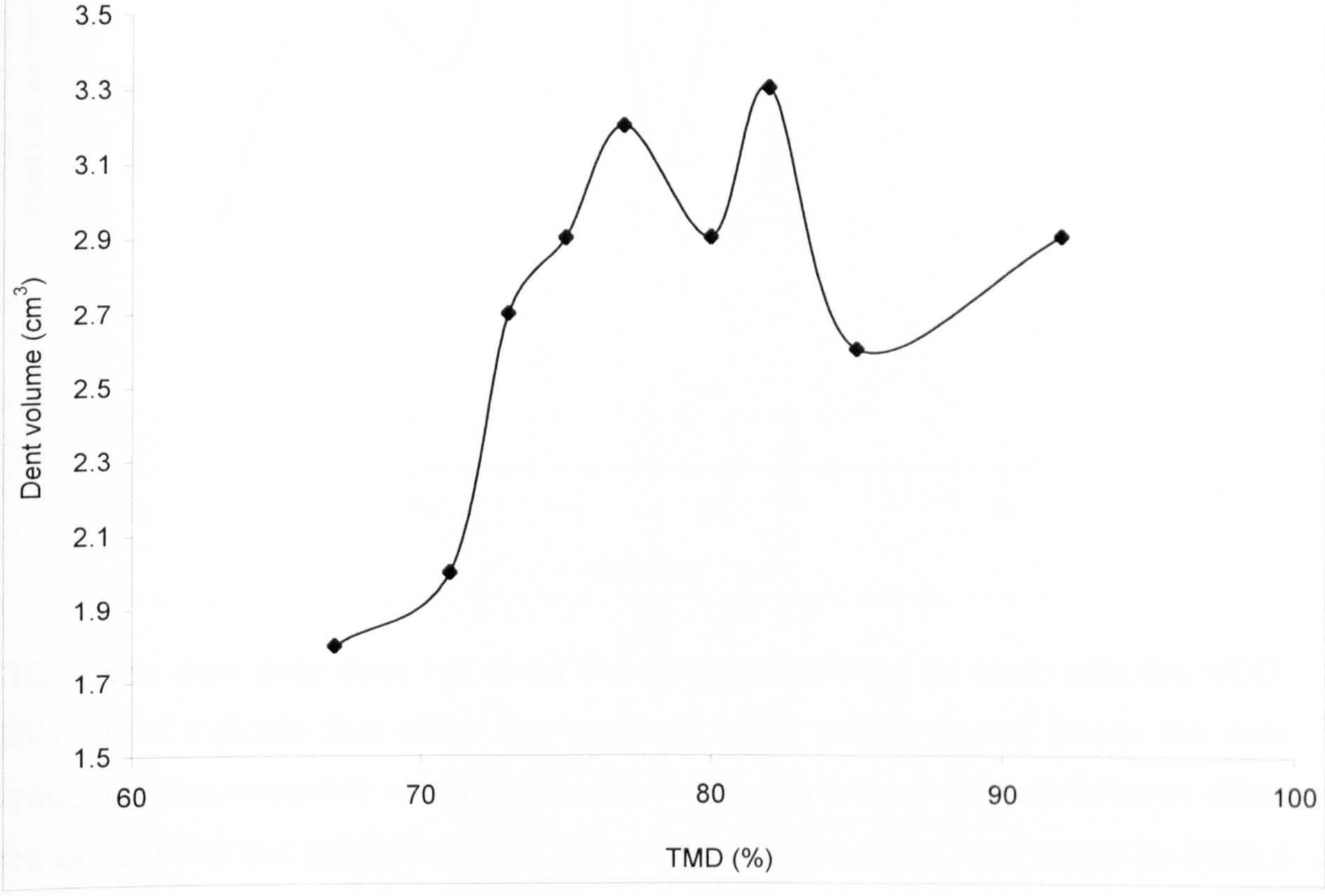

Figure 70 shows a similar profile to that of the 15% water content, except that there was a more pronounced initial rise in the plate dent depth with %TMD. Overall, the plate dent depth at 20% water content was more consistent than that observed at 15% water content emulsion.

Figure 71 shows the data for 25% water content emulsion. There was a drop off in dent volume at ~83% TMD but this was followed by a subsequent increase at ~87% TMD.

Figure 71 Plate dent versus %TMD 25% water content

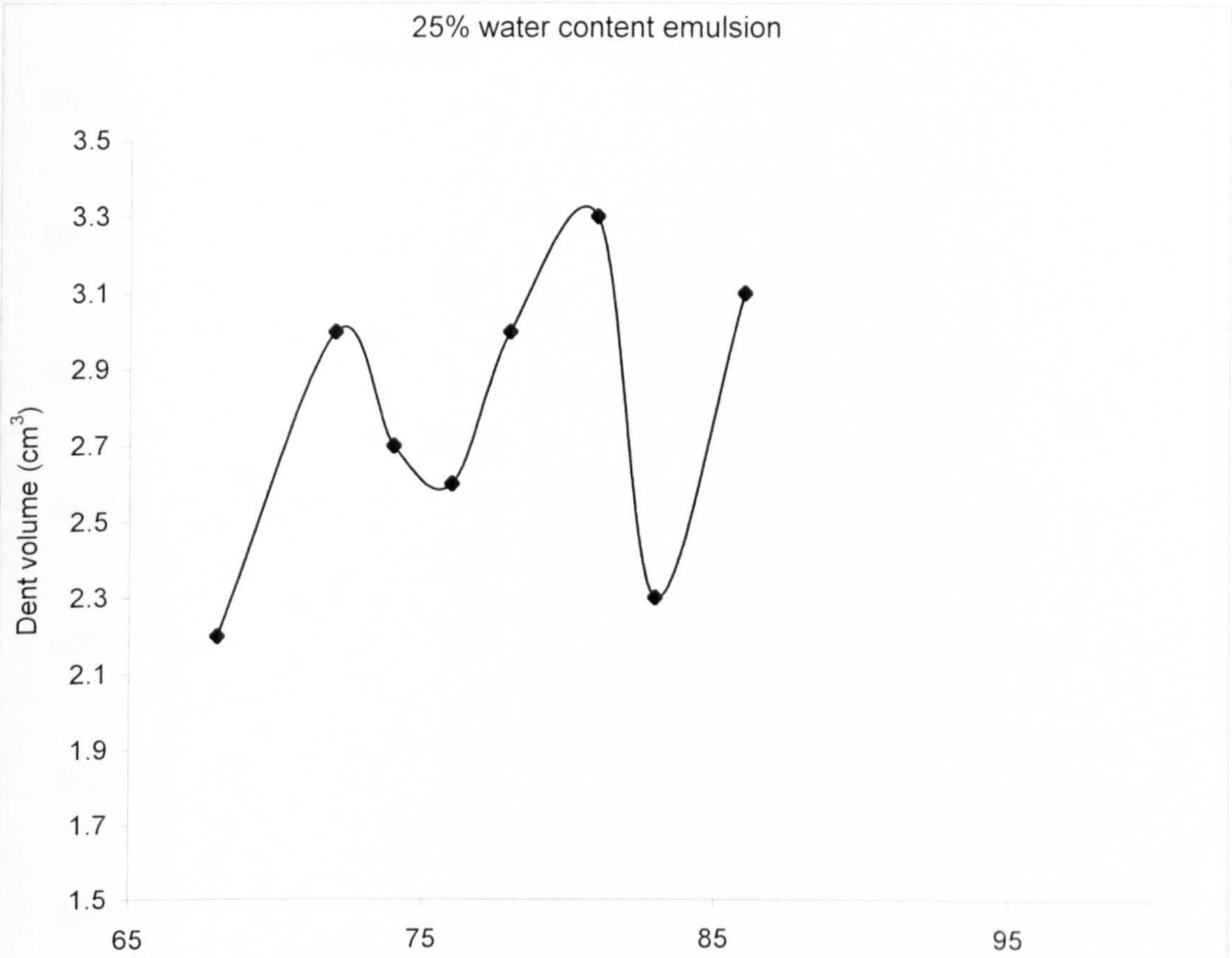

The plate dent data does not show the same correlation as seen with the VOD. This would indicate that either the test was to an extent flawed where the data produced was unusable or it indicates that VOD is not the only parameter to affect the brisance of the explosive. The size of the reaction zone itself could be such a parameter, with a detonation with a large reaction zone releasing energy over a longer time period, and therefore showing a lower brisance value to that of a detonation with the same VOD but a smaller reaction zone. This is discussed later in the context of a grain burning and thermal detonation.

In order to determine if there was a direct relationship between VOD and plate dent a graph of VOD versus plate dent was plotted and this is shown in Figure 72 and Figure 73.

Figure 72 VOD versus plate dent for 12% and 15% water content emulsion.

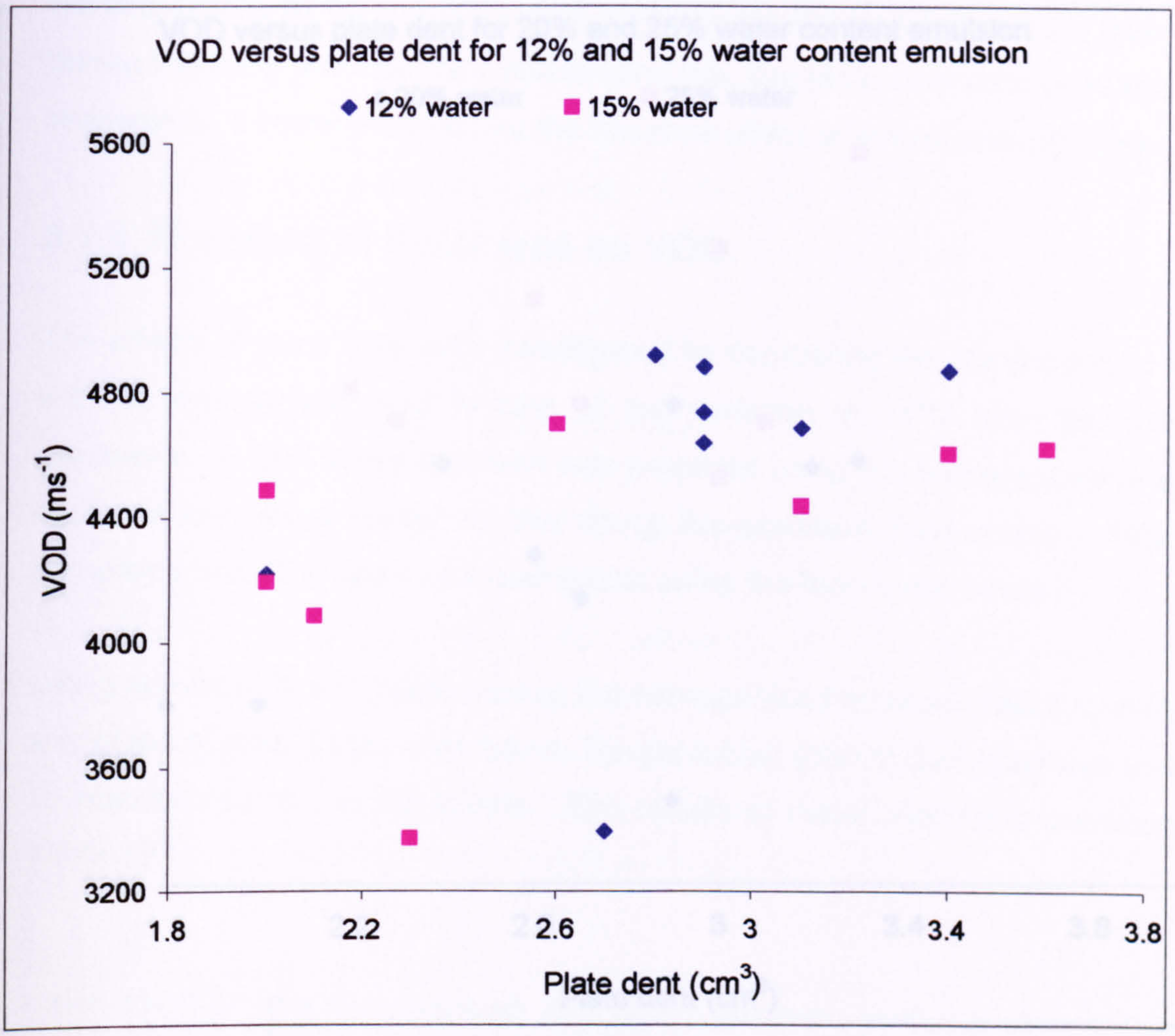

Figure 72 and Figure 73 shows that whilst it can be argued that there is an underlying trend of increasing dent volume with VOD the data is ambiguous.

Figure 73 VOD versus plate dent for 20% and 25% water content emulsion.

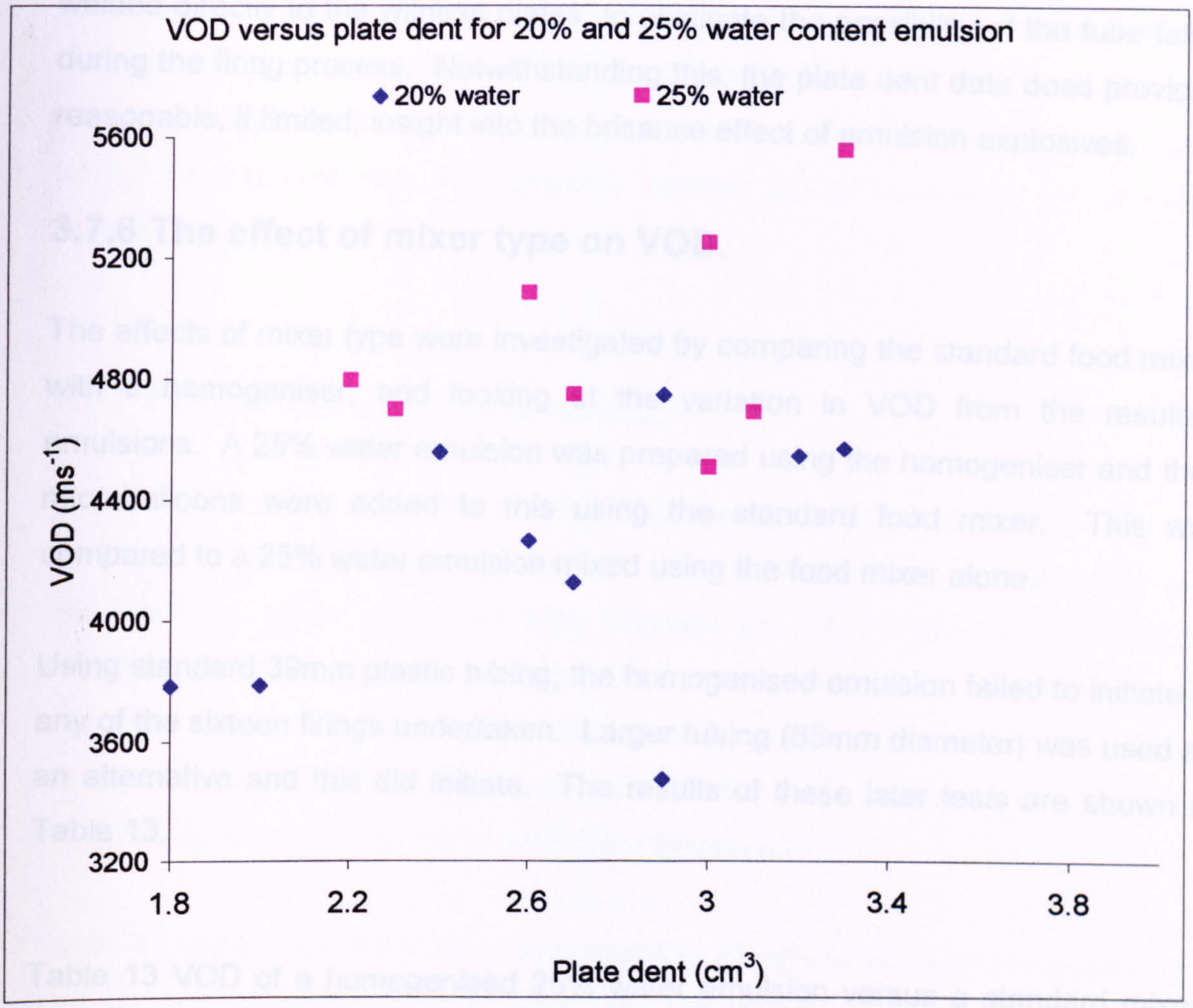

Plate dent tests are not the best method with which to determine the brisance effect of an explosive. The advantage they did offer, and a reason for their widespread use, is that the test was easily combined with VOD observations and was relatively inexpensive, in both materials and equipment. It was hoped that the double pipe test would produce data that would correlate directly to the plate dent data, but, unfortunately, this test was unsuccessful. Each firing undertaken using the double pipe test resulted in a steel cylinder being entirely flattened along the bottom surface. This was not the expected result as, according to the literature[77] this test has been used quantitatively for emulsion explosives.

For the plate dent tests itself, there are many improvements, which could have been adopted, to obtain results that are more consistent. These were not undertaken for fiscal reasons. Improvements would have included using a much

larger backing plate, replacing this as and when necessary, and using steel tubing welded directly to the witness plates, to eliminate the possibility of the tube falling during the firing process. Notwithstanding this, the plate dent data does provide a reasonable, if limited, insight into the brisance effect of emulsion explosives.

3.7.6 The effect of mixer type on VOD.

The effects of mixer type were investigated by comparing the standard food mixer, with a homogeniser, and looking at the variation in VOD from the resulting emulsions. A 25% water emulsion was prepared using the homogeniser and then microballoons were added to this using the standard food mixer. This was compared to a 25% water emulsion mixed using the food mixer alone.

Using standard 39mm plastic tubing, the homogenised emulsion failed to initiate in any of the sixteen firings undertaken. Larger tubing (65mm diameter) was used as an alternative and this did initiate. The results of these later tests are shown in Table 13.

Table 13 VOD of a homogenised 25% water emulsion versus a standard mixed 25% water emulsion.

Standard emulsion 65mm diameter tubing (25% water/3% microballoons)	Homogenised emulsion 65mm diameter tubing (25% water/3% microballoons)
5208ms^{-1}	3876ms^{-1}
5208ms^{-1}	3676ms^{-1}
5502ms^{-1}	3759ms^{-1}
5324ms^{-1}	3817ms^{-1}
5265ms^{-1}	3782ms^{-1}

The homogenised emulsion did not perform as well as a standard emulsion, exhibiting only around 70% of the VOD of a standard mixed emulsion. This was thought to have been due to the mixing action of the homogeniser, which had a

higher rate of energy deposition than the standard mixer. This had the effect of causing phase separation to occur on mixing. It was occasionally noted that, after homogenising, water would separate from the emulsion itself.

As the results from the homogeniser produced low VOD's it was not considered useful to examine the homogeniser further as a technique for emulsion manufacture.

3.7.7 Effects of mixing time on VOD.

The effect of mixing time on the VOD of an emulsion was measured. This was achieved by mixing a 5kg batch of 20% water emulsion and removing 1kg at a time from the mixer at various time intervals (2, 10, 20 and 30min). Before microballoons were added to the emulsion, particle size was measured for each batch (as shown in Figure 30). Microballoons were then added to make a standard mixture of 20% water emulsion with 3% microballoons. The explosive performance properties of these were then measured.

Figure 74 shows that the VOD of the emulsion steadily increased with mixing time until about 20min of mixing time. After 20min of mixing, the mixing process begins to have a detrimental effect on the emulsion VOD. This effect could be compared to the use of the homogeniser, as the emulsion is mixed it reaches an optimum after which breakdown of the emulsion matrix begins to occur. The homogeniser applied energy to the mixing process very rapidly, not giving the emulsion time to recover, whereas the food mixer applied energy much more evenly through the emulsion. Notwithstanding this, there was a point at which the addition of more energy, by mixing, has a detrimental effect on the VOD of the emulsion.

Figure 74 Effect of mixing time on VOD for 20% water emulsion/3% microballoon.

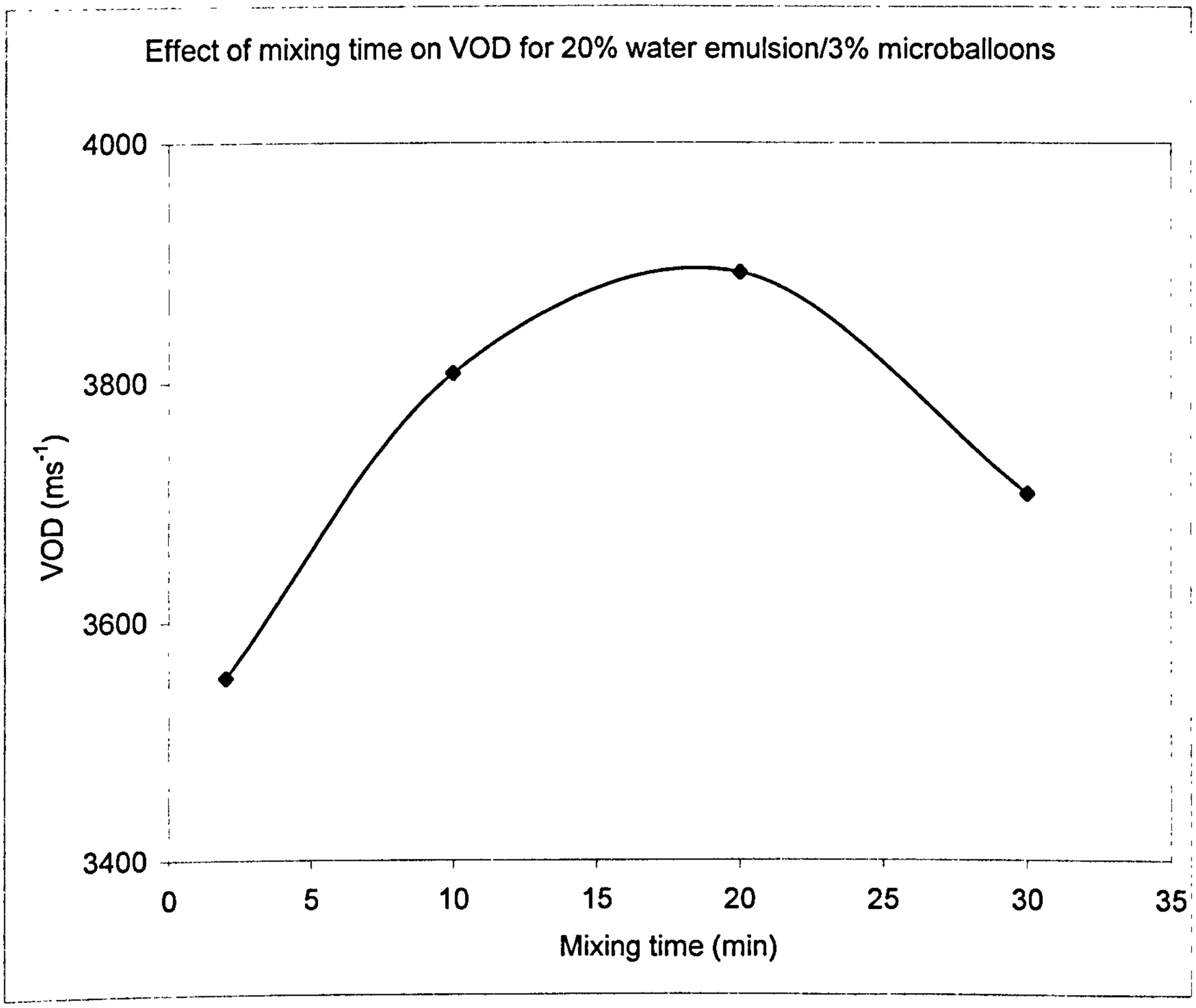

Figure 75 shows the same VOD data as in Figure 74, but this time plotted as a function of emulsion droplet size versus VOD. As discussed earlier, the more intimately mixed an explosive composition is, then the faster the reaction would be expected to occur. It would be expected that decreasing the average droplet size would lead to increase in VOD.

Figure 75 Effect of median particle size versus VOD 20% water 3% microballoons.

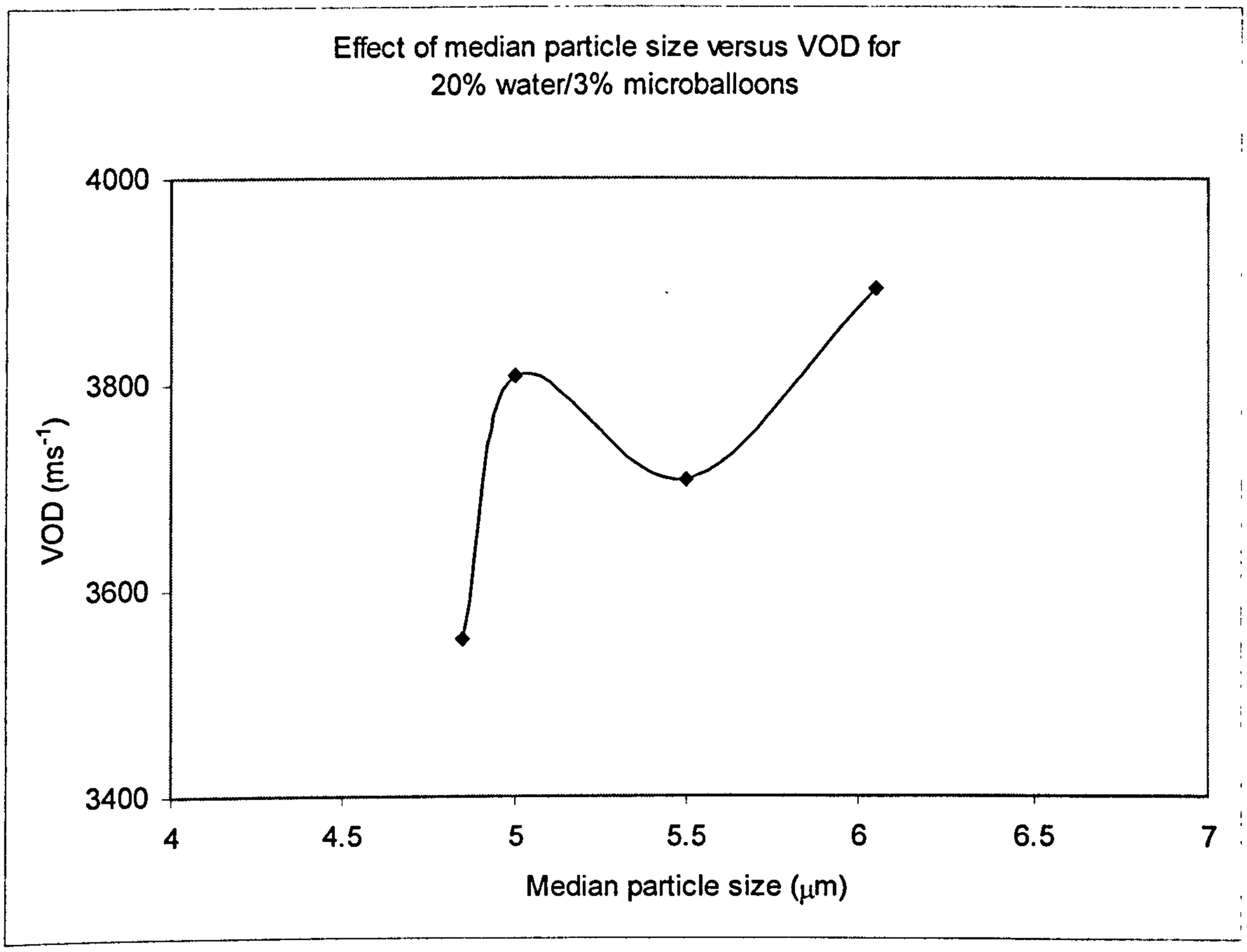

Figure 75 shows that for emulsion explosives this trend of increasing reaction rate with decreasing droplet size did not occur. From Figure 75 it can be seen that the converse is almost true, as the droplet size increases, so the VOD increases. Thus, whilst droplet size is important to emulsion stability, there was not a strict relationship between disperse phase droplet size and emulsion explosive VOD. It was also apparent that the change in average droplet size was not as important an effect on VOD, as mixing time itself, which showed a clear trend of increasing VOD with mixing time.

3.7.8 Viscosity versus VOD relationship

It was expected that emulsion explosives would display a relationship between viscosity and VOD. The viscosity of the emulsion determines the rate of movement of microballoons through the emulsion, as, in time, the low-density microballoons would begin to separate out. The behaviour of the emulsion under shock loading, to a certain degree, is also determined by the viscosity of the

emulsion. Figure 76 shows a graph of viscosity versus VOD, for various different water content emulsions.

Figure 76 Viscosity, as calculated from emulsions with no microballoons present, versus VOD for emulsions with 3% microballoons.

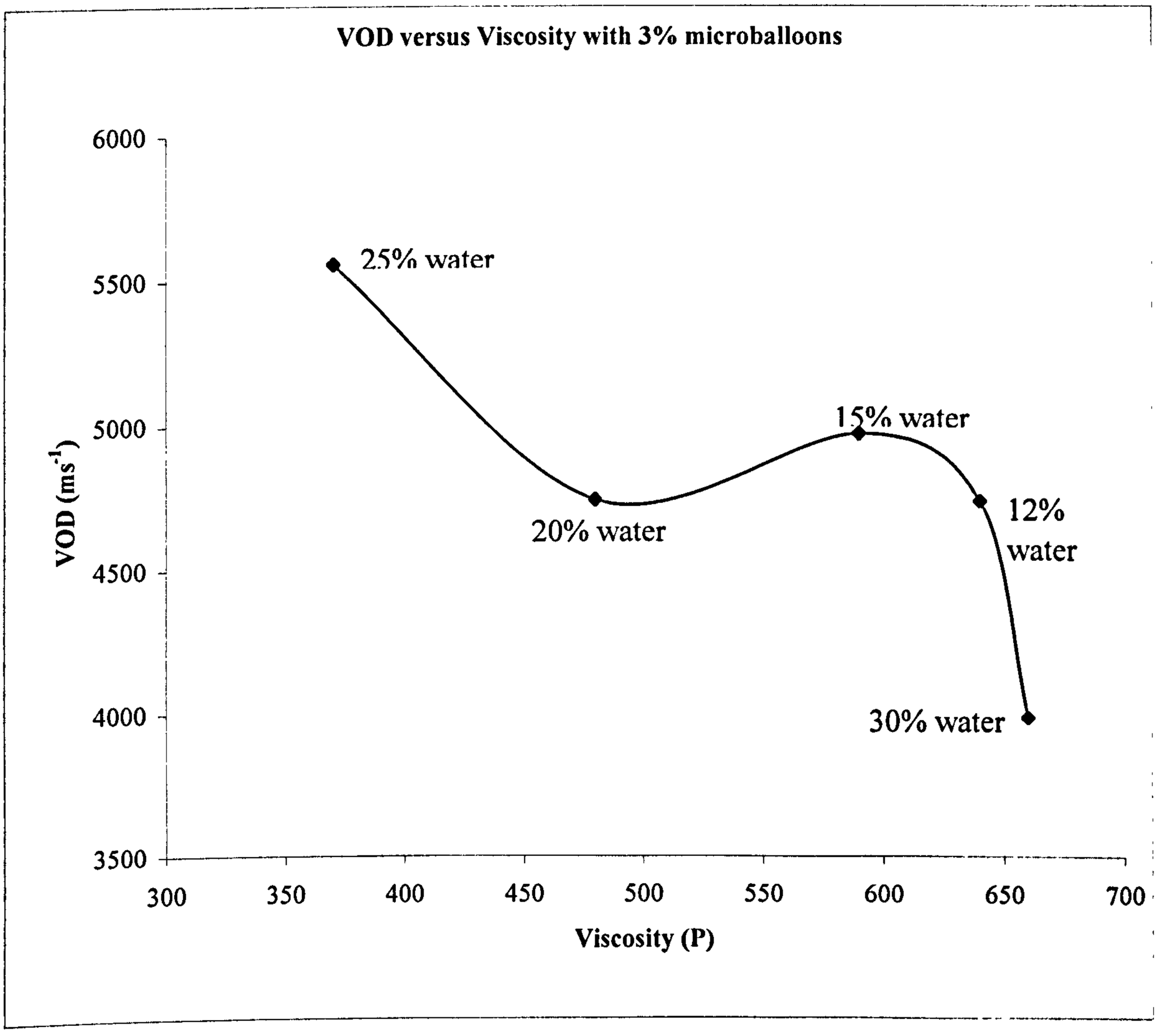

The graph shows that there was only a limited correlation between viscosity and VOD. The low viscosity at 25% displays the highest VOD but the expected trend of decreasing VOD with viscosity did not occur and no real trend can be determined from the data.

4 Further Discussion

The preceding results have shown that the explosive behaviour of emulsion explosives cannot easily be defined by their physical characteristics. Knowing the viscosity, density or the thermal conductivity of the emulsion does not allow the prediction of the VOD. This section attempts to account for the differing behaviour of the emulsions and show how emulsion explosives, whilst displaying type II non-ideal behaviour, could be further classified by the type of reaction that occurs upon detonation.

Figure 77 All explosive firing data plotted on a VOD versus density graph.

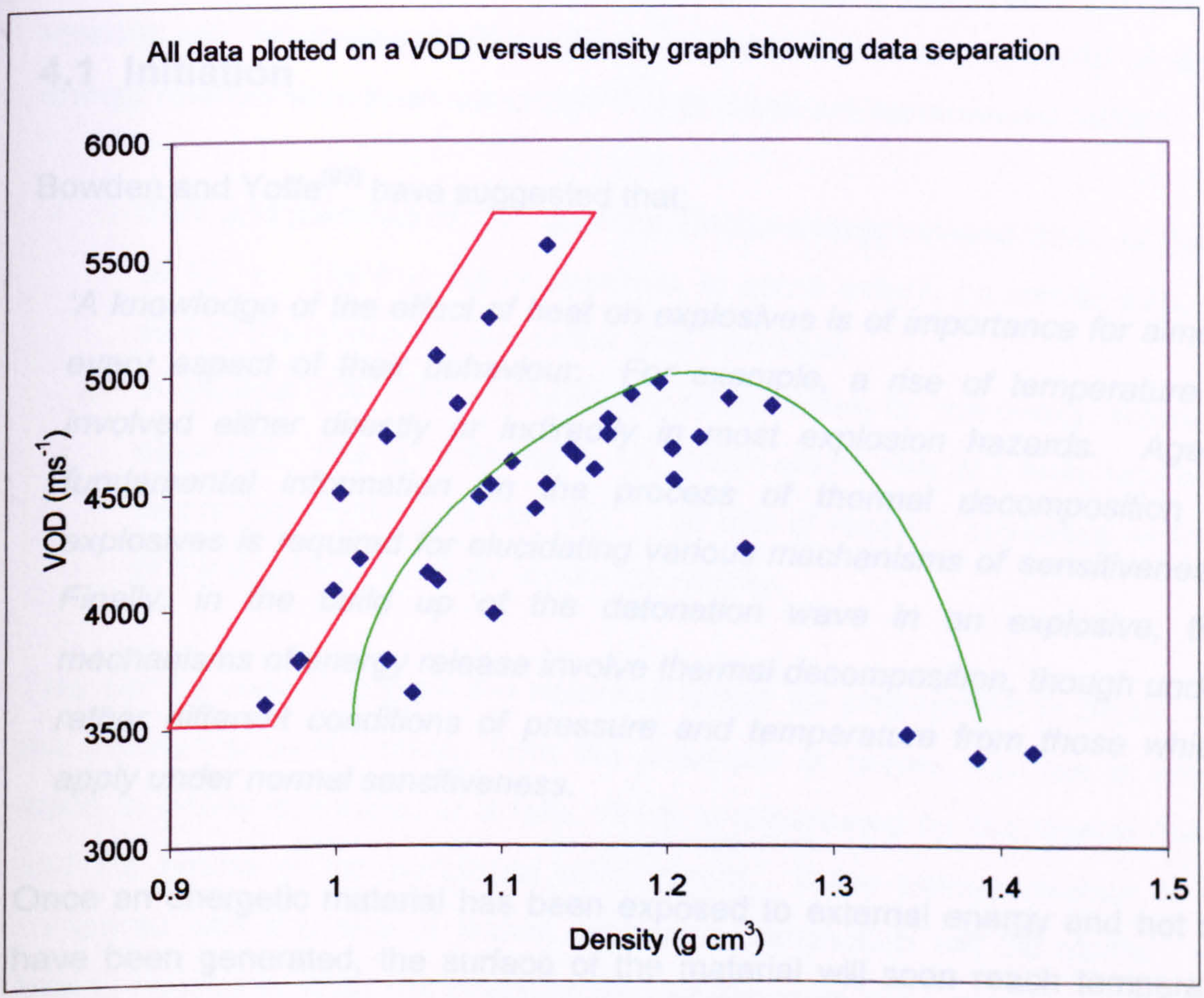

Figure 77 shows the data for all the explosive firings plotted as density versus VOD. Looking at this it was possible to see two distinct trends in the data. On this basis, it was subjectively split into one side of the graph, which showed a linear trend of increasing VOD with density, and one side, which showed a parabola.

This split was entirely based on the data as seen in Figure 77. Inspection of the data showed that the split in the data was not random. All the data, which formed the linear trend, was either high water content or high microballoon content. All the data in the parabola was low water content and microballoon content. This process of splitting the data was repeated for the plate dent data and again the same trend was noted.

Discussions with colleagues[92] suggested that it was possible that emulsion explosives could display two differing reaction regimes, that of grain burning and a thermal explosion. How these two reaction regimes exist and how emulsions could display these regimes is discussed below.

4.1 Initiation

Bowden and Yoffe[93] have suggested that;

> *'A knowledge of the effect of heat on explosives is of importance for almost every aspect of their behaviour. For example, a rise of temperature is involved either directly or indirectly in most explosion hazards. Again, fundamental information on the process of thermal decomposition of explosives is required for elucidating various mechanisms of sensitiveness. Finally, in the build up of the detonation wave in an explosive, the mechanisms of energy release involve thermal decomposition, though under rather different conditions of pressure and temperature from those which apply under normal sensitiveness.*

Once an energetic material has been exposed to external energy and hot spots have been generated, the surface of the material will soon reach temperatures high enough to volatilise it. This process, referred to as the induction lag or ignition delay time, occurs in a very short time period (measured in microseconds). There is no standard lag time for explosive material since induction lag is dependent on the composition of the explosive mixture.

They further commented that the standard hydrodynamic equations of detonation do not refer to the physico-chemical mechanisms where energy is released in the detonation wave. In the case of mixed explosives some of the energy may be released a considerable way behind the detonation front. In fact, the usual theoretical equations refer to the behaviour of an infinite plane wave of detonation travelling through the explosive. However, experimental studies have shown[94] that detonation velocities depend, to some extent, on charge diameter, when this is small. This can be explained in terms of energy release. If the time of expansion of the charge is comparable with the time required to release the chemical energy of the explosive, the maximum pressure of the detonation wave will be less than that calculated for an infinite plane wave, and the detonation velocity will be correspondingly lower. Qualitative measurements of times of energy release have been computed[95] and these are summarised below.

1. TNT and mixtures of TNT and tetryl have energy release times of the order of 10^{-7} s. The true figure depends, to some extent, on crystal size, as the size of the crystal increases the time increases.
2. In amatols (TNT/AN), considerably longer times, for the energy release, are observed. This is attributed to AN, which reacts only at a finite rate with the detonation products of the TNT. The rate of reaction increases as the size of the ammonium nitrate crystal decreases.

This can be used to explain the nature of failure for propagation to occur. When the detonation wave arrives, from the detonator or primer, the rise in pressure leads to lateral expansion at a rate, which is determined by the charge diameter and the nature of the peripheral confinement. If the energy release is rapid, compared with the rate of lateral expansion, detonation will be stable. If the energy release is slow, the pressure and temperature may drop to a level, at the periphery of the charge, that the explosive in this region never releases its energy effectively. When this occurs detonation fails at the edges. The failure occurs in successive layers from the edge working inwards progressively, which explains both the fading inwards from the edges and the decrease in velocity as the diameter of what is left of the detonation front decreases. Failure of the explosive

to propagate can therefore be attributed to the slow rate of energy release in the explosive.

In single molecule explosives, and in mixtures of these, the critical diameter decreases with decreasing grain size and increasing initial density up to a density close to a critical density. At or very near the crystal density, the critical diameter is often found to increase, growing from a few millimetres to tens of millimetres. One explanation for this behaviour is the hot spot theory. A powdered or pressed explosive will contain a huge number of 'hot spots', or initiation centres and the reaction can be assumed to be dominated by the spread of reaction from the hot spots. It is assumed that the rate of reaction at each hot spot will be greater with a greater shock pressure therefore implying that there will be a greater concentration of energy, initially, at each hot spot. There will be an induction lag before the energy from the hot spots dissipates and the bulk of the explosive material reacts. The length of this lag depends upon the way the explosive reacts. This reaction can either be a grain burning type reaction or a thermal explosion.

4.2 Grain burning and thermal explosion

A grain burning type reaction can be thought of as a combustion type process, where the reaction proceeds stepwise through the explosive. The reaction is constantly fading and picking up as hot spots are formed. There is little time lag between the formation of the hot spot, and the subsequent reaction of the explosive.

In a thermal explosion, the hot spots are created by the initial shock wave and for a period there is no discernable reaction from the explosive, until the bulk of the explosive reaches a temperature where it all reacts in a short time period.

There is no increase in energy output or gas production in one process over the other, but there is an increase in the speed of the reaction rate in a thermal explosion.

This was demonstrated by Leiper et al[96] when they investigated the link between the physical form and ingredients of an explosive and its detonation performance. They were looking at low and high order detonations, as shown by explosives such as nitro-glycerine. They found that in a high velocity regime, thermal explosion was the process of heat release, but in low order detonation grain burning kinetics predominate. They went on to establish a link between charge diameter effects and the nature of heat release. They used data from previous studies and placed this in a slightly divergent flow detonation model, CPEX, to produce constant pressure to heat release rates for the formulations. Thermo-hydrodynamic calculations for the ideal Chapman-Jouguet state for a variety of explosives were carried out using the JCZ3 equation of state.

Equation 19

$$\dot{\beta} = (1-\beta)\left(\frac{a_h(p-p_c)}{\tau_h} + \frac{a_l p}{\tau_l} + \frac{a_s p}{\tau_s}\right)$$

where

β Mass fraction reacted

$\cdot$ Time differentiation

p pressure

a_i shape functions depending only on initial formulations

τ_l time constants

p_c critical pressure

Subscripts h,l,s refer to various phases in the explosive, nominally hot spot, liquid and solid.

The four fitting parameters were τ_l, τ_h,τ_s, and p_c.

They used an automatic fitting algorithm, based on a simple line search followed by a constrained minimisation routine, to generate a least squares fit to the experimental data with a failure point that lay at a smaller diameter and lower

velocity than experimental data. The explosives used, and their compositions, are shown below in Table 14.

Table 14 Key to graph and composition of explosives examined by Lieper et al[96].

Explosive	Line label	Composition
NG98 (high velocity)	A	98% Nitro-glycerine blasting gelatine
NG98 (low velocity)	B	98% Nitro-glycerine blasting gelatine
NG29 (high velocity)	C	29% Nitro-glycerine plaster gelatine
NG29 (low velocity)	D	29% Nitro-glycerine plaster gelatine
NG15	E	15% Nitro-glycerine powder
NG8	F	8% Nitro-glycerine powder

NG98 and NG29 both had a high velocity regime, a low velocity regime, and an unstable transition regime.

Their graph, Figure 78, shows the differing reaction regimes. Line A (NG98 high velocity) shows an induction time where no or very little reaction occurs. After this, the reaction is exceptionally fast, rising to completion very quickly. Line C (NG29) shows a similar trend, but the induction period is shorter and the rise time slower. Both these reactions show typical thermal explosion type characteristics as would be expected by an ideal military high explosive. Thermal explosions produce high VOD's with the explosive reacting rapidly.

The remaining lines (D, B, E and F) show the characteristics of a grain burning reaction. In this, the explosive reacts almost immediately with the shock wave but in a cellular type process. This means that the reaction takes a relatively long time to go to completion. Line B shows that the reaction rate is at a maximum as the shock wave passes and slowly tails off in an exponential manner. This leads to lower velocities of detonation and lower detonation pressures.

Figure 78 Plot of reaction rate versus normalised time[96].

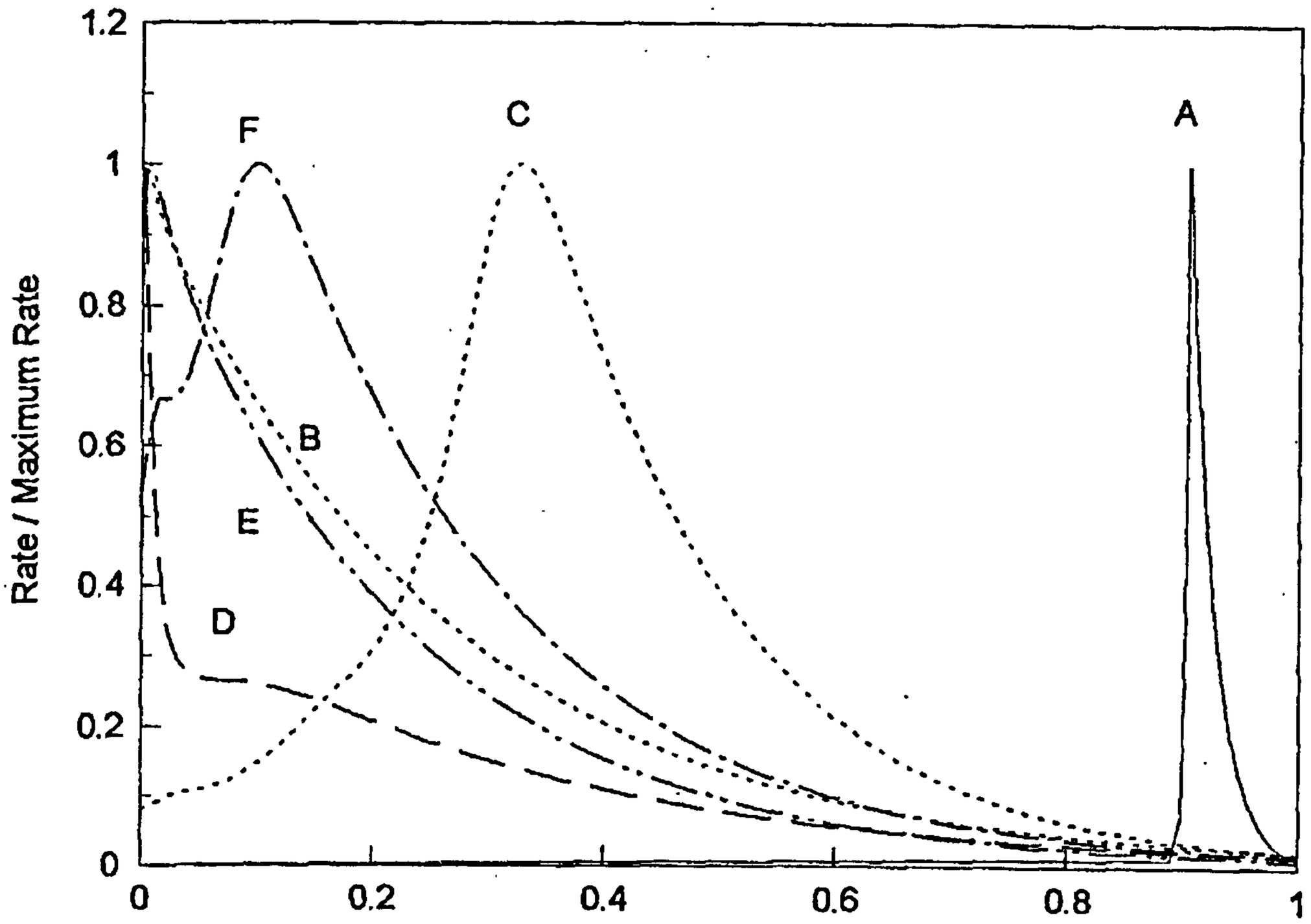

To demonstrate that emulsion explosives do not display standard type I explosive behaviour, their explosive performance was modelled, using a computer-modelling program. This was accomplished using a standard military computer modelling code, CHEETAH, which is based on ideal explosive behaviour, utilising a BKW equation. Emulsions explosives, as used in this study, were modelled with this software.

This is a standard Lawrence Livermore computer code that is used for modelling military high explosives. It allows no divergent flow and gives a linear response in respect of density versus VOD. Figure 79 shows the results obtained from using this code, based upon the density and formulation of the emulsion explosives.

Figure 79 Density versus VOD calculated by Cheetah using BKW equation

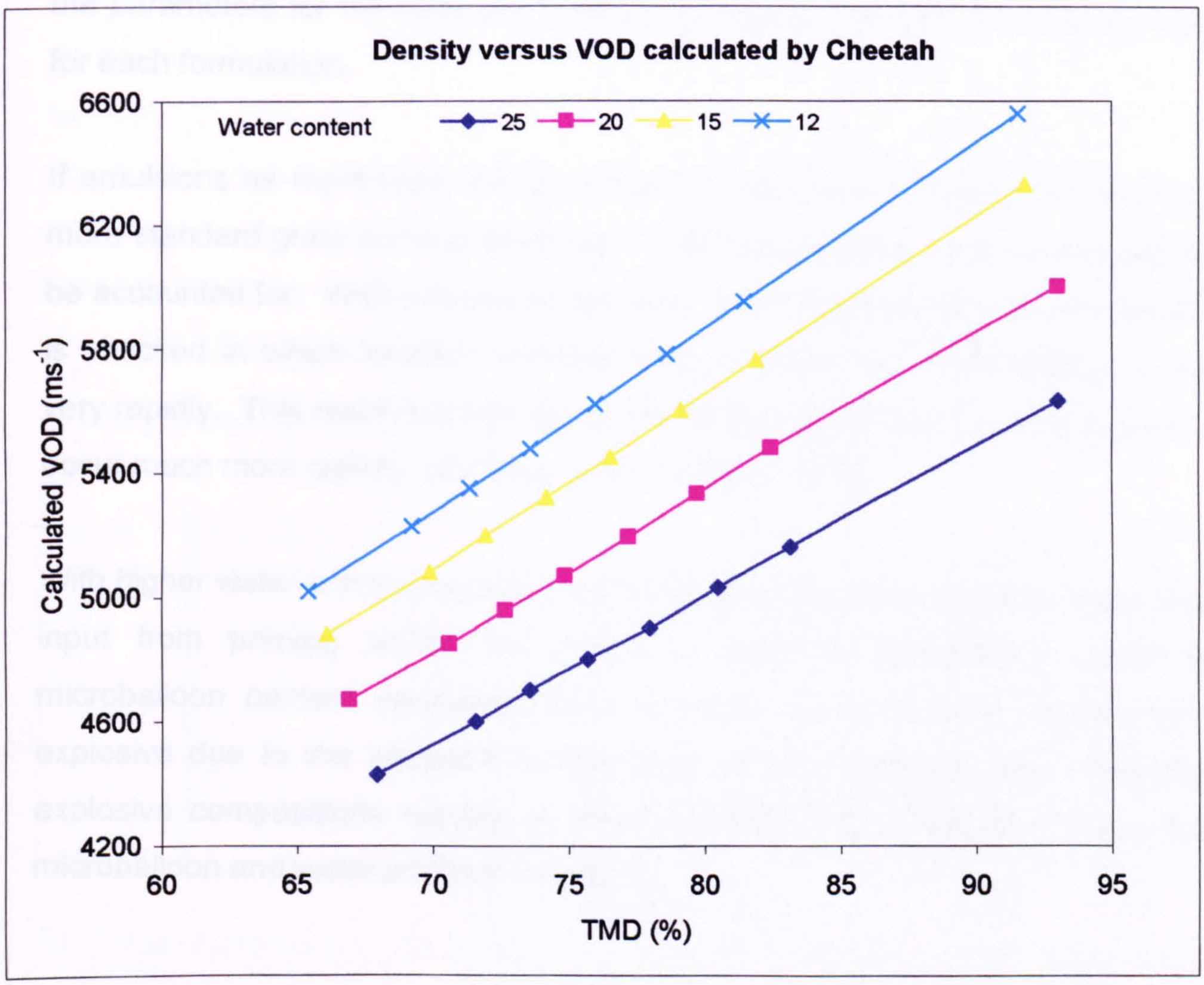

As the graph shows the lower water content emulsions, having a higher energy content, are predicated to have a higher VOD. This is the expected response for a Type I military explosive and at no point should the higher water content explosives give a higher VOD than a lower water content. The actual velocities predicated by the code are, principally, significantly higher than seen in this study, although the code makes no account for charge diameter effects. The code shows that the highest expected VOD for a 25% water content emulsion was around 5500ms at 93%TMD, which was similar to that found in this study, although at a different %TMD.

This variation in performance from that predicated can be accounted for by the slightly divergent flow expected from an emulsion and from the highly curved detonation front. Lateral losses, as mentioned are also not accounted for by the code, which, again, would lead to lower observed velocities than expected. None

of this accounts for why the 25% water emulsion achieves the highest VOD, as all the parameters for the code are based upon giving the maximum energy release for each formulation.

If emulsions as mentioned exhibited thermal explosion behaviour as well as the more standard grain burning detonation regime then some of the anomalies could be accounted for. With a thermal explosion, there is a time lag after the explosive is shocked in which localised heating occurs before the whole explosive reacts very rapidly. This rapid reaction allows the release of energy from the explosive to occur much more rapidly, ultimately giving a higher VOD.

With higher water content explosives, the emulsion requires a greater initial energy input from priming before the explosive goes to detonation. With high microballoon content emulsions there is much more localised heating of the explosive due to the adiabatic compression of the glass balloons. Both these explosive compositions require or have a greater initial heat input than lower microballoon and water content emulsions.

4.3 Low water content emulsions – Grain burning reaction

These emulsion formulations exhibited the classical type II non-ideal explosive behaviour. This data was taken from Figure 77, and comprised points on the graph described by the parabola. Although, as previously discussed, this data was separated subjectively (initially without recourse to the identity of the data), all these data points, except two, were low water content emulsions. Table 15 shows the emulsion formulations that made up this group.

Table 15 Emulsions exhibiting grain burning type detonation

Water content (%)	Microballoon content (%)							
35								
30				3				
25		2						
20	1	2	2.5	3	3.5	4	4.5	5
15	1	2	2.5	3	3.5	4	4.5	5
12	1	2	2.5	3	3.5	4	4.5	5

All these formulations are low water content emulsions, which were relatively easily initiated and when plotted individually as separate water content displayed type II non ideal explosive behaviour.

The only exceptions to the low water content emulsion were the 25 and 30% water content emulsions. Although there was only one data point from each, and that was the highest density of each emulsion and the most difficult to initiate. These two results can be accounted for as they were the highest density of each formulation to successfully initiate and thereby the detonation front in these would probably have been unstable. This means that the detonation was close to failure and parts of the explosive would not have been entirely consumed in the reaction. On this basis, the fact that results from higher water content emulsions are included in the grain burning type reaction is not considered significant.

Figure 80 shows this data plotted as density versus VOD and this shows the classical type II non-ideal profile.

Figure 80 Grain burning detonation VOD versus density

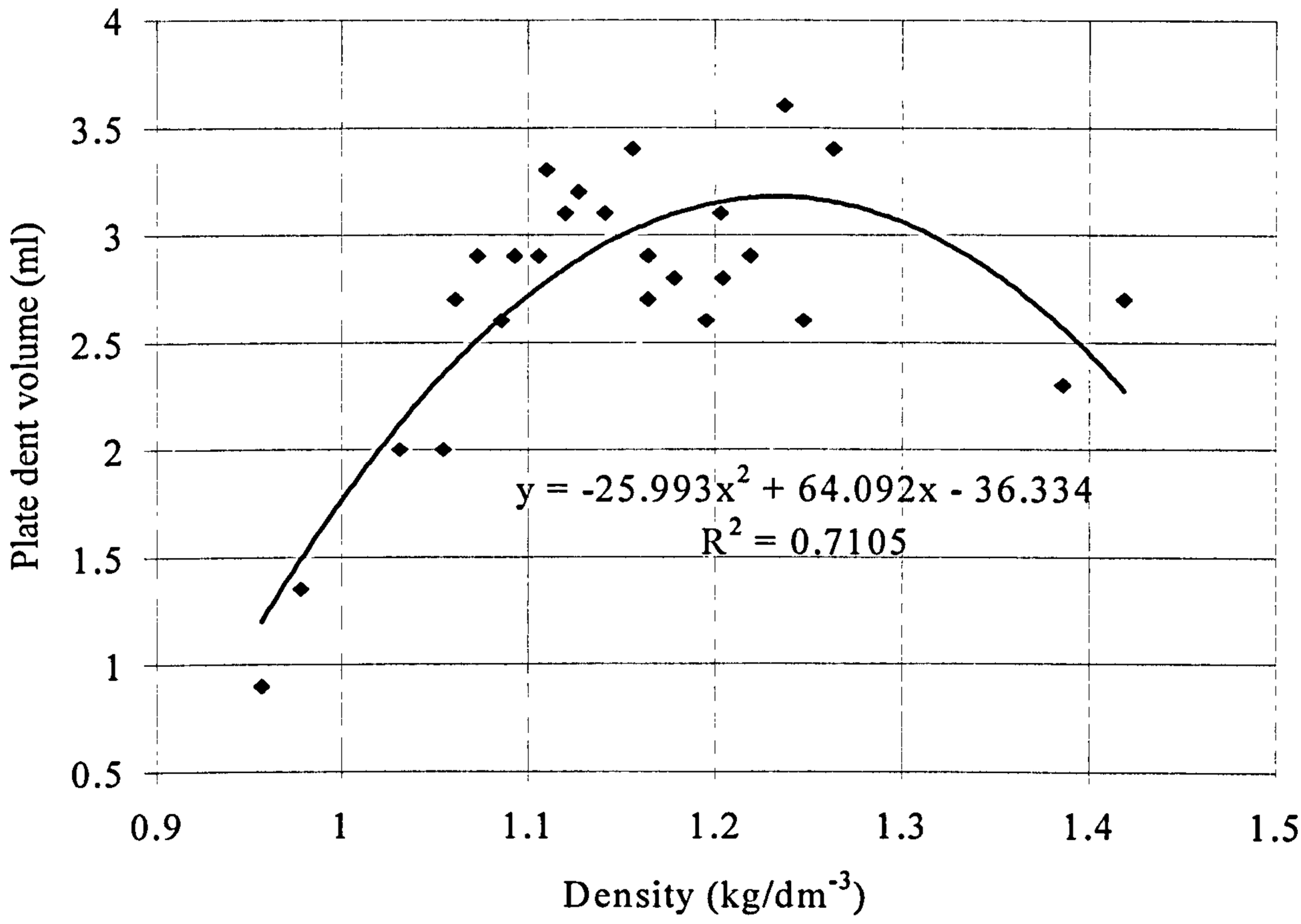

Figure 81 shows the same emulsion formulations plotted as density versus plate dent. The same trend, of initially increasing plate dent volume with density followed by a region of stability before rapidly leading to failure, is noted.

Figure 80 Grain burning detonation VOD versus density

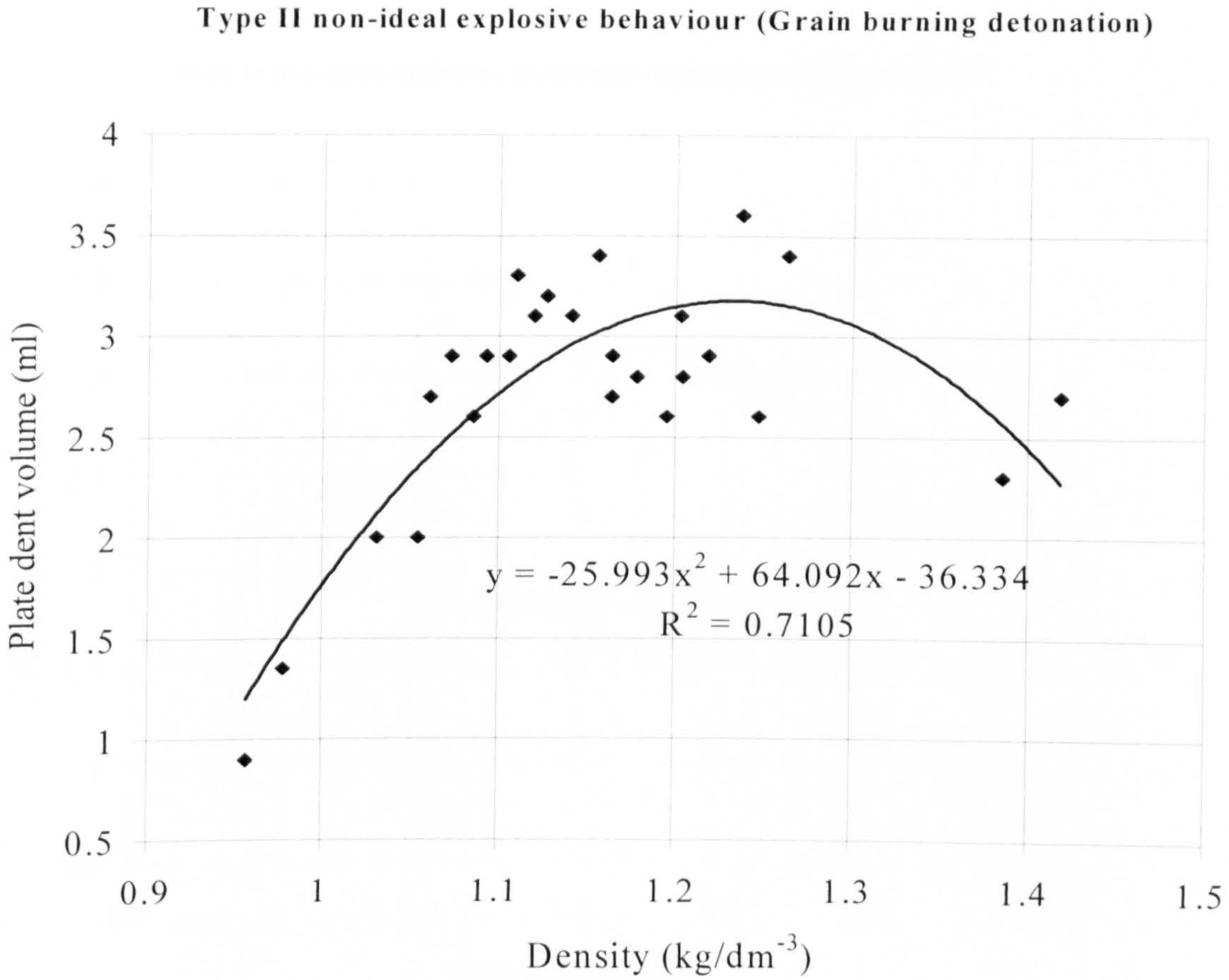

Figure 81 shows the same emulsion formulations plotted as density versus plate dent. The same trend, of initially increasing plate dent volume with density followed by a region of stability before rapidly leading to failure, is noted.

Figure 81 Type II non-ideal explosive behaviour plate dent volume versus density.

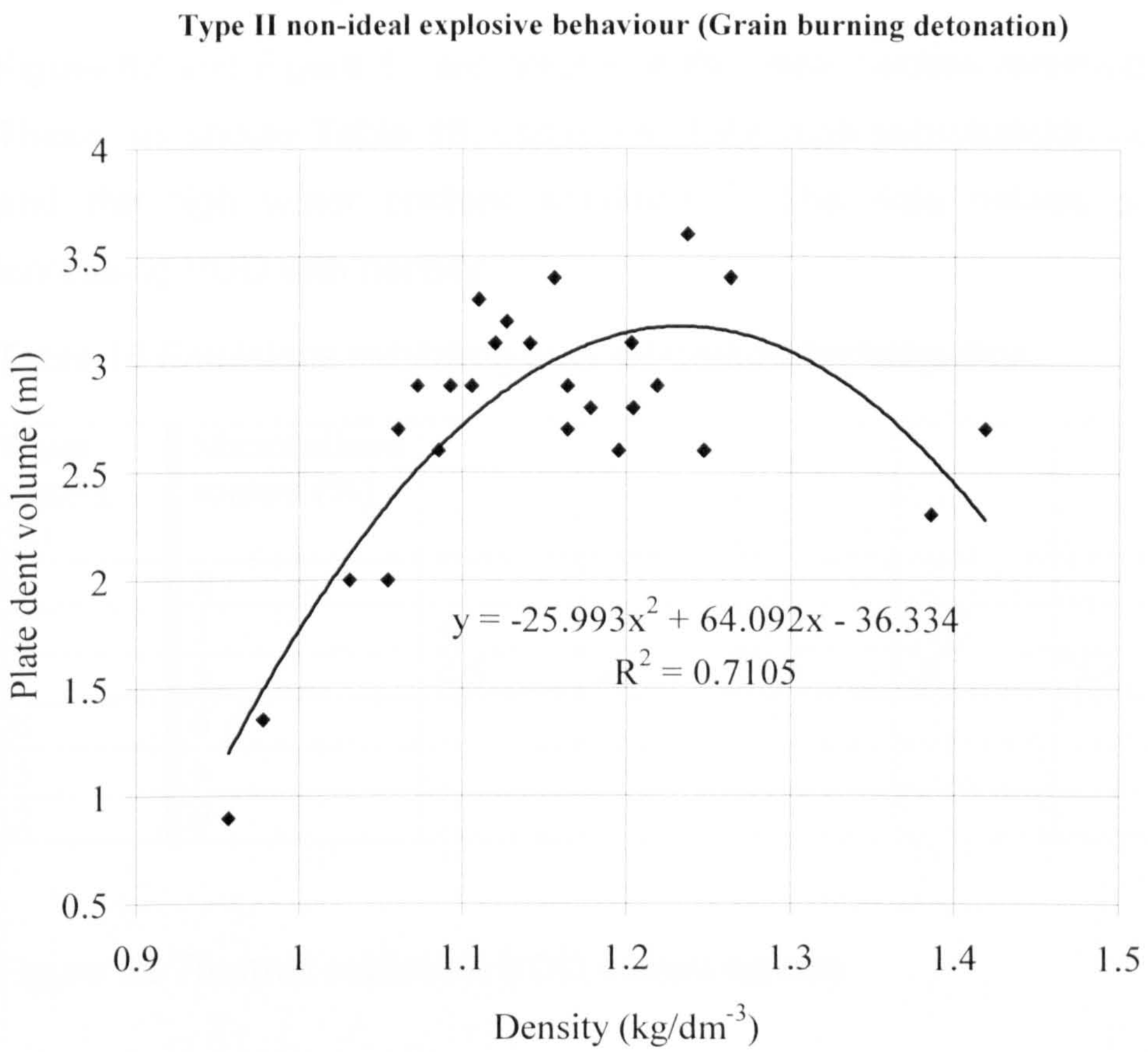

When the plate dent data was previously plotted no significant correlation with the VOD versus density data could be seen, but when the data was separated out in to two reaction regimes, a relationship can be seen between density and plate dent and VOD and density.

4.4 High microballoon and high water content emulsions- Thermal explosion

Figure 82 and Figure 83 are graphs of the linear section removed from Figure 77. These, as shown *Table 16, comprise* of the high microballoon content emulsions and the high water content emulsions. The data follows a linear trend of increasing VOD with density.

Table 16 Emulsions exhibiting thermal detonation behaviour.

Water content (%)	Microballoon content (%)					
35	5					
30	5	4				
25	5	4.5	4	3.5	3	2.5
20	6					
15	6					
12	6					

Figure 82 Thermal explosion VOD versus density

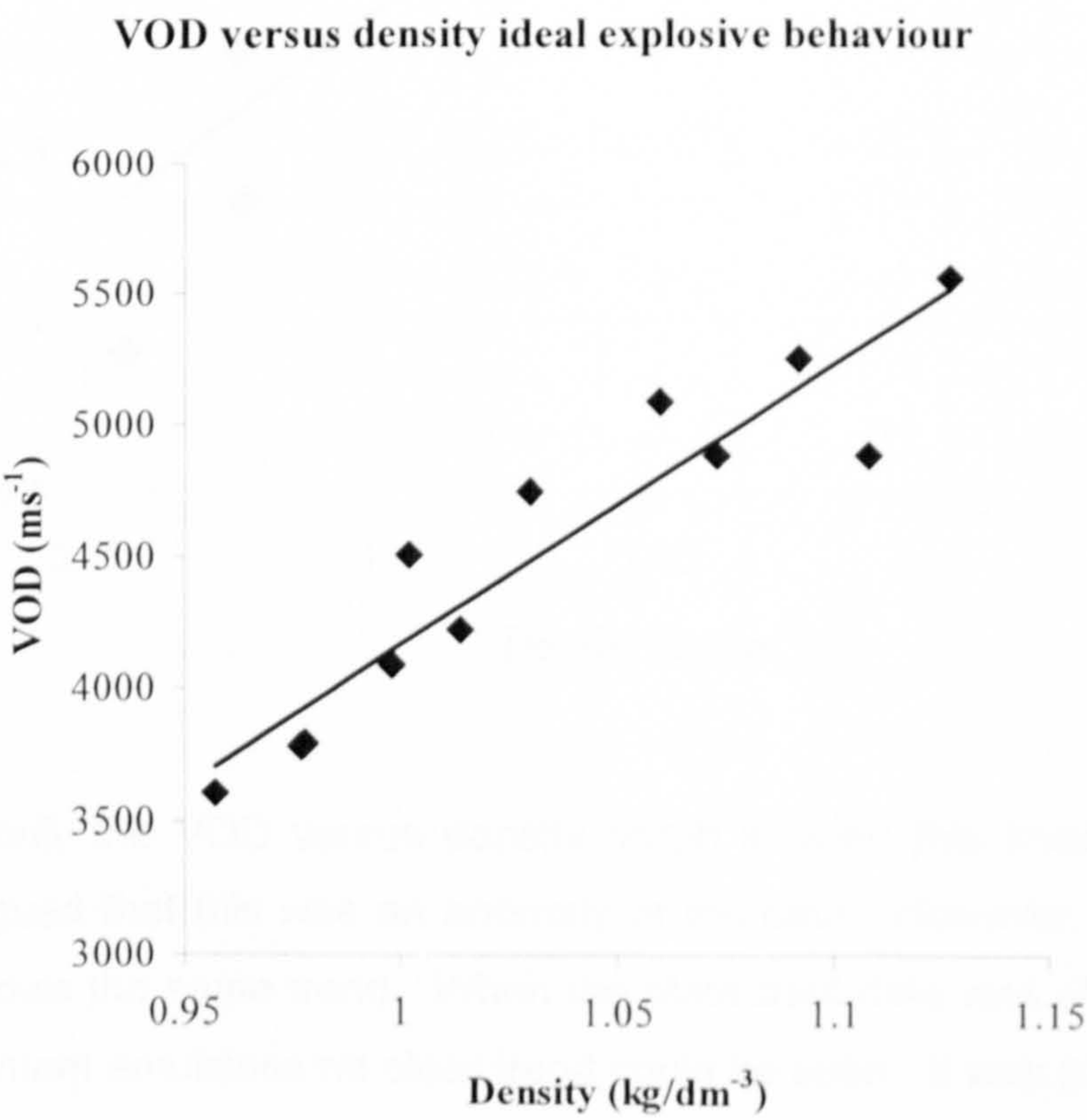

The trend shows that VOD increases directly with density, as would be expected with a type I ideal explosive. Only a small density range was represented by this graph, in comparison to Figure 80, but there was a clear linear trend.

Figure 83 shows the plate dent data and this shows a linear trend of increasing plate dent volume with density.

Figure 83 Plate dent versus density thermal explosion

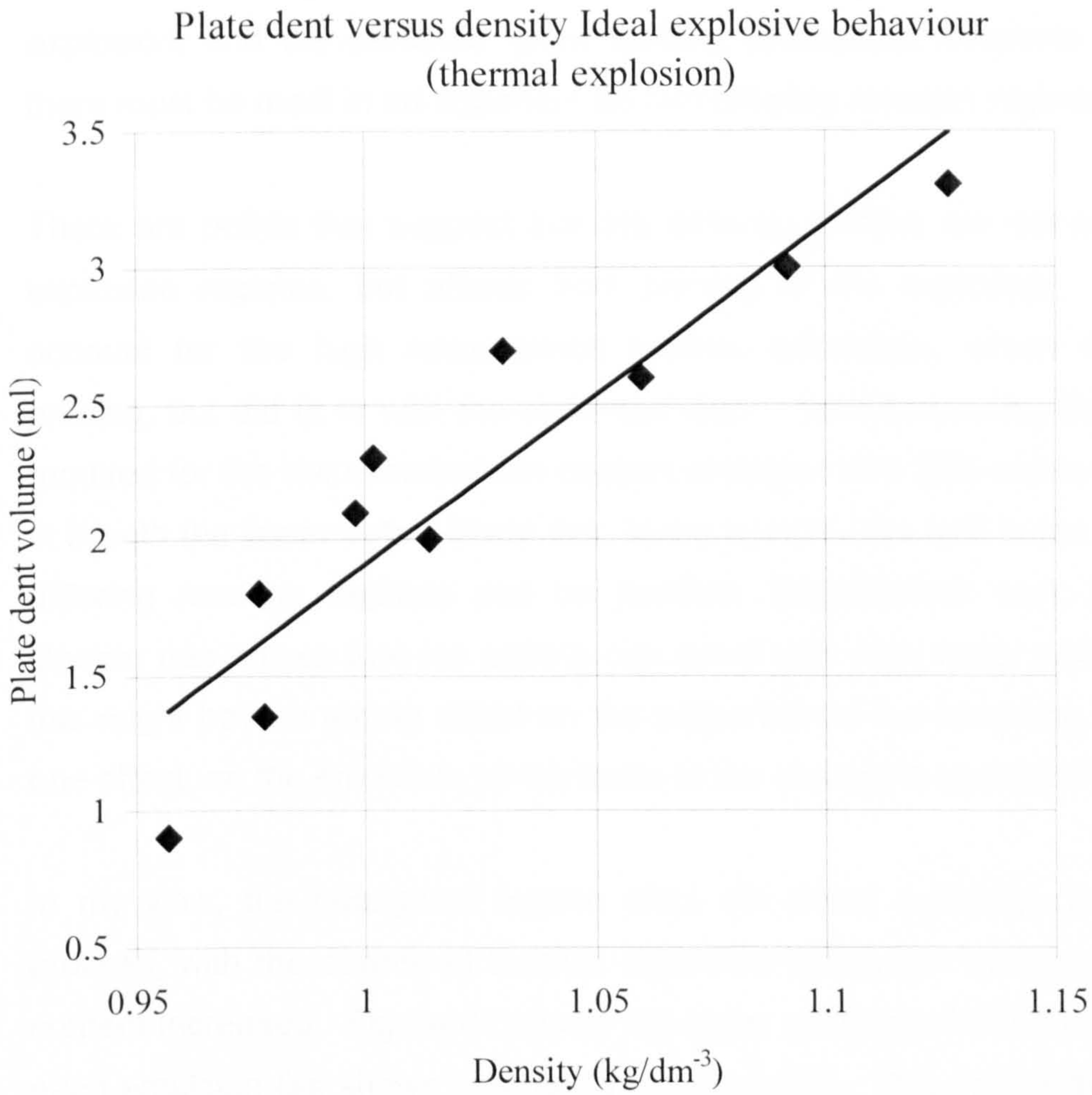

If only the VOD versus density graph showed this linear trend then it could be argued that this was an anomaly of the data. However, the plate dent data also shows the same trend. When the plate dent data was plotted for individual water content emulsions no clear trend could be seen. It was previously discussed as to whether the plate dent test was actually showing the brisance of the explosive.

With the data now separated, even though somewhat arbitrarily, the dent volumes show a relationship with the VOD of the explosives.

4.5 Discussion

Splitting the data into two sets fits with the concept of two differing detonation regimes, but it must be disputed as to whether the results do support the premise of two reaction regimes. Given that the plate dent data for the linear trend, thermal explosion, and the parabola, grain burning detonation, supports the VOD data, there must be merit in an argument for two differing reaction regimes.

There are points that suggest that the differing profiles are not actually differing explosion regimes, but affects from priming of the explosive. This does not account for the high microballoon content emulsions, which did not require priming, but did fit in with the observed data. Notwithstanding this, priming was required for the low microballoon content emulsion with 20% water and this did not fit in with the linear data. Given this, in my opinion, the split in the data leading to differing reaction regimes can be justified. Unpublished work by Dr Graham Cooper has shown that ion pairing can occur with high water content emulsions, this might have a strong effect on the properties of the emulsion. This could be one effect on the emulsion, which leads to the change in reaction regime.

In my view, the change in regime does not occur suddenly, but is a gradual process, with the degree of thermal explosion behaviour increasing as the water content increased. Figure 84 shows the linear sections of VOD versus density for each emulsion (as shown separately in Figure 66). This shows that as the water content of the emulsion increases so the rate of increase in VOD with respect to density increases. This indicates that there is an increase in thermal explosion type reaction with the increasing water content. At low water content, there is little difference in VOD with density because the rate of energy release is slow, even though there is more energy available to be released. At higher water content,

the energy is released more rapidly, which indicates thermal explosion type behaviour.

Figure 84 Comparison of the initial slope in VOD versus %TMD

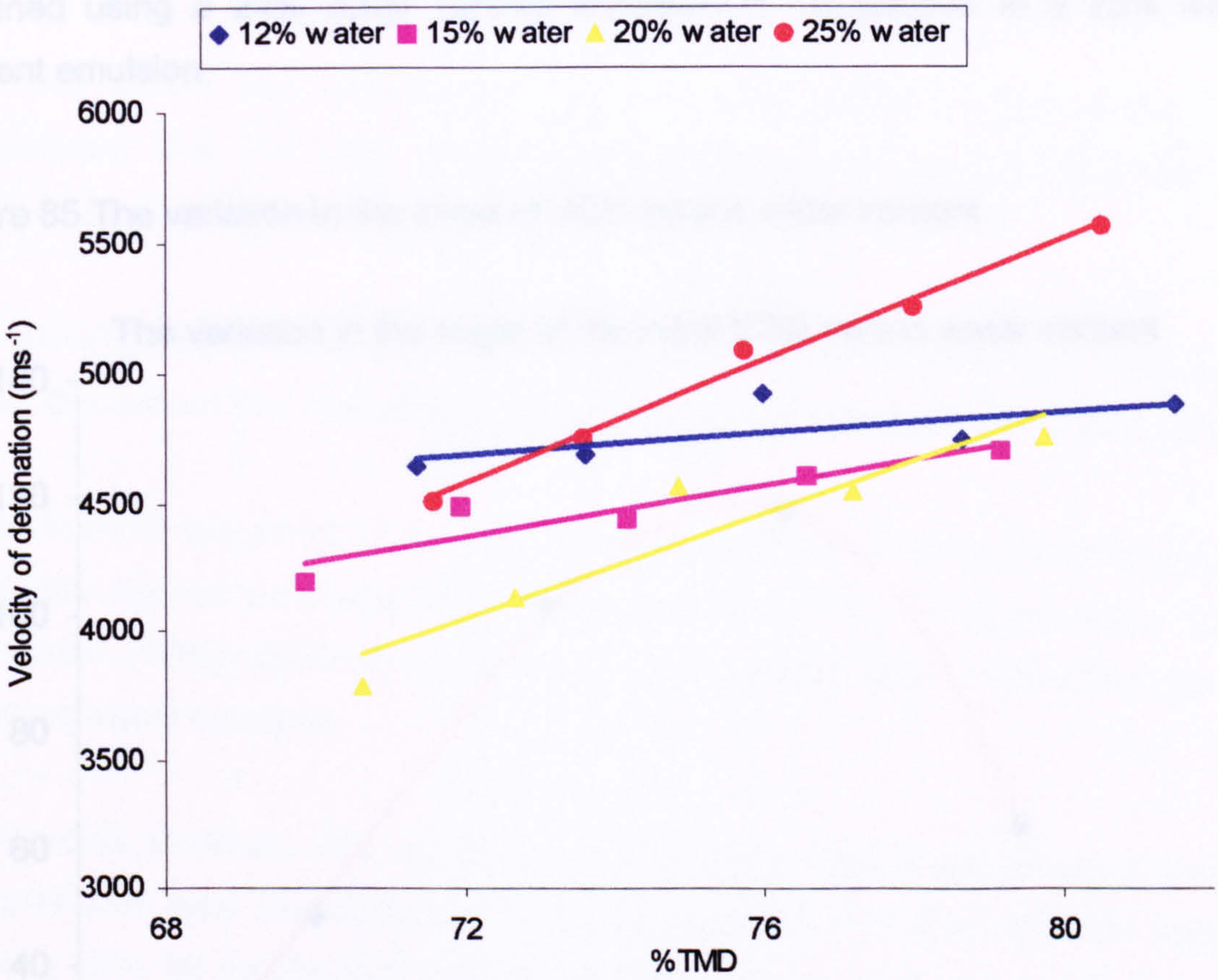

The 25% water content emulsion was the only emulsion to achieve the VOD predicated by CHEETAH. This program was based on ideal explosives, where all the energy is released rapidly, in a thermal explosion reaction. For the emulsion to have obtained this VOD, the rate of energy release must be equal to that of a type I military high explosive, with thermal explosion kinetics. As the lower water contents failed to reach the predicated VOD's then the rate of energy release must

be lower than that of a thermal explosion type reaction, which indicates a grain burning reaction.

There was further evidence that indicated the slow change from grain burning to thermal explosion kinetics. This is shown in Figure 85, which shows the angle from the line of best fit for the linear section of each of the emulsions. This graph shows that the rate of increase in the slope is at a maximum at about 24% water content. This would indicate that perhaps increased performance could be obtained using a 24% water content emulsion in comparison to a 25% water content emulsion.

Figure 85 The variation in the slope of VOD versus water content.

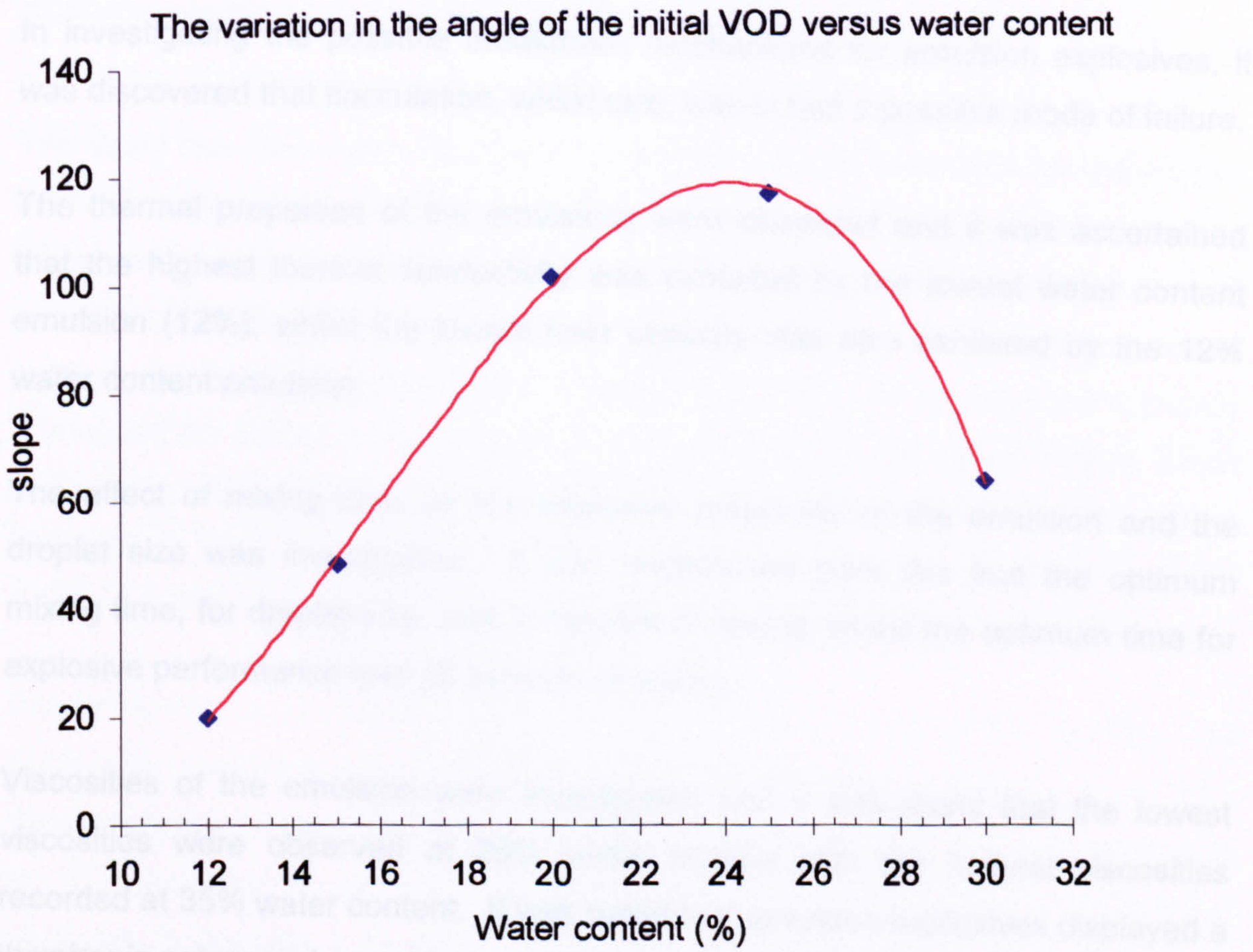

In my opinion, the evidence suggests that emulsion explosives do show a change in reaction regime with increasing water content.

5 Conclusions

This study set out to characterise emulsion explosives with the aim of gaining a better scientific understanding of their behaviour. Whilst some of these objectives have been achieved, such as showing that low water content is not a prerequisite to high VOD performance, others objectives have not been achieved and the results obtained require further work to elucidate their significance.

It was shown that microballoons had a greater affect on the density of the explosive, than the water content, and emulsions can be compared directly by altering the microballoon content.

In investigating the possible breakdown mechanisms for emulsion explosives, it was discovered that flocculation, whilst rare, was in fact a possible mode of failure.

The thermal properties of the emulsions were observed and it was ascertained that the highest thermal conductivity was exhibited by the lowest water content emulsion (12%), whilst the lowest heat capacity was also exhibited by the 12% water content emulsion.

The affect of mixing time on the explosive properties of the emulsion and the droplet size was investigated. It was ascertained from this that the optimum mixing time, for droplet size, was 2 minutes of mixing, whilst the optimum time for explosive performance was 20 minutes of mixing.

Viscosities of the emulsion were investigated and it was found that the lowest viscosities were observed at 25% water content with the highest viscosities recorded at 35% water content. It was noted that emulsion explosives displayed a thixotropic nature and as such viscosities varied with time.

The study endeavoured to link the physical properties of the emulsion directly to the explosive performance, but no physical property was found which allowed the accurate predication of the emulsion explosive performance.

The study showed that emulsion explosives exhibit two distinct explosion regimes, namely that of a thermal explosion and a grain burning regime. At low water contents the explosive follows a grain burning regime, with the reaction occurring rapidly with respect to the shock front and the explosive exhibiting a classical type II explosive behaviour. As the water content increased, then the regime began to change to that of a thermal detonation. At 25% water content, the emulsion displayed this thermal explosion behaviour, and as such increased VOD and brisance was seen for this formulation.

The study showed that at 25% water content with 3% microballoons the VOD achieved (5558ms^{-1}) was similar to that predicated by computer modelling software (CHEETAH). This indicated that the emulsion was undergoing a thermal explosion reaction, which is type I ideal explosive behaviour.

The study has also shown that there is commercial work that could be undertaken in this area as the increased performance in the emulsion explosive occurs at higher water contents. This makes for a more stable emulsion as the increased water helps to inhibit breakdown of the emulsion matrix. The increase in water content also leads to an increase in safety of the explosive, as more initial energy is required for initiation. Notwithstanding this, increasing the water content, whilst decreasing the oil and ammonium nitrate content, makes commercial sense on a cost basis.

6 Further Work

There is a great deal of further work that could be undertaken in this area, some of it having commercial implications.

Commercially emulsion explosive formulations could be further developed with investigations into the increased performance noted at 25% water content. Initially this would require looking at different diameter tubes to determine if the high VOD noted is an affect of the diameter of the charge. Current formulations use low water contents, and this is an area where significant cost benefits, along with increased performance, could be gained.

The thermal results obtained in this study were mostly comparative. With modern thermal instrumentation, it is possible to determine thermal conductivity whilst running TGA and DSC. Undertaking this would help to elucidate the phase changes that occur in the emulsion. If this was coupled with X-ray crystallography then the processes involved, which cause the phase changes to occur in AN could be more fully understood.

Whilst particle size was measured in the study, this was undertaken using an old instrument at the limit of its design capability. Using a modern technique, which would allow the whole emulsion including large droplet sizes to be analysed, would better determine if droplet size has a direct effect on explosive performance.

It is believed that emulsion explosives undergo two distinct reaction regimes and there are experimental techniques, which could help elucidate this. The measurement of VOD with resistance probes to allow continuous measurements would determine run up distances and reveal more information on the way the explosive undergoes transition to detonation. This could be coupled with fibre optic probes connected to a fast video recording device, and if placed on the edge of the charge, would allow limited measurements of the reaction zone to be made. The use of high-speed video itself would allow some determination of the reaction processes occurring in the explosive. To further determine what is happening

inside the explosive reaction zone then the use of flash x-ray would yield much information.

The main problem with all the above techniques is that they usually require large testing facilities and expensive equipment to usefully undertake the analysis. Fiscal limitations severely hampered the present study, but without this limitation, it would be possible to fully characterise emulsion explosives and link their explosive behaviour to their physical properties.

7 References

1 'Explosives Engineering', P.Cooper; Wiley-VCH, 1997.

2 'Detonation' W.Fickett and W.Davies; University of California Press, 1979.

3 'The Mathematics of Combustion', Editor J.Buckmaster, SIAM, 1985.

4 P.Vieille *Comptes Rendes Academie des Sciences,* 1893, **130**.

5 E.Mallard, Le Chatelier, *Comptes Rendes Academie des Sciences*, 1881, **93**.

6 'Explosives in the Service of Man', Editors J.Dolan and S.Langer: The Royal Society of Chemistry 1997; W. Mather 120-138.

7 M.Bertholet, *Comptes Rendes Academie des Sciences*, 1881, **93**.

8 M.Bertholet, P.Vieille, *Annales de Chimie at de Physique*, 1883, 5th Seiers, **28**, 289.

9 M.Bertholet, *Comptes Rendes Academie des Sciences*, 1882, **94**.

10 H.Dixon, *Philosophical Transitions A*, 1893, **184**. 93-98.

11 'Introduction to the Technology of Explosives', P.Cooper, S.Kurowski; VCH 1996.

12 'Numerical Modelling of Detonations', C.Mader; University Of California Press, 1979.

13 'Detonation of Condensed Explosives', R.Cheret; Springer-Verlag, 1992.

14 'Detonation in Condensed Explosives', J.Taylor; Oxford University Press, 1952.

15 'Theory of Detonation', Z. Kompaneets; Academic Press, 1960.

16 'Combustion: a study in theory, fact and application', J.Chomiak; Abacus, 1990.

17 D.Chapman, *Philosophical Magazine*, 1889, **47**.

18 E.Jouguet, *Comptes Rendes Academie des Sciences*, 1904, **140**.

19 'On the Normal Ignition Velocity of Explosive Gaseous Mixtures', V.Michelson; Moscow University Printing Service, 1893, **10**.

20 'Explosives and Rock Blasting,' R.Morhard; Atlas Powder, 1987.

21 Y.Zeldovich, *Zh. Exp. I Teor. Fiz.*, 1940, **10**.

22 J.Neumann, 'Theory of Stationary Detonation Waves' *Selected Works*, 1942, **6**.

23 W.Doering, Annalen der Physik 1942 **43**.

24 'Explosive Effects and Applications', Editors: A.Zukasj, W.Walters; Springer-Verlag, 1998.

25 'Initiation and Growth of Explosions in Liquids and Solids', F.Bowden, Y.Yoffe; Cambridge University Press 1952.

26 J. Dear, *J. Fluid Mech*, 1988, **190**, 409-425.

27 N.Bourne, J.Field, *J. Fluid Mech,* 1992, **244**, 225-240.

28 N.Bourne, J.Field, *Proc. R. Soc. Lond. A,* 1991,435, 423-435.

29 J. Dear, J.Field, A.Walton, Nature, 1988, **332**, 505-508.

30 K.Feng, W.Chung, J.Yu, *Symposium on Detonation,* Maryland, 1981, 343-351.

31 J.Austing, A.Tullis, D.Brzycki, *Symposium on Detonation,* Maryland, 1981, 47-56.

32 J.Johnson, P.Tang, C.Forest, *Journ. Appl. Phys,* 1985,. **57**, 4323-4334.

33 J.Field, G.Swallowe, S.Heavens, *Proc. R. Soc. Lond. A*, 1982, **382**, 231-244

34 J.Field, N.Bourne, S.Palmer, S.Walley, *Phil. Trans. R. Soc. Lond.A*, 1992, **339**, 269-283.

35 S.Walley, J.Field, S.Palmer, *Proc.R.Soc.Lond.A*, 1992,.**438**, 571-583.

36 N.Bourne, , *Proc. Ninth Symp. on Detonation*, 1989, 869-878.

37 J.Field *Acc. Chem. Res*, 1992, **25**, 489-496.

38 P.Tang, J.Johnson, C.Forest *Proc. Ninth Symp. on Detonation* 1989, 375-384.

39 C.Mader, J.Kershner *Proc. Ninth Symp. on Detonation* 1989, 366-374.

40 P.Taylor, *Proc. Ninth Symp. on Detonation*,1989, 358-365.

41 'American Instiute of Physics Handbook', 2nd Edition.

42 Frank-Kamenetskii, *Acta Physiochimica*, 1939, **10**, 365.

43 'Explosives Engineering' P.Cooper; Wiley-VCH, 1997.

44 M.Cook, 'The Science of High Explosives', Chapman & Hall London, 1958 (Reprint 1971).

45 D.Price, Proc.*11th Symp (International) on Combustion*, 1967, 693-702.

46 'Detonics of High Explosives' C.Johansson, P.Persson, Academic Press, 1970.

47 'Explosives', R. Meyer; VCH, 1987.

48 'Emulsions and Foams', Berkman & Egloff; Reinhold, 1941.

49 'Introduction to Colloid & Surface Chemistry', D.Shaw; Butterworth-Heinemann, 4th Edition, 1994.

50 'Emulsifiers Functionality and Applications', Editors: K.Berger & R.Hamilton; Society of Chemical Industry, 1998.

51 'An Introduction to Rheology', H.Barnes,J.Hutton & K.Walters; Elsevier, 1989.

52 'Surfaces, Interfaces, and Colloids: Principles and Applications', M.Drew; VCH, 1990.

53 'Basic Principles of Colloid Science', D.Everett; RSC Paperbacks,1988.

54 'Food Emulsions –What Are They?' Emulsifiers Functionality and Applications', N.Krog; SCI, 1998.

55 Grete Hyldig: PhD Thesis 'Influence of Technological Parameters on the Enzymatic Reaction and Gel Formation in Milk and UF-Retentates', 1993, KVL.

56 'Emulsions: Theory and Practice', Becher; Reinhold, 1957.

57 'Encyclopaedia of Emulsion Technology', Editor:P.Becher; Marcel-Deker,1983.

58 US Patent 3,161,551, R.Egly, Dec 1964.

59 US Patent 3,164,503, N.E.Gehrig, Jan 1965.

60 H.Dautriche, *Comptes Rendes Academie des Science*, 1906,**143.**

61 US Patent 4,110,134, H.F.Bluhm, June 1969.

62 US Patent, 4,110,134, Wade, 1978.

63 'Encyclopaedia of Emulsion Technology, H.Bampfield, J.Cooper; Marcel Deckker, 1988.

64 'Explosives in the Service of Man' Editor:J.Dolan, S.Langer, Royal Society of Chemistry, 1997.

65 P.Worsy, B.Weeks, *J. Explos. Eng Des,* 1997 18-21.

66 'Encyclopedia of Chemical Technology', Kirk-Othmer;Wiley, 1991, **2.**

67 B.Luca, M.Ahtee, A.Hewat, *Acta Cryst*, 1979, **B35**, 1038-1041.

68 M.Ahtee, K.Smolander, B.Luca, A.Hewat *Acta Cryst,* 1983, **C39**, 651-655.

69 'Encyclopaedia of Explosives' Picatinny Arsenal',B.Fedoroff, 1960 ,**1**.

70 'Differential Thermal Analysis', R.Mackenzie; Academic Press, 1973.

71 D.Tramoundanis, '*Phase Stabilisation Of Ammonium Nitrate*' Msc Thesis Nov.1988.

72 U.Teipel, *Propellants, Explosives, Pyrotechnics*, 1995, **20**, 20-265.

73 O.Listh, *Propellants and Explosives*, 1978, **3**, 36-41.

74 Y.Alymova, V.Annikova, N.Vlasova, B.Kondrikov, *Combustion, Explosion and Shock Waves*, 1994, **30**, 340-345.

75 L.Wang, *J. of Thermal Analysis,* 1995, **45**, 261-268.

76 A.Martin, D.Bastos-Netto, *Propellants, Explosives, Pyrotechnics,* 1999, **24**, 308-313.

77 V.Mohan, T.Tang, *Propellants, Explosives, Pyrotechnics*, 1984, **9**, 30-39.

78 E.Lee, C.Tarver, *Phys. Fluids*, 1980, **23**, 2362-2372.

79 'Analytical Chemistry Handbook', J.Dean, Mcgraw-Hill, 1995.

80 'Introduction to Thermal Analysis Techniques and Applications', M.Brown; Chapman and Hall, 1988.

81 'Advanced Physics', M.Nelkon, M.Detheridge; Pan Books, 1982.

82 G.Shankar, A.Kumar, V.Mohan, *Propellants, Explosives, Pyrotechnics*, 1996, **21**, 70-73.

83 M.Kenndy, D.Kerr, *Proc. Ninth Symp. on Detonation,* 1989, 1352-1359

84 J.Lee, P.Persson, *Propellants, Explosives, Pyrotechnics,* 1996, **15** 208–216.

85 K.Hattori,Y.Fukatsu, *Journal of the Industrial Explosives Society Japan*, 1982, **43**, 295-301.

86 'Explosives, Propellants and Pyrotechnics' A.Bailey, S.Murray; Brasseys, Vol 2, 1989.

87 Private communications with Dr J.Cooper and G.Lieper.

88 'Differential Thermal Analysis', R.Mackenzie; Academic Press, 1970.

89 AN Trace Provided by Dr.Cartwright.

90 Private Communications with Dr Cartwright.

91 H.Eyring, R.E.Powell, G.H.Duffy, R.B.Parlin, *Chemical Reviews*, 1949, **45**, 69-172.

92 Private communications with Dr J.Cooper and G.Lieper.

93 Science of High Explosives' Editor:C.Bawn and G.Rotter; Her Majesty's Stationary Office, 1956.

94 H.Jones, *Proc. R. Soc. Lond.* 1947, **189**, 415-422.

95 J.Copp, A.R.Ubbelohde, *Trans. Faraday Soc.* 1948, **44**, 646-658.

96 G.A. Leiper and J.Cooper , 28th ICT, Karlsrhue, 1997.